

**AN ANALYSIS OF OFF-GRID, OFF-PIPE HOUSING IN SIX U.S. CLIMATES**

A Dissertation

by

MINI MALHOTRA

Submitted to the Office of Graduate Studies of  
Texas A&M University  
in partial fulfillment of the requirements for the degree of

DOCTOR OF PHILOSOPHY

December 2009

Major Subject: Architecture

**AN ANALYSIS OF OFF-GRID, OFF-PIPE HOUSING IN SIX U.S. CLIMATES**

A Dissertation

by

MINI MALHOTRA

Submitted to the Office of Graduate Studies of  
Texas A&M University  
in partial fulfillment of the requirements for the degree of

DOCTOR OF PHILOSOPHY

Approved by:

Chair of Committee,	Jeff S. Haberl
Committee Members,	David E. Claridge
	Charles H. Culp
	Anat Geva
Head of Department,	Glen Mills

December 2009

Major Subject: Architecture

## ABSTRACT

An Analysis of Off-grid, Off-pipe Housing in Six U.S. Climates. (December 2009)

Mini Malhotra, B.Arch., Birla Institute of Technology, Mesra, India;

M.S., Texas A&M University, College Station

Chair of Advisory Committee: Dr. Jeff S. Haberl

This dissertation addresses the issues of climate change and depletion of non-renewable resources of energy and water, and aims at eliminating the use of non-renewable resources of energy and water for the building operation in single-family detached residences in the U.S. With this aim, this study investigated the feasibility of the off-grid, off-pipe design approach in six climate locations across the U.S. to achieve self-sufficiency in a house for building energy, indoor water use, and household wastewater and sewage disposal using only on-site available renewable resources.

For the analysis, a 2,500 ft<sup>2</sup>, 2000/2001 International Energy Conservation Code standard reference house with typical building and usage characteristics was selected as the base case. The six U.S. climate locations included: Minneapolis, MN, Boulder, CO, Atlanta, GA, Houston, TX, Phoenix, AZ, and Los Angeles, CA. The renewable resources considered for this study included: solar radiation, wind, biomass for building energy needs; rainwater for indoor water use. In addition, the building site was considered for the disposal of household wastewater and sewage. The selected climate locations provided different scenarios in terms of base-case building energy needs and availability of renewable resources. Depending on these, energy and water efficiency measures were selected for reducing the building needs. For the reduced building needs, the sizing of systems for self-sufficiency was performed, including: solar thermal system for building's space heating and water heating needs, photovoltaic and wind power systems for building's electricity needs; rainwater harvesting system for indoor water needs; and septic system for the on-site disposal of household wastewater and sewage. In this manner, an integrated analysis procedure was developed for the analysis and design of off-grid, off-pipe homes, and was demonstrated for six U.S. climate locations.

The results of the analysis indicated that achieving self-sufficiency for energy, water and sewage disposal was possible in all climates provided the systems for the collection and storage of renewable resources were large. On the other hand, the utilization of these systems was small for locations, where the year-to-year and seasonal variations in the weather conditions and availability of climate resources was large. For increased system utilization, minimization of the peak building needs, utilization of harvested energy for secondary purposes, and considering alternative systems for such applications are preferred.

**DEDICATION**

*To my parents*

## ACKNOWLEDGMENTS

I would like to express my sincere gratitude to the chair of my advisory committee, Dr. Jeff Haberl, for guiding my work with his dedicated attention, expertise and knowledge. I would like to thank Dr. David Claridge, Dr. Charles Culp and Dr. Anat Geva for being on the committee and for giving their valuable time and input to my dissertation.

The study utilized several resources developed for the Texas Emissions Reduction Program (Senate Bill 5) of the Texas State Legislature. In this context, I am grateful to the Senate Bill 5 team at the Energy Systems Laboratory who have helped this study in various ways. My special thanks to Dr. Juan-Carlos Baltazar for his expert advice on the solar thermal and PV system analysis and Dr. Zi Liu and Jaya Mukhopadhyay for sharing their views and knowledge, which helped me solve various issues related to this study.

I would like to thank my advisor, Dr. Jeff Haberl, once again, for encouraging me to participate in the Texas A&M team of 2007 Solar Decathlon, which provided me an unparalleled learning opportunity and helped develop this study. I would also like to extend my appreciation to all the team members for sharing their knowledge and expertise.

My special thanks to my uncle, Dr. Rajiv Kohli, for his support and encouragement throughout and for providing an exceptional model for me to follow as a researcher and one that continues to inspire me.

Finally and most importantly, I am deeply grateful to my family for their love, support, patience, and encouragement which helped me overcome obstacles and accomplish my goals.

## TABLE OF CONTENTS

	Page
ABSTRACT .....	iii
DEDICATION .....	iv
ACKNOWLEDGMENTS .....	v
TABLE OF CONTENTS .....	vi
LIST OF FIGURES .....	x
LIST OF TABLES .....	xiv
CHAPTER	
I    INTRODUCTION .....	1
1.1. Background.....	1
1.2. Theoretical Framework.....	3
1.3. Purpose and Objectives.....	5
1.4. Organization of the Dissertation .....	5
II   LITERATURE REVIEW .....	7
2.1. Off-grid House: the Concept and Application .....	7
2.1.1. Introduction .....	7
2.1.2. Pioneering Off-grid Efforts .....	8
2.1.3. Reasons and Concerns for Going Off-grid .....	11
2.1.4. Key Considerations for Off-grid Houses .....	11
2.2. Climatic Classification Approaches.....	11
2.3. Building Characteristics.....	15
2.4. Measures for Energy and Water-efficiency for Off-grid Applications .....	16
2.4.1. Building Envelope .....	16
2.4.2. Fenestration System.....	17
2.4.3. Lighting and Appliances.....	18
2.4.4. Mechanical Systems .....	19
2.4.5. Water-efficiency Measures .....	20
2.5. Renewable Energy Technologies and Analysis Methods .....	21
2.5.1. Passive Solar Systems .....	22
2.5.2. Active Solar Thermal Systems .....	23
2.5.3. Photovoltaic System .....	25
2.5.4. Wind Power System .....	26
2.5.5. Micro-hydroelectric System .....	27
2.5.6. Biomass and Biodiesel .....	28
2.5.7. Rainwater Harvesting System .....	29
2.5.8. Renewable System Selection Priorities .....	30
2.6. Climate Maps and Weather Data Sources.....	30
2.6.1. Typical Meteorological Year (TMY2) Weather Data: .....	31
2.6.2. Measured Wind and Rainfall Data .....	31

CHAPTER	Page
2.6.3. Meteorological and Solar Energy Datasets.....	31
2.6.4. Special Concerns About Weather Data .....	32
2.7. Tools and Methods for an Integrated Analysis .....	33
2.7.1. Whole-Building Energy Simulation Programs .....	33
2.7.2. Analysis Programs for Solar Systems .....	35
2.7.3. Tools for Integrated Analysis .....	36
2.7.4. Approaches for Integration of Various Tools.....	38
2.8. Summary of the Literature Review.....	38
<b>III SIGNIFICANCE OF THE STUDY.....</b>	<b>41</b>
3.1. Expected Contributions of the Study .....	41
3.2. Scope and Limitations of the Study .....	41
<b>IV METHODOLOGY .....</b>	<b>43</b>
4.1. Overview of the Methodology .....	43
4.2. Selection of Representative Climate Locations .....	45
4.2.1. Preliminary Selection of Locations .....	46
4.2.2. Determination of the Base-case Building Characteristics .....	47
4.2.3. Simulation of Base-case Energy Use.....	53
4.2.4. Final Selection of Locations.....	55
4.3. Analysis of Climate Characteristics.....	58
4.4. Selection of Water Efficiency Measures.....	58
4.5. Selection of Energy Efficiency Measures .....	59
4.5.1. Investigation of the Base-case Energy Use .....	59
4.5.2. Investigation of the Peak Load Components .....	60
4.5.3. Selection of Energy Efficiency Measures.....	61
4.6. Quantification of On-site Harvestable Renewable Resources .....	62
4.6.1. Analysis of the Active Solar Thermal System.....	63
4.6.2. Analysis of the Photovoltaic System .....	66
4.6.3. Analysis of the Wind Power System .....	68
4.6.4. Analysis of the Rainwater Harvesting System .....	69
4.7. Sizing and Integration of Systems for Self-sufficiency .....	72
4.7.1. Sizing of the Solar Thermal System .....	73
4.7.2. Sizing of Electricity Generation System.....	73
4.7.3. Sizing of Biomass-based Heating System .....	74
4.7.4. Sizing of Electricity Storage System .....	74
4.7.5. Sizing of the Rainwater Harvesting System .....	75
4.7.6. Sizing of Sewage Disposal System .....	76
4.7.7. Checking Inter-relationship of the Building, Site and Systems.....	76
4.8. Summary of Methodology .....	77
<b>V ANALYSIS AND RESULTS.....</b>	<b>78</b>
5.1. Climate Characteristics of the Selected Locations.....	78
5.1.1. Minneapolis, MN.....	79
5.1.2. Boulder, CO.....	80
5.1.3. Atlanta, GA .....	80
5.1.4. Houston, TX.....	80
5.1.5. Phoenix, AZ.....	80

CHAPTER	Page
5.1.6. Los Angeles, CA .....	80
5.2. Selection of Water Efficiency Measures.....	83
5.3. Selection of Energy Efficiency Measures.....	85
5.3.1. Investigation of the Base-case Energy Use .....	85
5.3.2. Investigation of the Base-case Peak Load Components .....	93
5.3.3. Selection of Energy-efficiency Measures.....	97
5.3.4. Determination of the Optimum Building Configuration .....	100
5.3.5. Reduced Energy Use .....	104
5.4. Quantification of On-site Harvestable Renewable Resources .....	114
5.4.1. Analysis of the Solar Thermal System .....	114
5.4.2. Performance of the Photovoltaic System.....	123
5.4.3. Performance of Wind Turbines .....	127
5.4.4. Determination of Sizing Parameters for the Rainwater Harvesting System.....	133
5.5. Sizing of Systems for Self-sufficiency .....	136
5.5.1. Solar Thermal System for Heating Needs .....	136
5.5.2. Photovoltaic and Wind Power System for Electricity Needs .....	137
5.5.3. Electricity Storage System .....	141
5.5.4. Rainwater Harvesting System for Indoor Water Use .....	144
5.5.5. Septic System for Sewage Disposal .....	145
<b>VI SUMMARY AND CONCLUSIONS .....</b>	<b>147</b>
6.1. Summary of Research Objectives.....	147
6.2. Summary of the Methodology .....	147
6.3. Summary of Analysis and Results .....	148
6.3.1. Energy Use for the Base-case and Proposed House .....	149
6.3.2. Sizing of Systems for Self-sufficiency .....	150
6.4. Discussion.....	152
6.4.1. Criteria for the Analysis Procedure .....	153
6.4.2. Opportunities .....	153
6.4.3. Challenges .....	154
6.4.4. Building and System Design Priorities.....	155
6.4.5. Recommended Architectural Policy .....	156
6.4.6. Limitations of the Analysis Procedure Specific to This Study .....	157
6.5. Conclusions .....	159
6.6. Recommendations for Future Research.....	161
REFERENCES.....	163
APPENDIX A: SIMULATION CAPABILITIES ADDED TO THE DOE-2.1E INPUT .....	175
APPENDIX B: ESTIMATION OF DOMESTIC HOT WATER ENERGY USE.....	179
APPENDIX C: DETERMINATION OF HEATING AND COOLING LOAD COMPONENTS .....	182
APPENDIX D: SYSTEMS PERFORMANCE DATA.....	187
APPENDIX E: ANALYSIS OF SOLAR THERMAL SYSTEM.....	189
APPENDIX F: ANALYSIS OF PHOTOVOLTAIC SYSTEM.....	195



	Page
APPENDIX G: ANALYSIS OF WIND POWER SYSTEM.....	197
APPENDIX H: ANALYSIS OF RAINWATER HARVESTING SYSTEM .....	216
APPENDIX I: SPREADSHEETS FOR THE INTEGRATION OF RESULTS .....	220
APPENDIX J: COST ESTIMATE OF SYSTEMS.....	227
VITA.....	229

## LIST OF FIGURES

		Page
Figure 1	Theoretical Framework (modified from Chen et al. 2009) .....	3
Figure 2	Climate Classification for the 2000/2001 IECC .....	13
Figure 3	Climate Classification for the 2000 by Briggs et al. (2003).....	13
Figure 4	An Overlay of Climate Classification Maps by the U.S. DOE Building America Program (US DOE 2007) and Lechner (2001) .....	14
Figure 5	Research Methodology .....	44
Figure 6	Procedure for Selecting Six Representative Climate Locations.....	45
Figure 7	Preliminary Selection of Locations.....	46
Figure 8	Base-case House .....	48
Figure 9	Schedule for Combined Domestic Hot Water Use .....	50
Figure 10	Schedule for Lighting Use, Equipment Use, and Occupancy .....	51
Figure 11	Indoor Water End-use Estimates by: (a) Mayer and DeOreo (1999), and (b) Vickers (2001).....	52
Figure 12	Base-case Annual End-use Energy Use and Peak Monthly Total Thermal Energy Use for Seventeen Locations .....	56
Figure 13	Base-case Annual End-use and Peak Monthly Total Electricity Use for Seventeen Locations .....	56
Figure 14	U.S. Annual Average Solar Radiation (1961-1990) .....	57
Figure 15	U.S. Annual Average Wind Resource Potential .....	57
Figure 16	U.S. Annual Precipitation (1971-2000). .....	57
Figure 17	Procedure for Climate Analysis.....	58
Figure 18	Procedure for the Selection of Water and Energy Efficiency Measures.....	59
Figure 19	Procedure for the Quantification of On-site Harvestable Renewable Resources.....	62
Figure 20	Procedure for Analyzing Solar Thermal System .....	63
Figure 21	Procedure for Analyzing the (a) Wind Power System, and (b) Photovoltaic System .....	67
Figure 22	Procedure for Deriving Normalized Sizing Parameters for the Rainwater Harvesting System .....	70

	Page
Figure 23 Procedure for Determining Rainwater Storage Volume based on One-year Rainfall Data.....	71
Figure 24 Procedure for the Sizing and Integration of Systems for Self-sufficiency.....	72
Figure 25 Procedure for the Sizing of Electricity Storage System for the PV Electricity Production.....	75
Figure 26 TMY2 Monthly Climate Statistics for Temperature, Humidity and Solar Radiation in the Six Selected Climate Locations.....	81
Figure 27 Monthly Statistics for Wind, Rainfall, Frost Days and Daylight Hours (based on the NOAA and NASA Measured Data) in the Six Selected Climate Locations.....	82
Figure 28 Indoor Water Use for the Base Case and with Water Efficiency Measures.....	84
Figure 29 Base-case Annual End-use Electricity Use in the Six Selected Climate Locations.....	88
Figure 30 Base-case Annual End-use Thermal Energy Use in the Six Selected Climate Locations.....	88
Figure 31 Base-case Monthly End-use Electricity Use in the Six Selected Climate Locations.....	89
Figure 32 Base-case Monthly End-use Thermal Energy Use in the Six Selected Climate Locations.....	90
Figure 33 Base-case Peak Summer Day Hourly End-use Electricity Use in the Six Selected Climate Locations.....	91
Figure 34 Peak Winter Day Hourly End-use Thermal Energy Use in the Six Selected Climate Locations.....	92
Figure 35 Base-case Peak Load Components in the Six Selected Climate Locations.....	94
Figure 36 Base-case Peak Heating Load Components in the Six Selected Climate Locations.....	95
Figure 37 Base-case Peak Cooling Load Components in the Six Selected Climate Locations.....	96
Figure 38 Impact of the Building and Window Configuration on the Monthly Peak Heating and Cooling Energy Use of the Proposed Design in the Six Selected Climate Locations.....	101
Figure 39 Impact of the Building Aspect Ratio and Overhang Depth on the Monthly Peak Heating and Cooling Energy Use of the Proposed Design in the Six Selected Climate Locations.....	102
Figure 40 Peak Load Components of the Base-case House and Proposed Design in the Six Selected Locations.....	106

	Page
Figure 41	Peak Heating Load Components of the Proposed Design for the Six Selected Climate Locations ..... 107
Figure 42	Peak Cooling Load Components of the Proposed Design for the Six Selected Climate Locations ..... 108
Figure 43	Minimized Annual End-use Thermal Energy Use in the Six Selected Climate Locations ..... 109
Figure 44	Minimized Annual End-use Electricity Use in the Six Selected Climate Locations ..... 109
Figure 45	Minimized Monthly End-use Electricity Use in the Six Selected Climate Locations ..... 110
Figure 46	Minimized Monthly End-use Thermal Energy Use in the Six Selected Climate Locations ..... 111
Figure 47	Minimized Peak Summer Day Hourly End-use Electricity Use in the Six Selected Climate Locations ..... 112
Figure 48	Minimized Peak Winter Day Hourly End-use Thermal Energy Use in the Six Selected Climate Locations ..... 113
Figure 49	Test Slope ( $F_R U_L$ ) and Test Intercept ( $F_R \tau \alpha$ ) for: (a) All Solar Thermal Collectors on an x-y Scatter Plot, and (b) Selected Solar Thermal Collectors using Collector Efficiency Curves ..... 116
Figure 50	Incident Angle Modifiers $K_\theta$ for: (a) Flat Plate Collectors, (b) Evacuated Tube Collectors ..... 117
Figure 51	Product of Test Slope and Incident Angle Modifiers $K_\theta$ for: (a) Flat Plate Collectors, (b) Evacuated Tube Collectors ..... 118
Figure 52	Determination of Building UA and $T_{bal}$ for the Six Selected Climate Locations ..... 119
Figure 53	Performance of Flat Plate and Evacuated Tube Collectors in the Six Selected Climate Locations ..... 122
Figure 54	Performance of Mono-crystalline and Thin-film PV Arrays in the Six Selected Climate Locations ..... 125
Figure 55	Electricity Output from Mono-crystalline and Thin-film PV Arrays at Varying Tilts in the Six Selected Climate Locations ..... 126
Figure 56	Wind Turbine Power Curves ..... 127
Figure 57	Twelve-year Wind Speed Distribution and Turbine Power Output at the NOAA Weather Station in the Six Selected Climate Locations ..... 129
Figure 58	Critical Year Wind Speed Distribution and Turbine Power Output in a Suburban Terrain at the Tower Height in the Six Selected Climate Locations ..... 130

	Page
Figure 59	Rainfall Characteristics in the Six Selected Climate Locations ..... 135
Figure 60	Rainfall Harvesting Potential in the Six Selected Climate Locations Indicated by: (a) Rainfall Intensity per Unit Catchment Area, (b) First-flush Volume per Unit Catchment Area, (c) Catchment Area Requirement per Unit Daily Water Demand, and (d) Rainwater Storage Requirement per Unit Daily Water Demand..... 136
Figure 61	Sizing of the Solar Thermal System in the Six Selected Climate Locations..... 138
Figure 62	Monthly Wind Turbine Electricity Output versus Monthly Electricity Needs in the Six Selected Climate Locations ..... 139
Figure 63	Sizing of the Photovoltaic and Wind Power Systems in the Six Selected Climate Locations ..... 140
Figure 64	Determination of the Electricity Storage Requirements for NO-SUN days in the Six Selected Climate Locations ..... 142
Figure 65	Determination of the Electricity Storage Requirement for EXTRA SUN Days in the Six Selected Climate Locations ..... 143
Figure 66	Procedure for an Integrated Analysis of Off-grid, Off-pipe Homes ..... 159
Figure 67	Schematic Design of the Proposed Off-grid, Off-pipe Residence ..... 160

## LIST OF TABLES

		Page
Table 1	Annual Energy Consumption due to Appliances and Sensible and Latent Heat Gain Fractions.....	50
Table 2	Base-case Indoor Water Use.....	53
Table 3	General Characteristics of the Base-case House.....	54
Table 4	Sources for Monthly and Hourly End-use Energy Use.....	60
Table 5	Climate Characteristics of the Six Selected Locations .....	83
Table 6	Water-efficiency Measures and the Resulting Indoor Water Use Reductions .....	84
Table 7	Climate-specific Characteristics of the Base-case House in the Six Selected Climate Locations.....	86
Table 8	Energy-efficiency Measures for Lighting and Appliances .....	97
Table 9	Measures for Achieving Maximum Energy-efficiency in the Six Selected Locations .....	103
Table 10	Climate Location Specific F-CHART Input Parameters .....	120
Table 11	Collector-specific F-CHART Input Parameters.....	120
Table 12	Common F-CHART Input Parameters (for All Climate Locations and Collector Types).....	121
Table 13	Photovoltaic Panel Specific PV F-CHART Input Parameters .....	124
Table 14	Climate Location Specific PV F-CHART Input Parameters .....	124
Table 15	Wind Turbine Specifications .....	127
Table 16	Wind Turbine Electricity Output .....	131
Table 17	Sizing of the Rainwater Harvesting System .....	145
Table 18	Sizing of the Septic System .....	146

## CHAPTER I INTRODUCTION

### 1.1. Background

Climate change and the depletion of fossil fuels have become major political issues worldwide (IPCC 2007; Fletcher 2007). The root cause of both issues lies in the increasing use of fossil fuels in all sectors (US EIA 2008a). Fossil fuels (i.e., coal, oil, natural gas) are non-renewable resources because they took millions of years to create, yet are being depleted much faster than being formed. Their combustion releases carbon dioxide and other greenhouse gases, which contribute to climate change (US EPA 2006).

One of the potential solutions to these issues is minimizing the use of fossil fuels by adopting energy-efficiency measures and switching to alternative clean energy sources in all sectors (Kutscher 2007; Socolow and Pacala 2006). The building sector has been identified as the largest and fastest growing energy consuming and CO<sub>2</sub> emitting sector in the U.S. (US EIA 2008b,c; Mazria 2003). Therefore, using energy efficiency and renewable energy technologies in buildings can help mitigate climate change and provide a measure of energy security in the U.S. from reduced dependence on the use of fossil fuels purchased from foreign sources.

Currently, there are several approaches aimed at minimizing the use of fossil fuels in buildings and addressing the climate change, which utilize net-zero, carbon-neutral, plus-energy and carbon-negative designations. “Net-zero” is currently the most commonly used approach in the U.S. It is aimed at achieving zero energy (i.e., in the contexts of either source energy use, site energy use, energy cost or energy emissions) on an annual basis by generating electricity on-site using renewable sources and selling excess electricity back to the utility grid to balance purchased energy from non-renewable sources (Torcellini and Crawley 2006; Torcellini et al. 2006). The “carbon-neutral” building, which is a target for greenhouse gas reduction set by Mazria’s “The 2030 Challenge” to be achieved by the year 2030, calls for adopting the “net-zero” approach in the context of annual carbon emissions (Mazria and Kershner 2008). A “plus-energy (or energy-plus)” approach, conceptualized in late 1970s and currently more common in Europe, aims at producing more energy than the building consumes over a pre-defined period, which can then be sold on the utility-grid or used for other purposes such as recharging an electric vehicle (Yde 1996). A “carbon-negative” building approach aims to exceed the “carbon-neutral” goal and offset the carbon debt embodied in the manufacture of construction materials and building construction process. It combines energy-efficiency and renewable energy measures with a modest form of carbon capture and storage strategy (i.e., the use of construction materials, which act as carbon dioxide sinks due to their high carbon-content or carbon-absorbing properties) (Wald 2008).

Unfortunately, all these approaches require the electricity grid for the electricity storage and back up. In addition, the balancing equation often involves more than one fuel types, which have different costs per unit and site-to-source conversion. Therefore, these approaches can have different implications and can favor the selection of different strategies depending on the context of energy balance. Also, any single approach may not achieve the goals of another approach (Torcellini et al. 2006). Furthermore, the energy used for providing potable water (which includes municipal water supply) and sewage disposal is usually not considered in an energy balance. By using an approach that is aimed at achieving self-sufficiency for energy, water supply and sewage disposal using only renewable energy and water resources, all the above concerns can be addressed and the non-renewable energy use eliminated for all building operations.

The “off-grid” building design approach utilizes a stand-alone system for electricity generation and storage to achieve the goal of zero energy in terms of site energy use, source energy use as well as energy cost (US DOE 2009c). The term “off-grid” was modified to be “off-grid, off-pipe” to suggest the disconnection from both – utility grid for electricity and utility pipes for natural gas supply (Vliet 2007). However, the “off-pipe” term has more commonly been used to suggest the disconnection from municipal water supply and sewage services (Alter 2007a,b, 2008). Combining these implications, a comprehensive definition of the “off-grid, off-pipe” would imply independence from the utility grid for energy, water supply and sewage disposal. By utilizing only those renewable resources of energy and water that arrive at the site for providing all the energy and water needs of the building and facilitating on-site sewage disposal, this approach can eliminate all non-renewable energy use for all building operations. Thus, an “off-grid, off-pipe” design approach qualifies to be used for designing a completely self-sufficient, stand alone, zero-energy building. In addition, the potential exists in some locations for a “carbon-neutral” or a “carbon-negative” building that produces more energy than it uses during certain seasons and fully-utilizes the excess energy for transportation or other purposes to possibly offset the carbon debt associated with the building materials and construction.

Considering that among all building types, single-family detached residences usually have the maximum design flexibility and access to solar radiation and wind, they can be considered as potential candidates to depend solely on on-site renewable resources. In the past, an off-grid, off-pipe design approach has been considered for houses in locations with inefficient or no utility-grid services (such as rural areas and remote locations) (Rosen 2007). However, this design approach also has a potential in new suburban development, where the housing lot can accommodate systems for the collection and storage of renewable energy and rainwater, and the treatment and disposal of sewage from the residence.

Therefore, this study seeks to eliminate the use for all non-renewable sources of energy and the need for municipal water supply and waste water services in single-family detached residences by using an off-grid, off-pipe building design approach and utilizing only on-site harvestable renewable resources of energy and water.



## 1.2. Theoretical Framework

According to Chen et al. (2009), the theoretical framework for an “autonomous house” involves three overlapping domains, which include: sustainable environment, architectural design and energy applications. Using this model in context with this study, the key essentials for the off-grid, off-pipe design approach are shown in Figure 1, which include: the three domains of the environment, architectural design and energy systems, supported by the social, political, technological and logistical support systems. It implies that the off-grid, off-pipe design approach requires:

1. A favorable social environment, which can act as a driving force for adopting this approach; a favorable political environment, with policies, codes and regulations supporting this approach; and a favorable climatic environment, which can provide resources for achieving self-sufficiency for energy and water;
2. An architectural design, which can support an independent living from the viewpoint of building form and layout, functional spaces, structural system, and use of building materials and construction methods;
3. Building systems, which are essential for achieving self-sufficiency, and are robust, cost-effective, and easy-to-install, maintain and operate.

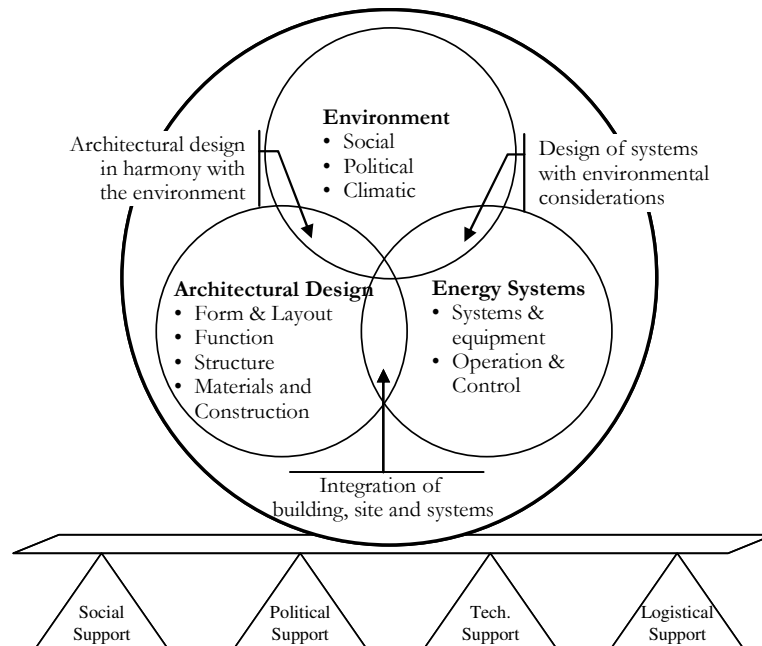


Figure 1 Theoretical Framework (modified from Chen et al. 2009)

Turning to the interconnections among the three domains, the key essentials of an off-grid, off-pipe house would include:

1. A harmony between the architectural design and its environment – social, political and climatic, such that the architectural design of the house fulfils the aspirations of the occupants, meets the building codes and regulations, and at the same time, is responsive to the climate of its location;
2. The selection and sizing of building systems in accordance with the environment, such that they are socially acceptable from the viewpoint of cost-effectiveness, operation and maintenance; meet the building codes and regulations; and can harvest on-site climate resources as much as possible; and
3. An integration of the building, site and its systems, such that the building design incorporates functional spaces, structural support system, and provisions for installing systems at their optimal performance; and a system design and installation that considers the integrity of the design, livability, and the use of indoor and outdoor spaces.

In addition, several other factors influence the overall feasibility of this approach on a macro scale, which can be categorized under the following four support systems:

1. Technical Support System: This includes the development of new technologies as well as the improvement of conventional technologies related to building materials, systems, and construction methods, which as cost-effective, durable, and easy-to-implement, operate, maintain, and service. Alternatively, an easy-to-approach technical support from the service providers for more sophisticated building systems and components is favorable.
2. Political Support System: This includes carrying out programs to raise public awareness for the benefits of this approach, if deemed valuable; providing financial incentives such as rebates, tax credits, and property value appraisal to encourage public participation; and the development and adoption of building codes, regulations, and standards addressing and crediting this approach. In addition, any subdivision planning and layout should consider: i) the access to on-site renewable resources, and ii) site area requirement for accommodating systems for self-sufficiency.
3. Social Support System: The acceptance of this approach in the society as a whole is influenced by the public perception for: i) financial benefits (initial investment and long-term cost-effectiveness), ii) livability (comfort, health, usability and quality of indoor and outdoor spaces, safety and security), and iii) technical and political support systems, as discussed above.
4. Logistical Support System: With all the above factors favoring this approach, it is essential that all the resources involved in the concept-to-creation process flow (including the human resources, process resources, and natural resources) are well coordinated, and properly managed and allocated.

In view of this framework, it can be inferred that the individual sustenance of such a design depends on the interactions among the building design, its systems and the climatic environment, and the overall feasibility of an off-grid, off-pipe design approach depends on the support systems, which provide

and realize economical and effective solutions for the building design and systems. This study acknowledges the significance of the support systems discussed above. However, the focus of this study is the interactions among the building design, its systems and the climatic environment for an independent sustenance of an off-grid, off-pipe house in different climate contexts.

### **1.3. Purpose and Objectives**

The purpose of this study is to investigate the feasibility of the off-grid, off-pipe building design approach for a typical single-family detached residence in different climate regions across the U.S., using only on-site harvestable renewable resources. This requires:

1. Investigation of measures for reducing the energy use, water use and sewage disposal needs of a house, and technologies for harvesting on-site resources of renewable energy, rainwater and land on a residential scale.
2. Formulation of a comprehensive general procedure for the analysis and design of off-grid, off-pipe home, which could be applied to a variety of scenarios in terms of the building energy and water needs and the availability of renewable resources.

With these as the core objectives, the specific tasks of this study are:

1. To analyze energy and water use of a code-compliant, single-family detached residence in different climates in the U.S. to establish a base case.
2. To use energy and water-efficiency measures to reduce the energy and water use of the residence to a practical minimum.
3. To investigate the potential of on-site renewable resources for supplying all of the energy and water needs of the house in different climate regions across the U.S.
4. To size the renewable energy, rainwater harvesting and sewage systems to provide all the household energy and water needs from on-site resources, and facilitate on-site sewage disposal.

### **1.4. Organization of the Dissertation**

This dissertation is divided into six chapters, which include: i) Introduction, ii) Literature Review, iii) Significance of the Study, iv) Methodology, v) Analysis and Results, and vi) Summary and Conclusions.

Chapter I presents an introduction to this study by providing a background, establishing the need, and stating the purpose and objective of this study.

Chapter II reviews literature related to the objectives of this study, which provide a basis for conducting this study. The topics of the literature reviewed include: the concept and application of off-grid design approach in housing, climate classification approaches, building characteristics; measures for energy and water-efficiency for off-grid application, renewable energy technologies and analysis methods; and tools and methods for energy analysis.

Chapter III discusses the importance of this study, its expected contributions to this area of research, and the scope and limitations of this study.

Chapter IV describes the methodology applied in this study. To begin with, it demonstrates the selection of representative climate locations in the U.S., and establishes the base-case building used in this study. Using the base-case building in the selected climate locations, and the analysis tools and methods selected for this study, it outlines the integrated analysis procedure for the design of off-grid, off-pipe homes.

Chapter V presents the analysis and results for six locations selected across the U.S. For each location, the findings are presented in terms of: the climate and site-specific opportunities and liabilities; the selection of energy and water-efficiency measures, and the resulting reduced energy use, water use and sewage disposal needs; the potential of harvesting on-site renewable resources; and the sizing of renewable energy, rainwater harvesting and sewage disposal systems for achieving self-sufficiency in each location. Thus, this chapter demonstrates the integrated analysis procedure for design of off-grid, off-pipe residences for six U.S. climate locations.

Finally, Chapter VI summarizes this study, discusses the key findings of this study including the limitations, and presents a conclusion. Finally, based on the limitations identified in this study, recommendations for future research are proposed.

## CHAPTER II

### LITERATURE REVIEW

The literature review categories that are most relevant to this dissertation are: i) the concept and application of an off-grid design approach in housing, ii) climate classification approaches, iii) residential building characteristics, v) energy and water-efficiency measures for off-grid applications, v) renewable energy technologies and analysis methods, vi) climate maps and weather data sources, and vi) analysis tools and techniques for an integrated design.

The sources of literature that were reviewed include: research journals and publications (ASHRAE Transactions, Building and Environment, Building Services Engineering Research and Technology, Development in Water Science, Energy, Energy and Buildings, Solar Energy, Solar Energy Engineering, Environmental Management, Urban Water, Water Science and Technology, and Water Research); conference proceedings (ACEEE, IBPSA, SimBuild, Hot and Humid Symposium, ICEBO and IEEE); ASHRAE standards and handbooks (ASHRAE 2004, 2005, 2007, 2008); building energy codes (ICC 1999, 2001, 2003, 2004, 2006); books about building energy-efficiency and renewable energy technologies (AIA Research Corporation 1978; Duffie and Beckman 2006; Givoni 1998; Gould and Nissen-Petersen 1999; Hastings and Wall 2007a,b; Lechner 2001; Pahl 2007; Rosen 2007; Stein and Reynolds 2000; Vale and Vale 1975, 2000; Vickers 2001); publications by: the Lawrence Berkeley National Laboratory (Aresteh et al. 2006; Huang et al. 1999; Lutz 2005; Winkelmann et al. 1993), the Los Alamos National Laboratory (Balcomb et al. 1980; Jones et al. 1982), the Energy Systems Laboratory (Haberl and Cho 2004 a,b,c), the Department of Energy (NREL 2003, 2005; US DOE 1999, 2000, 2006, 2007, 2008a,b,c, 2009 a,b,c; US EIA 1994, 2008a,b,c, 2009), the American Solar Energy Society (Kutscher 2007), the American Wind Energy Association (AWEA 2009), and the American Water Works Association (Mayer and DeOreo 1999); and articles from the Home Energy magazine, Mother Earth News, Home Power magazine, Solar Today, Renewable Energy, Scientific American, and TreeHugger. The findings of the literature review are discussed in the following sections.

#### **2.1. Off-grid<sup>1</sup> House: the Concept and Application**

##### **2.1.1. *Introduction***

The term “off-grid” refers to a self-sufficient way of living that relies solely on on-site harvestable renewable resources of energy, water and land rather than the traditional public utility “grid” (i.e., utility services, in general) for electricity, natural gas, water supply or sewage services. An off-grid

---

<sup>1</sup>The term “off-grid” in this section is used instead of “off-grid, off-pipe” to ensure consistency with the literature reviewed. Other terms found in the literature include: “autonomous”, “self-sufficient” and “stand-alone”. All these terms in this section imply independence from the utility services and reliance on the on-site harvestable renewable resources for energy, water supply, and sewage disposal, at a minimum.

house is therefore autonomous, i.e., it is designed to operate independently of any other resources except those in its immediate environment, such as the sun, wind, hydro and on-site harvested vegetation to provide energy for the house, rain to provide water, and soil and vegetation to process its wastes (Vale and Vale 1975).

### 2.1.2. *Pioneering Off-grid Efforts*

There have been a number of notable efforts to design, build and operate self-sufficient houses in the past that demonstrated several approaches to address the different objectives. The following are some of the examples, which include: Dymaxion houses (Baldwin 1996), the Autarkic House (Vale and Vale 2000, Fowles 2004, Webb 2005), Bioshelters (Barnhart 2007), Earthships (Reynolds 1991), the Biosphere II (Anker 2005), and the U.S. Solar Decathlon (US DOE 2009a). Although, most of these examples were implemented as prototypes and operated for a limited period, yet they demonstrated state-of-the-art technologies and concepts, which have proved instrumental for the future projects in several ways.

#### 2.1.2.1. *Dymaxion Houses by Buckminster Fuller*

Some of the earliest published efforts to design a self-sufficient house were the Dymaxion Houses –designed by Buckminster Fuller between 1927 and 1950. Aiming for resource efficiency, space efficiency, and adaptability for universal application, these houses were designed: i) as compact, cylindrical/ hexagonal-shaped, lightweight, self-sufficient units; ii) with a flexible interior space achieved by moveable partition walls housing storage spaces, iii) to be mass-produced, affordable and easily transportable. The design of these houses was influenced by a tensile structural system (with most of its components suspended from the top through cables) as opposed to the conventional system that depends on gravity and friction for structural strength. The features demonstrating autonomy included: natural heating and cooling means, a diesel generator for power, and provisions for sewage composting and rainwater collection. These houses demonstrated examples of water conserving systems such as waterless bathrooms, a "fog gun" shower, waterless packaging toilets, and were designed to implement future technology such as a built-in wind turbine. The proposed designs were not publicly accepted due to limited resources and higher material costs at that time (except their deployment as housing shelters during the World War II). However, the concept paved the way for several design approaches aiming for self-sufficiency (Baldwin 1996).

#### 2.1.2.2. *The Autarkic House by Alexander Pike*

In view of the planning implications of self-sufficient homes, this concept of “the autonomous house” was first and formally proposed in 1972 at the United Nations Conference on the Environment in Stockholm by Alexander Pike, who coined this term in the 1960’s. The aim was to have complete self-sufficiency with a fully-integrated service system for houses, which could reduce dependence on the utility services and allow outlying and marginal lands to be utilized (Vale and Vale 2000, Fowles 2004). With

this motive, the Autarkic House project examined the potential of self-sufficiency in a house by building a scale model at the Martin Centre at the University of Cambridge. This scale model demonstrated measures for energy-efficiency, recycling of resources, elimination of energy waste, and provisions for self-sufficiency, such as a conservatory with moveable shutters for passive solar energy collection, underground thermal storage for winter heating, roof-mounted wind turbine for electricity generation, underground water storage and other provisions for rainwater harvesting, and sewage digester for producing methane for cooking. Unfortunately, due to limited funding resources, further research on the proposed systems and building a prototype house could not be accomplished. However, the concept was widely published and has proved influential (Stansbury and Flattau 1975; Webb 2005).

#### *2.1.2.3. Bioshelters by the New Alchemy Institute*

With a broader objective of creating ecologically-driven human support system, the New Alchemy Institute designed several prototypes and conceptual models of “Bioshelters” beginning in the 1970s. These bioshelters utilize renewable energy, agriculture, aquaculture, housing and landscapes to provide food, water, and shelter. They were designed as closed ecosystems of soil life, insect life, aquatic life and terrestrial plants, enclosed in greenhouses to create a year-round self-regenerating growing environment. In addition, they were to have provisions for natural space heating and cooling, rainwater harvesting, waste disposal, and wind-based water pumping and electricity systems. Several Bioshelters have been built as prototypes with a range of building shapes, layout and materials. The common design features include: a greenhouse with large solar aperture, passive thermal storage due to massive interior walls, rock bed and/or water ponds, and vents for a better control of indoor thermal environment. These designs evolved over the years to incorporate improved glazing, active solar systems and photovoltaic systems (Barnhart 2007).

#### *2.1.2.4. Earthship Bioteecture by Mike Reynolds*

Concurrently, Mike Reynolds – an architect in New Mexico, founded “Earthship Bioteecture” in 1970s, to develop sustainable, independent, living communities, which utilize indigenous materials and construction techniques for building economically-feasible, self-powered, off-grid, off-pipe homes, called “Earthships”. The earliest such community was built in Taos, NM, which became a legal subdivision in 1998. Earthships, in general, incorporate passive heating and cooling strategies such as high thermal mass, shading, sunspaces, and natural ventilation; wind and solar electricity generation systems; and provisions for rainwater harvesting and waste treatment for individual sustenance, which together influence their form and layout. A typical Earthship is a U-shape packaged single unit, an assembly of individual U-shape modules, or custom designed units, with large solar aperture and three sides embedded in the earth. The early designs of Earthships utilized rammed earth and reused materials from discarded sources such as waste tires and aluminum cans. The more recent designs, built across the U.S. and in many European

countries, also incorporate insulated walls, which have been found to be more viable in selected climatic contexts (Reynolds 1991). Although, the individual stand-alone Earthship provides individual sustenance, the Earthship communities with small clusters of such units have been described as a more affordable solution addressing to the current economic crisis, achieving higher efficiency through shared systems (such as parking area, roads, collection area for garbage and recyclable materials, community wells for fire and emergency situations, etc.), and addressing the social need for people to interact and help sustain each other. In addition, the barriers of existing living concepts, codes and regulations, faced by such development in different parts of the world, are easier to overcome on a community scale (Earthship Bioteecture 2009).

#### *2.1.2.5. Biosphere II by the Space Biosphere Ventures*

One of the most ambitious projects aiming for self-sufficiency at a very different scale was Biosphere II, which aimed to replicate earth's ecosystem within a man-made enclosed structure. Biosphere II was designed by Space Biosphere Ventures between 1987 and 1991 in Oracle, AZ, with the objective of understanding the interactions within the earth's ecosystem and exploring the possibility of its use for space colonization. Its structure enclosed five areas of natural biomes, an agricultural area, a human habitat and the underground technical infrastructure. The provisions for self-sufficiency included: sustainable and non-polluting agriculture system and chemical-free waste recycling system. Although, it utilized passive solar energy for sustaining the ecosystem, the electricity supply was derived from natural gas. It was inhabited by a crew of eight people for two years (i.e., from 1991 to 1993), during which it underwent many unforeseen operational and management issues. This demonstrated the complexity and vulnerability of small artificial ecosystems (Anker 2005).

#### *2.1.2.6. Solar-powered Houses for the U.S. Solar Decathlon Competition*

Since 2002, the U.S. Solar Decathlon – a competition among college and university students to design, build, and operate independent solar-powered house – has provided the opportunity to demonstrate different approaches for integrating state-of-the art energy-efficiency and renewable energy technologies for building and system design for different climates. The competition criteria includes demonstrating self-sufficiency for energy (and not necessarily for water supply and sewage disposal) by performing daily household activities, maintaining comfort conditions and driving an electric car using solar energy only. The 2002, 2005 and 2007 Solar Decathlon competition required designing a stand-alone, solar-powered house. On the other had, the 2009 Solar Decathlon competition is aimed at designing grid-tied, net-metered, zero energy homes. More than 50 entries showcasing off-grid houses have participated in the competitions held in 2002, 2005 and 2007. A discussion of some of these houses in terms of the strategies and technologies used for the building envelope and systems as well as the design and analysis procedure is included in the corresponding sections in this chapter (US DOE 2009a).



### 2.1.3. *Reasons and Concerns for Going Off-grid*

There are several reasons for adopting self-sufficient living, which include: remote location, high cost of bringing in utility lines, increased energy security, sustainability, environmental concerns, land use policies and personal choices (Rosen 2007). The main concerns for going off-grid include: the possibility of draining surplus energy and water when storage is full, and the need for back-up sources, which most of the time has been from non-renewable sources. Therefore, for grid-connected locations, an off-grid home is an attractive choice only when the local utility does not allow selling surplus electricity. Despite of these concerns, off-grid homes are good examples of the responsibilities and challenges of gradually making the grid more and more sustainable (Woofenden 2007a).

### 2.1.4. *Key Considerations for Off-grid Houses*

Achieving complete self-sufficiency with “only” on-site renewable resources is an even greater challenge for designing an off-grid house. Firstly, the building design and the site area should be able to accommodate the collection and storage systems for the on-site harvesting of renewable resources. Secondly, for the sizing of the systems, the energy and water collected on-site should exceed daily loads, and provide storage for cumulative energy and water needs for periods when renewable resources are unavailable. This requires the use of energy and water-efficiency measures for minimizing the energy and water needs, while at the same time, sizing the renewable systems for maximizing the collection and storage of on-site renewable resources. Finally, provisions for back-up are essential for periods when daily/seasonal resources to recharge the energy and water storage are unavailable.

## 2.2. **Climatic Classification Approaches**

Detached single-family residences are usually “skin-dominated” buildings, where space heating and cooling loads are determined primarily by the heat gain and loss through the building envelope, and therefore, are largely driven by the local climate conditions. In addition, the climate parameters indicate the availability of solar radiation, wind and rainwater as natural resources. Therefore, an understanding of the climate characteristics across the U.S. is important to this study to: i) identify representative locations based on heating and cooling energy use, and availability of renewable resources, ii) determine climate-specific measures for energy-efficiency, and iii) sizing solar, wind and rainwater harvesting systems.

To begin with the selection of representative locations, several approaches for the climate zoning of the U.S. were reviewed<sup>2</sup>, which include those proposed by: ASHRAE (2005), Lstiburek (2000), AIA Research Corporation (1978), Lechner (2001), International Code Council (ICC 1999) and Briggs et al. (2003).

---

<sup>2</sup> A more detailed review of some of the climate classification approaches discussed here is presented in Briggs et al. (2003).

Most of the climate classification schemes are based on the Koppen climate classification, in which the climate classification boundaries were determined based on the native vegetation distribution that combines average annual and monthly temperatures and precipitation, and the seasonality of precipitation (Peel et al. 2007). The traditional climate classification of the U.S. for energy-efficient building design developed by the U.S. Department of Energy (DOE) in the early 1980s used a simple five-region map similar to the Koppen classification, which featured separate heating and cooling dominant climates with humid and dry zones. Similar climate zoning was found in the publications by ASHRAE (ASHRAE 2005), the Building Science Corporation (Lstiburek 2000), and the U.S. Department of Energy's Building America program (US DOE 2007), which were based on the Herbertson's thermal regions (Herbertson 1905) - a modified Koppen's classification. These classifications were adopted for developing climate-specific codes, standards and recommendations for the building construction in order to address the thermal and moisture related issues in the building assemblies in different climates.

Another climate classification approach, based on the climate-specific heating and cooling needs of homes in the U.S., was developed by the AIA Research Corporation (1978). It identified 16 climate regions in the U.S. based on how the four climate elements: sun, wind, temperature and humidity act as liabilities that drive the heating and cooling needs, or act as assets for natural heating and cooling of homes. This subdivision system was also used in Lechner (2001), which shows 17 climate regions, including a coastal area of California as a separate climate region.

The climate zoning used in building codes and standards are based on degree-days that focus primarily on controlling the envelope conductance. The International Code Council (ICC) identified 33 climate zones for the 2000 International Energy Conservation Code (IECC) (ICC 1999), which include nineteen 500 degree-day bands (zones) of HDD65°F and three subdivisions of selected zones in order to address different cooling-related requirements (Figure 2). However, the residential code requirements do not differentiate between the cooling-related subdivisions.

This classification scheme was adopted in the 2001 Supplement to the 2000 IECC (ICC 2001) and the 2003 IECC (ICC 2003). The 2004 Supplement of the IECC (ICC 2004) classification scheme, which was continued in the 2006 IECC (ICC 2006) and the 2009 IECC (ICC 2009), has only 17 climate zones. The 17 zone classification scheme by Briggs et al. (2003) was developed using the cluster approach for temperature, radiation, wind and humidity, which identified eight 1,800 degree-day zones and three subdivisions for moist, dry and marine climates (Figure 3). The climate zones, including the subdivisions, are defined by heating degree-day, cooling degree-day and precipitation that are correlated with humidity, radiation, cloud cover and wind. The climate boundaries of groups of certain climate zones of the 2000 IECC (ICC 1999) combined with the subdivisions for humidity conditions are similar to the scheme developed by Briggs et al. (2003). Further grouping of certain climate zones results in the boundaries identical to the climate classification scheme by US DOE (2007).

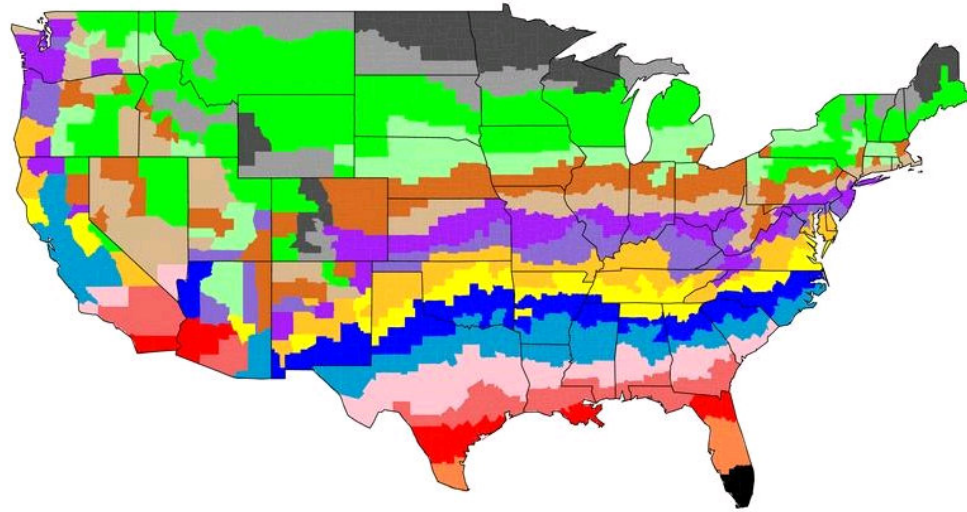


Figure 2 Climate Classification for the 2000/2001 IECC<sup>3</sup>

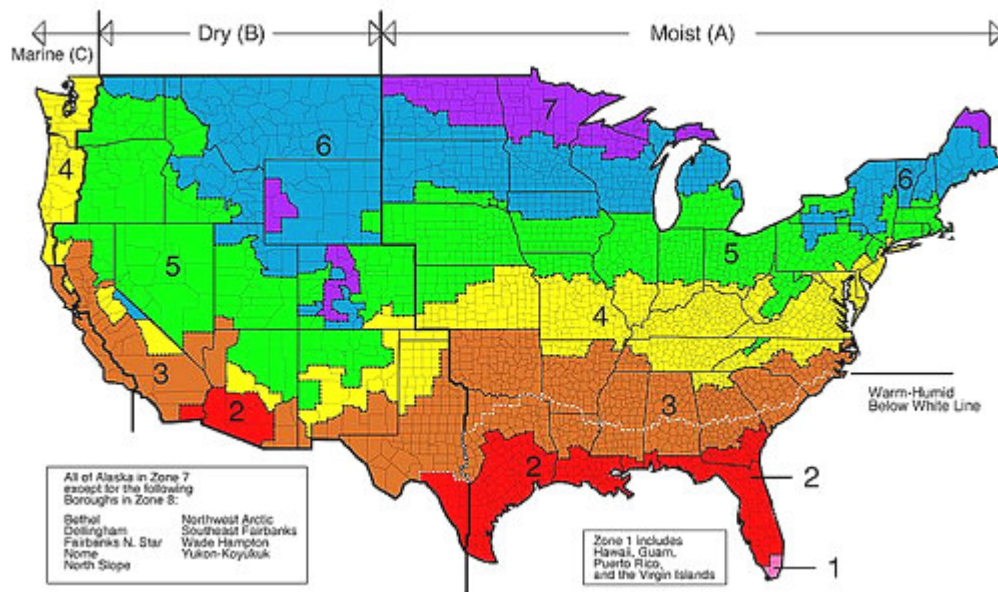


Figure 3 Climate Classification for the 2000 by Briggs et al. (2003)<sup>3</sup>

<sup>3</sup> Source: PNL (2009)

To investigate the correspondence between the two climate classification approaches discussed above (i.e., the one based on the building's heating and cooling requirements and humidity conditions, and the other one based on the assessment of the climate elements for thermal comfort by passive means in homes), an overlay of the climate maps by US DOE (2007) (indicated as five colored zones) and Lechner (2001) (numbered 1 through 17) is shown in Figure 4. It shows that only some the climate zones of Lechner (2001), when grouped, matched with those of US DOE (2007) to certain extent. Furthermore, the climate zone boundaries of the two maps did not match, as several climate zones of Lechner (2001) extended up to three climate zones of US DOE (2007).

This indicates that the locations that are different from one aspect may represent very similar scenario in another aspect. Therefore, for this study, a preliminary analysis of the energy use and the availability of renewable resources for several locations is necessary, in order to select representative climate locations. Furthermore, the conclusions drawn from this study for one climate location may not be applicable to the corresponding entire climate zone classified using only one approach.

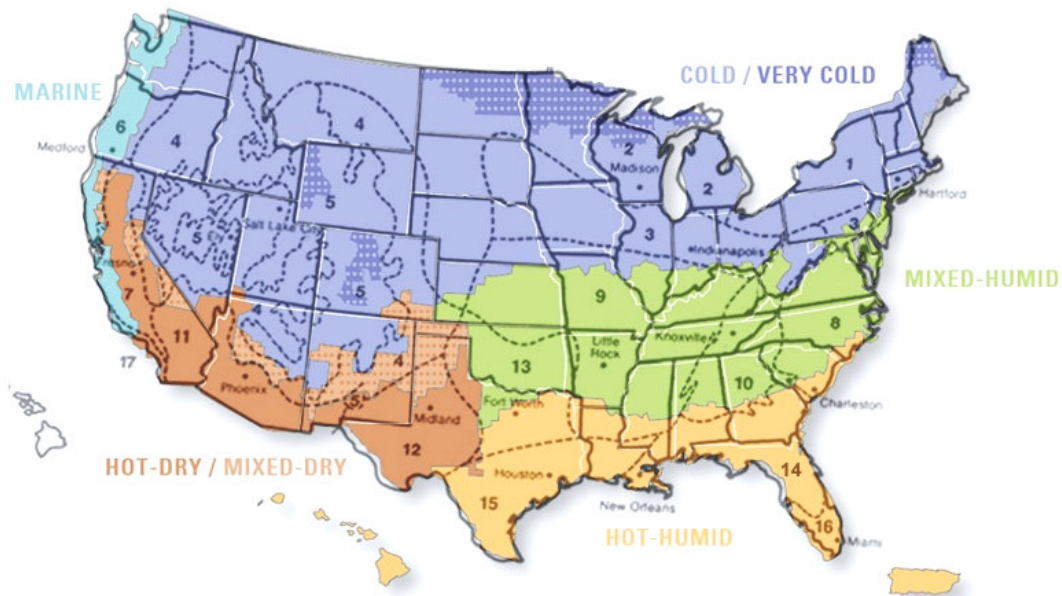


Figure 4 An Overlay of Climate Classification Maps by the U.S. DOE Building America Program (US DOE 2007)<sup>4</sup> and Lechner (2001)<sup>5</sup>

<sup>4</sup> Source: US DOE (2007)

<sup>5</sup> Copyright © 2001 by John Wiley & Sons, Inc. (Reprinted with Permission)

### 2.3. Building Characteristics

This study requires defining a base case with typical building characteristics in order to determine the residential energy and water use in each climate and to evaluate strategies for energy-efficiency and renewable energy. Several sources from the previous literature were reviewed, which provided information about building characteristics. The most relevant resources include: the housing survey data by the U. S. Census Bureau (2009), data contained in the International Energy Conservation Codes (ICC 1999, 2001, 2003, 2004, 2006), by the U.S. DOE's Building America publication (Hendron 2008), and data from ASHRAE (2007).

The general characteristics of a house such as lot size, floor area, the number of bedrooms and bathrooms, the construction type and building system types were determined from the national sample survey of new housing construction by the U.S. Census Bureau (2009). Based on the national and regional data for single-family houses completed or sold in 2008, the average house had a 2,534 ft<sup>2</sup> floor area and was built on an 18,433 ft<sup>2</sup> lot size<sup>6</sup>. In addition, the most common characteristics of the surveyed houses include: four bedrooms and three bathrooms, two or more stories<sup>7</sup>, basements<sup>8</sup>, wood frame construction, vinyl siding on the exterior wall<sup>8</sup>, and air conditioners with heat pumps as the primary heating system.

There are several residential energy codes that have been adopted in different states in the U.S., which establish minimum performance requirements for energy-efficient building envelope and systems. The State Energy Code Database (BECF 2008) lists the Residential State Codes and the enforcement status in all states across the U.S. The database indicates that the 2000/2001 IECC and the 2003 IECC (ICC 1999, 2001, 2003) are the most widely used energy codes. However, some states enforce less stringent Model Energy Codes (i.e., MEC, which are older versions of the IECC (US DOE 1999)) or more stringent state-specific codes (such as Title-24 in California (DGS 2007), and 2003 IECC with amendments in Washington and North Carolina). The 2001 IECC and the 2003 IECC are identical in all respects except for the fixed internal gains in the 2001 IECC and variable internal gains in the 2003 IECC. In the 2001 IECC, the three compliance methods include: i) a component performance approach (Chapter 5, 2001 IECC), ii) a prescriptive approach (Chapter 6, 2001 IECC), and iii) a system analysis method (Chapter 4, 2001 IECC) that requires annual energy use simulation and allows renewable energy to be subtracted from total energy consumption.

Finally, user profiles were reviewed from Hendron (2008) and ASHRAE (2007). The Building America benchmark (Hendron 2008) provides a series of user profiles for lighting, appliances and domestic hot water in detached and attached single-family housing. ASHRAE (2007) also provides DHW system size and usage profile for different family structures and lifestyles.

---

<sup>6</sup> The average lot size was larger in the Northeast and smaller in the West.

<sup>7</sup> Less common in the Midwest and the South

<sup>8</sup> Less common in the West and the South

## 2.4. Measures for Energy and Water-efficiency for Off-grid Applications

The literature providing guidelines for climate-responsive, passive design and measures for building energy and water-efficiency were investigated to determine strategies for minimizing residential energy and water use in different climates. Sources surveyed included: Huang et al. (1999), Givoni (1998), ASHRAE (2005), Miller et al. (2002), US DOE (2000), SIPA (2004), VanderWerf et al. (1997) for building envelope measures; Aresteh et al. (2006), Fine and McElroy (1989), Mayfield (2000), Givoni (1998), RMI (1995), Hunn et al. (1990), and Pletzer et al. (1988) for fenestration measures; Hastings and Wall (2007b), Wiehagen and Sikora (2003), the Davis Energy Group (2006), Johnson and Wyatt (1997) and Lutz (2005) for HVAC and DHW systems; Geltz (1993), ACEEE (2007), and Woofenden (2007b) for lighting and appliance measures; and Roaf et al. (2007), Mayer and DeOreo (1999), Vickers (2001), and Dixon et al. (1999) and for water and waste water measures.

### 2.4.1. *Building Envelope*

Residential buildings, especially detached units, are classified as “skin-dominated” buildings, where heating and cooling loads are mainly driven by building envelope characteristics (Huang et al. 1999). These characteristics include: building shape, orientation and shading conditions, thermal properties of opaque and glazed materials (i.e., conductance, thermal mass, reflectance, transmittance and emissivity) and type of construction. The building shape determines the surface area, relative to the floor area or the volume, through which heat transfer occurs. It also affects a building’s potential for daylighting and natural ventilation (Givoni 1998). The building orientation and window shading conditions determine the solar and wind exposure of glazed and opaque elements of the building’s envelope. Properly installed thermal insulation retards heat loss/gain by reducing conduction, infiltration and, in some cases, radiative heat transfer. Thermal mass and phase-change materials, if strategically incorporated, can shift peak heating/cooling load conditions and stabilize indoor temperatures, resulting in reduced HVAC system size. Reflectance and emissivity of opaque exterior surfaces impact the surface temperature and heat transfer through the envelope, and in some cases, the surrounding temperatures. High reflectance and high infrared emittance surfaces reduce cooling loads, whereas selective surfaces with high absorptance and low infrared emittance reduce heating loads (Miller et al. 2002). An airtight construction with reduced leaks, gaps, cracks and joints in the envelope reduces heat loss/gain due to air-infiltration (Lechner 2001, ASHRAE 2005).

In general, compact designs elongated along an east-west axis, high R-value insulation, airtight construction, and protected building entrances (i.e., vestibules) are desired for climates where heating or cooling loads are extreme. However, the extent to which this is used depends on the climate and other building characteristics. Thermal mass is an important element of passive solar design, which requires proper orientation and placement with respect to the solar aperture. The benefits of thermal mass used in

the building envelope depend on the layering of the wall assembly and the climate conditions. Thermal mass is more effective with exterior insulation when an HVAC system operates continuously, and conversely, with interior insulation when an HVAC system operates for short periods or when thermostat setup/setback is used. Optimizing thermal mass in relation to insulation placement is therefore an important criterion for off-grid construction (ASHRAE 2005).

Although, light-weight wood frame construction with 2x4 studs placed 16 inches on center is the most common construction for residences in the U.S., other construction techniques such as advanced framing (also known as optimum value engineering (OVE)), structural insulated panels (SIPs) and insulated concrete forms (ICFs) can provide improved insulation and airtight construction when installed properly. Advanced framing or OVE consists of a wall assembly with 2x4 studs (for one-story) or 2x6 studs placed 24 inches on center that allows the floor, walls and roof framing members vertically in line with one another allowing the loads to be transferred directly downward. This allows single lumber headers and top plates where appropriate, which results in more space for insulation and a higher whole-wall R-value (US DOE 2000).

SIPs are high-performance panels for walls, floors and roofs that are typically made using expanded polystyrene (EPS) or polyisocyanurate rigid foam insulation sandwiched between two structural skins of oriented strand board (OSB). Having no thermal breaks or penetrations in the panels, SIPs have higher R-values (R-15 to R-50, depending of the EPS core thickness) and are 85% more airtight than wood-frame construction (SIPA 2004). ICFs are foam insulation forms for poured concrete walls that stay in place as a permanent part of the wall assembly. These forms provide a near-continuous insulation and an improved sound barrier, and can provide a backing for interior and exterior wall finishes. ICF walls have high R-values (R-17 to R-26, compared to R-9 to R-15 for wood-frame walls), high thermal mass, and are 50% more airtight than wood-frame walls (VanderWerf et al. 1997). SIP and ICF construction techniques can result in a reduction in the heating or cooling loads when compared to conventional wood-frame walls and allow smaller HVAC systems.

#### 2.4.2. *Fenestration System*

Windows in the U.S. account for about 30% of building heating and cooling energy use, and have an even larger impact on peak energy demand and occupant comfort. Therefore, a high performance fenestration system design should aim at minimizing winter-time heat loss, reducing summer-time solar gain, while at the same time providing daylighting benefits, natural ventilation when needed, and winter-time solar heat gain (Aresteh et al. 2006).

Potential design strategies and available technologies for high performance fenestration design include: i) window shape and size with respect to the depth of the interior space, and location on the wall with respect to the perpendicular interior surfaces, for the daylighting benefits; ii) properly sized and strategically aligned operable windows relative to the prevailing wind direction or the stack effect for an

effective natural ventilation in selected climates; iii) shading devices such as overhangs, vertical fins, decks and porches, awnings, light shelves, screens, blinds and rolling shutters (Mayfield 2000), and automated shading systems (Givoni 1998); iv) high-efficiency glazing options, such as insulated glazings (i.e., multiple layers of glazings with aerogel, vacuum, or low conductance gas-fill between the panes) with low-e and spectrally-selective coatings, and dynamic glazings (i.e., electrochromic, photochromic, or thermochromic with switchable properties) (Aresteh et al. 2006, Fine and McElroy 1989); v) insulated frames and spacers, such as aluminum with thermal break, wood, fiberglass or vinyl; and vi) good edge seals that provide airtightness and minimize infiltration. By combining the design strategies with appropriate glazing type, shading devices, frame and spacer materials, and good quality construction, the benefits of daylighting and natural ventilation can be achieved without significant energy penalty that could otherwise result from large window openings with operable shutters.

The Rocky Mountain Institute (RMI 1995) has quantified the energy savings from different shading options in different climates. For cold-weather, the RMI reported improvements in heat loss reductions of 25-40% from installing plastic barriers on single-pane windows, up to 50% by storm windows and up to 40% increase in solar gain by providing clear solar access on south windows. For warm-weather, it reported a solar heat gain reduction of 40-50% from window shades and blinds, and 60-80% from insect screens or bamboo shades. Two simulation studies for analyzing the impact of interior and exterior shading devices in residences reported annual cooling energy savings and summer peak electric demand reductions of up to over 30% and 20%, respectively, in Minnesota (Hunn et al. 1990) and up to 32% and 22%, respectively, in Austin, TX (Pletzer et al. 1988).

#### 2.4.3. *Lighting and Appliances*

Lighting energy saving measures include: using efficient lamps (i.e., compact fluorescent lamps, LEDs and exterior HID lighting) and fixtures, task-oriented lighting, small-scale fixtures, multiple switching schemes, occupancy sensors, daylighting with glare control, and dimmers and timers (Geltz 1993).

Among household appliances, the refrigerator, clothes washer, dryer, dishwasher, cooking equipment and home electronics constitute the major loads in a residence. Together they accounted for 25% of the U.S. residential energy use in 2005 (US DOE 2009b). For off-grid applications, the most energy-efficient appliances that meet the needs of the resident are of paramount importance for reducing appliance energy use and limiting back-up generator use during long periods of cloudy or windless weather. Also, to avoid losses due to conversion of DC electricity to AC electricity, using DC appliances such as a DC refrigerator fed directly from the DC batteries or solar PV array is preferable. However, this would increase the cost of electric wiring. Home electronics with low standby power, convection ovens, microwave ovens, induction cooktops, dishwashers and horizontal axis clothes washer with variable wash



cycles and hot water feed from solar thermal DHW system, electric clothes dryer with advanced sensors and timers are recommended (ACEEE 2007, Woofenden 2007b).

#### 2.4.4. *Mechanical Systems*

Heating, ventilating and air-conditioning (HVAC) systems appropriate for off-grid, off-pipe application include those that utilize solar thermal energy for heating and cooling. In addition, since solar energy is available during the day, the use of passive thermal storage (such as thermal mass or phase change materials) or actively-charged thermal storage (hot water and cold water/ice) is preferred over the use of electricity storage to provide space heating or cooling during the night. Furthermore, converting the surplus electricity from the PV system during the day into thermal energy using thermal storage can further reduce the electricity storage requirements for space heating/cooling during the night. The HVAC systems, which can utilize solar heated water include: radiant heating system, water-to-water heat pump system<sup>9</sup>, absorption chillers<sup>10</sup> for cooling, and desiccant systems<sup>11</sup> for cooling and dehumidification, which have been used in a number of off-grid homes including several Solar Decathlon homes. Unfortunately, although such systems offer higher utilization of the solar thermal system, the currently available systems of the size needed for residential application can be less efficient than larger commercial versions. Since solar absorption cooling system requires high water temperature, the solar thermal energy collected is not useful below a critical level. Other priorities for the selection, design, and operation of HVAC systems include: use of high-efficiency equipment; improving equipment performance (using appropriate equipment size); minimizing losses; avoiding prolonged and low temperature setbacks to ensure smaller peak loads, which allows smaller system sizes; and recovering waste heat (using an exhaust air heat pump, air-to-air heat exchangers and heat recovery units) (Hastings and Wall 2007b).

On the air distribution side, the design priorities for minimizing duct losses include: providing adequate duct insulation, minimizing duct runs, minimizing duct leakage, or installing ducts in the conditioned space. Carefully designing diffusers could eliminate uneven space temperatures in the conditioned space and avoid delayed response for ducts embedded in the structure. These measures must then be combined with efficient operation and control to achieve the comfort conditions.

---

<sup>9</sup> This system was used in the 2007 University of Colorado Solar Decathlon team, which also utilized thermal storage tanks. During the winter, it provides domestic hot water and charges hot water storage tank during the day, and the stored hot water provides hot water and space heating at night. During summer, the high-efficiency heat pump (which operates more effectively at lower ambient temperatures, i.e. at night during the summer) exploits waste heat from the house to make encapsulated ice during the night, which can provide space cooling during the day.

<sup>10</sup> This system was used by 2007 Santa Clara and Cincinnati Solar Decathlon teams in different configurations. Both teams used single-effect LiBr absorption chillers (which uses LiBr as the absorbent and water as the refrigerant), with the absorption cycle energized by high-temperature solar heated water. However, the cooling of the condenser water was accomplished through a cooling tower in the Santa Clara team's house, and by an in-built rotation technique in the Cincinnati team's house.

<sup>11</sup> This system was used in various configurations by the Solar Decathlon teams, such as: a liquid desiccant/vapor compression cooling system (by 2002 Puerto Rico team); a desiccant wheel energy recovery ventilator (by Cornell and Rhode Island teams in 2005), and a liquid desiccant water fall system (by 2007 Maryland team).

For domestic hot water (DHW) systems, the type and efficiency of system, and the plumbing layout impact the energy losses due to leaks, as well as conduction to the concrete slab or soil, and intentional wasting of the cold/warm water before the arrival of hot water. Lutz (2005) showed 20% hot water and associated energy savings from an efficient plumbing layout including the location of hot water fixtures and appliances. Wiehagen and Sikora (2003) compared different configuration of DHW system comprised of a demand vs. storage tank-type water heater with a copper trunk and branch (tree) vs. cross-linked polyethylene (PEX) parallel piping system in high and low hot water use homes, and showed that a system with a demand water heater and insulated PEX type distribution system was the most efficient. Storage tank-type systems with copper tree-type distribution system were the least efficient. The energy savings were higher in the low-use homes because of higher standby and distribution losses with tank systems. In high-use homes requiring high flow rates and simultaneous use, distributed (point-of-use) systems showed better performance than a single demand water heater in terms of sufficiently heating the water. A similar study by Davis Energy Group (2006) reported 30-40% hot water distribution savings, shorter waiting time and less water wasted at the end use point from a PEX parallel piping system compared to a standard copper trunk and branch installations. In addition, by using waste heat recovery systems such as drain-water heat recovery devices for DHW system (Johnson and Wyatt 1997), additional savings can be achieved.

Depending on the availability of the resources, the renewable energy based back-up space heating system can be a ground source, air-source, or water source heat pump system with a supplementary electric resistance heater using electricity from PV, or a biomass system such as a pellet oven. The back-up DHW system can be an electric tankless water heater, a heat pump water heater, or a biomass-fired boiler. In addition to the installation of a properly sized, energy-efficient water heater, switching to energy and water-efficient fixtures and appliances, and adhering to water conserving practices is also important for minimizing DHW consumption (RMI 2004).

#### 2.4.5. *Water-efficiency Measures*

Measures for reducing indoor water use include installing water efficient appliance and fixtures such as efficient toilets and cisterns (i.e., not just reduced flush volume), tap aerators and sprays, low-flow showerheads, optimized bath shape, and optimized water pipe dead-legs. Unfortunately, water use is habit-dependant. Therefore, technical innovations such as taps with automatic water shut-off, dual-flush toilets, flow regulators, automatic leak detectors and automatic tap closure would minimize the waste of water without reducing the standard of performance or require changing habits (Roaf et al. 2007). According to the American Water Works Association Research Foundation (Mayer and DeOreo 1999), the mean per capita indoor water use is 69.3 gallons per day. By using water-efficient fixtures and appliances, the indoor water use can be reduced to 45.3 gallons per capita per day (Vickers 2001).

Further reduction in water use can be obtained by reusing and recycling the water using a greywater system (Dixon et al. 1999). A greywater reuse system can reuse wastewater from the kitchen, showers, faucets, dishwasher and clothes washer for reuse in flushing toilets and irrigation. This can eliminate an additional 9.6 gallons per person per day for toilet flushing. This system includes a greywater filtration and storage system, and requires electricity for repressurization of greywater or pumping the greywater into an overhead tank before reuse. Recycled greywater can be used for non-potable indoor and outdoor water use including clothes washing and car washing. However, the use of recycled greywater for indoor use is subjected to local regulations and public acceptance. Recycling greywater also introduces the need for electricity for disinfection (e.g., for ultraviolet treatment and for certain chemical treatment). The potential concerns from greywater include: risk of pathogenic micro-organisms occurring in greywater impacting human health; corrosion, fouling and microbiological growth in the plumbing system; and the risk of ground water contamination, and potential for blockages in the greywater treatment system. Backflow prevention and accidental cross-connection between potable and greywater systems are also main concerns (Roaf et al. 2007).

Up to 20% of the total hot water use can be saved from using measures avoiding water waste due to improper water distribution planning (Lutz 2005). The Davis Energy Group (2003) reported shorter waiting time and less water wasted at the end-use point from PEX parallel piping systems compared to the standard trunk and branch installations using copper piping, which are often buried in the concrete slab. Finally, outdoor water use for irrigation can be reduced by implementing the principles of xeriscaping.

Reducing water use eventually will result in the reduced need for sewage collection and treatment, which is critical for an off-grid, off-pipe residence that requires on-site sewage treatment system. A typical on-site sewage treatment system consists of a wastewater storage and treatment tank (i.e., a septic tank or an aeration tank), and a soil absorption and filter system for the treated wastewater (i.e., a leaching field). For a more through and fast treatment of sewage, septic tanks can be coupled with other on-site wastewater treatment units such as biofilters or aerobic systems involving artificial forced aeration. However, the aerated system uses electricity to operate the mixing mechanism, requires frequent maintenance, and is more expensive compared to a septic system. In addition, the use of a septic system or an aerated system is subjected to local regulations and building practices (AGWT 2008). With the use of incinerating or composting toilets, a septic system is required for only greywater treatment and therefore, has less potential impact on the environment (Roaf et al. 2007).

## **2.5. Renewable Energy Technologies and Analysis Methods**

The renewable technologies suitable for off-grid homes include: passive solar, active solar, photovoltaic, wind energy, micro-hydroelectric and biomass systems for energy, and rainwater harvesting for water. These systems were investigated in terms of working principles, system types and components, analysis methods, applicability and concerns. A review of analysis methods for the active solar and

photovoltaic systems is presented in Section 2.7.2. The commercially available technologies were identified by reviewing the Mother Earth News, Home Power magazine, Solar Today magazine and the resources provided by the International Solar Energy Society (ISES), the American Solar Energy Society (ASES) and the American Wind Energy Association (AWEA). Procedures for the sizing of the systems reviewed included Balcomb et al. (1980) and Jones et al. (1982) for passive solar systems, Duffie and Beckman (2006) for passive and active solar thermal, Dahl (2008) and the German Energy Society (2008) for photovoltaic systems, Gipe (2004) for wind energy systems, and Gould and Nissen-Petersen (1999) for rainwater harvesting system.

#### 2.5.1. *Passive Solar Systems*

Passive solar systems utilize the form and fabric of the building to collect, store and distribute solar energy by natural means only. The traditional approaches to passive solar systems for heating include: i) direct gain, which requires south-facing glazed openings, thermal mass exposed to the sun inside the space, and moveable insulation for the glazed openings, ii) thermal storage walls, usually masonry walls or containers filled with water or a phase-change material, iii) an attached sun space, separated from the heated space by a thermal storage wall and moveable insulation, iv) a thermal storage roof, which utilizes water-filled containers or a roof pond and movable insulation, and v) a convective loop system, which utilizes a natural thermosiphon to move heat from collector to storage (Balcomb et al. 1980). Passive solar designs for cooling utilize natural ventilation, thermal mass with night ventilation, a thermal storage roof with a movable insulation for night radiation or a Sky-Therm system (Hay and Yellott 1970), thermally driven natural convection and evaporative cooling. Passive solar design can also include strategies for daylighting.

A building's solar performance can be measured by calculating the Solar Saving Fraction (SSF) (i.e., the extent to which a solar design reduces a building's auxiliary heat requirement relative to a "reference" building – one that has, instead of a solar wall, an energy neutral wall that experiences neither solar gain nor heat loss). In addition to sizing the solar aperture for achieving solar gains that can offset heat losses through the building envelop, the amount and distribution of thermal mass necessary to store the solar heat collected during the day is important, especially, in buildings with high SSF (Stein and Reynolds 2000). Balcomb et al. (1980) and Jones et al. (1982) provided rules-of-thumb that can be used to guide the conceptual design of passive solar energy systems. These rules-of-thumb are based on extensive hourly simulations with the PASOLE program (McFarland 1978) developed at the Los Alamos National Laboratory. These provide SSF values that can be achieved for a range of south glazing area with/without night insulation in various locations, and the amount of thermal storage required. In addition, correlations and tables were developed that can be used to determine the characteristics of a passive solar system to achieve desired SSF in a building with known envelope characteristics in a given location.

Another simple analytic method for predicting long-term thermal performance of passively-heated solar houses was proposed by Gordon and Zarmi (1981a,b). This method can be applied to buildings with varying building parameters (e.g., amount of thermal mass, storage absorptance, ratio of glazing to storage mass etc.) with any type of passive heating elements (e.g., direct gain exposure, water wall, massive storage wall, phase change wall etc.). It uses closed-form equations to calculate the solar heating fraction (SHF, the fraction of house heating load supplied by solar energy) as a function of solar load ratio (SLR, the ratio of the insolation transmitted into the house and the house heating load) and the building and climatic parameters. It accounts for the variations in total daily insolation by weighting different values of the SLR by the frequency of their occurrence, and it suited for monthly and annual calculations.

The P-Chart method is another simplified method for passive solar heating system sizing, which determines the cost-optimal passive solar collector area. It is based on the solar load ratio (SLR) passive prediction method developed at Los Alamos Scientific Laboratory. It uses two closed form equations, which calculate: (i) the economically optimum area of a passive solar collector, and (ii) the annual solar fraction for the calculated collector area and a given location. For a direct application, a P-chart nomograph is also available. The P-chart method applies strictly to a standard passive system of the direct gain, masonry storage wall, or water storage wall types. It can be used for residential or commercial buildings. (Arney et al. 1981; Kreider and Kreith 1982).

The potential risks associated with passive solar environments include: overheating in the summer, excessive heat loss in the winter, large temperature swings, temperature stratification, variation in indoor lighting levels and glare, which can cause discomfort and increase dependence on purchased energy consumption (Nutt 1994; Yakubu 1996). The performance of passive solar buildings can be improved by incorporating optimal shading to avoid overheating, and high-efficiency windows with moveable night insulation to avoid winter heat losses, and can be used to block summer heat gain. The key design parameters which influence the performance, cost and comfort are glazing area, number and type of glazings, mass storage volume (wall thickness \* area), night insulation options, shading devices, allowable interior temperature swings, and thermocirculation flow vents (Noll and Wray 1978). With these considerations, building envelope and systems characteristics become more important in energy-efficient designs (Hastings and Wall 2007a). Therefore, these strategies combined with energy-efficient measures for building systems and equipment will be considered for maximizing residential energy savings in the selected location.

### 2.5.2. Active Solar Thermal Systems

Active solar thermal systems for space heating and domestic water heating use solar energy to heat a heat transfer fluid such as air, water, or an anti-freeze solution (directly or through heat pipes). The thermal energy can then be stored as hot water, in a high-density building material, or phase-change

material, and used when needed. The components of an active solar thermal system include solar collectors, thermal storage, heat exchangers, a heat transfer fluid, circulating pumps/fans, controls, piping/ducts, valves and gauges (Ramlow and Nusz 2006).

For combined space heating and water heating applications in residences, flat plate, integral collector-storage (ICS) or evacuated tube collectors can be used. Flat plate collectors can supply hot water or air up to temperatures 200°F, although relative efficiency diminishes rapidly above 160°F and during cold ambient conditions. Flat plate collectors are more efficient than evacuated tube collectors under certain operating conditions, when the temperature difference between the collector inlet temperature and the ambient temperature is less than 70°F (i.e., swimming pools). Evacuated tube collectors have reduced convection and conduction losses, so the tubes can operate at higher temperatures than flat-plate collectors. In addition, in some designs, the cylindrical absorber area, which passively tracks the sun throughout the day, allows evacuated tube collectors to have higher day-long performance. Evacuated tubes are suitable for applications requiring very high temperatures (over 160°F), for very cold climates and also work well for climate locations with overcast conditions (ASHRAE 2008, Ramlow and Nusz 2006).

The sizing of a solar thermal system depends on the available solar energy, collector efficiency, local climate, and domestic water heating loads and space heating requirements. For domestic water heating application, the sizing is determined to meet the daily hot water needs, whereas for a space heating application, the sizing is optimized to meet the nighttime, winter heating loads. A solar thermal system for space heating requires a much larger collector area than a DHW-only system, significant storage volume, and a highly efficient building envelope (NREL 2003).

For best performance, the thermal storage tank should be well insulated. The delivery temperature from the collector, flow rate through the storage tank and position of the inlet and outlet should be determined to take advantage of thermal stratification in the tank. Storage volume should be determined based on an accurate estimation of heating loads and the hot water usage schedule. Oversized storage may result in an unacceptably low storage temperature that would then require auxiliary heating to reach the desired supply temperature. Undersizing the storage can limit the collection and use of available solar energy during periods when the storage is fully charged. Storage tanks are usually sized as 40-100 liters per m<sup>2</sup> (1-2.5 gal/ft<sup>2</sup>) of collector area. Typically, a storage volume of 75 liters per m<sup>2</sup> (1.8 gal/ft<sup>2</sup>) of collector area provides enough heat for a one day sunless period (ASHRAE 2007).

Finally, solar thermal systems require auxiliary or back-up systems for overcast days and times of increased demand. A renewable-based back up system suitable for off-grid application may use one of several types of systems, including: a PV-powered tankless electric water heater or heat pump water heater; a heat-pump space heating system that uses solar thermal storage as the cold reservoir; or a biomass-combustion system for space heating and domestic water heating.

### 2.5.3. *Photovoltaic System*

Solar energy is a low-density source of thermal radiation. Solar electric systems are one of the several ways of capturing the low-density solar thermal energy and converting it to useful electricity using the photovoltaic effect, (i.e., the process of converting sunlight directly into electricity using solar or photovoltaic (PV) cells). A solar cell is configured as a large-area p-n junction of semiconductor materials (such as silicon, which is the most commonly used PV material). When exposed to light, electricity is generated across the junction between the two materials (Wenham et al. 2007). A group of series-connected solar cells is packaged into a PV module. A number of modules fixed together on a single surface is called a solar panel. PV panels that are wired together to obtain the desired power, voltage and current are called a PV array (Eiffert and Kiss 2000). Solar panels integrated into the building envelope components such as the façade, atrium, awning and shading, or roofing systems are called building-integrated photovoltaic (BIPV)\_systems<sup>12</sup>, which are now commercially available (Eiffert and Kiss 2000, Sylvester and Haberl 2001).

Based on manufacturing technologies, commercially available PV materials are classified as mono-crystalline, polycrystalline or thin film. Mono-crystalline silicon panels are the most efficient (15%-18%), and are suitable for applications requiring high voltage (i.e., where the DC power has to travel some distance before being utilized or stored in a battery). With recent improvements, up to 25% efficiency has been achieved in photovoltaic panels<sup>13</sup>. Polycrystalline panels have efficiencies ranging between 13%-16% and are less expensive. Thin-film panels are the least expensive and are more flexible for applications, but they have lower efficiencies ranging between 5%-7% (stabilized condition), which diminishes over time due to light-induced degradation before leveling off at a stable value or nominal power rating. However, with the use of a stack of PV cells (e.g., in triple junction cells) the aging effect can be reduced (German Energy Society 2008). To achieve higher efficiency and maximum output, an optimum orientation and tilt or a tracking hardware should be used. The tilt of the panels can be optimized for summer-only, winter-only or annual energy production using low tilt, high tilt or latitude tilt angles, respectively. For heavy overcast conditions (with decreased direct-beam radiation), low tilt angles better utilize diffuse radiation from the sky. On the other hand, for overcast conditions coupled with snow-covered surfaces, higher tilt angles can capture reflected light from the snow-covered ground. Furthermore, the solar panel should be installed for uninterrupted solar access, avoiding shading and shadowing from nearby structures, trees and other panels. (Krauter 2006, Dahl 2008).

---

<sup>12</sup> The 2007 Colorado team used a solar system with 8.8 kW of PV panel with the solar hot water system underneath the PV paneling. This increases the PVs efficacy due to a cooling effect and maximizes solar utilization for a given area.

<sup>13</sup> In 2006, a 40.7% efficient multi-junction PV cells were developed, which achieve a higher efficiency by capturing more of the solar spectrum. In a multi-junction structure, individual cells are made of layers, where each layer captures part of the sunlight passing through the cell. These cells rely on an optical concentrator to focus sunlight onto the cell (US DOE 2006).

The main components of a photovoltaic electric system for off-grid applications include:

i) photovoltaic panels, ii) mounting structure, iii) batteries for electricity storage, iv) a charge controller to convert the array voltage to the proper voltage for charging the battery bank and prevent the battery bank from being overcharged, v) inverters to convert DC current from the array/batteries to AC current for use in the house, vi) disconnecting means, and vii) wires and fuses (Russel 2004, Wiles 2001). A solar electric system should be sized to generate enough power to be stored in the batteries for meeting building loads for several days without sufficient solar radiation. The sizing of the PV array is determined based on the daily average sun hours and daily electrical loads. The sizing of the battery-storage is determined based on the total electricity requirement for the period the system must support (specific to the location), battery efficiency due to charge/discharge cycle, allowable depth of discharge of the batteries, performance of the batteries as affected by the extreme winter conditions, battery voltage, and system voltage. In addition, the sizing of the charge controllers and inverters should be determined based on the system's electrical output and building's electrical loads (Dahl 2008).

#### 2.5.4. Wind Power System

Wind is a low-density source of kinetic power. Energy can be extracted from the wind by transferring the momentum of the passing air to rotating blades. The kinetic energy of the wind is converted into mechanical energy of the rotating shaft that runs a generator to produce electricity. The quantity of energy generated is a function of the rotor area and the cube of the wind speed (AWEA 2009). Thus, the power from a wind turbine is greatly impacted by wind speed and the rotor diameter.

The efficiency of a wind power system can be as high as 30%. Small wind systems range from 20 Watt to 30 kW capacities, and can provide 50-90% of a home's electricity needs. They are applicable if a site receives a steady wind (> 5 mph), has enough space (at least 1/4 acre), and has no restrictions for towers up to 50 ft. or higher. Selection of a wind turbine is usually based on the average local wind speed and energy needs of the house. Cost is another consideration which depends on the output and the energy needs of the house (NREL 2005).

Wind turbines are primarily available as horizontal-axis and vertical-axis wind turbines. Vertical-axis wind turbines may require additional energy to start the rotor turning due to low starting torque, and may also require larger land area for guy wires to hold them in place. Most of the commercially available small scale wind turbines for residential applications are horizontal-axis turbines (Sagrillo 2008). A wind-powered electric system consists of: i) a wind generator, which includes rotor blades coupled with permanent magnet alternators, ii) a tower, capable of withstanding the lateral thrust of the wind and the weight of turbine, and iii) brakes, either mechanical brakes, dynamic brakes or mechanical furling for emergency stopping of the rotating blades, iv) a balance-of-system that includes charge-controller, inverter and wires, and v) batteries for off-grid applications (Gipe 2004, Woofenden 2005).



Wind electric systems generate electricity in a specific range of wind speeds. The estimate of energy production from a wind turbine can be made using a wind turbine power curve (i.e., a graph showing a wind turbine's power output across a range of wind speed), the average annual wind speed at the site, the height of the tower, and the hourly frequency distribution of the wind speed during an average year, with adjustments made for the site elevation. A typical power curve shows: i) cut-in wind speed (i.e., the speed at which a wind turbine begins to generate electricity. At the start-up wind speed the wind turbine rotor begins to spin without producing electricity), ii) cut-out speed, where the turbine ceases to generate electricity, iii) rated speed, at which the rated output is given, and iv) maximum design wind speed, above which the power production starts diminishing or ceases due to the furling of turbine blades. In some cases, a mechanism in which the rotor shaft folds either up or around the tail vane in order to protect the turbine from damage (NREL 2005). The most accurate power generation estimate of a wind energy system is accomplished by combining a turbine performance curve with an hourly frequency distribution of the wind speed at the hub height of the turbine (AWEA 2009).

Considerations for installing wind turbines include: annual wind speed, prevailing wind direction, existing obstacles as well as future obstructions. For best results, the turbine should be 30 feet above anything within 300 feet, and needs enough space to raise and lower the tower for maintenance. The concerns for installing a wind turbine include: high maintenance, aesthetics, "perceived" noise levels (typically, 52 to 55 decibels, which is equivalent to the noise from an average refrigerator), danger to birds and bats (Rogers 2009), cost, zoning regulations, and permitting requirements (NREL 2005, Woofenden 2005).

#### 2.5.5. Micro-hydroelectric System

Hydroelectric resources also have great potential for electricity generation for residential properties near a usable water source, such as a creek or a stream. For a site with a suitable water source, it can be the most cost-effective and reliable renewable source with predictable electricity output, due to the relatively constant flow of a stream compared to the sun and wind's variability. Micro-hydroelectric systems can also complement photovoltaic systems in locations where water flow is the highest in the winter when solar energy is at a minimum (Davis 2003).

Micro-hydroelectric systems typically produce power within 200 Watt to 25 kW range (Alexander and Giddens 2008). They generate electricity from small water-powered alternators. The energy potential of a water resource is evaluated by measuring the head (vertical drop) and the flow of the stream (Davis 2003). The potential energy of the falling water and kinetic energy of its flow is converted into rotational motion (mechanical energy) by spinning shaft of the turbine. This shaft is usually coupled directly or belted to either a permanent magnet alternator, or a "synchronous" or induction AC generator that produces electricity (Cunningham and Woofenden 2007).

According to Davis (2003), useful power can be generated from a flow as low as two gpm and a large drop, or a drop of as small as two feet and 500 gpm water flow. A more precise estimation of electricity output range was provided by Alexander and Giddens (2008), which indicated that from a 1,550 rpm turbine, a minimum of 40 gpm discharge at 56 feet of head, or a minimum of 5.6 ft. site head with a 475 gpm discharge was required for a 200 Watt electrical output.

Depending on the hydro sites and energy needs, a micro-hydroelectric system consists of a wide range of equipment and system configurations that include: i) an intake – either a submerged, screened box or complete damming of the stream; ii) a pipeline from the water source to the turbine, preferably buried to prevent freezing in extremely cold climates, shifting, damage or ultraviolet degradation from exposure to sunlight; iii) a turbine; and iv) a balance-of-system (BOS) that includes charge controller, invertors, a load shedding device, and the proper wiring. An off-grid application also requires batteries for seasonal water sources and/or any seasonal and daily variation in energy needs (Cunningham and Woofenden 2007).

The concerns associated with this technology include: local regulations about creating stream diversions, environmental concerns such as fish passing through the stream, drying of the remaining creek, seasonal droughts or floods, and the need for regular maintenance and periodic replacement of the moving equipment (Cunningham and Woofenden 2007).

#### 2.5.6. Biomass and Biodiesel

Biomass is a very broad term that refers to non-fossilized, renewable materials derived from plants. Biomass energy is, essentially, solar energy stored in plants in the form of chemical energy through the process of photosynthesis, which is released when the biomass is consumed, burnt or converted into fuels (AGORES 2009). Biomass energy is usually derived from three distinct energy sources: i) wood; which includes harvested wood, wood by-products and wood waste; ii) waste, which includes municipal solid waste, manufacturing waste and landfill gas; and iii) alcohol fuels, derived from the conversion of agricultural products/waste (US EIA 1994). Using biomass is, essentially, completing the natural carbon cycle, from vegetation growth through decay and returning to the growth cycle. Burning biomass simply accelerates this degradation process producing no more CO<sub>2</sub> than would occur by decomposition, and therefore, is considered carbon-neutral if no fossil fuels are consumed in the transport of the biomass to the conversion site (Hastings and Wall 2007b). Biomass technologies range from individual home systems to industrial-sized facilities that can either produce electricity or be converted to fuel for later use (AGORES 2009). For residential applications with high heat-demand, biomass-based micro combined heat and power (microCHP) systems would be beneficial. These systems are driven by heat-demand and deliver electricity as a byproduct, which can be stored for later use. For this study, only individual dwelling-scale biomass technologies for space heating will be investigated.

Wood-fired space heating technologies have evolved with remarkable improvements regarding both efficiency and emissions. Concerns about air quality and creosote formation due to incomplete combustion in older versions of wood stoves have been addressed to some extent with catalytic converter-equipped wood stoves (Mother Earth News 1984). Masonry heaters have an added advantage over other types of stoves since they allow more complete combustion by burning fuels at full-temperature with controlled airflow. The large thermal mass of some masonry stoves can slowly radiate the captured heat over long periods without the need of constant firing (Pahl 2007). The most recent development in biomass stoves are pellet ovens for space heating as well as domestic water heating applications. Pellet ovens burn compressed wood or compressed wood waste called pellets in a highly efficient, low-emission combustion process in a thermostatically controlled burn cycle and can include an automated fuel supply to the boiler and a forced-air exhaust system. Unfortunately, the operation and control of pellet ovens requires electricity (Hastings and Wall 2007b). The average heat content of paper pellet is 6,515 Btu/lb compared to 4,980 Btu/lb for wood/wood waste and 10,377 Btu/lb for coal (USEIA 1994, 2009).

#### 2.5.7. Rainwater Harvesting System

Rainwater harvesting is an ancient method of collecting, storing and delivering water, and is a viable source of water for off-grid homes for both indoor and outdoor use under suitable climatic conditions. A rainwater harvesting system typically consists of a catchment surface (e.g., a roof or ground area), a conveyance system (i.e., gutter, glides, and surface drains or channels) and a storage reservoir (such as a surface or an underground tank) (Gould and Nissen-Petersen 1999). The possibility of microbiological and chemical contamination of rainwater due to roof debris, compounds contained in roofing materials and airborne pollution (Chang et al. 2004, Simmons et al. 2001) requires filtering and treatment of collected rainwater using fowl water-flushing, screens and membranes, settling chambers, aeration, ultraviolet and ozone treatments (Yaziz et al. 1989; Gould and Nissen-Petersen 1999; Kim et al. 2005). Rainwater harvesting systems can provide clean, safe and reliable water so long as they are properly sized, built and maintained, and the rainwater is stored appropriately for intended uses (Zhu et al. 2004). Factors affecting the design of rainwater system include: the rainfall amount and distribution, demand schedule, available space for catchment and storage, runoff coefficient, ease of treatment, maintenance and water extraction, and possibilities of water contamination (ITDG 2008).

Several techniques are available for calculating appropriate water storage reservoir volumes, either for maximizing supply for a given catchment or for meeting a required target demand. These methods range from simple spreadsheet-based and graphical methods (where the storage requirement is determined by comparing cumulative rainfall supply versus cumulative water use) to detailed methods such as mass curve analysis and statistical methods (for determining the reliability of supply and probability of system failure) (Gould and Nissen-Petersen 1999). McMahan and Mein (1978) identified three general types of reservoir sizing models, namely: i) the critical period method, which uses historical

data and identifies sequences of flows where demand exceeds supply to determine the storage capacity; ii) Moran's theory of storage, where a system of simultaneous equations is used to relate reservoir capacity, demand and supply (Moran 1959); and iii) behavioral models, which simulates the spatial and temporal fluctuations in the operation of the reservoir to predict system performance in terms of their water-saving efficiency for different combinations of roof area, demand, storage volume and rainfall level (Fewkes and Butler 2000, Fewkes 2000). For simple methods, an accurate estimation of rainwater supply requires at least ten years of reliable rainfall data and a good estimate of household water demand considering the variation due to family characteristics and seasonal changes in consumption rates.

For areas with limited supply and uncertain rainfall, a large catchment area (possibly using the ground surface) can offset the need for having very large storage, and will require extensive treatment before use. In such locations, the need for having very large storage can significantly be offset by combining strategies for water-efficiency and conservation measures such as recycling and reuse.

#### 2.5.8. Renewable System Selection Priorities

Woofenden (2007a) ranked energy-efficiency and renewable energy measures for small scale and large scale applications. Assuming equal resources, the order listed for home-to-ranch scale is: energy-efficiency, solar pool heating, micro-hydroelectric systems, solar hot water systems, photovoltaic systems and wind energy systems. In addition, the selection of renewable systems and components is also subjected to the installation, operation and maintenance issues specific to the climate of the building location. Acknowledging that in the real world, each region and property has more or less of each source, the best procedure is to implement energy conservation and efficiency strategies, and then move toward using local renewable resources.

### **2.6. Climate Maps and Weather Data Sources**

This study required the determination of representative climate locations in the U.S. which have different heating and cooling energy needs as well as the availability of renewable resources. Therefore, climate resource maps of the U.S. including Solar Radiation Resource Maps (NREL 2008), Wind Energy Resource Atlas (Elliot et al. 1986) and precipitation maps (PRISM Group 2006) were obtained to identify the potential of solar, wind and rainwater as renewable resources across the U.S. In addition, information in Kutscher (2007) was reviewed, which included several maps indicating the potential of concentrating solar power, photovoltaics, wind power, geothermal, biomass and biofuel in the U.S., and also, an overlay of these maps showing the high-potential renewable resources in different parts of the U.S.

For determining the building energy, water and sewage disposal needs, and the sizing of renewable systems for providing the daily needs as well as the cumulative needs for periods with limited or unavailability of renewable resources, weather data for typical and extreme conditions was required. Since a single weather dataset does not usually represent both typical and extreme conditions for all the

relevant climate parameters, a number of sources were accessed to obtain the necessary weather data. The data obtained were then processed and formatted, as needed, to be used at different steps throughout the analysis. The climate data sources used and the processing steps are described in the following sections.

#### 2.6.1. Typical Meteorological Year (TMY2) Weather Data:

The analyses of building energy use (with DOE-2.1e) and solar systems (with F-CHART and PV F-CHART) were performed with TMY2 weather data. A TMY2 weather file for a location is comprised of hourly measured data of the months with the most representative temperature and solar radiation characteristics selected from 30 individual years (1961-1990), which are concatenated to form a complete, contiguous year. However, TMY2 data does not represent typical rainfall and wind conditions. TMY2 hourly datasets were available in the format required for the analysis with DOE-2.1e. TMY2 monthly average data available with F-CHART and PV F-CHART programs were compared and matched with the TMY2 monthly statistics obtained from (USDOE 2008) to ensure consistency across the programs.

#### 2.6.2. Measured Wind and Rainfall Data

The characteristics of wind and rainfall as renewable resources were determined from measured hourly data obtained from the National Climatic Data Center (NCDC) (NOAA 2008). Twelve years of measured data for the period 1997-2008 were obtained for each location to analyze the availability of wind and rainwater, and identify critical years within this period (i.e., with minimum availability of these resources). For the analysis of wind, hourly measured data for each month was analyzed using histograms of hourly wind speed. The typical and critical conditions for each month were then determined using a statistical procedure. Using a time-series analysis, the longest period without any useful wind for on-site electricity generation was determined.

For the analysis of rainfall, twelve years of measured hourly data were analyzed to determine the amount of daily harvestable rainwater. This required analyzing the frequency of rainfall, and the elapsed time between two (harvestable) rainfall events. In addition, after a gap of 24-hours, a fixed amount of rainwater at a minimum rate was assumed to be deliberately diverted (i.e., a first flush). Using these criteria, daily and annual water harvested per unit area was determined for each year. Finally, the average and critical years were identified using average and minimum rainfall harvested amounts, as well as the largest storage needs (i.e., to cover the longest elapsed time between rainfall events).

#### 2.6.3. Meteorological and Solar Energy Datasets

The NASA Surface Meteorology and Solar Energy datasets (SSE 2008) were reviewed, which provided monthly solar radiation data for average and extreme conditions. These datasets were developed for the photovoltaic and solar thermal applications, and are available as monthly values based on a twenty-two year period of measured data. These datasets were for used for the sizing of electricity storage system.

#### 2.6.4. *Special Concerns About Weather Data*

Due to a lack of one consistent weather data source that could be used for an integrated analysis for energy-efficiency, water-efficiency, and renewable measures, weather data from different sources were used. This introduced several concerns, which could not be avoided as follows:

1. **Non-concurrent Meteorological Data:** The analysis of building energy use and solar systems were based on TMY2 weather data, and the analysis of wind and rainfall would be based on ten-year measured hourly data (probably different years). Thus, even though concurrent data would be used with one analysis method (i.e., temperature, humidity and solar radiation), the analysis across other renewable resources used in the study involved non-coincident data (i.e., wind and rainfall). By integrating the results on monthly basis, the effect of non-coincidence was reduced to some extent.
2. **Typical vs. Extreme Year:** With TMY2 weather data, typical building energy needs and the average performance of solar systems were determined. On the other hand, the performance of the wind power system and the sizing of the rainwater harvesting system would be based on an extreme year (i.e., the most unfavorable year with minimum availability of wind resource and rainwater). Therefore, achieving complete self-sufficiency requires considering extreme weather years with opposite conditions, for example higher than typical building energy use and lower than typical solar system output. Although, the analysis of building energy use with the DOE-2.1e simulation program could be performed for extreme years, the performance of the solar systems using the F-CHART and PV F-CHART analysis can be predicted only on long-term average basis because the algorithms are based on correlations that are applicable to average weather conditions (Duffie and Beckman 2001).
3. **Assumptions for the Analysis based on Monthly and Annual Data:** In this analysis, the DOE-2.1e program was used, which is an hourly whole-building energy simulation program that takes into account short-term (i.e., hourly) weather records. Whereas, F-CHART and PV F-CHART predict monthly-average daily performance (and monthly total output) of the solar systems based on monthly average data. Finally, wind power curves were used that provide turbine output based on instantaneous (at least hourly) wind speed data. In addition, the performance of the wind electric systems will be based on the monthly total output meeting the monthly total electricity use. Therefore, an integration method that was used is based on a monthly basis that is applicable only if the storage system is sized to have enough capacity so that no load dumping occurs during one month. Similarly, the design of the rainwater harvesting system (especially, the size of catchment area) was based on the annual rainwater supply and water demand. This required the storage tank to be sized for surplus and/or deficit accumulated over the whole year, so that no dumping of rainwater occurs until there is enough stored water to provide for the cumulative demand during extended periods with reduced rainfall, which are determined by the analysis of the long-term record.

4. Limited Synchronization: Given the concerns listed above, the inputs across the methods/tools used for this study were assumed to be synchronized to a limited extent. For example, the roof tilt optimized for PV panels and solar collectors can be modeled in DOE-2. However, the thermal impact of the building integrated photovoltaic (BIPV) panels and solar collectors cannot be modeled accurately (Sylvester and Haberl 2001) without the use of special routines to calculate the changes to that portions of the building envelope now occupied by the BIPV. In addition, the electricity used for operating the solar thermal pump was only approximated assuming that the pump operates from sunrise to sunset. Whereas in reality, the operation is automated and usually controlled based on a temperature difference between the collector and storage tank temperatures with the pump shutting down for the day once the thermal storage is up to temperature. Similarly, the schedule for the pump pressurization for the building's potable water supply was based on another set of operating assumptions.

## **2.7. Tools and Methods for an Integrated Analysis**

For the past 50 years, numerous tools and techniques for building energy analysis have been developed, which include databases, spreadsheets and simulation programs (US DOE 2008a). While some programs are limited to certain applications (e.g., for the analysis of specific building components and systems, ventilation/air flow, daylighting, solar/climate analysis, and code-compliance), others have the capability of performing whole-building energy analysis (with or without renewable energy systems). Crawley et al. (2008) provided an up-to-date comparison of various whole-building energy simulation programs. Among these, five programs for whole-building analysis were reviewed for this study, which include: BLAST (Hittle 1977, 1979a,b), TRNSYS (Klein et al. 2004), DOE-2.1e (Winkelmann et al. 1993), ESP-r (ESRU 2002; Clarke 2001) and EnergyPlus (Crawley et al. 2004). In addition, F-CHART (Klein and Beckman 1993a) and TRNSYS (Klein et al. 2004) were reviewed for active solar thermal system, and PV F-CHART (Klein and Beckman 1993b), PVFORM (Menicucci 1985, Menicucci and Fernandez 1988) and PVSIM (King et al. 1996) were reviewed for photovoltaic system analysis.

### **2.7.1. Whole-Building Energy Simulation Programs**

In the U.S., computer simulations for predicting the thermal performance of buildings began in the late 1960s with the development of NBSLD (National Bureau of Standards Load Determination) computer program by Kusuda (1974, 1976). The NBSLD program combined algorithms for transient conduction in the building structure, solar heat gains, radiant transfer, and convection between building surfaces and the room air in order to predict interior temperatures and heating/cooling loads of a single-zone building under dynamic conditions. The NBSLD algorithms provided the basis for the development of the U.S. Army Construction Engineering Research Laboratory's (CERL) Building Loads Analysis and System Thermodynamics (BLAST) program, released in 1977, which incorporated algorithms to simulate

multiple rooms and integrate building loads with algorithms for air handling systems and plant equipment for predicting energy consumption in buildings (Hittle 1977). BLAST was one of the first hourly fixed-schematic simulation program that used: i) the response factor method for transient heat transfer through multilayered walls (Mitalas and Stephenson 1967; Stephenson and Mitalas 1967); and ii) the heat-balance method for calculating overall heat transfer, hourly fuel and electricity consumption, and plant life cycle cost (Hittle 1979a,b). The latest version is BLAST 3.0 includes a user interface – Heat Balance Load Calculation (HBLC) (US DOE 2008b).

About the same time, the Energy Research and Development Administration (ERDA) (now known as the Department of Energy (DOE)), sponsored the development of the Post Office program for the U.S. Postal Service for building energy analysis. After proceeding through progressive stages of development (i.e., NECAP, CAL-ERDA, CAL/CON and DOE-1) by several organizations, it was finally released as DOE-2 by the Lawrence Berkeley Laboratory (LBL) in 1978, with the latest version released as DOE-2.1e. DOE-2.1e is also an hourly fixed-schematic, whole-building energy simulation program that uses one subprogram for translation of inputs (the BDL Processor) and four simulation subprograms (i.e., LOADS, SYSTEMS, PLANT and ECONOMICS) executed in sequence. It uses: i) the response factor method (the same as BLAST), and ii) the ASHRAE weighting factor method, a simpler approach for calculating overall heat transfer within each thermal zone (Winkelmann et al. 1993). DOE-2.1e has been widely used for evaluating the energy performance of buildings, and offers a great capability for simulating a wide range of design features. It has been extensively validated for accuracy and consistency and is usually the program against which other programs are compared (Judkoff and Neymark 1995; Haberl and Cho 2004a).

TRNSYS (TRAnsient SYstem Simulation program) was developed by the Solar Energy Laboratory at the University of Wisconsin, primarily as a program for simulating solar thermal systems (Klein 1973), which later incorporated general HVAC system simulations. It is a transient system simulation program with a modular structure that allows simulation of complex energy systems by configuring and assembling a series of smaller components (Klein et al. 2004). The subroutines representing the physical components are combined and solved simultaneously with the building envelope thermal balance and the air network at each time step. The TRNSYS library includes components for a multizone building models, low energy buildings, HVAC systems, and renewable energy systems, including passive solar, active solar thermal and photovoltaic systems, wind energy, fuel cells and cogeneration, etc. Furthermore, the modular nature of TRNSYS facilitates the addition of new mathematical models to the program (Klein et al. 2004), which cannot be easily accomplished with BLAST and DOE-2, which are fixed schematic programs.

ESP-r is a general purpose, multi-domain simulation environment for building thermal, inter-zone air flow, intra-zone air movement, HVAC systems and electrical power flow simulations, developed by



Strathclyde University in Glasgow, Scotland. It follows a pattern of “...simulation follows description...” where additional technical domain solvers are invoked as the building and system description evolves. Users control the complexity of the geometric, environmental control and operations to match the requirements of particular projects. ESP-r uses explicit finite difference conservation equations for energy, mass and electric power for each zone and each surface, and message passing between the solvers to support inter domain interactions. It uses the finite-volume calculation method to describe the spatial variation of temperature, humidity and heat flux (ESRU 2002, Clarke 2001).

EnergyPlus is also a modular, structured code based on a platform that combines the best features of BLAST and DOE-2.1e. Similar to BLAST and DOE-2.1e, EnergyPlus also uses the response factor method for transient heat transfer through multilayered walls. The simulation modules are integrated with the heat balance method for the zone simulation. The input and output data structures are tailored to facilitate third party interface development. It allows user-specified time steps of less than an hour, and performs load calculation and simulation of the response of systems and plant at the same time step. This integrated solution provides more accurate space temperature prediction, which is crucial for system and plant sizing, occupant comfort and occupant health calculations. It also allows users to evaluate realistic system controls, moisture adsorption and desorption in the building elements, radiant heating and cooling systems, and interzone air flow, photovoltaic systems and fuel cells (Crawley et al. 2001, 2004).

All these programs have a different level of capability for the analysis of renewable energy systems. The modular structure of TRNSYS and ESP-r allow modeling of passive solar, active solar thermal, photovoltaic and wind power systems. EnergyPlus can model Trombe wall passive solar, active solar thermal systems with flat plate collectors and photovoltaic systems. The early versions of DOE-2 (i.e., DOE-2.1a,b,c) incorporated algorithms for simulating solar systems, which were disabled in later versions. The current version (i.e., DOE2.1e), can simulate only a Trombe wall and passive solar sunspace systems. However, this limitation of DOE-2.1e can be overcome by integrating the results of DOE-2.1e with other programs for analyzing the performance renewable energy systems, such as those described in the next section.

### 2.7.2. Analysis Programs for Solar Systems

F-CHART and PV F-CHART are simplified programs for the design and analysis of solar thermal and photovoltaic systems, respectively (Klein and Beckman 1993a,b). These are simplified models that use monthly average weather data, synthesize hourly data (in PV F-CHART), and require a general description of the system to predict long-term system performance. The F-CHART program is based on the “*f*-chart” method developed by Klein (1976), which provides a means of estimating the fraction of the total heating load supplied by solar energy for a given system. “*f*-chart” is a correlation of hundreds of simulation results of solar heating systems using the TRNSYS simulation program (Klein et al. 1976) for many climates, conditions and system designs. The correlations give the fraction “*f*” of the

monthly heating load supplied by solar energy as a function of two dimensionless parameters: the ratio of collector losses to heating loads, and the ratio of absorbed solar radiation to heating loads.

The PV F-CHART program is based on the concept of utilizability – a radiation statistic, which is the fraction of the incident solar radiation that can be converted to useful energy (Duffie and Beckman 2006). PV F-CHART was developed by Klein and Beckman (1983) based on the methods by Siegel et al. (1981) and Clark et al. (1983, 1984), simulation studies performed with TRNSYS (Klein 1973), and photovoltaic component models developed by Evans et al. (1978). The PV F-CHART method consists of a combination of correlations and fundamental expressions for the hourly calculations of solar radiation at a given location. The F-CHART and PV F-CHART programs correlations have been extensively compared and validated with other solar simulation programs (Haberl and Cho 2004b,c).

PVFORM (Menicucci 1985, Menicucci and Fernandez 1988), developed at the Sandia National Laboratory for simulating the hourly performance of PV flat-plate systems, incorporates improved integrated modeling techniques which include: the anisotropic diffuse radiation model (Perez 1984) to accurately compute the insolation in the plane of the array (as opposed to isotropic model by Liu and Jordan (1963)), the Fuentes model (Fuentes 1985) to predict the installed NOCT (normal operating cell temperature) as a function of the module mounting configuration (as opposed to a constant NOCT values in other models), and DC-power and AC-power submodels in order to improve the accuracy of the predicted performance. PVFORM is being used for the web-based hourly simulation program PVWATTS (Marion et al. 2005, NREL 2007). PVSIM, also developed at the Sandia National Laboratory, addresses the interactive behavior of modules in arrays by accurately simulating the characteristics of individual cells in the module. It also analyzes the effects of cell mismatch or reverse bias (hot-spot) heating in modules (King et al. 1996).

### 2.7.3. *Tools for Integrated Analysis*

There are number of simulation programs that can perform an integrated analysis of energy-efficiency and renewable energy measures. These programs include: TRNSYS, ESP-r and EnergyPlus. TRNSYS, ESP-r and EnergyPlus have modular structures that facilitate the addition of new mathematical models to the program. In TRNSYS, the user can specify building and system components and the manner in which they are connected. It can perform simulations for building energy use, and renewable energy systems including passive and active solar thermal, photovoltaic, wind electric, and fuel cell system. ESP-r also has the same capabilities except that only flat-plate solar collectors can be simulated. EnergyPlus has a limited capability of analyzing passive solar systems, and can only analyze flat-plate collectors. As of version 3.1.0, wind electric systems cannot be analyzed with EnergyPlus. In addition, there are other software programs available with different overall objectives. These include: Energy-10, BEopt, and HOMER. Among these, HOMER and BEopt can provide cost-optimized results.

Energy-10 version 1.8 is a conceptual design tool for low-energy buildings below 10,000 ft<sup>2</sup> in conditioned area that can be characterized by one or two thermal zones. The simulation engines include: the DOE-2 split flux method for daylighting simulation, the CNE (California Nonresidential Engine) for the thermal network based simulation and TRNSYS for the photovoltaic simulation, to perform an integrated analysis (Balcomb et al. 2001). It can also perform a life-cycle cost analysis.

BEopt is a computer program designed to find optimal building designs along the path to a zero net energy (ZNE) building that is grid-tied, with net-metered photovoltaic (PV) and active solar systems. BEopt has three analysis modes: (a) design mode, (b) parametric mode, and (c) optimization mode. In BEopt, a user selects from predefined number of options in various categories to specify options to be considered in the optimization. BEopt calls the DOE-2.2 program for building load calculation and calls TRNSYS for PV and solar DHW system simulations. In the optimization mode, BEopt sequentially searches the available building options for the lowest cost building designs at various levels of energy savings. BEopt handles special situations with positive or negative interactions between options in different categories. The renewable systems that can be analyzed with BEopt are limited to PV system and flat-plate solar thermal system for domestic hot water only, and the analysis of PV systems is performed only for grid-connected homes, which does not consider parameters such as battery capacity, battery efficiency and load dumping that impact the usability of the generated power. Therefore, for off-grid applications, BEopt could be used to perform the analysis of building energy use with predefined energy-efficiency options, and to compare the cost-effectiveness of various combinations (Christensen et al. 2005).

HOMER is an optimization program for small power systems (including photovoltaic systems, wind turbines, hydroelectric systems, fuel cells; generators using biogas, stored hydrogen or fossil fuels; and optional battery storage). It allows the user to analyze the cost-effectiveness, optimum system sizing, and the adequacy of renewable resources for off-grid and grid-connected applications. The required inputs include: i) thermal and electrical loads, ii) characteristics of the components, and performance and costs of the systems, and iii) availability of resources such as solar, wind, and hydro and biomass, and fuel costs. With the optimization and sensitivity analysis capabilities, HOMER finds the least cost combination of the components from various combinations of different system sizes and types that meet electrical and thermal loads, and generates results of the sensitivity analyses on most inputs. It simulates the operation of a system by making hourly energy balance calculations using thermal, electrical loads, available energy from user-selected system(s) including optional batteries and fuel-powered generators. Unfortunately, the current version of HOMER cannot analyze solar thermal systems. Thus, for analyzing measures for energy efficiency and obtaining building thermal and electrical loads for HOMER, a whole-building simulation program would be required. With these inputs, HOMER can perform the analysis of certain renewable energy systems and provide cost-optimized results (NREL 2004). For the analysis and design of off-grid

homes, the building thermal and electrical loads with cost-optimized energy-efficiency measures obtained from BEopt could be used with HOMER to select cost-effective renewable power systems.

#### 2.7.4. *Approaches for Integration of Various Tools*

The literature that contained documented simulation approaches for designing off-grid homes includes the energy reports submitted by the teams participating in the 2002, 2005 and 2007 Solar Decathlon Competition. The design approach in most cases combines the analysis and results for individual systems using separate analysis tools. The reasons for following this approach were the limited capabilities of a single program, and the compromise between the ease of use and the level of detail sought by the teams.

Most of the 2002 Solar Decathlon teams performed separate analysis for building energy use, solar thermal system and photovoltaic system. For example, VisualDOE and Energy-10 (Texas team); Energy-10, PV-sol and T-sol (Carnegie-Mellon team); PowerDOE, F-CHART and PV DesignPro (Virginia Tech team); and Energy-10, PV DesignPro and SolarPro (Crowder team). However, the Colorado team used only TRNSYS and Maryland team used only Energy-10<sup>14</sup> (and simplified calculations for solar thermal system) for building energy use as well as photovoltaic system simulation.

In the 2005 Solar Decathlon, the suite of tools used was common among various teams. The teams combined the results of whole-building energy simulation programs (Energy-10<sup>15</sup>, eQuest, Ecotect or Energy Plus) with the analysis tools for the solar systems such as SolarPro<sup>16</sup>, F-CHART, MATLAB, MathCAD and RetScreen for solar thermal system, and PV-DesignPro and Dimensiona for PV system.

The 2007 Solar Decathlon teams have also used a similar approach. The teams used Energy-10 and PV-FCHART for conceptual design and EnergyPlus, MATLAB, TRNSYS for detailed hourly simulation (Colorado team), IES (Cornell team), TRNSYS and PHPP (Passivehaus Projektierungs Packet) for building performance, and INSEL (Integrated Simulation Environment Language) for solar systems (Germany team), EnergyPlus (Illinois), Energy-10, eQuest and TRNSYS (Lawrence Tech Team), EnergyPlus and PV-DesignPro (Santa Clara team), Energy-10 and Solar Design Studio (Penn. State team), CNE (California Nonresidential Engine), EnergyPlus (New York team), and DOE-2.1e, F-CHART and PV F-CHART (Texas A&M team).

## 2.8. Summary of the Literature Review

The literature review provided an understanding of available off-grid, off-pipe design approaches, energy-efficiency and renewable energy techniques best suited for off-grid applications, different climate

<sup>14</sup> Only Energy-10 v. 1.4 has the capability of analyzing photovoltaic system based on TRNSYS. This capability was later added in v. 1.8.

<sup>15</sup> Developed by National Renewable Energy Laboratory's (NREL) Center for Building and Thermal Systems, the new version of Energy-10 (version 1.8) includes photovoltaic module and solar domestic hot water module.

<sup>16</sup> These programs can perform hourly simulation of solar thermal and photovoltaic systems, and are included in the Solar Design Studio suit developed by the Maui Solar Design Corporation.

classification approaches for energy-efficient building design, typical residential building characteristics, and available tools and techniques for analyzing building energy use with energy-efficiency and renewable energy measures. The findings of the literature review are summarized below.

Designing an off grid, off-pipe house means achieving complete self-sufficiency in terms of energy, water and sewage disposal using only on-site resources. This should be accomplished by first implementing energy and water-efficiency measures, and then utilizing on-site renewable resources that include: solar, wind, hydro, biomass and rainwater. The energy and water-efficiency measures should aim at reducing the demand, increase the efficiency of equipment/devices, minimize waste and recover otherwise lost heat. The sizing of the renewable energy generation and water collection system should be performed to exceed the daily energy and water use, and provide sufficient storage for the cumulative needs during periods when renewable resources are not available, supplemented by a back-up system.

For minimizing energy use, energy-efficiency must be a priority for the design, which include: a higher amount of insulation and airtight construction with advanced framing techniques, (i.e., SIPs or ICFs); a high-performance fenestration system consisting of insulated glazing with low-e or spectrally-selective coatings, insulated window frames and spacers, window shading devices, moveable night insulation (for cold climates), and controls for window operation; an adequately sized, energy-efficient HVAC system and a properly insulated and sealed duct system, preferably, located in the conditioned space; energy-efficient lighting design with compact florescent lamps or LEDs, sensors, dimmers and timers, integrated with daylighting strategies; and energy and water-efficient appliances, and low standby power home electronics.

For minimizing the water use and water heating energy use, water-efficient appliances and fixtures must be selected, an efficient plumbing layout needs to be incorporated into the design, and measures for minimizing water waste should be considered. Water reuse and recycling provides further reduction of the water use, which is desired for climates with less rainfall. Reducing the water use also results in reduced sewage disposal needs, which requires a smaller septic system that can further be reduced by considering incinerating or composting toilets.

For utilizing renewable resources, passive solar, active solar thermal, photovoltaic, wind electric, micro-hydroelectric, biomass and rainwater harvesting systems were reviewed. Passive solar systems utilize solar thermal gains and thermal mass to maintain comfortable indoor environment, reduce space heating and cooling energy use and allow smaller HVAC systems. Active solar systems provide space heating and domestic hot water, but require electricity to operate. The design of active solar thermal systems should be optimized for winter loads, and sized for at least 80% of the winter-time space heating and water heating energy use. The excess thermal energy collected during the summer can be utilized for space cooling and dehumidification, if the appropriate thermally-driven systems are used. Photovoltaic, wind power, and micro-hydroelectric systems generate electricity for space cooling, appliances, lighting,

operating active solar thermal system as well as for back-up space heating and water heating. Depending on the resources available on-site, these systems can be combined to form a hybrid system requiring combinations of equipment for the balance-of-system and a single battery bank. The design of photovoltaic, wind-power or micro-hydroelectric system should be optimized for summer. The system should be sized to provide daily electricity use as well as charge the battery bank large enough to provide the cumulative electricity use for critical periods.

Rainwater is the only source of water supply in off-grid, off-pipe homes. Therefore, optimizing the collection and storage size of the rainwater harvesting system to exceed the cumulative water use for the dry-season is extremely important. While integrating these systems, the building design should be optimized to fully utilize the potential of these sources and minimize the dependence on “auxiliary” or back-up systems.

For the energy analysis of off-grid houses, five whole-building energy simulation programs were reviewed, including: BLAST, TRNSYS, DOE-2.1e, ESP-r and EnergyPlus. These programs are based on different simulation algorithms and programming structure, and have different capabilities for simulating building systems and renewable energy systems. Among these programs, BLAST and DOE-2.1 e are fixed-schematic programs, whereas TRNSYS, ESP-r and EnergyPlus are modular programs that enable the user to incorporate models for simulating advanced building systems and various renewable energy systems. In addition, F-CHART, PV F-CHART, PVFORM and PVSIM were reviewed for active solar thermal and photovoltaic system analysis. F-CHART and PV F-CHART predict long-term performance of active solar thermal and photovoltaic systems, respectively, using monthly average and synthesized hourly weather data. PVFORM and PVSIM use enhanced submodels for a more accurate simulation of the hourly performance of photovoltaic system.

Finally, sources for defining building characteristics were reviewed that include: housing survey data for general building characteristics, residential building energy code (IECC) for minimum performance requirements for the building envelope and systems, and Building America Research Benchmark Definition for the building usage profiles.

## CHAPTER III

### SIGNIFICANCE OF THE STUDY

#### 3.1. Expected Contributions of the Study

This study is intended to provide the following benefits towards the design of residential buildings that aim to minimize or eliminate the dependency on non-renewable sources used on-site as well as on non-renewable energy used through municipal services:

1. The identification of building and system design priorities for achieving self-sufficiency in terms of energy, water and sewage disposal,
2. The identification of essential features and resources required in different climates,
3. The development of a step-by-step procedure to guide the design of off-grid, off-pipe single-family detached houses in different U.S. climates,
4. The investigation of analytical resources required for the design and analysis of off-grid, off-pipe homes. These include: the analysis tools and methods for an integrated analysis, and weather data sources that could provide typical and extreme climate characteristics required for designing for self-sufficiency.

Finally, the limitations of using available resources for such a design an analysis approach were identified, which establish the need for future research in these aspects.

#### 3.2. Scope and Limitations of the Study

This study was conducted with the following limitations:

1. This study focuses on a specific building type: a single-family detached house with slab-on-grade floor. For this building type, a 2000/2001 IECC<sup>1</sup> standard reference design was considered as the base case for six U.S. climate locations, irrespective of the status of the state energy codes in those locations.
2. This study presents an analysis for six cities located in different climate regions. The selection of locations was intended to represent a range of scenarios with dissimilar building energy and water needs, and the availability of renewable resources. The analysis demonstrates a methodology to achieve self-sufficiency in different climates. These results may not be applicable directly to all location in those climates.
3. This study analyzed only those measures for energy-efficiency that could be simulated with DOE-2.1e version 119, F-CHART and PV F-CHART programs.

---

<sup>1</sup> In this manuscript, the 2000 IECC (International Energy Conservation Code) with the 2001 Supplement and 2006 NAECA (National Appliance Energy Conservation Act) revisions is denoted as the 2000/2001 IECC.

4. The study analyzed only solar, wind, biomass and rainwater as renewable sources of energy and water.
5. This study is based on only the macroclimate analysis of the representative locations, which was obtained from data collected from local airport weather stations by NOAA.
6. The selection of energy and water-efficiency measures, and the sizing of renewable systems were based on reduced building energy and water needs, to achieve self-sufficiency with only the available on-site renewable resources. The cost of these measures was not considered during the selection of the measures and sizing of the systems.
7. This study is a quantitative analysis of the feasibility of off-grid, off-pipe single-family residence for achieving self-sufficiency. Other aspects related the implementation of this approach, such as local building codes and regulations, cost-effectiveness, overall appearance of the house, and public perception, were not considered.



## CHAPTER IV METHODOLOGY

This chapter describes the methodology used in this study. The goal of this methodology is to form a comprehensive general procedure for the analysis and design of off-grid, off-pipe homes, which could be applied to a variety of scenarios in terms of building energy and water needs and the availability of renewable resources. In order to accomplish this goal, several supporting procedures were developed using analysis tools and methods for the individual building systems as well as the building as a whole, which were then combined to form an integrated analysis procedure. The following section provides an overview of the methodology. The supporting procedures involved are described in the subsequent sections.

### 4.1. Overview of the Methodology

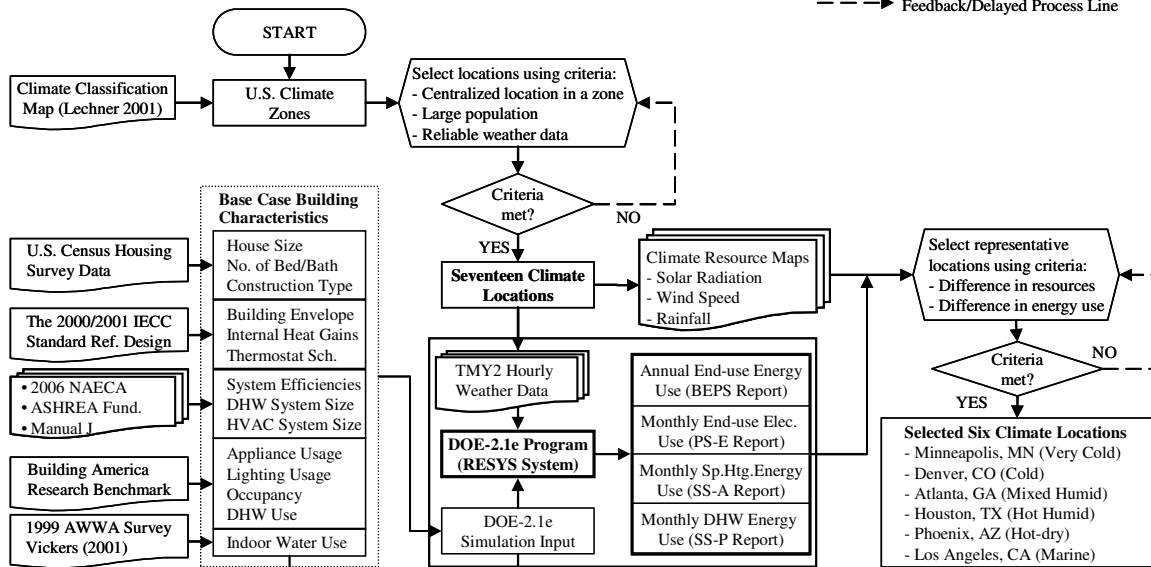
The aim of this study is to investigate the feasibility of off-grid, off-pipe design approach for single-family detached residences in different climate regions across the U.S. to achieve self-sufficiency for energy, water and sewage disposal using only renewable resources. To accomplish this, first six climate locations with dissimilar base-case<sup>1</sup> building energy requirements and availability of renewable resources (i.e., solar radiation, wind and rainwater) were selected. For each location, energy and water-efficiency measures were applied to reduce the building energy and water needs (i.e., to minimize the monthly peak energy and average daily indoor water use). Next, the harvestable on-site renewable resources were quantified in each location. For this, the performance of the renewable energy systems with different types/capacities of active solar thermal collectors, photovoltaic panels and wind turbines was analyzed for varying system and installation configurations. In addition, normalized system sizing parameters (i.e., per unit of daily water use) were derived for the rainwater harvesting system. Finally, the sizing of systems was performed to provide all the household energy and water needs, and facilitate on-site sewage disposal. In this manner, an integrated analysis procedure was developed for the analysis and design of off-grid, off-pipe homes, and demonstrated for six U.S. climate locations.

Figure 5 shows the flowchart of the overall research methodology. It consists of the following tasks: 1) selection of representative climate locations; 2) analysis of climate characteristics; 3) selection of water-efficiency and energy-efficiency measures; 4) quantification of on-site harvestable renewable resources; and 5) sizing and integration of systems for self-sufficiency. Task 4 and 5 calls for additional

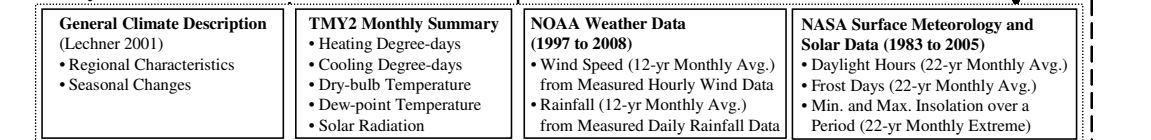
---

<sup>1</sup> The base-case house in this study is a 2000/2001 IECC standard reference house in each location, which provided a common ground for selecting representative climate locations as well as a reference point for minimizing the building energy and water use (i.e., the demand) before sizing the systems for harvesting renewable resources (i.e., the supply) for achieving self-sufficiency.

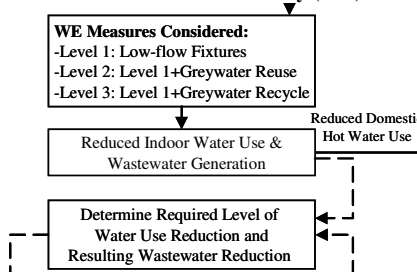
1. Selection of Representative Climate Locations



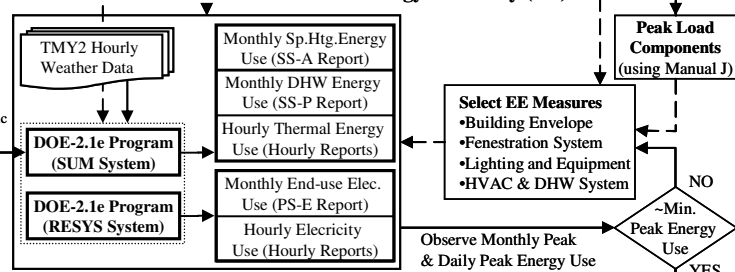
2. Analysis of Climate Characteristics



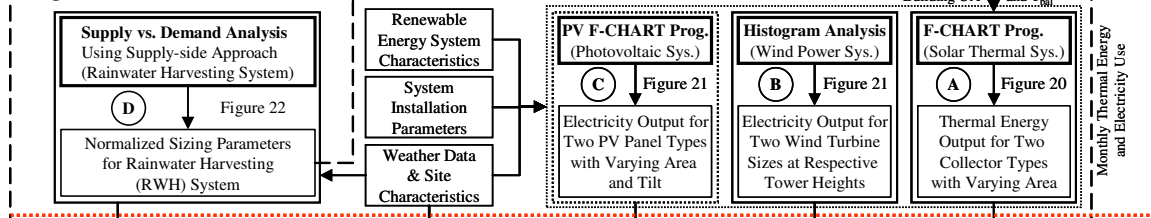
3. Selection of Water Efficiency (WE) Measures



4. Selection of Energy Efficiency (EE) Measures



5. Quantification of Harvestable On-Site Renewable Resources



6. Sizing & Integration of Systems for Self-sufficiency

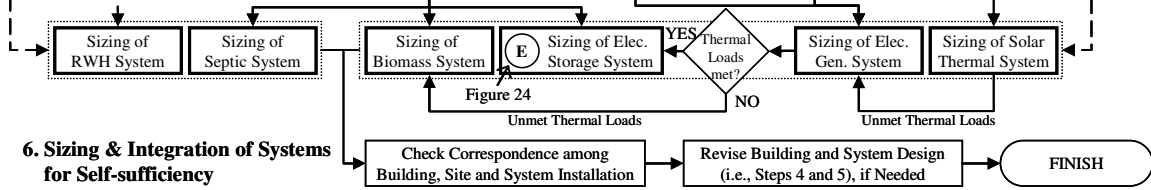


Figure 5 Research Methodology

flowcharts for the analysis of solar thermal, photovoltaic, wind power and rainwater harvesting systems, and for the sizing of electricity storage systems (shown in Figure 20 through Figure 23). A detailed description of each task is provided in the following sections.

#### 4.2. Selection of Representative Climate Locations

This study used six representative climate locations in the U.S. to demonstrate a variety of scenarios in terms of building energy requirements and availability of renewable resources. Therefore, a detailed investigation of building energy use and climate resources was performed for climate locations across the U.S. Figure 6 shows the procedure for selecting the six representative climate locations, which consists of four steps: i) preliminary selection of locations, ii) determination of the base-case building characteristics, iii) simulation of the base-case energy use, and iv) final selection of locations.

First, several locations were selected from different climate regions across the U.S. For each location, the base-case building characteristics were determined for a code-compliant residence. These building characteristics were modeled in DOE-2.1e program and simulated with the appropriate TMY2 weather data to obtain the base-case energy use in each location. In addition, U.S. climate resource maps for solar radiation, wind and precipitation were reviewed in order to compare the availability of renewable resources for these locations. Finally, by investigating the simulated base-case energy use and U.S. climate resource maps, six locations that covered a wide range of heating and cooling energy use and availability of renewable resources were selected. The following sections describe these steps in detail.

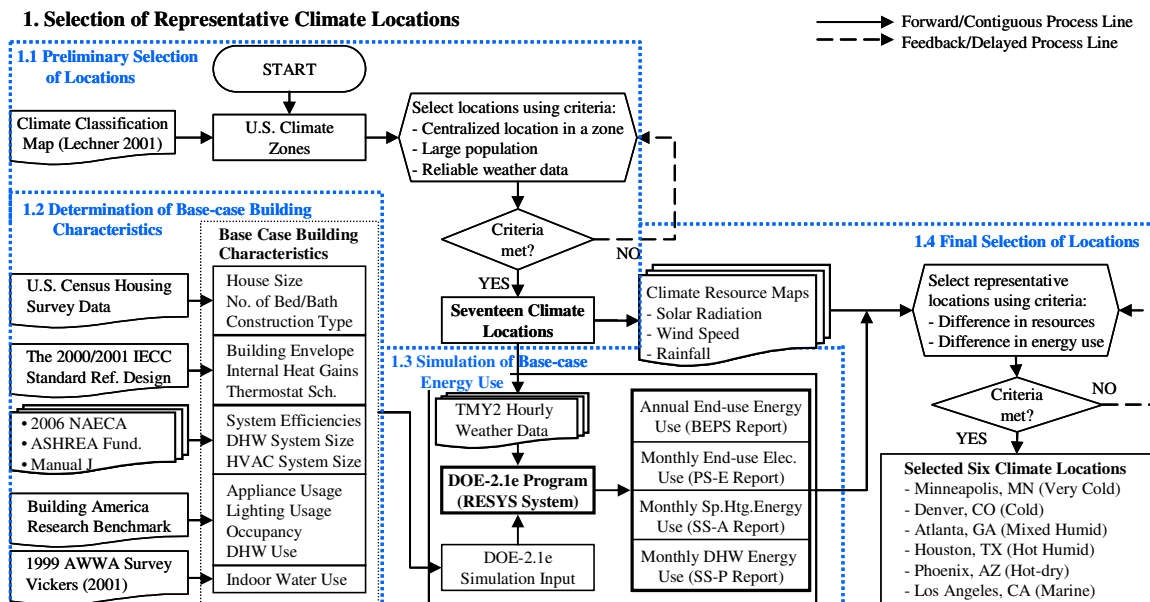


Figure 6 Procedure for Selecting Six Representative Climate Locations

#### 4.2.1. *Preliminary Selection of Locations*

This study used a 2000/2001 IECC<sup>2</sup> standard reference design to determine the base-case building characteristics. Instead of the climate zoning in the 2000/2001 IECC, which was based on heating-degree days, only (i.e., the variations in other climate elements were not taken into account), the climate classification proposed by Lechner (2001) was used for the preliminary selection of locations. This climate classification, originally developed by the AIA Research Corporation (1978), was based on how the four climate elements: sun, wind, temperature and humidity act as liabilities that drive the heating and cooling needs, or as assets for natural heating and cooling of homes. Using this climate classification map, one location from each of the seventeen proposed climate regions was selected using the following criteria:

1. The location should be a city with large population, where residences are predominantly located;
2. The location should have good-quality weather data for all relevant weather parameters (i.e., TMY2 weather data, Class I solar radiation data, and measured wind and rainfall data);
3. The location should represent average weather conditions of the climate region it belongs to.

Considering these criteria, international airport weather stations in major cities located well within these climate zones were selected. Figure 7 shows the selected seventeen locations marked on the U.S. climate classification map by Lechner (2001). From each of these locations, the base-case house characteristics were determined in order to simulate the building energy use and determine the availability of renewable resources.

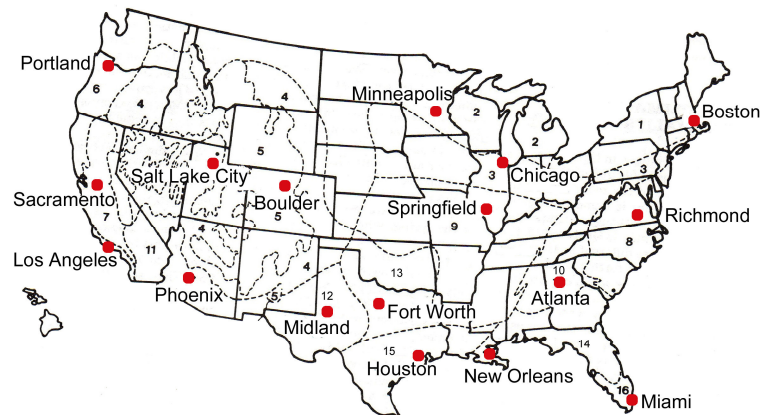


Figure 7 Preliminary Selection of Locations<sup>3</sup>.

<sup>2</sup> In this manuscript, the 2000 IECC (International Energy Conservation Code) with the 2001 Supplement and 2006 NAECA (National Appliance Energy Conservation Act) revisions is denoted as the 2000/2001 IECC.

<sup>3</sup> Source: Lechner (2001, p.40). Copyright © 2001 Wiley & Co. (Reprinted with Permission)

#### 4.2.2. *Determination of the Base-case Building Characteristics*

This study is focused on single-family detached residences. It uses a 2000/2001 IECC standard reference design as the base case. Several other resources were used for determining other building characteristics. The general characteristics of the house including the floor area, the number of bedrooms and bathrooms, and the construction type were determined from the housing survey data by the U.S. Census Bureau (2009). The thermal characteristics of the building envelope, internal heat gains, and thermostat settings were determined to conform to the 2000/2001 IECC standard reference design (ICC 1999, 2001). The capacity of the HVAC and DHW systems were determined using Manual J (Rutkowski 2004) and ASHRAE (2007), respectively. The efficiency of the HVAC and DHW systems were determined from the 2006 NAECA (National Appliance Energy Conservation Act) revisions to the 2000/2001 IECC. Since the 2000/2001 IECC does not specify the details of internal heat gains, the U.S. DOE's Building America Research Benchmark Definition (Hendron 2008) was used to obtain the schedules for lighting usage, appliance usage, occupancy and domestic hot water use, and the sensible and latent fractions of the internal heat gains. The base-case indoor water use was determined using the estimates by Vickers (2001). The domestic wastewater estimate for the base case was determined using the indoor water use estimate. The base-case house characteristics are described in the following sections.

##### 4.2.2.1. *General Building Characteristics*

A 2,500 ft<sup>2</sup> single-family detached residence with four bedrooms and three bathrooms (U.S. Census Bureau 2009) was considered as the basis for this study. For the base-case house, a square-shape plan with equal areas on the north, east, south and west exposures was used to comply with the 2000/2001 IECC. To ensure consistency, identical building and system configurations were assumed for the base-case house in all locations. This includes: a one-story house with slab-on-grade floor and an unconditioned, vented attic; all-electric equipment for space heating, space cooling and domestic water heating; the air distribution system located in the attic; and the domestic water heating system located in the conditioned space<sup>4</sup>. A simplified image of the residence is shown in Figure 8.

##### 4.2.2.2. *Building Envelope*

The base-case house was assumed to have light-weight wood-frame construction with 2x4 wall studs spaced at 16 inches on center (i.e., 25% framing factor<sup>5</sup>) and 2x6 ceiling joists/roof rafters spaced at 24 inches on-center (i.e., 7% framing factor<sup>5</sup>), a slab-on-grade floor with 4-inch heavy-weight concrete, and an unconditioned, vented attic with an 18.4° roof tilt (i.e., a 4:12 slope). The gross window area of the

---

<sup>4</sup> The internal heat gains from the domestic hot water tank were assumed to be the same as the stand-by tank losses (i.e.,  $(UA)_{\text{tank}} * (T_{\text{supply}} - T_{\text{ambient}})$ ). For simplification, constant temperatures for the DHW tank and the ambient (i.e., the conditioned space) were used.

<sup>5</sup> Source: ASHRAE (2005)

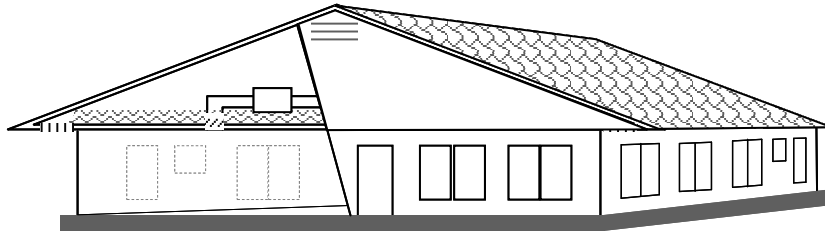


Figure 8 Base-case House

house equaled 18% of the conditioned floor area, which was distributed equally on all four sides for the base-case house. In addition, the base-case windows had no exterior shading, and had interior shading values of 0.7 in summer and 0.9 in winter (ICC 1999, 2001).

The base-case house had 2000/2001 IECC specified climate-specific exterior wall assembly and ceiling assembly U-values, slab perimeter insulation level, and fenestration system U-factor and solar heat gain coefficient. To achieve the required overall wall U-value, the exterior wall assembly was assumed to have 3.5" fiberglass-batt cavity insulation and varying thickness of continuous insulation between the ½" plasterboard interior finish and 4" facia-brick exterior finish. Similarly, the ceiling assembly was assumed to have varying thickness of cellulose-fill insulation placed between and above the ceiling joists over a ½" plaster board. The roof assembly included ½" plywood over rafters and grey asphalt shingle roofing. The slab perimeter insulation, if required for the 2000/2001 IECC standard reference design for certain climate locations, was assumed to be provided vertically, on the outside of the foundation.

The air infiltration for the base-case house was determined using a specific leakage area of 0.00057 for the one-story conditioned zone, which assumed a 0.57 normalized leakage (ICC 1999); and 0.0033 for the attic, which assumed 1 ft<sup>2</sup> of aperture area per 300 ft<sup>2</sup> of attic floor area (ICC 2004).

#### 4.2.2.3. Space Conditioning and Air Distribution System

The base-case HVAC system included a SEER 13 central air-conditioner with a 7.7 HSPF electric heat pump (conforming to the 2006 NAECA revisions to the 2000/2001 IECC). The heating and cooling capacities of the HVAC system were determined from Manual J Average Load Procedure (Rutkowski 2004). The heating and cooling coil airflow was determined using a 30 cfm/kBtu of capacity (RESNET 2007). The heating and cooling set-points were 68 °F for the winter and 78 °F for the summer, with a 5 °F setback for six hours (11 p.m. to 5 a.m.) during the winter and a 5 °F setup for six hours (9 a.m. to 3 p.m.) during the summer (ICC 1999).

The ducts for the base-case house were located in the unconditioned, vented attic. The supply and return duct areas were 27% and 5% of the conditioned floor area, respectively (ASHRAE 2004)<sup>6</sup>. The insulation levels for the supply and return ducts were obtained from ICC (2001)<sup>7</sup>. A 10% supply and a 10% return duct leakage were assumed for the base-case house (Cummins et al. 1991).

#### 4.2.2.4. Domestic Hot Water Use and System Characteristics

For the base-case house with four bedrooms and three bathrooms, a 66-gallon, 5.5 kW electric water heater (ASHRAE 2007) with a 0.84 energy factor (ICC 1999) was used, which provided hot water at 120 °F supply temperature (ICC 1999) according to the combined hourly profile by Hendron (2008) shown in Figure 9. The daily hot water consumption and resulting domestic water heating loads for each location were determined using the following procedure, which is based on the average daily water consumption end-use estimates and equations for calculating water mains temperature obtained from Hendron (2008). This procedure is explained in detail, and demonstrated for six climate locations in Appendix B.

#### 4.2.2.5. Occupancy, Lighting, and Equipment Usage

The annual electricity consumption due to interior lighting was calculated as 2,455 kWh/yr, which included 86% incandescent lamps and including 14% fluorescent lamps installed as 80% hard-wired lighting and 20% plug-in lighting. All electricity consumed by lighting system was assumed to be converted to sensible heating loads. Figure 10(a) shows the hourly interior lighting profile for the base-case house obtained from Hendron (2008).

The base-case house was assumed to be equipped with electric appliances with an hourly normalized end-use profile for combined residential equipment use shown in Figure 10(b). Table 1 shows the annual electricity consumption due to appliances and the associated sensible and latent internal heat gains. The electricity use for the appliances were calculated as a function of the number of bedrooms and finished floor area, with the exception of the refrigerator and miscellaneous electrical loads that were constant regardless of the number of bedrooms. The sensible and latent internal heat gain fractions indicate that not all of the electricity consumed by appliances is converted into internal heat gains. For the base-case house, the appliance electricity use was 6,808.2 kWh/yr, which was converted to a sensible heat gain of 4,201.3 kWh/yr (62% of the appliance electricity use) and a latent heat gain of 554.6 kWh/yr (8% of the appliance electricity use).

In addition, sensible internal heat gains of 220 Btu/h per person and latent internal heat gains of 164 Btu/h per person from 3.5 occupants were included in the simulation model. The schedule of the

<sup>6</sup> According to ASHRAE Standard 152-2004 (ASHRAE 2004): Supply duct area =  $0.27 * F_{out} * A_{floor}$ ; Return duct area =  $b_r * F_{out} * A_{floor}$ ; where  $F_{out}$  shall be set to 1.0 for single-story houses and 0.75 for houses with more than one story;  $A_{floor}$  = conditioned floor area;  $b_r$  =  $(0.05 * \text{number of return registers})$  or 0.25, whichever is less.

<sup>7</sup> According to the 2001 Supplement to the 2000 IECC (ICC 2001), the minimum duct insulation levels are: R-8 for the supply duct and R-4 for the return duct for locations with annual heating degree days below or equal to 7,500, and R-11 for the supply duct and R-6 for the return duct for locations with annual heating degree days above 7,500.

occupancy used in the simulation model is shown in Figure 10(c), which amounts to 16.5 hrs per day per occupant.

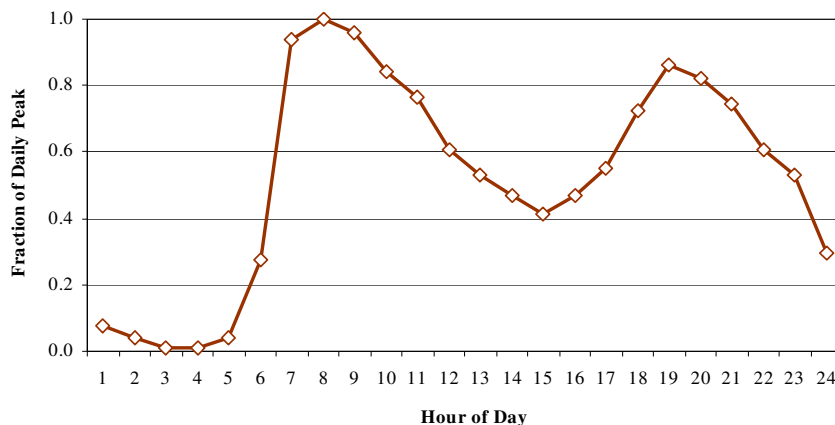


Figure 9 Schedule for Combined Domestic Hot Water Use<sup>8</sup>

Table 1 Annual Energy Consumption due to Appliances and Sensible and Latent Heat Gain Fractions<sup>8</sup>

End Use	Calculations for End-use Electricity Use kWh/yr = (a + b*N <sub>br</sub> + c*FFA)*Multiplier <sup>9</sup>					Internal Heat Gains (Fraction)		Internal Heat Gains (kWh/yr)	
	a	b	c	Multiplier	kWh/yr	Sensible	Latent	Sensible	Latent
Refrigerator	669.0	-	-	1.0	669.0	1.00	-	669.0	0.0
Clothes Washer (3 cu. ft.)	52.5	17.5	-	1.0	122.5	0.80	-	98.0	0.0
Clothes Dryer (Elec.)	418.0	139.0	-	1.0	974.0	0.15	0.05	146.1	48.7
Dishwasher (8 place)	103.0	34.3	-	1.0	240.2	0.60	0.15	144.1	36.0
Range (Elec.)	302.0	101.0	-	1.0	706.0	0.40	0.30	282.4	211.8
Variable MELs <sup>10</sup>	1231.0	194.0	0.32	1.0	2,797.0	0.81	0.02	2,265.6	55.9
Fixed MELs <sup>10</sup> (All Elec.)	349.0	58.0	0.09	1.0	808.5	0.13	0.25	105.1	202.1
Plug-in lighting	455.0	-	0.80	0.2	491.0	1.00	-	491.0	0.0
Annual Total Electricity Use					6,808.2	Total Internal Gains		4,201.3	554.6
Average Electricity Use (kW)					0.78	Fraction of Annual Total Electricity Use		0.62	0.08

<sup>8</sup> Source: Hendron (2008)

<sup>9</sup> N<sub>br</sub> = Number of bedrooms, FFA = Finished floor area

<sup>10</sup> MELs = Miscellaneous Electrical Loads



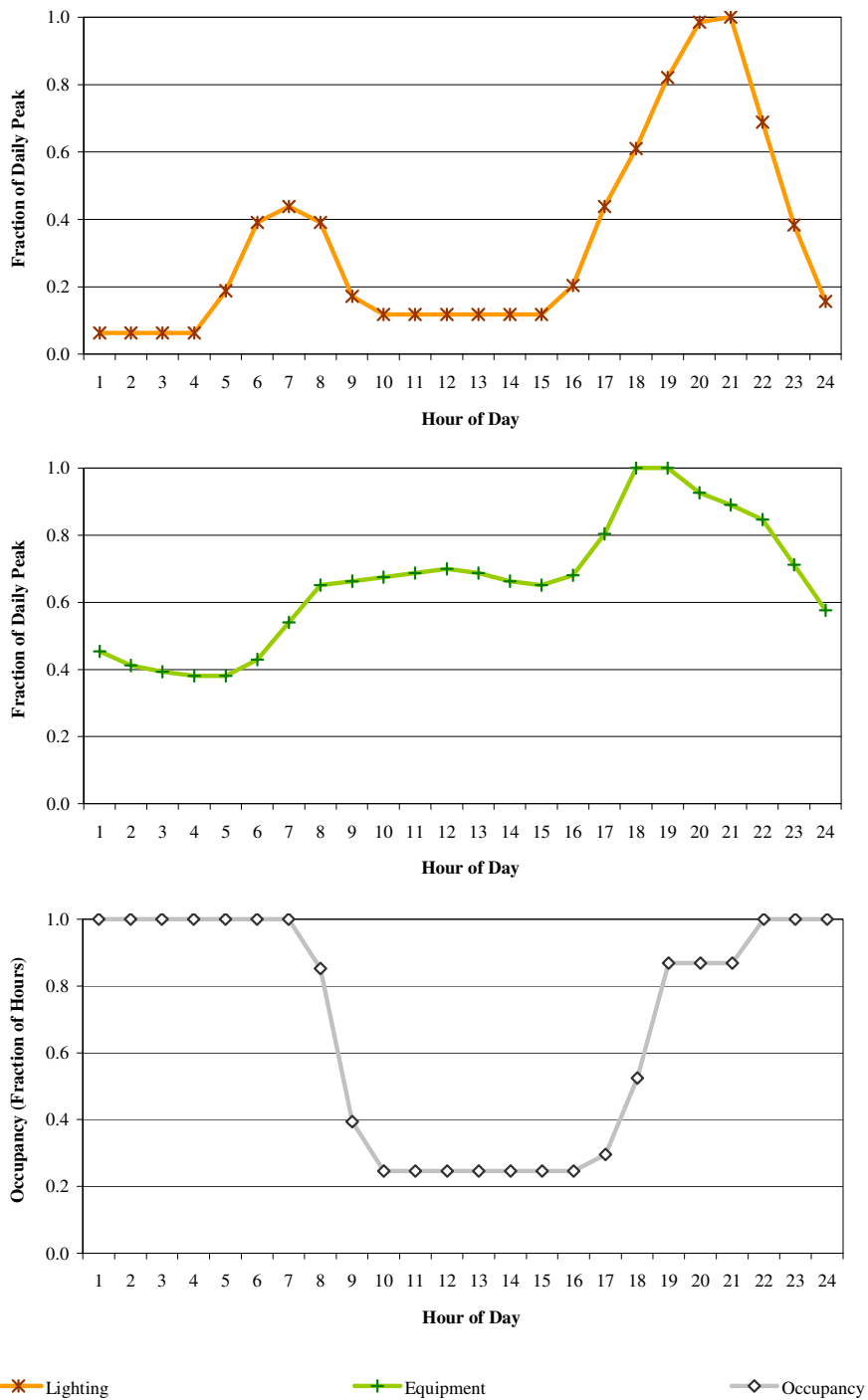


Figure 10 Schedule for Lighting Use, Equipment Use, and Occupancy<sup>11</sup>

<sup>11</sup> Source: Hendron (2008)

#### 4.2.2.6. Base-case Water Use and Wastewater Generation

For the base-case house in all locations, an estimate of 45.3 gallons per capita per day (i.e., 181 gallons per day<sup>12</sup> for a household of four occupants) of indoor water use was used. This is an estimate by Vickers (2001), who revised the results of an empirical study of indoor water use in the U.S. (Mayer and DeOreo 1999) to consider if all the installed fixtures were in compliance with the 1992 U.S. Energy Policy Act (EPAct). Figure 11 shows the indoor water end-use estimates with and without these revisions. The maximum allowable water flow rates of various fixtures based on 1992 EPAct, average daily fixture utilization, and the revised estimates of indoor water end-use are listed in Table 2. These values were used for determining the indoor water use reduction from various water-efficiency measures.

Based on the national U.S. Geological Survey database of combined indoor and outdoor water use reported by public water supply systems (USGS 2004) and the study of indoor water use by Mayer and DeOreo (1999), the U.S. average daily outdoor single-family residential water use (for landscape water use, car washing, cleaning, and swimming pools) was estimated as 31.7 gallon per capita per day. However, it was found that the outdoor residential water use could vary from a few gallons to hundreds of gallons per capita per day due to local climatic conditions and landscape design (Vickers 2001). Therefore, in this study, only indoor water use was considered as the criteria for the selection of water-efficiency measures and the sizing of rainwater harvesting and sewage disposal systems. For the outdoor water use, only the estimate of the first-flush volume was made, which, if collected separately, could be used for site irrigation.

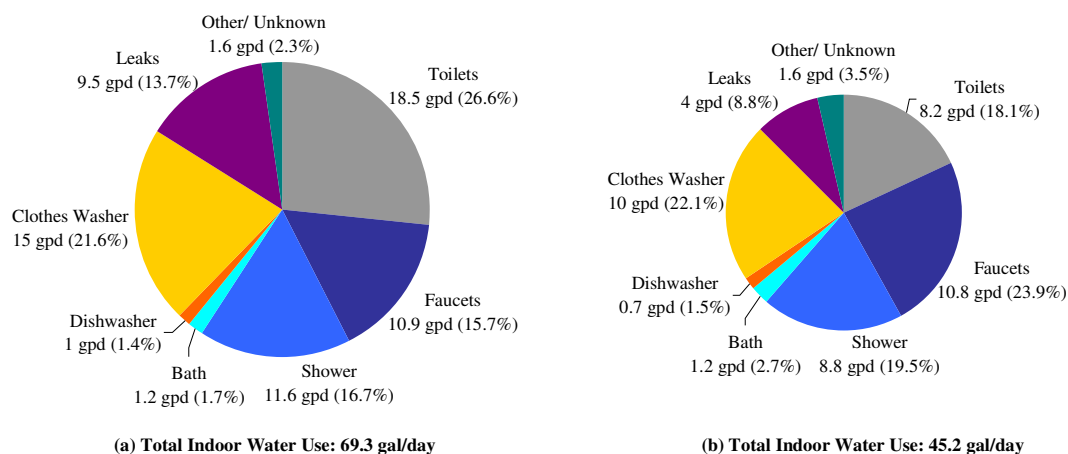


Figure 11 Indoor Water End-use Estimates by: (a) Mayer and DeOreo (1999), and (b) Vickers (2001)

<sup>12</sup> This was assumed to include (approximately) 70 gal/day domestic hot water use at 120 °F water temperature. The climatic variation and seasonal fluctuations in the cold water (mains) temperature impacts the domestic hot water use, which was considered for the energy analysis. However, the daily total indoor water use was assumed to be same throughout the year, across the U.S.

Table 2 Base-case Indoor Water Use<sup>13</sup>

Type of Use	Max. Water Flow rates	Fixture Utilization (Average Daily)	Usage (gal per capita per day)
Toilet	1.6 gal/flush	5.05 times per capita	8.2
Faucet	2.5 gal/min	8.1 minute per capita	10.8
Shower	2.5 gal/min	0.75 per capita (shower and bath, combined)	8.8
Bath	-		1.2
Dishwasher	7 gal/load	0.1 loads per capita	0.7
Clothes Washer	27 gal/load	0.37 loads per capita	10.0
Leaks	-	21.9 gallons	4
Other Domestic	-	-	1.6
Total			45.3

#### 4.2.2.7. Summary of Base-case Building Characteristics

Table 3 summarizes the general building characteristics of the base-case house including the building configuration, construction details, space conditions, and mechanical systems. The resources used for determining these characteristics included: 2000/2001 IECC, housing survey data, and Building America Research Benchmark Definition. Several building characteristics, such as house size, construction type, floor and roof configuration, system type and efficiency were assumed to be common for all climate locations. Certain building characteristics such as the insulation levels of the building envelope components and HVAC ducts, and window properties varied depending on the climate location. In addition, the domestic hot water use varied with the climate location due to difference in the water mains temperature.

#### 4.2.3. Simulation of Base-case Energy Use

For this study, the residential simulation model “RES.INP v3.00.10”, developed by the Energy Systems Laboratory (ESL), was used, which simulates a single-family house as a single-zone building. This model uses parameters for various building and system characteristics, which can be assigned different values using external DOE-2 include files. The simulations were performed in a batch mode using the Desktop DOE-2 Processor (DDP) (Liu et al. 2008).

Using this model, the house was simulated in a delayed thermal construction mode (i.e., using the DOE-2.1e custom-weighting factors) to account for the thermal mass of the construction materials and the slab-on-grade foundation. The domestic water heating energy use was simulated using a user-defined

<sup>13</sup> Source: Vickers (2001)

Table 3 General Characteristics of the Base-case House

CHARACTERISTIC	DESCRIPTION
<b>Building Configuration:</b>	
Building Type	Single family, detached house with four bedrooms and three bathrooms for a family of four.
Building Geometry	2,500 ft <sup>2</sup> , square-shape, one-story, oriented N, S, E, W (south-facing); eight foot ceiling height; unconditioned vented attic with an 18.4 deg. (4:12) roof tilt.
Surroundings	Ground (grass with reflectance = 0.24); No obstructions.
<b>Construction Details:</b>	
Structure	Light-weight wood frame walls and roof; slab-on-grade concrete floor.
Exterior walls	2x4 wall studs spaced at 16" on center (i.e., 25% framing factor); R-11 fiberglass-batt cavity insulation and climate-specific continuous insulation on the exterior to conform to the 2000/2001 IECC standard reference design requirements; facia brick exterior (absorptance: 0.75).
Ceiling/Roof	2x6 ceiling joists/roof rafter spaced at 24" on center (i.e., 7% framing factor); cellulose-fill ceiling insulation (R-value: based on HDD65°F and window-to-wall area ratio); grey asphalt-shingle roofing (absorptance: 0.75).
Foundation/Floor	Slab-on-grade floor with 4" heavy-weight concrete (perimeter R-value: based on HDD65°F and window-to-wall area ratio); carpet flooring over 80% of slab-on-grade floor area.
Windows	Window area: 18% of conditioned floor area, distributed equally on all orientations; window U-factor: based on HDD65°F; SHGC: 0.4 for HDD < 3500, 0.68 for HDD ≥ 3500; no external shading; internal shade factor: 0.7 in the summer and 0.9 in the winter.
Infiltration	Specific leakage area: 0.00057 for the conditioned space and 0.0033 for the unconditioned, vented attic.
<b>Space Conditions:</b>	
Space Temperature Set-point	68 °F for heating, 78 °F for cooling, 5 °F set-back in the winter (from 11 p.m. to 5 a.m.) and 5 °F set-up in the summer (from 9 a.m. to 3 p.m.).
Internal Heat Gains	Lighting: 1,964 kWh/yr electricity use converted to 100% sensible heat gains; Equipment: 6,808 kWh/yr electricity use converted to 62% of the total as sensible heat gains and 8% of the total as latent heat gains (i.e., 30% of the total drained/exhausted to the outdoors); Occupants: From 3.5 persons, assuming 224 Btu/hr.person as sensible heat gains and 164 Btu/hr.person as latent heat gains.
<b>Mechanical Systems:</b>	
HVAC System	A central system with a SEER 13 air-conditioner and 7.7 HSPF heat pump; heating and cooling capacity determined from Manual J.
DHW System	66-gallon tank-type electric water heater with 0.84 energy factor (EF) to supply approximately 70 gal/day <sup>14</sup> hot water at 120 °F.
Thermal Distribution System	Ductwork located in the unconditioned, vented attic; 5% supply and 5% return duct leakage, supply and return duct R-value based on IECC requirements; Static pressure: 0.5, Supply air-flow rate: 360 cfm/ton

DOE-2.1e subroutine function based on the water heater analysis (WHAM) model (Lutz et al. 1998), which accounts for different water heater characteristics and operating conditions (as anticipated in this study due to different climate locations). The simulations were performed using pre-processed TMY2 weather data (Hirsch 2006) for the airport weather stations in these locations.

<sup>14</sup> The daily hot water use varies with location depending on the water mains temperature.

To determine the base-case energy use for the final selection of locations, the simulation model of the base-case house was run with DOE-2.1e system-type “RESYS” in the seventeen selected climate locations. From the DOE-2.1e output, the annual end-use energy use was obtained from the Building Energy Performance Summary in Utility Units (BEPU report), the monthly peak electricity use was obtained from the Plant Monthly Energy End Use Summary (PS-E report), and the monthly peak thermal energy use was obtained from the Systems Monthly Loads Summary (SS-A report, for space heating energy use), and the Load, Energy and Part Load DHW Tank Operation report (SS-P report, for DHW energy use). The annual and monthly peak energy use for the base-case house in these locations are shown as combined space heating and domestic water heating energy use (i.e., thermal loads for the solar thermal system) in Figure 12, and combined space cooling, HVAC fans, lighting, equipment and miscellaneous electricity use (i.e., electricity loads for the PV/wind electricity generation system) in Figure 13.

#### 4.2.4. *Final Selection of Locations*

The final selection of locations considered the simulated base-case annual and monthly peak electricity as well as the thermal energy use in the seventeen climate locations versus the availability of renewable resources indicated in the climate resource maps. To determine the availability of renewable resources, climate resource maps for annual average solar radiation (NREL 2008), wind (Elliot et al. 1986), and rainfall (PRISM Group 2006) were obtained, which are shown in Figure 14 through Figure 16. Based on the base-case heating and cooling energy use, and average solar radiation, wind and rainfall characteristics, six locations were selected for further analysis, which include:

1. Minneapolis, MN (very cold climate), with the largest heating energy use and moderate availability of all resources including solar, wind and rainwater;
2. Boulder, CO (cold climate), with a large heating energy use, high potential of using solar and wind energy resources, but a moderate availability of rainwater;
3. Atlanta, GA (mixed-humid climate), which has significant heating and cooling energy use, a higher solar resource, a limited wind resource, and a good rainwater availability,
4. Houston, TX (hot-humid climate), with high cooling energy use, moderate solar resource, inconsistent (seasonal) wind resource, and a good rainfall availability,
5. Phoenix, AZ (hot-dry climate), which has the highest cooling energy use, a very high solar resource, no wind resource, and a very limited availability of rainwater,
6. Los Angeles, CA (marine climate)<sup>15</sup>, with the minimum heating and cooling energy use, good solar resource, moderate wind resources and very limited availability of rainwater.

---

<sup>15</sup> Climate classification by Briggs et al. (2003) assigns Los Angeles, CA to the hot-dry climate zone because the available land for new development extends into the hot-dry climate zone.

In this manner, the selected locations present a diverse scenario with different needs and availability of energy and water.

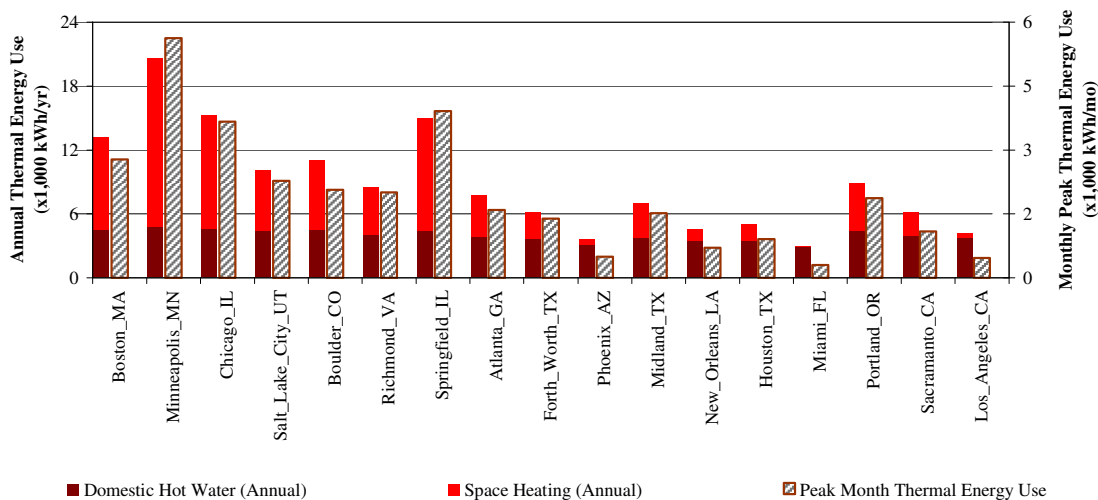


Figure 12 Base-case Annual End-use Energy Use and Peak Monthly Total Thermal Energy Use for Seventeen Locations

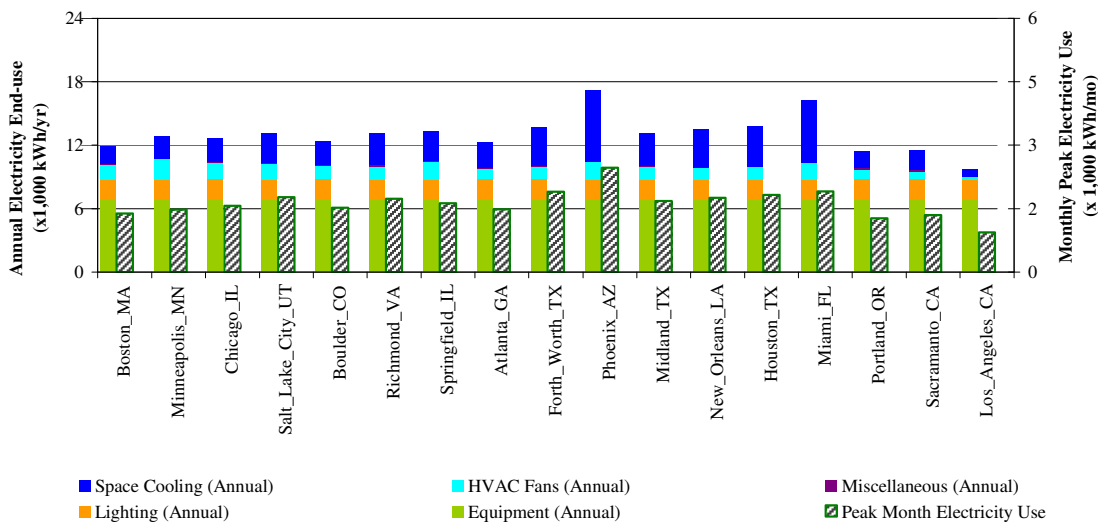


Figure 13 Base-case Annual End-use and Peak Monthly Total Electricity Use for Seventeen Locations

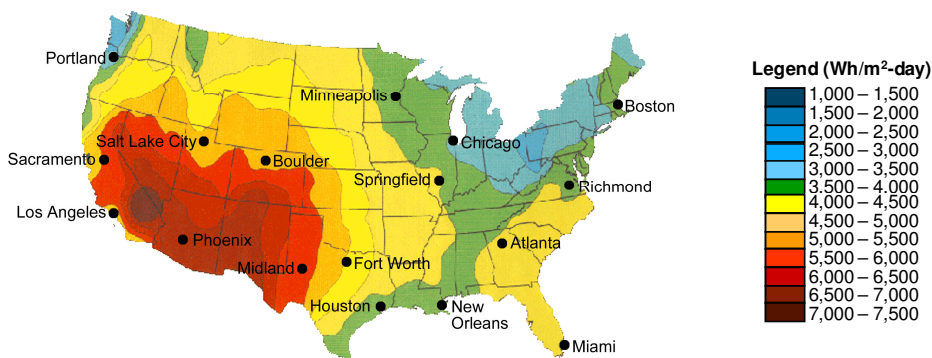


Figure 14 U.S. Annual Average Solar Radiation (1961-1990)<sup>16</sup>

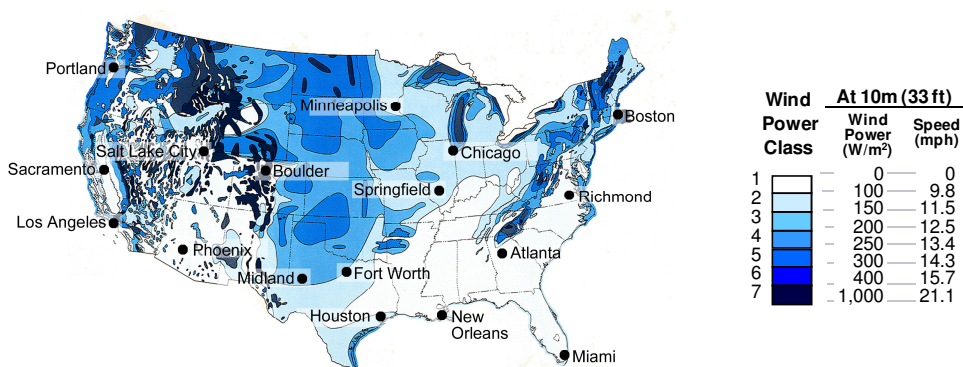


Figure 15 U.S. Annual Average Wind Resource Potential<sup>17</sup>

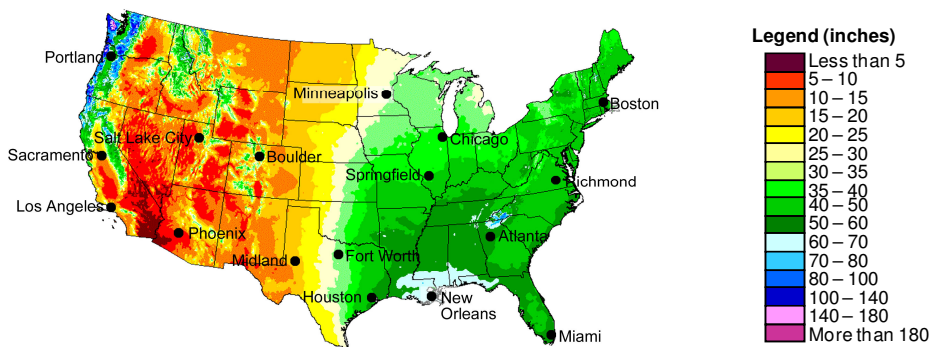


Figure 16 U.S. Annual Precipitation (1971-2000)<sup>18</sup>.

<sup>16</sup> Source: NREL (2008)

<sup>17</sup> Source: Elliott et al. (1986)

<sup>18</sup> Source: PRISM Group (2006). Copyright © 2006 PRISM Group, Oregon State University, <http://www.prismclimate.org>. Map created June 16, 2006 (Reprinted with Permission).

### 4.3. Analysis of Climate Characteristics

The climate characteristics of the six selected locations were investigated as determinants of building heating and cooling loads, as well as the availability of resources for renewable energy and rainwater. Figure 17 outlines the procedure for the analysis of climate characteristics. To begin with, the general climate characteristics of the climate regions corresponding to the selected locations were reviewed from Lechner (2001). In addition, to obtain the necessary data for typical weather conditions, the monthly statistics of several weather parameters were obtained from the following weather data sources:

1. The monthly summary reports, based on TMY2 weather data (US DOE 2008c), for obtaining heating degree day (base 65 °F), cooling degree day (base 50 °F), average dry-bulb temperature, minimum and maximum dry-bulb temperatures (obtained from the average hourly statistics for dry-bulb temperatures), average dew-point temperature, and average daily global horizontal solar radiation;
2. Measured hourly wind and daily rainfall data for 12 years (1997 to 2008) by NOAA (2008), for determining average wind speed and monthly total rainfall; and
3. NASA surface meteorology and solar energy data, for total number of frost days, average number of daylight hours, and surface albedo. These data are available as monthly values based on the average for 22 years (July 1983 to June 2005) of measured data (NASA 2008).

These weather data sources were also used for analyzing the building energy use, the performance of renewable energy systems, the potential of rainwater harvesting; and finally, for the sizing of systems for self sufficiency including the electricity storage. The data for the detailed analysis were processed and formatted, as needed, to be used at different steps throughout the analysis.

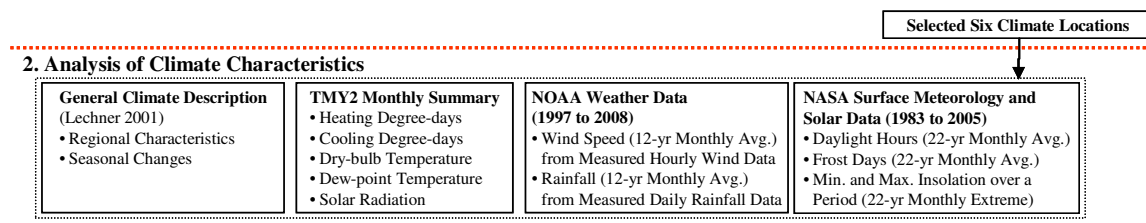


Figure 17 Procedure for Climate Analysis

### 4.4. Selection of Water Efficiency Measures

The procedure for selecting water-efficiency measures is shown in Figure 18. For all location, the base-case indoor water use was assumed to be the same. However, the selection of water-efficiency measures for each location was based on the availability of harvestable rainwater. Considering the large variation in the availability of rainwater among the six selected location, three levels of water-efficiency and conservation measures were considered, including: (i) water-efficient fixtures and appliances, such as



low-flow faucets and showers, low water use clothes washer and dishwasher, (ii) water-efficient fixtures and appliances with greywater reuse for toilets, and (iii) water-efficient fixtures and appliances with greywater recycling for non-potable water use. The indoor water use with water-efficiency measures was investigated by end-use to account for the water use reduction in the associated end-use categories. In this manner, first the total indoor water use was estimated for each level. Then, depending on the normalized sizing parameters (i.e., per unit of average daily water use) for the rainwater harvesting system for each location (which would be derived using the procedure described in Section 4.6.4) the required level of water use reduction was determined, and finally, the selection of water-efficiency measures was made.

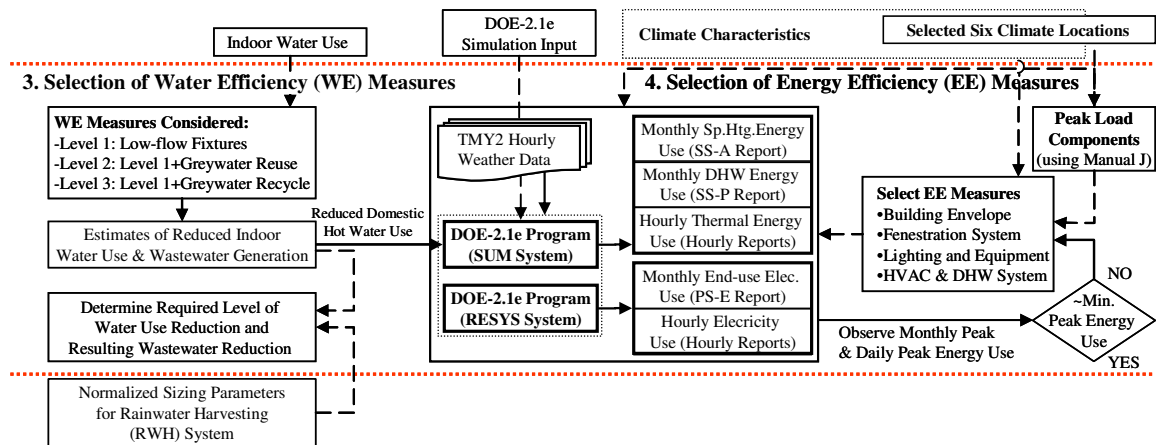


Figure 18 Procedure for the Selection of Water and Energy Efficiency Measures

#### 4.5. Selection of Energy Efficiency Measures

The selection of energy-efficiency measures was aimed to minimize the peak thermal energy and electricity use, in order to minimize the sizing requirements for the renewable energy systems. This required an investigation of the base-case monthly and peak day hourly electricity and thermal energy use as well as the contribution of the building envelope and energy end-use components to the base-case peak heating and cooling energy use. With the peak heating and cooling load components identified, and peak month thermal and electricity use quantified, energy-efficiency measures were selected and applied to base case in order to minimize the peak energy use.

##### 4.5.1. Investigation of the Base-case Energy Use

To investigate the energy use, two sets of simulations were performed for the base-case house using the DOE-2.1e system types SUM and RESYS. The system type SUM simulates building heating and cooling loads considering the thermostat set-points without simulating a system. Thus, it provided space

heating loads excluding the impacts of the efficiency and part-load performance of the heating system. The domestic water heating loads were added to the space heating loads to obtain total thermal loads the active solar thermal system should provide. The system type RESYS with electric cooling and heat pump heating was used to determine the base-case electricity use for space cooling, lighting and equipment, and heating and cooling fans. In addition, the monthly average operating efficiency of the heating system was estimated by dividing the monthly space heating loads by monthly space heating energy use. This estimate was later used for converting the unmet monthly space heating thermal loads (if any, by the active solar thermal system) to the monthly electricity loads, while sizing the PV/wind electricity generation system.

From the DOE-2.1e output using system type SUM, the monthly space heating energy use was obtained from SS-A report, the monthly DHW energy use was obtained from SS-P report, and the peak winter day hourly space heating and domestic water heating loads were obtained from the hourly reports in SYSTEMS for VARIABLE-TYPE = PLANT-ASSIGNMENT and VARIABLE-LIST 2 and 131, respectively. From the DOE-2.1e output with system type RESYS, the monthly end-use electricity use were obtained from PS-E report, and the peak summer day hourly electricity loads was obtained from hourly reports in SYSTEMS for VARIABLE-TYPE = END-USE and VARIABLE-LIST 1, 3, 6, 8, and 9 for lighting, equipment, cooling, miscellaneous and fans, respectively. Table 4 lists the DOE-2.1e reports required for obtaining the various loads.

*Table 4 Sources for Monthly and Hourly End-use Energy Use*

	Monthly Loads		Peak Day Hourly Loads	
	DOE-2 Report	DOE-2.1e Sub-program	VARIABLE-TYPE	VARIABLE-LIST
Outdoor Dry-bulb Temperature	-		GLOBAL	8
Room Temperature	-	LOADS	RM-1 (Name of Space)	1
Attic Temperature	-		ATTIC-1 (Name of Space)	1
Space Heating Loads	SS-A	SYSTEMS	<Name of PLANT- ASSIGNMENT>	2
Domestic Water Heating Loads	SS-P			131
Lighting				1
Equipment				3
Space Cooling Loads	PS-E	SYSTEMS	END-USE	6
Miscellaneous				8
Heating and Cooling Fans				9

#### *4.5.2. Investigation of the Peak Load Components*

The contribution of building envelope and energy end-use components to the base-case peak heating and cooling energy use was investigated in order to identify the potential energy-efficiency measures. For this, the load components for the heating and cooling loads were calculated for the summer and winter design conditions using the Manual J average load procedure (Rutkowski 2004). The

components of the heating and cooling load that were accounted for included: fenestration loads, opaque panel loads (exterior walls, doors, ceiling/roof and slab-on-grade floor), infiltration loads, and internal loads. For the fenestration and opaque panel load calculations, the base-case construction characteristics were used. For calculating infiltration loads, the winter air infiltration rate was assumed as 1.2 times and summer air infiltration rate was assumed as 1.6 times the code-specified annual average air infiltration rate (EnergyGauge USA 2009). For the internal loads, the heat gains from the lighting, equipment and occupants including the corresponding sensible and latent fraction, as specified for the base-case house, were considered.

#### 4.5.3. *Selection of Energy Efficiency Measures*

The selection of energy-efficiency measures was aimed at minimizing the energy needs for the peak months and peak days. To accomplish this, first potential energy-efficiency measures for the building envelope, lighting, appliances, and systems were selected. These include: increased ceiling insulation, structural insulated panels (SIPs) for the exterior walls providing a continuous high insulation and airtight construction, and increased slab perimeter insulation for the cold climate locations. For all locations, heat-mirror glazing<sup>19</sup> with the appropriate thermal properties and vinyl frames were selected. For cold climates, windows with a higher SHGC on the south and a higher U-value on the east, west and north were selected. For warm climates, glazing with a lower SHGC values were selected for all orientations. In addition, moveable window insulation was considered for the cold climate locations.

Similar measures for the lighting, equipment and systems were considered for all locations. This includes: increased number of fluorescent/compact florescent lamps, energy-efficient appliances, a high SEER air-conditioner with a heat pump/electric resistance for the back-up heating, and a high-efficiency water heater for a back-up. In addition, the air-distribution system was located in the conditioned space. These measure were then applied to the base-case simulation model in combination and the reduced peak electricity and thermal energy use were observed.

Next, the building geometry and fenestration system characteristics were fine-tuned. To accomplish this, parametric runs were performed in a combined simulation with the above energy-efficiency measures, by varying the number of stories, building aspect ratio, window distribution on the four sides and the overhang depth. By observing the heating energy use during the peak winter month and cooling energy use during the peak summer month, the optimal design was determined, which would result in a minimum heating requirement during the peak winter month and the least penalty on the cooling requirement during the peak summer month.

---

<sup>19</sup> Heat mirror glazing consists of a low-e film suspended inside an insulating glass unit, resulting in a triple unit with two airspace's.

#### 4.6. Quantification of On-site Harvestable Renewable Resources

The availability of renewable resources for a location can be assessed from the climate resource maps and weather data. However, the potential of utilizing these resources for achieving self-sufficiency depends on the performance of the systems used for harvesting these resources at that climate location for the given installation conditions. Therefore, several renewable energy system types/components were reviewed to select the ones with higher performance ratings. The performance of the selected systems was then quantified in the six selected locations for varying installation conditions. In addition, normalized system sizing parameters (i.e., sizing requirements per unit of daily water use) were derived for the rainwater harvesting system.

Figure 19 shows the procedure for quantifying on-site harvestable renewable resources. In general, the analysis was performed for the six selected climate locations using the selected renewable energy system characteristics and varying installation configurations. The harvestable solar thermal energy was quantified for an active solar thermal system with two types of collectors (i.e., a flat plate collector and an evacuated tube collector) tilted at a winter-optimized angle. The analysis was performed using the F-CHART program with TMY2 monthly weather data, and the thermal energy output was obtained for varying collector area.

The harvestable solar energy for electricity generation was quantified for a photovoltaic system with two types of PV panels (i.e., mono-crystalline PV panels and thin-film PV panels) of equal capacity. The analysis was performed using the PV F-CHART program with TMY2 monthly weather data, and the electricity output was obtained for varying panel tilts. The harvestable wind energy for electricity generation was quantified for two wind turbines of different capacities and at different tower heights (i.e., a 7.5 kW wind turbine at 60 ft. tower height, and a 2.5 kW wind turbine at 40 ft. tower height). The analysis was performed using the wind turbine power curves with the histogram of wind speed corrected for the local terrain, which was developed using measured hourly wind data obtained from the NOAA

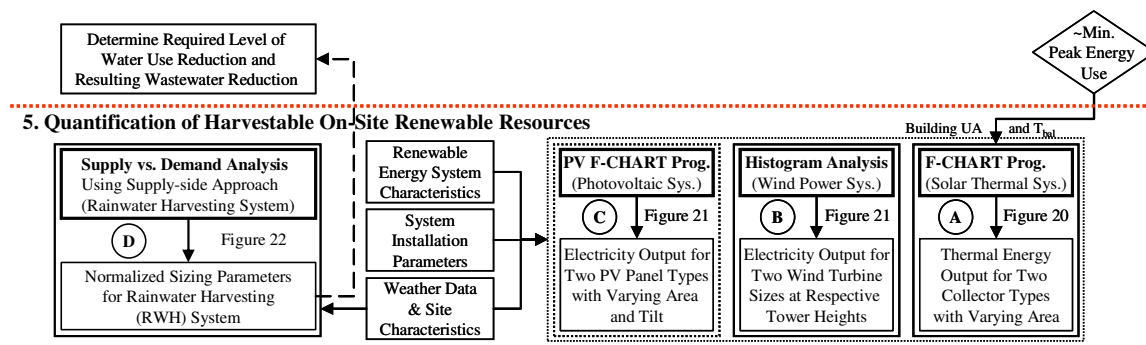


Figure 19 Procedure for the Quantification of On-site Harvestable Renewable Resources

weather stations. The normalized sizing parameters for the rainwater harvesting system were derived using the supply versus demand analysis with the supply-side approach (Gould and Nissen-Petersen 1999) (i.e., assuming full utilization of the harvested rainwater, and comparing the rainwater supply with the average demand fulfilled) and the measured daily rainfall data obtained from the NOAA weather stations.

#### 4.6.1. *Analysis of the Active Solar Thermal System*

The procedure for analyzing the performance of solar thermal system using the F-CHART program is shown in Figure 20. It shows three main tasks including: i) selection of solar collectors with higher performance ratings, ii) determination the F-CHART input parameters, and iii) interpretation of the F-CHART results for use while sizing the solar thermal system.

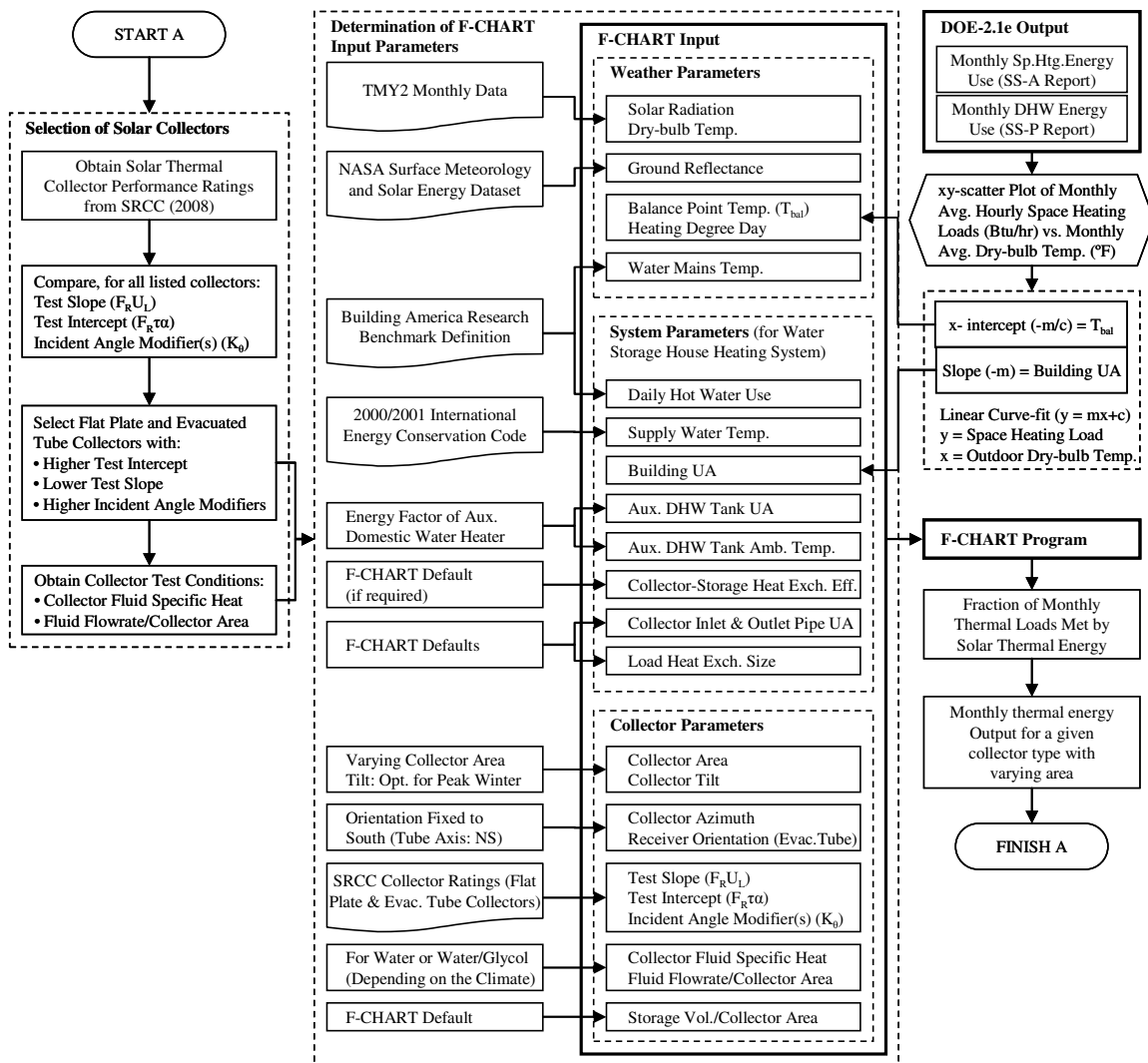


Figure 20 Procedure for Analyzing Solar Thermal System

#### 4.6.1.1. Selection of Solar Collectors with Higher Performance Ratings

The characteristics of a solar thermal collector, which determine the performance of the system in different climates, are: (i) test intercept ( $F_R\tau\alpha$ ), which represents the efficiency of the collector; and (ii) test slope ( $F_RU_L$ ), which represents the heat loss from the collector surface. In addition, the incident angle modifiers ( $K_\theta$  or  $(\tau\alpha)/(\tau\alpha)_n$ ) represent how the collector efficiency is modified with the position of the sun from east to west during a day and north to south over a year. For an increased output, collectors with a higher test intercept, a lower test slope and higher incident angle modifiers are desirable.

Considering that the collectors are available with a broad range for these parameters, a number of collectors were reviewed using the collector ratings listed in SRCC (2008), and two flat plate collectors and two evacuated tube collectors with higher performance ratings (i.e., with the highest test intercept and the highest test slope from each collector type category) were selected.

#### 4.6.1.2. Determination of the F-CHART Input Parameters

The F-CHART program requires three sets of input parameters, which include: weather parameters, system parameters, and collector parameters. A description of these sets of parameters and the use of these parameters for the F-CHART calculations are described below:

1. *Weather Parameters:* These include climate and location specific parameters (latitude, monthly average values for global horizontal daily solar radiation ( $H_o$ ), dry-bulb temperature ( $T_{DBT}$ ), water mains temperature ( $T_{mains}$ ), and ground reflectance ( $\rho_g$ ); and parameters that reflect the interaction of the building with the climate elements (i.e., the balance point temperature ( $T_{bal}$ )<sup>20</sup> for space heating and corresponding monthly heating degree days ( $HDD_{Tbal}$ )<sup>21</sup>).
2. *System Parameters:* These include parameters for determining the space heating loads (building heat loss coefficient (building UA)<sup>22</sup>) and domestic water heating loads (daily hot water use ( $V_{supply}$ ), supply water temperature ( $T_{supply}$ ), auxiliary DHW tank ambient temperature ( $T_{amb,tank}$ ) and heat loss coefficient of the auxiliary DHW tank (aux. tank UA)) on the system; the heat loss coefficient of the hot water supply and return pipes, and the characteristics of the collector-storage heat exchanger (if present) and the load heat exchanger.
3. *Collector Parameters:* These include the collector installation parameters (i.e., the area, tilt and orientation of the collector; and the specific heat and flow rate of the heat transfer fluid, as installed) and collector performance parameters (i.e., test slope ( $F_RU_L$ )<sup>23</sup>, test intercept ( $F_R\tau\alpha$ )<sup>24</sup>, and incident

<sup>20</sup> Balance point temperature ( $T_{bal}$ ) indicates the temperature at which the heat loss through the envelope is balanced by solar, infiltration and internal heat gains.

<sup>21</sup> In F-CHART, an algorithm by Erbs et al. (1983) calculates monthly heating degree-days at a given base temperature ( $HDD_{Tbal}$ ) using monthly ambient temperatures.

<sup>22</sup> Building UA represents the overall heat loss coefficient of the building (including the combined effect of infiltration, internal heat gains, solar heat gains), and indicates an increase in space heating loads per unit decrease in ambient temperature.

<sup>23</sup> The test slope represents the heat loss from the collector surface.

<sup>24</sup> The test intercept is the maximum efficiency the collector can achieve when there is no heat loss to the ambient.

angle modifier(s) ( $K\tau\alpha = (\tau\alpha)/(\tau\alpha)_n$ ) for the collector; and the specific heat and flow rate of the heat transfer fluid during the collector test).

In the F-CHART program, the calculations are performed for an average day for each month and summed for the number of days of the month ( $N_{\text{month}}$ ). For each month, first the collector parameters (tilt and azimuth) are used with the location and weather data (i.e., latitude,  $H_o$  and  $\rho_g$ ) to determine daily incident radiation on the collector plane ( $H_T$ ). Then, the system parameters are used with weather data to determine the monthly total thermal loads on the system ( $L$ ). These include: i) space heating loads (building  $UA * HDD_{Tbal}$ ), ii) domestic water heating loads ( $V_{\text{supply}} * (T_{\text{supply}} - T_{\text{mains}}) * N_{\text{month}}$ ), and iii) DHW auxiliary tank standby losses, ( $\text{auxiliary tank } UA * (T_{\text{supply}} - T_{\text{amb,tank}}) * N_{\text{month}}$ ).

Next, the collector test slope ( $F_R U_L$ ) and test intercept ( $F_R \tau\alpha$ ) are modified to take into account the installation factors, which include: i) heat transfer fluid characteristics ( $C_p$  and  $\dot{m}$ ), if different from the collector test conditions, and ii) hot water supply and return pipe  $UA$ . In addition, other correction factors are calculated, which include: iii)  $F_R / F_{Rc}$ , for collector-storage heat exchanger, if present, iv)  $(\tau\alpha)/(\tau\alpha)_n$ , for collector incident angle modifiers, v) hot water storage volume per unit of collector area, if different from the F-CHART standard assumption (i.e., 75 liters per square meter of collector area), and vi) load heat exchanger effectiveness ( $\epsilon_L$ , if different from F-CHART standard assumption)<sup>25</sup>.

Using the collector area, loads, average incident radiation, dry-bulb temperature, and all the correction factors determined above, the dimensionless variables  $X$  and  $Y$  are calculated. Finally, the fraction of loads met by solar  $f$ , is obtained from correlations between the variables  $X$  and  $Y$ . The equations used in F-CHART calculations are listed in Appendix E.

For the F-CHART weather parameters, TMY2 monthly data for average daily global horizontal solar radiation and average dry-bulb temperature were used. The monthly average water mains temperatures were obtained using the procedure described in Section 4.2.2.4<sup>26</sup>. For the ground reflectance, monthly average values for surface albedo, obtained from NASA (2008), were used. The balance point temperature for space heating was obtained from the DOE-2.1e simulation results, as described below while determining the F-CHART system parameter – building  $UA$ .

For the F-CHART systems parameters, the domestic hot water loads were specified using a 120 °F supply water temperature, the monthly average daily domestic hot water use was obtained from the procedure described in Section 4.2.2.4<sup>26</sup>. The auxiliary tank  $UA$  was calculated from the energy factor of the auxiliary water heater using the water heater analysis model (WHAM) by Lutz et al. (1998). The auxiliary tank environment temperature of 73 °F was used, which assumed that the auxiliary storage tank was located in the conditioned space.

<sup>25</sup> The f-chart for liquid system was developed with  $\epsilon_L * C_{\text{min}} / (UA)_h = 2$ , where  $(UA)_h$  is building  $UA$  and  $C_{\text{min}}$  is the minimum fluid-capacitance rate ( $mC_p$ )<sub>min</sub> in the load heat exchanger, generally that of the air.

<sup>26</sup> The monthly water mains temperatures are calculated in Appendix B.

For specifying the space heating loads in F-CHART, the system parameter - building UA and the weather parameter - balance point temperature were obtained from the DOE-2.1e simulation results for the system-type SUM. As explained in Section 4.2.3, the system-type SUM, the energy use can be obtained without simulating a system, and thus the efficiency and part-load performance of the system does not impact the results. From the DOE-2.1e SYSTEMS monthly load summary report (SS-A), the monthly space heating energy use (MMBtu/month) was obtained and converted to monthly average hourly space heating energy use (Btu/h). These twelve monthly average hourly values were plotted on an x-y scatter plot against monthly average dry-bulb temperatures. From the three-parameter, change-point, linear curve-fit to the twelve data points, using the ASHRAE's Inverse Modeling Toolkit (IMT) (Kissock et al. 2003), the slope and intercept were obtained that represent building's total heat loss coefficient (building UA) and balance-point temperature ( $T_{bal}$ ), respectively.

For the F-CHART collector parameters, the SRCC collector ratings datasheets for the selected collectors were used to obtain the test slope, test intercept, and incident angle modifiers of the collector, and the specific heat and flow rate of the heat transfer fluid during the collector test. The collector orientation was oriented due south, and the collector tilt for each location was determined to ensure a maximum thermal energy output during the peak winter month. The collector area was varied in order to compare the collector utilization during different months of the year for varying system sizes.

#### *4.6.1.3. Interpretation of the F-CHART Results*

Using the above F-CHART input parameters for the selected collector types and varying collector area, the fraction ( $f$ ) of thermal loads met by the solar thermal energy was obtained by month for the six selected climate locations. By multiplying the monthly fractions with the thermal loads, the monthly solar thermal system output could be obtained. Since the fraction  $f$  is reported as 1 for monthly thermal energy output exceeding the loads (which is likely to occur for large collector areas during the summer), the absolute thermal energy output in such cases cannot be determined directly from the F-CHART results without further modifications to the system configuration. Therefore, for these cases, the absolute thermal energy output was estimated by extrapolating the results for smaller collector areas for the same months. In this manner, the monthly thermal energy output for two collector types and varying collector area was obtained for the six selected climate locations, which would guide the sizing of the solar thermal system.

#### *4.6.2. Analysis of the Photovoltaic System*

The procedure for analyzing the performance of a photovoltaic system is shown in Figure 21. It shows three main tasks including: i) selection of PV panels with higher performance ratings, ii) determination the PV F-CHART input parameters, and iii) interpretation of the PV F-CHART results for use while sizing the PV system.



The characteristics of the PV panels that determined their performance in different climates are: (i) the panel reference efficiency that represents the efficiency of converting incident radiation into electricity ( $\eta_r$ ) at reference condition, (ii) the panel's temperature coefficient ( $\beta$ ) that represents the performance degradation of PV cells at high temperatures, and (iii)  $T_{NOCT}$  - the cell temperature at NOCT (nominal operating cell temperature) conditions (i.e., 800 W/m<sup>2</sup>, 20 °C ambient air temperature, and 1 m/s wind velocity). For increased output, a higher reference efficiency, a lower temperature coefficient, and a lower cell temperature are desirable. In general, mono-crystalline PV cells have higher efficiencies and thin-film PV panels have lower temperature coefficients. Therefore, thin-film PV cells perform better in hot climates compared to mono-crystalline PV cells of equal capacity. Furthermore, thin-film PV cells are less sensitive to the light intensity and shading conditions, and perform better in diffuse light compared to mono-crystalline PV cells. Therefore, both types of PV panels were considered for the analysis.

The sizing of the photovoltaic system was performed using the PV F-CHART program with TMY2 weather data. The PV F-CHART input included: i) the PV panel characteristics - array reference efficiency, cell temperature at NOCT condition, array reference temperature, and the maximum power temperature coefficient (obtained from the manufacturer's specifications); ii) the PV system parameters - efficiency of the maximum power point electronics and power conditioning electronics, using the PV F-CHART defaults; and iii) installation parameters – array area for equal capacity, varying array slope and array azimuth facing due south. With these inputs, the monthly PV system electricity output was determined using a stand-alone system under no load conditions.

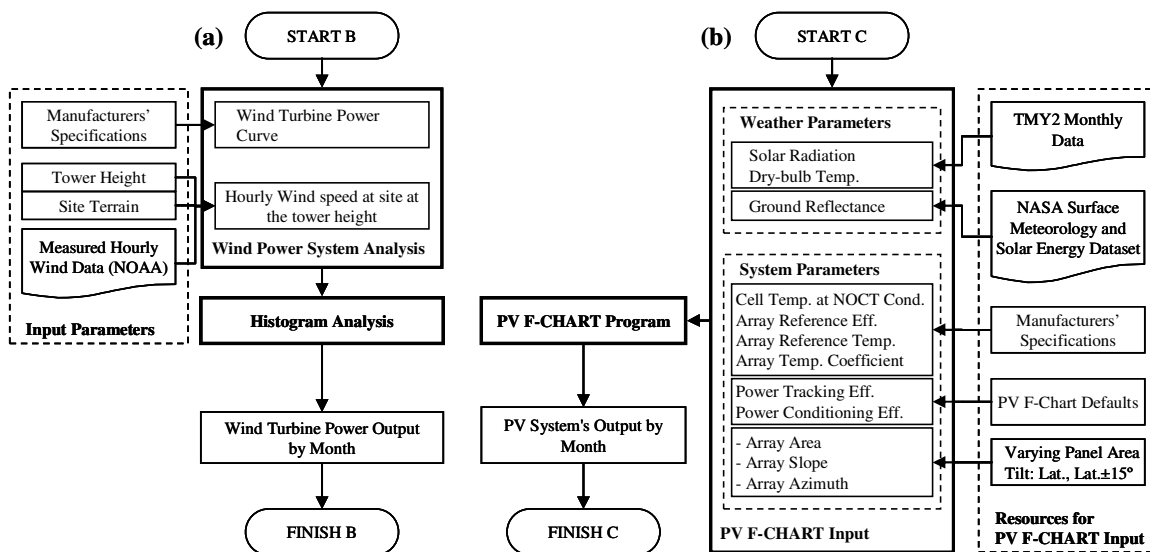


Figure 21 Procedure for Analyzing the (a) Wind Power System, and (b) Photovoltaic System

#### 4.6.3. *Analysis of the Wind Power System*

In general, residential wind turbines with smaller rated capacities (i.e., less than 5 kW) have a lower cut-in wind speed, and are therefore more suitable for grid-connected applications in urban locations where the wind speed is usually lower than in rural areas. For off-grid residential applications, wind turbines of larger capacities (up to 10 kW) are preferred, which could provide a large portion of the household electricity needs. However, such turbines have a higher cut-in speed, and may require auxiliary power for the start-up. Considering that this study is based on six climate locations with different wind and solar resource availability (i.e., wind power system would be providing a large or small part of the electricity needs of the house), wind turbines with different rated capacities were analyzed. For each turbine, product specifications and power curves were obtained from the manufacturer's product data sheets. From the comparison of the power curves, wind turbines from two different capacity range were selected that have lower cut-in speed and higher power output at lower wind speeds.

To analyze the performance of wind turbines at the site, hourly wind speeds at the site at the tower height should be used. Therefore, the measured hourly wind speed data obtained from the NOAA airport weather station<sup>27</sup> for each location were corrected to account for the local terrain and tower height. The corrected wind speed was calculated using the equation found in ASHRAE (2005). According to this equation, the hourly average wind speed  $U_H$  at height  $H$  above the local obstacles, weighted by the plan area, assuming an undisturbed approaching wind in the local terrain, can be calculated from the hourly wind speed  $U_{met}$  from a nearby meteorological station as follows:

$$\text{Equation 1: } U_H = U_{met} \left( \frac{\delta_{met}}{H_{met}} \right)^{a_{met}} \left( \frac{H}{\delta} \right)^a$$

where,  $H_{met}$  is the anemometer height at the meteorological station (which is 33 ft. above ground level for the NOAA weather stations) that records  $U_{met}$ .  $\delta_{met}$  - the wind boundary layer thickness, and  $a_{met}$  - the exponent are the atmospheric boundary layer parameters for the meteorological station (which are 900 ft. and 0.14, respectively, for a flat, open terrain of the NOAA weather stations). The wind boundary layer thickness  $\delta$  and the exponent  $a$  are for the building site (which are 1,200 ft. and 0.22, respectively, for the suburban terrain). Substituting these values in Equation 1, the average hourly wind speed at the tower heights 40 ft. and 60 ft. can be calculated from:

$$\text{Equation 2: } \begin{aligned} U_{40ft} &= 0.752 \cdot U_{met} \\ U_{60ft} &= 0.822 \cdot U_{met} \end{aligned}$$

---

<sup>27</sup> The hourly measured wind speed are the average wind speed for the most recent two-minute period prior to the observation time (calculated from a series of 24 five-second average values).

Equation 3:

$$P_{40ft} = (0.752)^3 \cdot P_{met} = 42.5\% \text{ of } P_{met}$$

$$P_{60ft} = (0.822)^3 \cdot P_{met} = 55.5\% \text{ of } P_{met}$$

To determine the wind turbine output<sup>28</sup>, first the histogram of hourly wind speed at site at the tower height was plotted for each year using wind speed bins of one mile per hour, and the critical year with higher wind speed frequencies at lower wind speeds was identified for each location. Using the wind turbine power curves for the selected wind turbines with the wind speed histogram for the critical year, the annual electricity output from the wind turbines was calculated. This provided an estimate for the harvestable wind resource for different locations using wind turbines of different capacities. Furthermore, monthly electricity output from the selected wind turbines was calculated for the critical year in the same manner. These monthly estimates were compared with the monthly electricity needs of the house in order to determine the appropriate wind turbine capacity and number to be installed, and calculate the remaining electricity loads for the sizing of PV system.

#### 4.6.4. Analysis of the Rainwater Harvesting System

The major sizing components of a rainwater harvesting system include: the catchment area and rainwater storage volume. The parameters for sizing these components include: i) rainfall characteristics (i.e., quantity and distribution over a year), ii) catchment surface characteristics (e.g., area and run-off coefficient), and c) the water demand for indoor and outdoor use. The variation in the rainfall characteristics from year-to-year indicates the degree of utilization of the designed system over a period. Using water-efficiency and conservation measures, water demand can be reduced significantly, which reduces the sizing requirements and maximizes the utilization of the rainwater harvesting system.

To achieve self-sufficiency for indoor water use, the sizing should be performed for critical rainfall conditions (i.e., the minimum annual rainfall and the longest dry-period), However, for a given location, these critical conditions may not occur during a single year. In addition, the water demand for the system sizing calculations would be undetermined at this point, since the level of water use reduction would be determined based on the availability of harvestable rainwater. Therefore, normalized values of the catchment area and rainwater storage requirements (i.e., per unit of daily water demand) were calculated, which could address the critical rainfall conditions and be applied to any climate location with different rainfall characteristics, which will help in selecting water-efficiency measures. These sizing parameters would be used with the indoor water use estimates for several levels of water-efficiency measures to determine the required level of water use reduction, and the catchment area and rainwater storage requirements to meet the reduced water demand solely from rainwater.

---

<sup>28</sup> For a simplified estimation of the wind turbine output at a modified wind speed, consider that the turbine power output is proportional to the wind speed. The turbine power output at the above installation conditions can be estimated using:  $P_{40ft} = (0.752)^3 \cdot P_{met} = 42.5\% \text{ of } P_{met}$ ; and  $P_{60ft} = (0.822)^3 \cdot P_{met} = 55.5\% \text{ of } P_{met}$ .

The flowchart shown in Figure 22 demonstrates the steps for the analysis of rainwater harvesting system for a location. The input parameters include measured daily rainfall data and first-flush volume diversion criteria. For each year, the calculations were first performed for a unit catchment area. The resulting values (i.e., the average demand fulfilled from a unit catchment area and the corresponding storage volume requirement) were then converted to normalized catchment area and storage volume requirements (i.e., per unit of daily water demand) for each year. These two sets of estimates for twelve years provide the minimum-maximum range for the catchment area and the storage volume requirements, respectively. The largest of the values from the two sets were used as normalized system sizing parameters, which represent the critical rainfall conditions in terms of the amount of harvestable rainwater and length of dry-period, respectively.

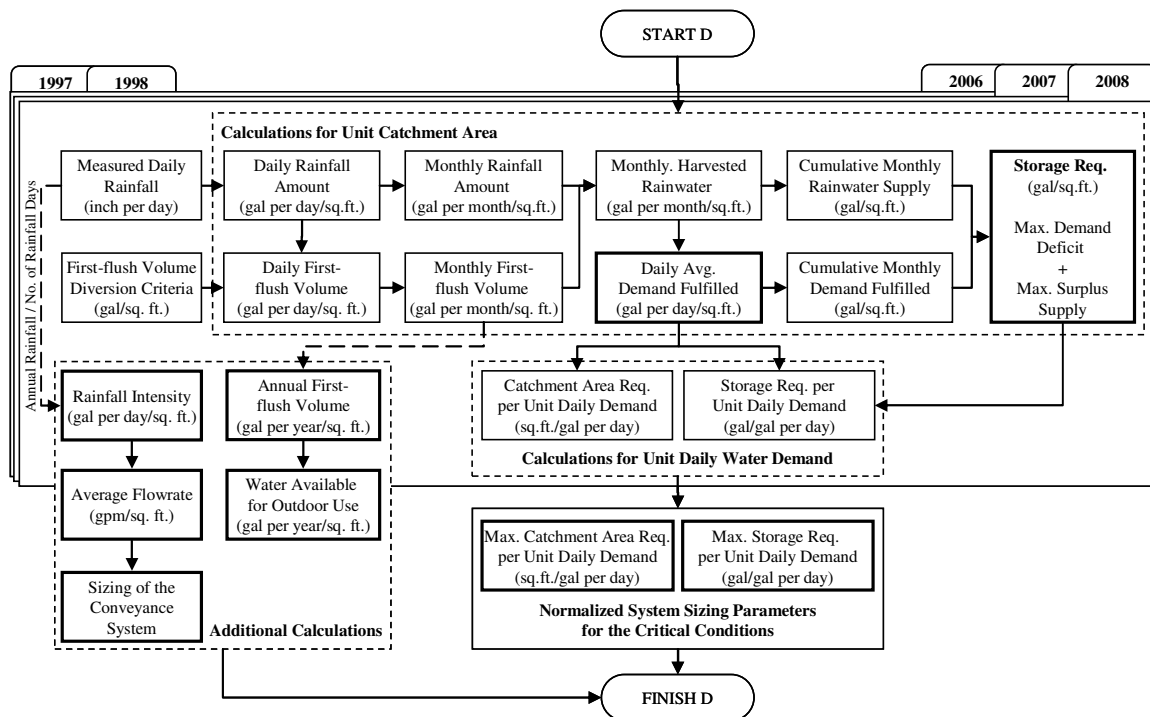


Figure 22 Procedure for Deriving Normalized Sizing Parameters for the Rainwater Harvesting System

#### 4.6.4.1. Calculations for a Unit Catchment Area

The procedure for determining rainwater storage volume for a year is graphically represented in Figure 23, which follows the steps for the calculations for unit catchment area shown in Figure 22. First, the measured daily rainfall data (in inches per day) for several years were obtained from NOAA (2008),

and converted to daily and monthly amounts of rainfall per unit of catchment area (gal per day/ft<sup>2</sup> and gal per month/ft<sup>2</sup>, respectively).

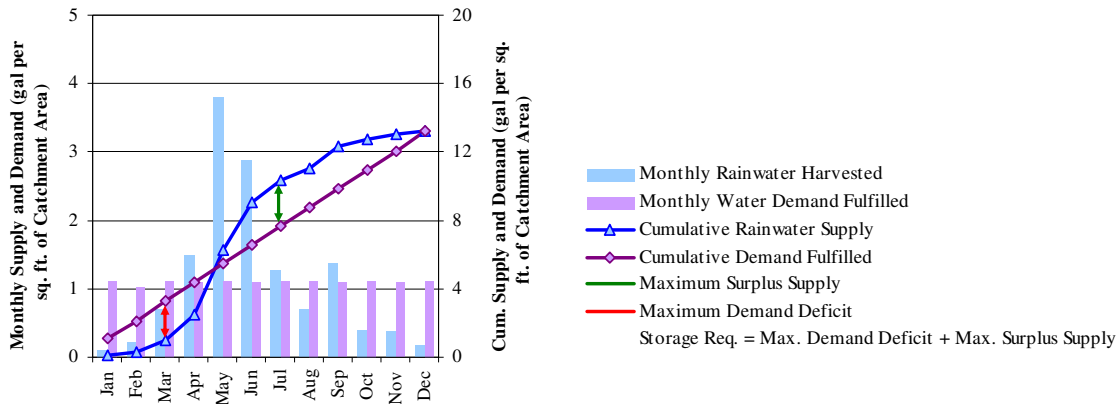


Figure 23 Procedure for Determining Rainwater Storage Volume based on One-year Rainfall Data

To determine the amount of harvestable rainwater, a criteria for the first-flush volume diversion was established. For this study, the criteria of up to one gallon of first-flush volume for every 100 ft<sup>2</sup> of catchment area diverted after a three-day dry-period was used for all locations. Using this criterion with the daily occurrence of rainfall, the first-flush volume diverted per unit of catchment area was estimated and summed for each month. By deducting the first-flush volume from the amount of available rainwater each month, the monthly harvestable rainwater per unit of catchment area (gal per month/ft<sup>2</sup>) was obtained (shown as blue bars in Figure 23). These values were used to calculate the cumulative harvestable rainwater (the curved line plot in Figure 23, which follows the rainfall distribution over a year). Considering full utilization of the harvested rainwater over a year, the average monthly total demand that could be met by the rainwater accumulated per unit catchment area (gal per month/ft<sup>2</sup>) was calculated (as shown as purple bars in Figure 23), and used to determine cumulative demand fulfilled, which is the straight line plot in Figure 23. For each month, the two cumulative values (or plots) were compared to obtain the maximum demand deficit and maximum surplus supply for a unit catchment area (gal/ft<sup>2</sup>). By adding these two quantities, the rainwater storage size per unit of catchment area (gal/ft<sup>2</sup>) required to fully store the harvestable rainwater and provide for the yearlong demand was obtained. In this manner, the daily average demand fulfilled per unit of catchment area (gal per day/ft<sup>2</sup>) and rainwater storage requirement per unit of catchment area (gal/ft<sup>2</sup>) were obtained.

#### 4.6.4.2. Calculations for a Unit Water Demand

Using the daily average demand fulfilled per unit of catchment area (gal per day/ft<sup>2</sup>) and rainwater storage requirement per unit of catchment area (gal/ft<sup>2</sup>) for each year, the catchment area and rainwater storage requirements were calculated using Equation 4 and Equation 5, respectively:

Equation 4: Catchment Area per Unit Water Demand (ft<sup>2</sup>/gal per day)

$$= [\text{Daily Average Demand Fulfilled per Unit Catchment Area (gal per day/ft}^2)]^{-1}$$

Equation 5: Rainwater Storage Requirement per Unit Water Demand (gal/gal per day)

$$= \left( \frac{\text{Storage Requirement per Unit Catchment Area (gal/ft}^2)}{\text{Daily Average Demand Fulfilled per Unit Catchment Area (gal per day/ft}^2)} \right)$$

#### 4.6.4.3. Determination of Normalized System Sizing Parameters

From these calculations performed for each year, the minimum-maximum range for the normalized sizing requirements were determined, which demonstrated the extreme rainfall conditions in terms of the amount of harvestable rainwater and length of dry-period for a location. The maximum values for the catchment area and rainwater storage requirements were used as the normalized system sizing parameters for the critical conditions.

### 4.7. Sizing and Integration of Systems for Self-sufficiency

Based on the on-site harvestable renewable resources and reduced building needs, the sizing of renewable energy, rainwater harvesting and sewage disposal systems was performed to achieve self-sufficiency, using the procedures described in the following sections. Figure 24 shows the procedure for the sizing and integration of systems for self-sufficiency.

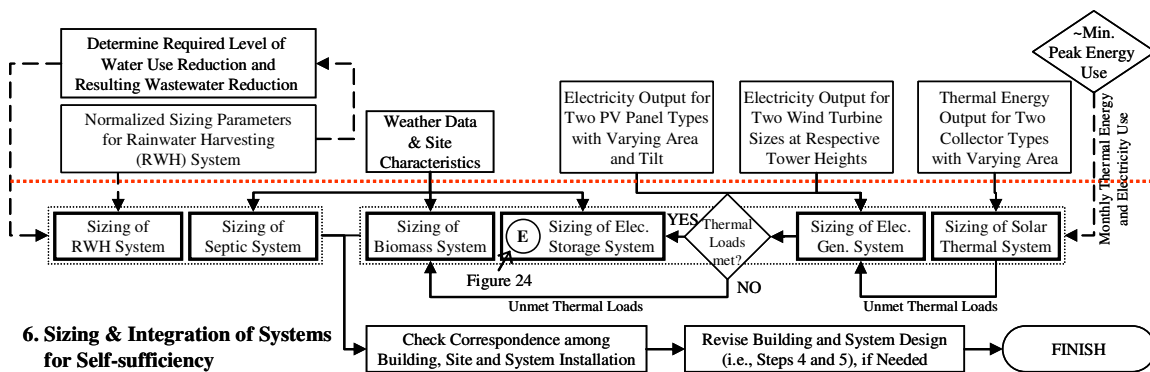


Figure 24 Procedure for the Sizing and Integration of Systems for Self-sufficiency

#### 4.7.1. *Sizing of the Solar Thermal System*

For the sizing of solar thermal system, the minimized monthly thermal energy needs of the house were compared with the monthly thermal energy output from the two collector types with varying collector area. For locations with large winter heating loads, the use of a larger collector area would result in smaller collector utilization on an annual basis, unless the thermal energy output from the collector during the summer was utilized. Since this study does not include the analysis of solar thermal cooling systems, a smaller collector area was considered, which could provide the peak winter thermal energy needs as much as possible, while ensuring that the unused summertime thermal energy is as small as possible. The remaining (unmet) monthly thermal loads were carried over to monthly electricity loads (using a conversion factor to account for the monthly operating efficiency of the electric heating system – a heat pump with supplementary electric resistance) for sizing the PV/wind electricity generation system. In addition, the electricity use for operating the solar thermal pumps was added to the electricity needs. The analysis then assumed that the remaining (unmet) electric heating energy requirements (if any) would be met by an auxiliary biomass-based heating system.

#### 4.7.2. *Sizing of Electricity Generation System*

The off-grid house used in this analysis requires electricity for operating the cooling system, heating and cooling fans, lighting and appliances, pumps for the solar thermal system, water supply pressurization pump, and equipment for the treatment of the harvested rainwater. For electricity generation, photovoltaic and wind power systems were considered based on the availability of solar radiation and wind. After determining the potential system type (i.e., photovoltaic, wind or hybrid), the sizing of systems was performed to exceed the daily electricity needs and provide for days with inadequate solar radiation and/or wind.

For the sizing of PV/wind electricity generation system, first the monthly electricity needs of the house were determined, which included the minimized electricity needs for space cooling, lighting and equipment, HVAC fan, and miscellaneous (obtained from the DOE-2.1e simulation results), the electricity use for operating the solar thermal pump<sup>29</sup> (NRC 2004) and the water supply pressurization pump, and the unmet thermal loads (from Section 4.7.1). The monthly electricity use was then compared with the monthly electricity output from wind turbines of different capacities and photovoltaic systems with two panel types with varying array area and tilt.

---

<sup>29</sup> According to NRC (2004), the pumping energy for an active solar thermal system can be computed as:  $Q_{\text{pump}} = N_{\text{coll}} * P_{\text{pump}} * A_c$ , where  $N_{\text{coll}}$  = number of hours per year the collector is in operation =  $[Q_{\text{dtd}} * (1 + f_{\text{ios}}) / (A_c * F_R(\tau\alpha) * H_T)] * N_{\text{daytime}}$ ;  $P_{\text{pump}}$  = pumping power per collector area =  $5 \text{ W/m}^2$  (assumed);  $A_c$  = collector area;  $Q_{\text{dtd}}$  = energy delivered to the system;  $f_{\text{ios}}$  is the fraction of solar energy lost to the environment through piping and tank = 10% (assumed),  $F_R(\tau\alpha)$  = collector efficiency without losses;  $H_T$  = monthly average daily solar radiation incident on collector surface; and  $N_{\text{daytime}}$  = number of daytime hours for the month.

For locations with wind and solar as potential resources, first the capacity and number of the wind turbines were determined to provide a significant part of the electricity needs for the months when photovoltaic system output was small compared to the electricity needs (which was likely to occur during peak winter and/or peak summer months). Then, the remaining electricity needs (or the total building electricity needs, if the wind electric system was not considered ) were compared with the monthly output from the photovoltaic system. Based on the comparison, the panel type<sup>30</sup> and tilt<sup>31</sup> were determined and the array area was scaled in order to meet/exceed the remaining loads for all months.

In general, for locations having significant wind turbine electricity output, one large or multiple smaller wind turbines were considered, depending on the monthly turbine electricity output per installed capacity (kWh/kWp). The tilt of the PV array was determined depending on the monthly electricity use. For locations having large summer electricity needs, a tilt favoring the summer was considered. On the other hand, for locations having large/comparable winter electricity needs (mostly due to unmet thermal loads), a panel tilt of higher than the latitude angle was considered. For locations with very large winter thermal loads, where higher panel tilt could not provide much benefit during the winter, compared to the reduced production during the summer, the panel tilt was optimized for the summer, leaving the unmet thermal loads for a biomass-based heating system.

#### 4.7.3. *Sizing of Biomass-based Heating System*

For the biomass-based heating system, wood pellets were considered which have a heating value of 8,200 Btu/lb (Biomass Energy Center 2008). The amount of wood pellets required to provide the unmet heating loads were then calculated. To produce the estimated amount of wood pellets using the on-site harvested vegetation, provisions for the harvesting, drying and manufacturing of the wood pellets would be required. This would require additional electricity from the house. However, the harvesting and production of the wood pellets most likely would occur during the summer or fall when there is ample electricity from the PV system and wind turbines. The growth of the vegetation for the wood pellets depends on the soil, rainfall conditions and climate.

#### 4.7.4. *Sizing of Electricity Storage System*

The sizing requirement for the electricity storage system was determined to store surplus electricity generated during periods of high solar insolation, and to provide electricity during periods when the weather is not favorable for electricity generation<sup>32</sup>. Figure 25 shows the procedure for the sizing of electricity storage system. To determine the total electricity use the system must support, the maximum number of equivalent NO-SUN days (obtained from NASA (2008)) over a consecutive-day period was

---

<sup>30</sup> For hot climates, thin-film PV panels were considered, and for cold climates, mono-crystalline PV panels were considered.

<sup>31</sup> For climates with large winter-time electricity needs, a higher tilt was considered.

<sup>32</sup> For this study, the sizing of electricity storage system was performed considering only the periods with extreme solar radiation. The availability of wind during these periods was not taken into account.



multiplied with average daily electricity needs for each month (obtained from DOE-2 output). The largest of these monthly cumulative electricity needs was used as the required capacity of electricity storage system. For determining the number of batteries, several other parameters needed to be determined including: battery efficiency due to charge/discharge cycle, allowable depth-of-discharge, performance of the batteries as affected by the extreme winter conditions, battery voltage and system voltage to be used.

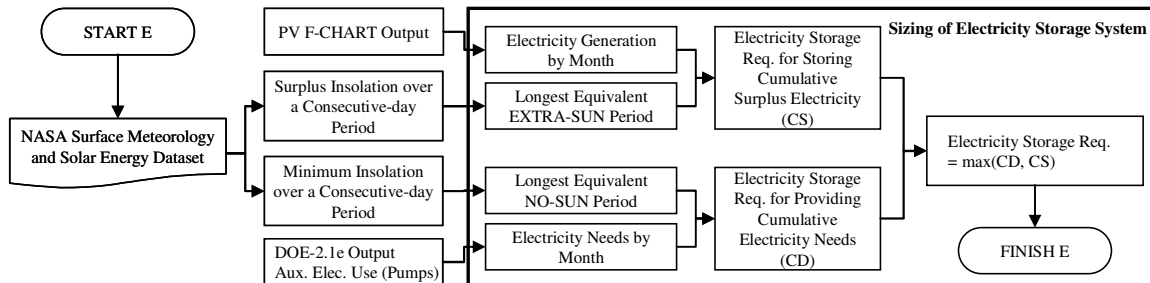


Figure 25 Procedure for the Sizing of Electricity Storage System for the PV Electricity Production

#### 4.7.5. Sizing of the Rainwater Harvesting System

The two normalized system sizing parameters obtained in Section 4.6.4.3 were used for determining the level of water use reduction and/or the increase in the catchment area required to meet the annual water demand. First, the catchment area per unit of water demand was compared with the available roof area (based on the building configuration determined in Section 4.5.3) and the three levels of water use reduction (estimated in Section 4.4). Based on this comparison, the required level of water use reduction versus the need for increasing the catchment area was evaluated. The reduction of water use was considered first, which would scale-down the rainwater storage requirement. For increasing the catchment area, the use of possible above-grade catchment surfaces such as the roof of the garage, storage rooms, porch, barns, and possible custom-designed ground catchment surfaces were considered. The estimation of the catchment area requirement for all surfaces was made by taking into account their run-off coefficients. Finally, the size of storage tank was estimated by multiplying the normalized storage volume with the reduced daily water use as determined above. This would ensure that the daily indoor water needs were met for the year with minimum annual rainfall and the cumulative water needs were met for the longest dry season.

In addition, an estimation of annual first-flush volume from the total catchment surface area was made, which could be used for outdoor water use. Finally, the average rainwater flow rate was estimated from the rainfall intensity for each catchment area, which guided the sizing of rainwater conveyance system from the catchment area(s) to the storage tank(s).

#### 4.7.6. *Sizing of Sewage Disposal System*

The need for sewage disposal is proportional to the indoor water use. The sizing of a sewage disposal system depends on the type of system used and the characteristics of the soil in the leaching field. For this study, a septic tank with a leaching field (i.e., an anaerobic system) was considered for all locations<sup>33</sup>. The amount of sewage generation in the six selected locations was estimated to account for the reduced indoor water use (which was determined based on the normalized sizing parameters derived for the rainwater harvesting system, combined with the area available for rainwater collection). After consideration of the level of water efficiency measures for the selected locations, the reduced design flows were calculated, and the septic tank size was determined.

#### 4.7.7. *Checking Inter-relationship of the Building, Site and Systems*

Finally, the inter-relationship of the building, site and systems was assessed. For this, the results of the analysis including the system sizing and configuration for all the systems were compared against the building design and site conditions. The main points to consider are available site area and site conditions, surroundings, roof area, roof tilt, etc. The methodology developed for this study allows flexibility in selecting the system size and installation conditions, which could be adapted to the building to a certain extent. However, in order to ensure that the systems are installed for maximized performance, the building design, site and landscaping should accommodate the systems to provide their best performance installation conditions, without compromising the functionality, livability, and structural integrity of the building. With these concerns, the specific considerations for an integrated design include:

1. Surroundings: The surroundings of the building should ensure no shading of the solar collectors and PV array, and should not be obstructions for the wind turbine;
2. Site and landscaping: The building site should accommodate systems for sewage disposal, provisions for water recycling, if considered, custom-designed catchment surfaces, if needed, and rainwater storage tank(s).
3. Building design: The design of the building should ensure sufficient roof area for mounting solar collectors and PV arrays, and should provide a roof catchment surface for rainwater harvesting, proper tilt(s) for the installation of building mounted system components; sufficient space for the installation, monitoring, and maintenance of equipment, and storage for biomass and batteries. The structure of the building should be designed to be able to support the building mounted system components. The layout of spaces indoor and outdoor (for outdoor activities), building entrance, and

---

<sup>33</sup> For a more thorough and rapid treatment of sewage, septic tanks can be coupled with other on-site wastewater treatment units such as biofilters or aerobic systems involving forced aeration. However, an aerated system uses electricity to operate the mixing mechanism, requires frequent maintenance, and is more expensive compared to a septic system with a leaching field. In addition, the use of a septic system or an aerated system is subjected to local code regulations and building practices (AGWT 2008).

location of windows with respect to the positioning of system components, and vice versa, should ensure avoidance of noise, undisturbed vision, and clear access.

4. Safety consideration: The installation of all systems including the PV/wind electric system, batteries, and solar thermal system, and access to the system's components should comply with the local building and safety codes. The rainwater harvesting system should be designed with proper considerations for providing safe and clean water with the potential to provide potable water. The back-up biomass system should ensure safe and clean combustion.

#### **4.8. Summary of Methodology**

The methodology used in this study was developed as a generalized procedure for the integrated analysis and design of off-grid, off-pipe single-family detached residences, which could be applied to different climatic contexts. Therefore, first six locations with dissimilar building energy requirements and availability of renewable resources (i.e., solar radiation, wind and rainwater) were selected across the U.S. For each location, the base-case building characteristics were determined in order to simulate its energy use and estimate the water use and sewage generation. Next, the performance of renewable energy systems (including different types/capacities of active solar thermal, photovoltaic and wind power systems) was quantified in each location. In addition, normalized system sizing parameters were derived for rainwater harvesting and sewage disposal systems. Based on the contribution of building envelope and energy end-use components to the base-case energy use, and the harvestable renewable resources, energy and water-efficiency measures were then selected to reduce the building energy and water needs to a level that could be met solely by on-site harvested renewable resources. Finally, with the performance of renewable systems quantified and system sizing parameters determined, the sizing of these systems was performed to provide all the household energy and water needs, and facilitate on-site sewage disposal. In this manner, the integrated analysis procedure developed for the analysis and design of off-grid, off-pipe homes was demonstrated for six U.S. climate locations.

## **CHAPTER V**

### **ANALYSIS AND RESULTS**

This chapter presents the results of the analysis for the six selected climate locations, which include: Minneapolis, MN (very-cold); Boulder, CO (cold); Atlanta, GA (mixed-humid); Houston, TX (hot-humid); Phoenix, AZ (hot-dry); and Los Angeles, CA (marine climate). The analysis for these locations is presented in terms of: (i) climate characteristics, (ii) base-case and reduced energy and water use, (iii) potential of harvesting on-site renewable resources, and (iv) sizing requirements of the systems for self-sufficiency.

In Section 5.1, the general climate characteristics of the selected locations are discussed, which indicate the climate-specific liabilities (as factors driving the heating and cooling loads) and opportunities (in terms of resources for energy and water), and form a basis for the subsequent analysis.

Section 5.2 describes the water efficiency measures considered in this study and provides estimates for the resulting indoor water use reductions. These estimates are used with the normalized sizing parameters for the rainwater harvesting system, derived in Section 5.4.4, to determine the required level of water use reduction and select the water efficiency measures for the six selected locations.

Section 5.3 investigates the base-case energy use, peak heating and cooling load components, potential energy-efficiency measures, and the resulting energy use reductions from the combined application of these measures for each location.

In Section 5.4, the potential of harvesting on-site renewable energy sources (i.e., solar radiation, wind and rainwater) is presented. This was accomplished by investigating the monthly performance of the active solar thermal system, wind power system and photovoltaic system for different types/capacities of system components and installation configurations, and deriving the normalized sizing parameters for the rainwater harvesting system.

Finally, Section 5.5 presents the analysis for the sizing of systems for self-sufficiency, which include: active solar thermal system, photovoltaic and wind electric systems, electricity storage system, biomass heating system, rainwater harvesting system, and septic system.

#### **5.1. Climate Characteristics of the Selected Locations**

The climate characteristics of the selected locations were investigated as determinants of the building heating and cooling loads, as well as the availability of resources for renewable energy and rainwater. To begin with, the general climate characteristics of the climate regions corresponding to the selected locations were reviewed from Lechner (2001). These include: (a) Minneapolis, MN, (b) Boulder, CO, (c) Atlanta, GA, (d) Houston, TX, (e) Phoenix, AZ, and (f) Los Angeles, CA. In addition, the monthly statistics of several weather parameters were obtained from:

1. The summary reports based on TMY2 weather data (US DOE 2008c),
2. The twelve years (1997 to 2008) of measured hourly and daily data (NOAA 2008), and
3. NASA surface meteorology and solar energy data (NASA 2008).

The monthly statistics from the TMY2 weather data files for each location are shown in Figure 26, which include: i) heating degree-days (base 65 °F), ii) cooling degree-days (base 50 °F)<sup>1</sup>, iii) average dry-bulb temperature, iv) minimum and maximum dry-bulb temperatures<sup>2</sup>, v) average dew-point temperature, and vi) average daily global horizontal solar radiation.

The monthly statistics based on the measured data by NOAA and NASA are shown in Figure 27, which includes: i) average wind speed, ii) total rainfall, iii) total number of frost days, iv) average number of daylight hours, and v) average surface albedo. The average wind speed and monthly total rainfall were calculated from measured hourly wind data and measured daily rainfall data, respectively, obtained from NOAA (2008). Other parameters were obtained from NASA (2008), which were available as monthly values based on the 22 years (July 1983 to June 2005) of measured data for the latitude and longitude corresponding to the selected locations. The summary of the climate characteristics is shown in Table 5.

Figure 26 and Figure 27 can be used to identify the general climate characteristics and to guide the design of renewable energy system. The heating degree-days and cooling degree-days roughly indicate the heating and cooling season in each location, and provide a means for a comparison among different locations. The number of frost days indicates the need for considering measures for freeze protection for the active solar thermal system, and protecting electricity storage batteries from low temperatures. The monthly surface albedo can be used to determine the preference for the solar thermal collector tilt (e.g., for a month with peak thermal energy use and a high reflectance of the snow-covered ground, a higher tilt may prove beneficial, which would receive a significant amount of radiation reflected from the ground). The average wind speed indicates the potential of considering wind power system, in general. The monthly rainfall indicates the required amount of water use reduction and the catchment area requirement.

The following sections discuss the climate characteristics of each location, which are relevant to the analysis and design of off-grid, off-pipe residential building and systems.

#### 5.1.1. *Minneapolis, MN*

Minneapolis is characterized by severe winter weather with very cold temperatures (often, well below freezing), snow and high winter wind speeds, and a short summer period of very hot and humid conditions. Solar radiation during the winter months is small (i.e., only 20% of the summer-time average

---

<sup>1</sup>The use of different base-temperatures for heating degree-day and cooling degree-day is to ensure consistency with the existing building codes and standards.

<sup>2</sup>The minimum and maximum dry-bulb temperatures were obtained from the monthly average hourly statistics for dry-bulb temperatures (US DOE 2008c).

radiation). The annual precipitation averaged 29 inches during the period 1998-2007, which occurred throughout the year. However, rainfall during the summer months was higher.

#### 5.1.2. Boulder, CO

Boulder is located in the semi-arid mountainous region. It has a cold windy winter with varying amounts of snow, and a summer with modest daytime temperatures, cool nights, and a high diurnal temperature range. Thus, heating is required about one-half of the year. The temperature and snow cover vary tremendously with the slope orientation and elevation. There is ample sunshine during winter (over 30-35% of the summer month). The annual precipitation averaged only 14 inches during the period 1998-2007, which occurred fairly uniformly for most of the year.

#### 5.1.3. Atlanta, GA

Atlanta, in the temperate region, can be characterized by a cool and windy winter; hot summer with modest humidity and a large diurnal temperature range; and a long and pleasant spring and fall. There is ample solar radiation throughout the year. The annual precipitation averaged 44 inches during the period 1998-2007, which occurred uniformly throughout the year.

#### 5.1.4. Houston, TX

Houston is characterized by cool and short winters, and hot and very humid summers with frequent rains and morning coastal breezes. The high humidity and clouds prevent the temperature from dropping much at night during the summer, resulting in a small diurnal temperature range. Ample sunshine can supply most of the winter heating demands, but increases the cooling loads in the summer. The annual precipitation averaged 53 inches during the period 1998-2007, which occurred uniformly throughout the year.

#### 5.1.5. Phoenix, AZ

Phoenix, in the southwest desert region, is characterized by extremely hot and dry summers with large diurnal temperature range and cool nights, and moderately cold winters. Skies are clear most of the year. The summer cooling load is the main concern for thermal comfort. The annual precipitation averaged only 7 inches during the period 1998-2007, which occurred mainly from July through September. April through June were the driest months.

#### 5.1.6. Los Angeles, CA

Los Angeles, in the semi-arid region, has a very mild and comfortable climate with moderate temperatures in the winters due to the cool winds with high humidity from the adjacent ocean, and occasional hot and dry winds from hot desert in summer. Sunshine is plentiful all year. The annual precipitation averaged only 12 inches during the period 1998-2007, which occurred mainly in the winter.

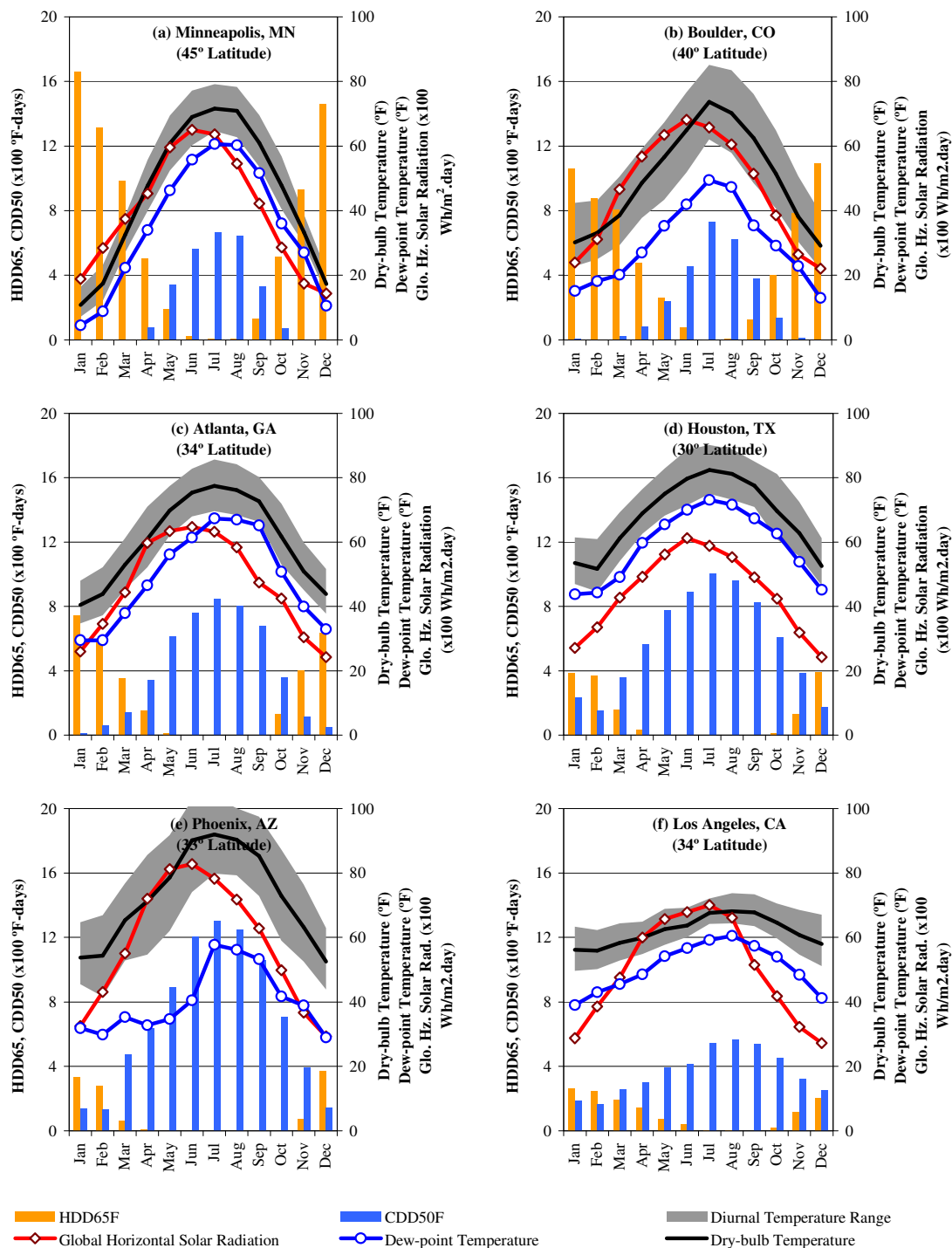


Figure 26 TMY2 Monthly Climate Statistics for Temperature, Humidity and Solar Radiation in the Six Selected Climate Locations

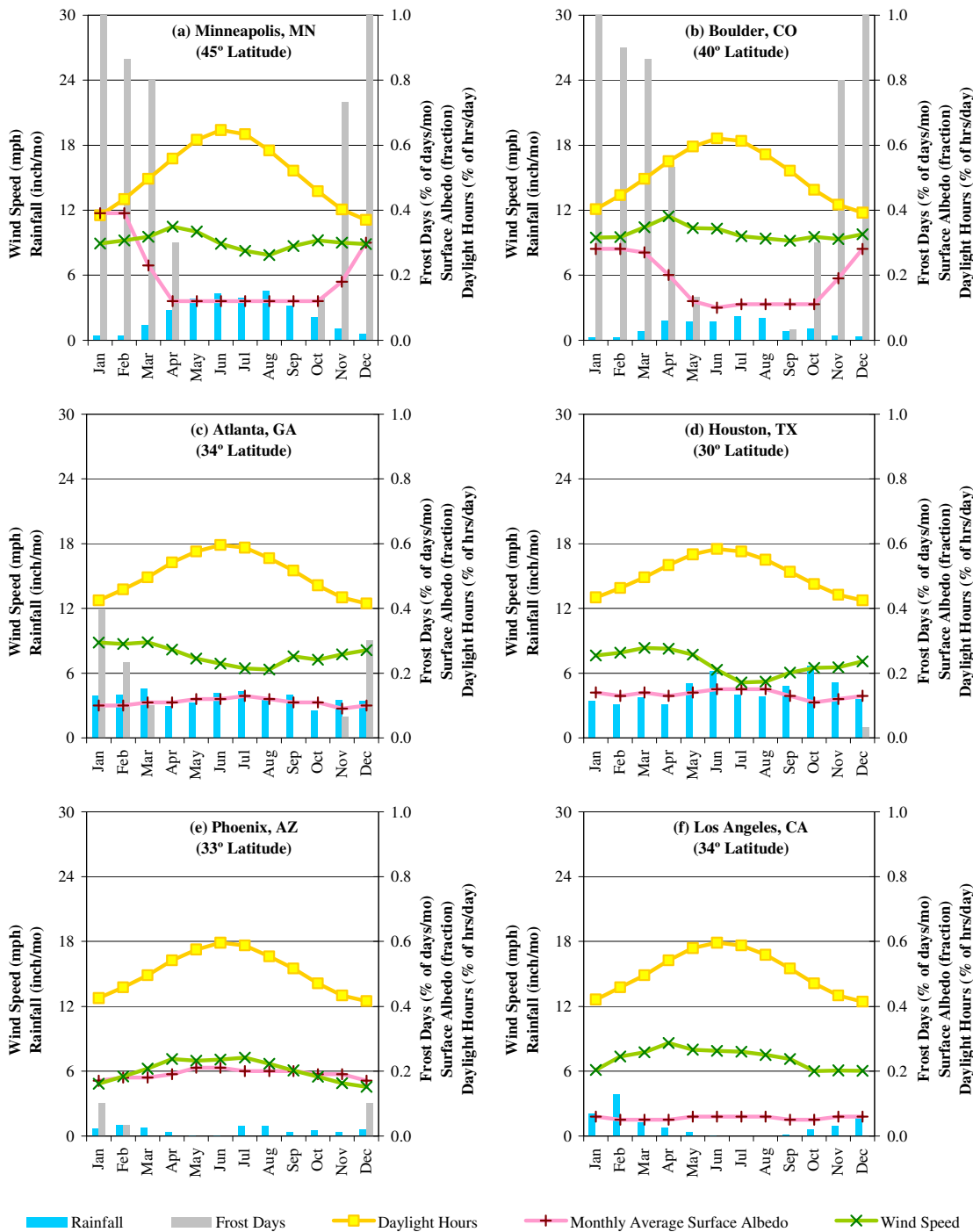


Figure 27 Monthly Statistics for Wind, Rainfall, Frost Days and Daylight Hours (based on the NOAA and NASA Measured Data) in the Six Selected Climate Locations



*Table 5 Climate Characteristics of the Six Selected Locations*

	Minneapolis, MN	Boulder, CO	Atlanta, GA	Houston, TX	Phoenix, AZ	Los Angeles, CA
Climate Region (Lechner 2001)	2	4	13	15	11	17
Climate Region (US DOE 2007)	Very Cold	Cold	Mixed-Humid	Hot-Humid	Hot-Dry	Marine
Latitude	44°52'	40°1'	33°39'	29°58'	33°25'	33°55'
Elevation above sea level (m)	255 m	1,634 m	315 m	33 m	339 m	32 m
HDD65 (°F-days)	7,735	5,980	3,013	1,487	1,129	1,296
CDD50 (°F-days)	2,716	2,686	4,790	6,943	8,327	4,376
Annual Avg. Dry-bulb Temp. (°F)	45.1 °F	49.8 °F	60.6 °F	68.1°F	72.5 °F	62.0 °F
Diurnal Temp. Range (°F)	13.4 °F	22.3 °F	15.5 °F	15.7 °F	24.8 °F	11.3 °F
Annual Avg. Dew-point Temp. (°F)	34.9 °F	29.6 °F	48.8 °F	58.9 °F	40.2 °F	50.7 °F
Solar Radiation, June/December (kWh/m <sup>2</sup> -day)	6.50/1.44	6.81/2.20	6.47/2.42	6.12/2.42	8.28/2.93	6.78/2.72
Annual Avg. Wind Speed (mph)	9.07	9.85	7.68	6.88	6.05	7.17
Annual Total Rainfall (inches/yr)	28.7	13.6	44.4	52.7	6.6	11.9
Daylight Hours, June/December	15.5/8.9	14.9/9.4	14.3/10.0	14.0/10.2	14.3/10.0	14.3/9.9
Annual Total Frost Days	145	167	33	1	7	0
Surface Albedo, June/December	0.3/0.12	0.1/0.28	0.12/0.1	0.15/0.13	0.21/0.17	0.06/0.06

## 5.2. Selection of Water Efficiency Measures

For the base-case house in all locations, an estimate of 45.3 gallon per capita per day (gpcd) of indoor water use was used, which assumed that all the installed fixtures comply with the 1992 U.S. Energy Policy Act (EPA Act) (Vickers 2001)<sup>3</sup>. This amounts to 181 gallon per day indoor water use for a household of four occupants.

The final selection of water-efficiency measures was based on the rainwater harvesting potential in each location. Considering a large variation in the availability of rainwater among the six selected locations, three levels of water-efficiency measures were considered. Table 6 lists these measures and the resulting reduced end-use and total water use estimates. Water use reduction at any level would result in an equal amount of reduction in the sewage disposal needs.

As shown in Figure 28, the water-efficiency measures at Level 1 include the use of high-efficiency fixtures and appliances such as, ultra-low flow showers and faucets, water-efficient clothes washer and dishwasher, and the elimination of leaks, which mainly occurs in aging toilet flush mechanism. This would reduce the average indoor water use to 122 gallons per day. For Level 2, greywater reuse for

<sup>3</sup> Vickers (2001) revised the results of an empirical study of indoor water use in the U.S. conducted in 1999 (Mayer and DeOreo 1999), which had estimated 69.3 gpcd average indoor water use.

Table 6 Water-efficiency Measures and the Resulting Indoor Water Use Reductions<sup>4</sup>

End-use	Fixture Utilization (per person per day)	Pre-1999 (From 1999 AWWA Survey)		Base Case (Current EPA Standards)		Level 1 (High -efficiency Fixtures)		Level 2 (Level 1 + Grey-water Reuse)		Level 3 (Level 1 + Grey-water Recycle)	
		gpcd	Fixture Rating	gpcd	Fixture Rating	gpcd	Fixture Rating	gpcd	Description	gpcd	Description
Toilets	5.05	18.5	3.5 gpf	8.2	1.6 gpf	8.2	-	0.0	Reused	0.0	Recycled
Faucets	8.1 minutes	10.9		10.8	2.5 gpm	8.1	1.5 gpm	8.1	-	8.1	-
Shower	0.75 times	11.6	3 gpm	8.8	2.5 gpm	5.3	1.5 gpm	5.3	-	5.3	-
Bath	(Shower & Bath Combined)	1.2	-	1.2	-	1.2	-	1.2	-	1.2	-
Dishwasher	0.1 times	1.0	10.5 gpl	0.7	7 gpl	0.5	4.5 gpl	0.5	-	0.5	-
Clothes Washer	0.37 times	15.0	40 gpl	10.0	27 gpl	5.5	14.8 gpl	5.5	-	0.0	Recycled
Leaks	-	9.5	-	4.0	-	0.0	No Leaks	0.0	-	0.0	-
Other/Unknown	-	1.6	-	1.6	-	1.6	-	1.6	-	1.6	-
Total (gpcd)		69.3		45.3		30.4		22.2		16.7	
Total (gallons per day) <sup>5</sup>		277.0		180.8		121.6		88.8		66.8	

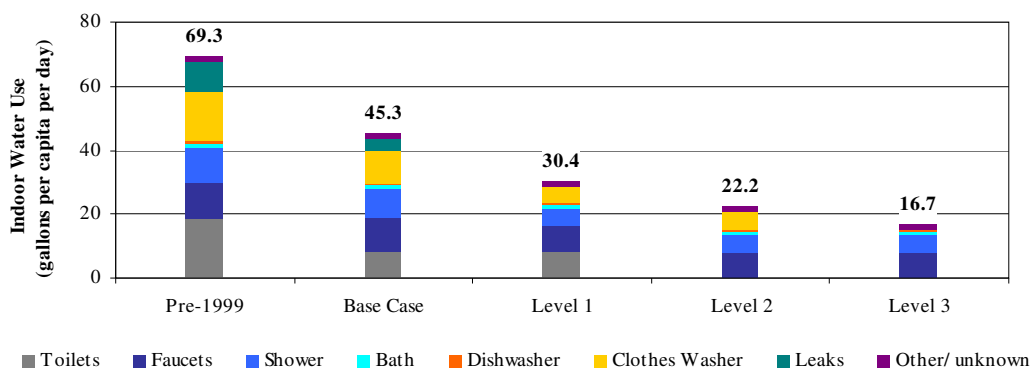


Figure 28 Indoor Water Use for the Base Case and with Water Efficiency Measures

toilets was considered. This would eliminate 8.2 gpcd water used for flushing toilets, and reduce the indoor water use to 88.8 gallons per day. It is noted that this measure would require a separate collection, storage and piping system for the greywater. Level 3 considers greywater recycling for the non-potable

<sup>4</sup> Sources: Vickers (2001), Mayer and DeOreo (1999).

gpcd = gallon per capita per day; gpf = gallons per flush; gpm = gallons per minute; gpl = gallons per load.

<sup>5</sup> This assumes four occupants in the base-case house. However, the household water use estimates in Vickers (2001) are based on the U.S. average of 2.64 persons per occupied household.

water end-uses including toilets and clothes washing<sup>6</sup>. This would reduce the indoor water use to 66.8 gallons per day. However, it would require systems for the filtration and treatment of greywater, as well as tanks for the storage of treated water. In addition, electricity would be required for the operation of this system.

### 5.3. Selection of Energy Efficiency Measures

For the selection of energy-efficiency measures, first the base-case energy use was analyzed for peak monthly thermal energy and electricity use. In addition, the contribution of the building envelope and energy end-use components to the base-case peak heating and cooling loads was investigated using the Manual J Average Load Procedure<sup>7</sup>. With the peak heating and cooling load components identified, and peak monthly thermal and electricity use quantified, the energy-efficiency measures were selected and applied to base-case house in order to minimize the peak energy use.

#### 5.3.1. *Investigation of the Base-case Energy Use*

The base-case energy use for the six selected locations was obtained from the DOE-2.1e output. These output were obtained by modeling the base-case characteristics in DOE-2.1e program using TMY2 weather data for each location, as described in Section 4.2.3. The base-case characteristics in the six locations include the general characteristics, as described in Table 3 of Section 4.2.2, and the climate-specific characteristics, as summarized in Table 7. The climate specific characteristics were determined from the standard reference design specifications of the 200/2001 IECC for the six selected locations.

For investigating the building thermal energy use and electricity use, the base-case house in each location was simulated using two DOE-2.1e system types: (i) RESYS with heat pump heating, to determine the base-case electricity use for space cooling, lighting and equipment, fans and pump, and (ii) SUM, to obtain the space heating loads without simulating a system to determine the base-case total thermal energy use for space heating and domestic water heating. From the DOE-2.1e output, the thermal energy use and electricity use were investigated on an annual, monthly, and peak-day hourly basis. The results of the simulation are shown in Figure 29 through Figure 34 for the six selected locations including: (a) Minneapolis, MN, (b) Boulder, CO, (c) Atlanta, GA, (d) Houston, TX, (e) Phoenix, AZ, and (f) Los Angeles, CA. Figure 29 and Figure 30 compare the annual electricity use and thermal energy use. Figure 31 and Figure 32 show the monthly electricity use and monthly thermal energy use, respectively. Figure 33 and Figure 34 show the peak winter day hourly electricity use and peak summer day hourly thermal energy use, respectively.

---

<sup>6</sup> The use of recycled greywater for indoor use is subjected to local regulations and public acceptance.

<sup>7</sup> The DOE-2.1e LOADS summary reports (i.e., LS-B for space peak load components and LS-C for building peak load components) show the peak heating and cooling load components, which are based on a fixed space temperature specified for each space in LOADS. Considering that the attic temperature in the summer and winter would be significantly different from the fixed value specified, the peak loads from the DOE-2.1e output were not used for this purpose.

*Table 7 Climate-specific Characteristics of the Base-case House in the Six Selected Climate Locations*

	Minneapolis, MN	Boulder, CO	Atlanta, GA	Houston, TX	Phoenix, AZ	Los Angeles, CA
HDD65°F	7,735	5,980	3,013	1,487	1,129	1,296
Ceiling Assembly U-value (Btu/h. ft <sup>2</sup> .°F)	0.026	0.026	0.036	0.042	0.044	0.043
Wall Assembly U-value (Btu/h. ft <sup>2</sup> .°F)	0.052	0.058	0.076	0.085	0.085	0.085
Window U-value (Btu/h. ft <sup>2</sup> .°F)	0.28	0.30	0.44	0.47	0.47	0.47
Window SHGC	0.68	0.68	0.40	0.40	0.40	0.40
Slab Perimeter R-value and Depth (Btu/h. ft <sup>2</sup> .°F) <sup>-1</sup>	R-6, 4 ft.	R-5, 4 ft.	R-4, 2 ft.	None	None	None
Supply and Return Duct Insulation (Btu/h. ft <sup>2</sup> .°F) <sup>-1</sup>	R-11, R-6	R-8, R-4	R-8, R-4	R-8, R-4	R-8, R-4	R-8, R-4

### 5.3.1.1. Annual Energy Use

Figure 29 and Figure 30 identify the major end-use components of the electricity use and thermal energy use for each location. Clearly, energy use for lighting and equipment (which were simulated in the same manner for all locations) contributes significantly to the total energy use. The short-period of hot summer weather in Minneapolis and Boulder combined with the high SHGC windows results in cooling energy needs similar to Atlanta. Variations in the cooling energy use in Houston, Phoenix and Los Angeles simply reflect the varying climate conditions of these locations. The thermal energy use for domestic water heating varies slightly across different locations, due to the water mains temperature that was calculated using the procedure by Hendron (2008). A large variation in the thermal energy use for space heating was observed for the different locations, which reflects the heating degree-days for each location, except for Boulder. In Boulder, the heating degree days were twice of Atlanta, but the space heating energy use was almost the same owing to the differences in the code-specified envelope characteristics in the two locations. An investigation of the monthly and peak summer and winter day energy use in these locations provides more insights about the occurrence of these loads.

### 5.3.1.2. Monthly Energy Use

Figure 31 and Figure 32 show the base-case end-use electricity and thermal energy use for each location as stacked bar charts, the outdoor dry-bulb temperatures as black line, and the global horizontal solar radiation as red lines. These plots indicate the base-case energy requirements in relation to the solar radiation that could potentially be used for providing these energy needs. In addition, they identify critical months with less solar radiation with respect to the energy requirements. For the critical months, the

major-end uses were identified in order to determine the strategies for minimizing energy use during these periods.

The lighting and equipment electricity use, which was specified the same throughout the year, was a significant part of the total electricity use. In addition, the internal heat gains from the lighting and equipment added to the space cooling loads, and helped to offset part of the space heating requirements. The outside dry bulb temperature was the main determinant of the cooling and heating energy use. The HVAC fan energy use was significant for those months with large heating and/or cooling loads. The variation in domestic water heating loads was very small across the year.

#### *5.3.1.3. Peak Day Hourly Energy Use*

Figure 33 and Figure 34 show the base-case peak day hourly electricity and thermal energy loads as stacked area graphs, and the outdoor dry-bulb temperature, indoor air temperature and attic air temperatures as line graphs. In contrast to the annual and monthly cooling as well as total electricity energy use, which varied significantly across the different locations according to the outdoor dry-bulb temperature; Figure 33 shows that the peak electricity loads were very similar for most of the locations (except for large cooling loads in Phoenix and small cooling loads in Los Angeles) and were largely influenced by the solar radiation. On the other hand, Figure 34 shows that the peak day hourly space heating energy use were very different for the six locations, including the largest loads in Minneapolis, followed by Atlanta, Boulder, Houston, Phoenix, and Los Angeles. Figure 33 also shows that the lighting and equipment energy use were a small portion of the peak day electricity use, as opposed to the monthly and annual total electricity use.

A comparison of the energy use profiles and solar radiation profiles indicates the critical months and the corresponding energy use, which would be targeted as the main criteria for selecting energy-efficiency measures. In Minneapolis, the main criteria would be minimizing the space heating loads in winter (otherwise, the unmet heating loads, added as electricity loads, would increase the winter peak electricity needs). With the space heating energy use minimized, the HVAC fan energy use in winter would be reduced. The resulting reduced winter peak electricity needs would be relatively easier to meet by utilizing the available solar radiation in the winter. This strategy applies to Boulder and Atlanta, too.

In Houston, the most important criteria would be to minimize the summer cooling loads, while avoiding the resulting winter heating loads penalty, if any. In Phoenix, minimizing the summer cooling energy use would be the only criteria. In Los Angeles, strategies for reducing lighting and equipment energy use would be the most important criteria for minimizing the peak day as well the monthly and annual energy use. Furthermore, the lighting and equipment energy use reduction strategies would also have significant impact on the monthly energy use rather than peak day energy use in other locations.

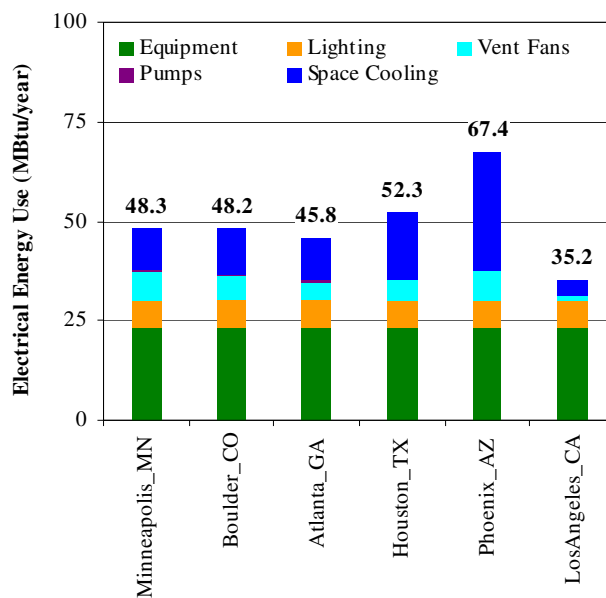


Figure 29 Base-case Annual End-use Electricity Use in the Six Selected Climate Locations

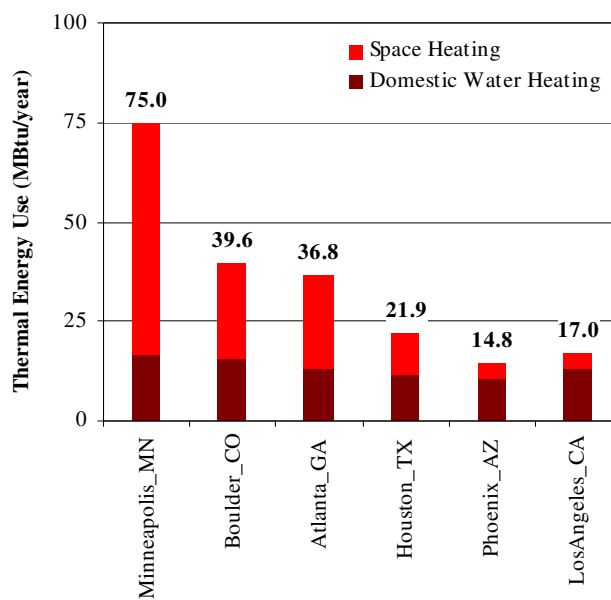


Figure 30 Base-case Annual End-use Thermal Energy Use in the Six Selected Climate Locations

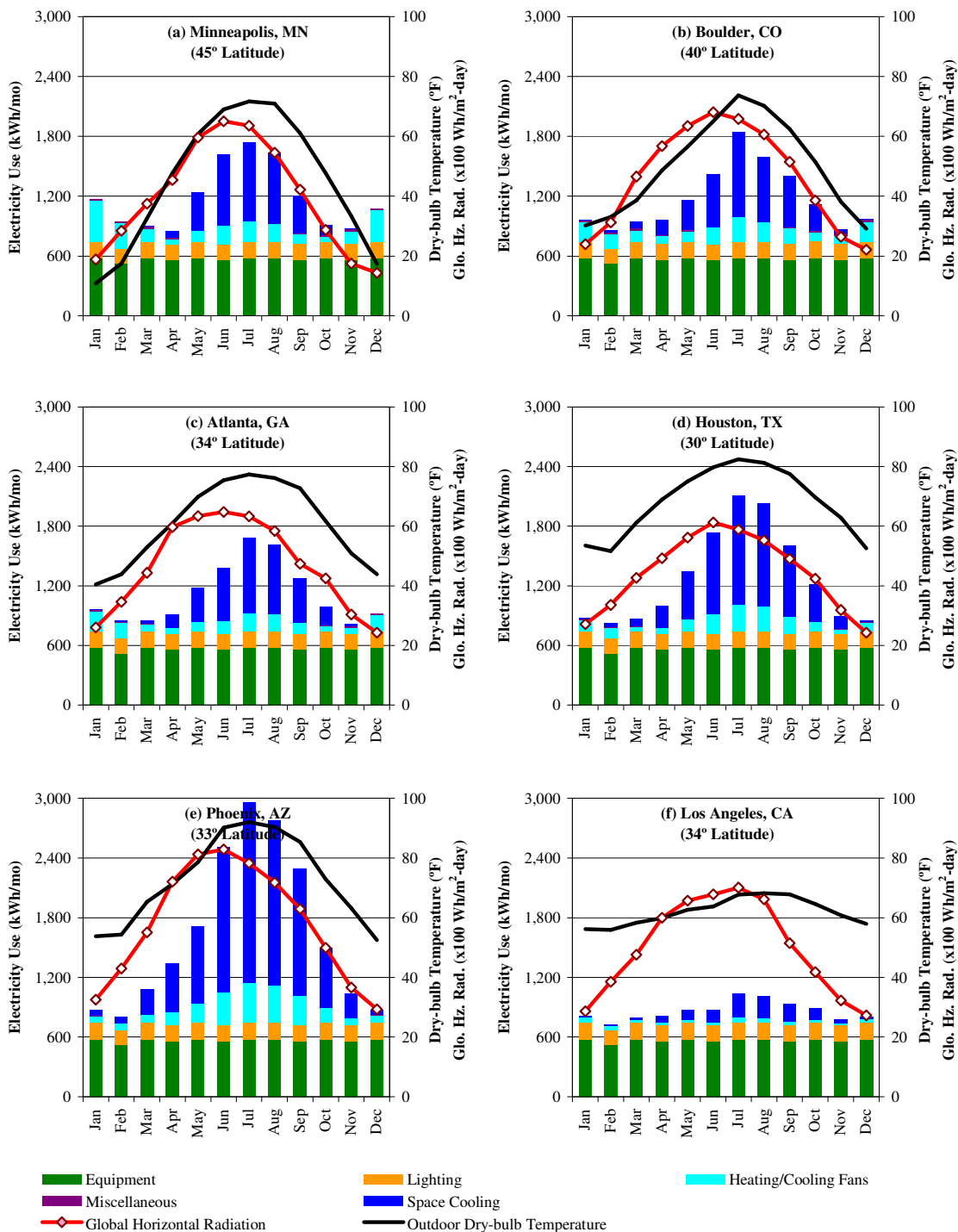


Figure 31 Base-case Monthly End-use Electricity Use in the Six Selected Climate Locations

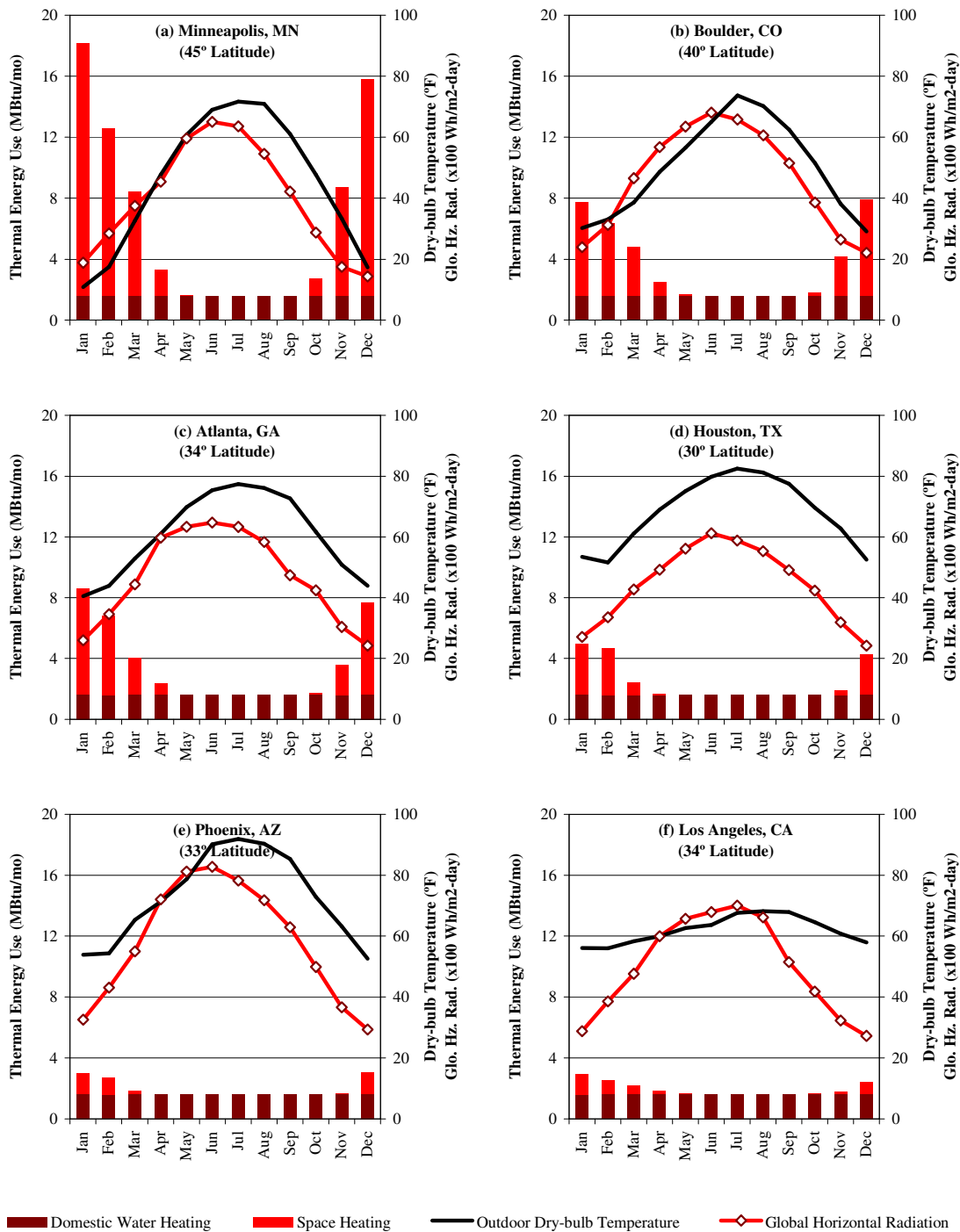


Figure 32 Base-case Monthly End-use Thermal Energy Use in the Six Selected Climate Locations



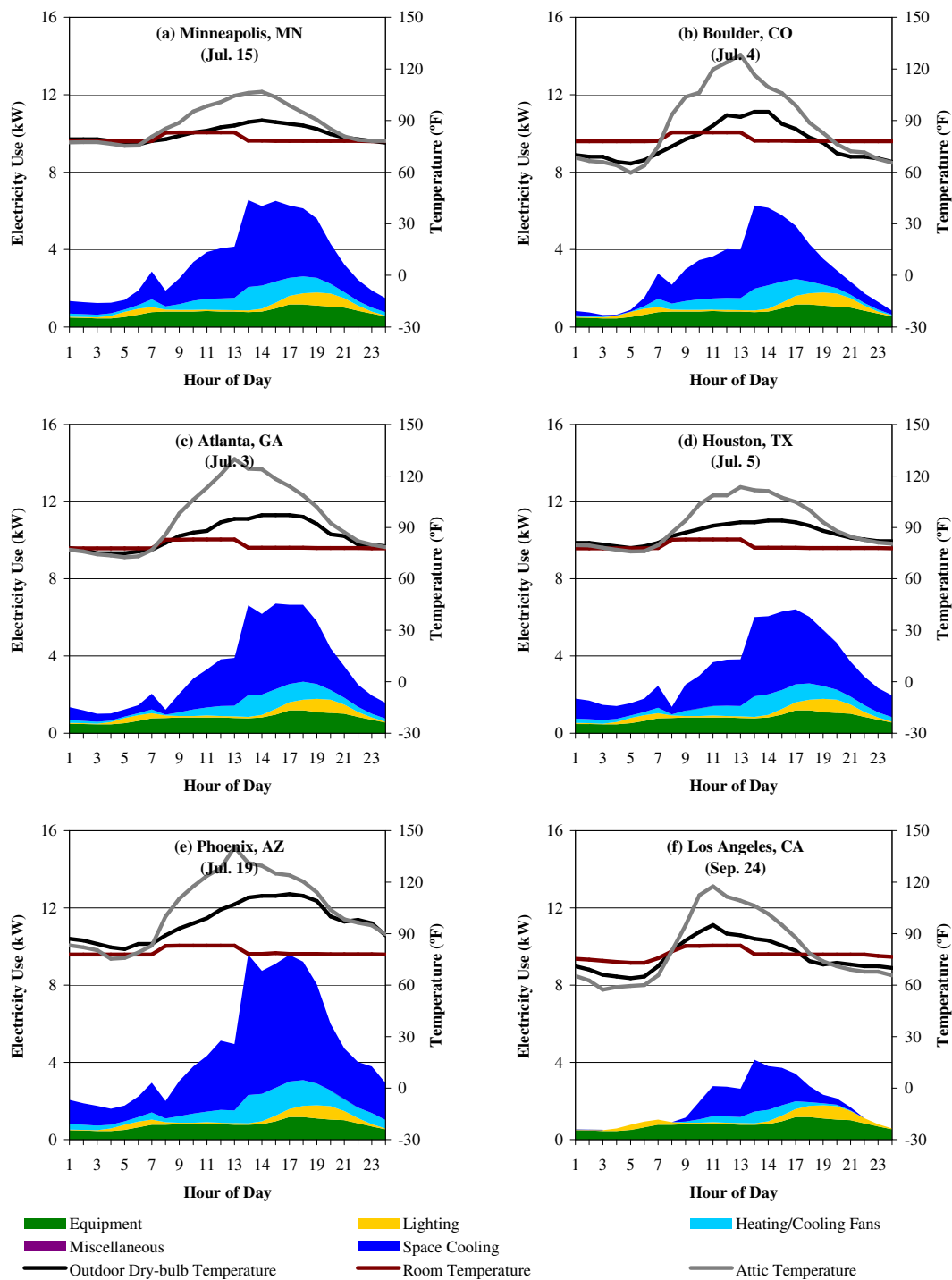


Figure 33 Base-case Peak Summer Day Hourly End-use Electricity Use in the Six Selected Climate Locations

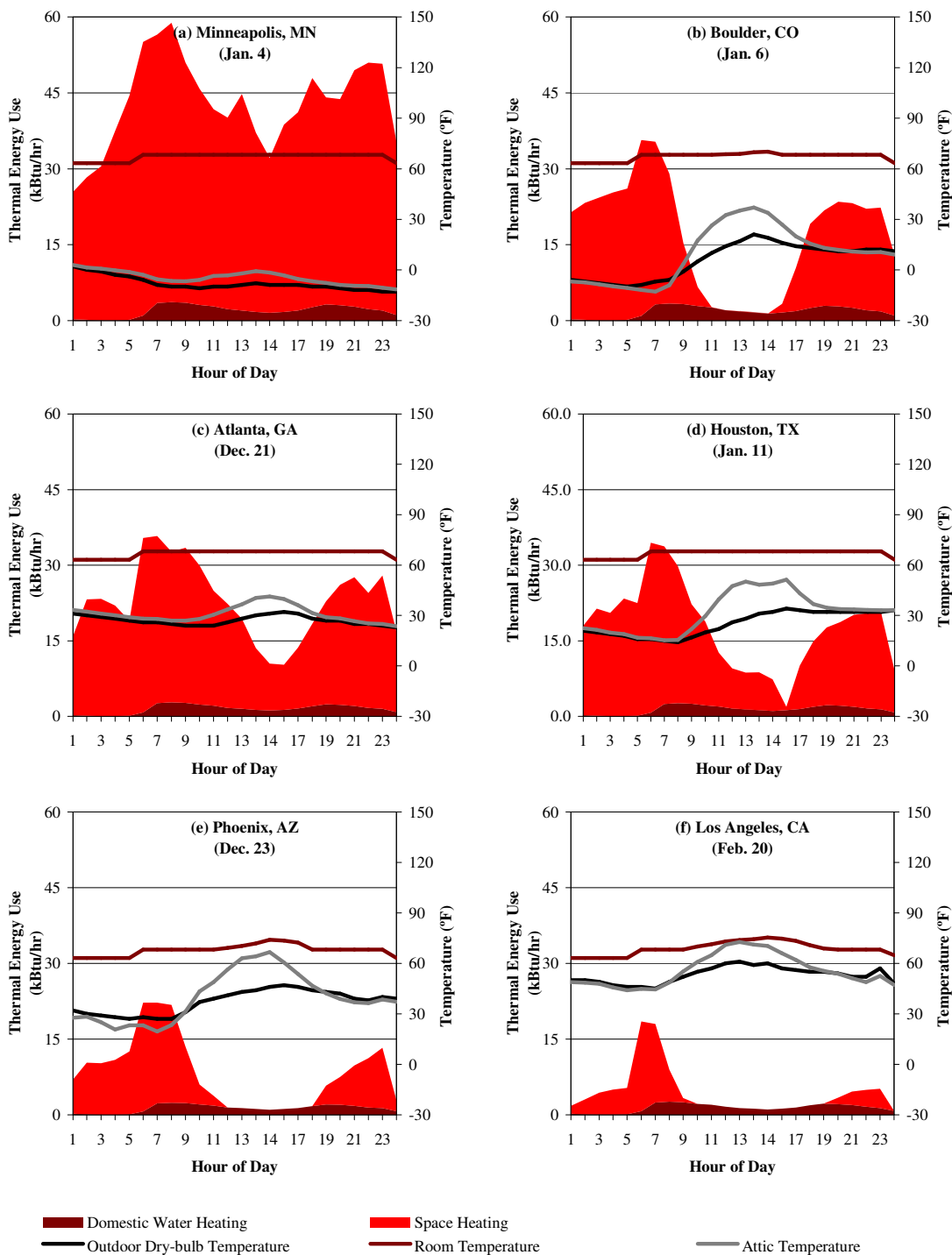


Figure 34 Peak Winter Day Hourly End-use Thermal Energy Use in the Six Selected Climate Locations

### 5.3.2. *Investigation of the Base-case Peak Load Components*

The base-case peak heating and cooling load components were calculated using the Manual J Average Load Procedure, as described in Section 4.5.2, to account for the fenestration loads, opaque envelope loads (exterior walls, doors, ceiling/roof and slab-on-grade floor), infiltration loads, and internal loads. The calculations are included in Appendix C, and the results are shown in Figure 35 through Figure 37.

Figure 35 shows a comparison of the base-case peak heating and cooling load components for the six locations. The stacked bars in the upper chart represent the heating load components due to windows, doors, exterior walls, ceiling, slab-on-grade floor, and infiltration, which are plotted with respect to the left hand y-axis. The difference between the heating design outdoor temperature (i.e., 99% dry-bulb temperature) and the heating design indoor temperature (70 °F) are shown as blue markers, and the winter infiltration rates are shown as black/grey markers, which are plotted with respect to the right y-axis. In the same manner, the stacked bars in the lower chart represent the cooling load components due to windows, doors, exterior walls, ceiling, sensible and latent heat gains from air infiltration, and sensible and latent internal heat gains, which are plotted with respect to the left hand y-axis. The difference between the cooling design outdoor temperature (i.e., 1% dry-bulb temperature) and the cooling design indoor temperature (75 °F) are shown as red markers, the summer infiltration rates are shown as black/grey markers, and the difference between the outdoor and indoor cooling design humidity ratio (based on the indoor relative humidity of 50%) are shown as purple markers, which are plotted with respect to the right y-axis. From this figure, following points can be observed:

1. Infiltration was the largest contributor to the winter heat loss in Minneapolis and Boulder due to low design temperatures combined with high infiltration rates.
2. Windows were the largest contributor to the summer heat gain due to the direct solar gains. Due to the high SHGC windows in Minneapolis and Boulder, the window heat gain for these locations was the same as in Phoenix.
3. Due to the code-specified high insulation levels of the exterior walls and ceiling and relatively lower solar radiation resulting in lower cooling load temperature difference (CLTD), the heat gain through walls and ceiling in Minneapolis and Boulder was quite small compared to that in Atlanta, Houston and Phoenix.
4. Despite of the high outdoor summer design temperature in Phoenix compared to Houston, the high latent infiltration loads in Houston resulted in an equal total heat gain in the two locations.

To analyze the contribution of the load components to the total heat gain/loss for each location, further investigations were performed using relatively sized pie charts to better compare the magnitude of the end-use loads, across the selected locations. Figure 36 shows the heating load components for the winter design day and Figure 37 shows the cooling load components for the summer design day for the six

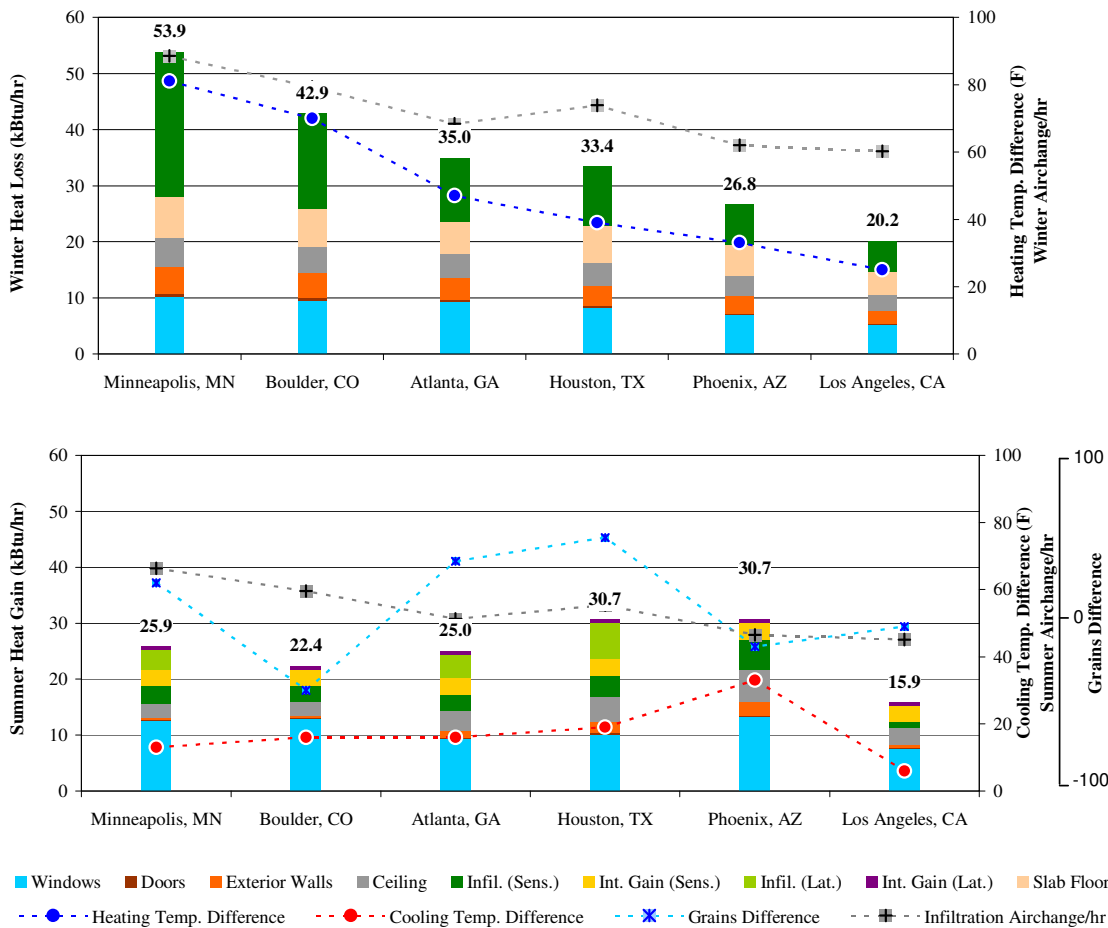


Figure 35 Base-case Peak Load Components in the Six Selected Climate Locations

locations. In these figures, the total area of the pie charts is proportional to the magnitude of the total loads, as well as the end uses. From these figures, following points can be observed:

1. Infiltration was the largest contributor (40 to 50%) to the total heat loss in cold climates, followed by windows (20%) and slab-on-grade floor (15%). Exterior walls and ceiling contributed equally (10% each) to the total heat loss in Minneapolis and Boulder.
2. For the other climate locations, the distribution of the load components was very similar, which included: 27-30% due to infiltration, 25-27% due to windows, 16-21% due to the slab-on-grade floor, and 11-13% each due to the exterior walls and the ceiling. Because of the code-specified slab perimeter insulation requirement in Atlanta, the heat loss through slab was smaller.

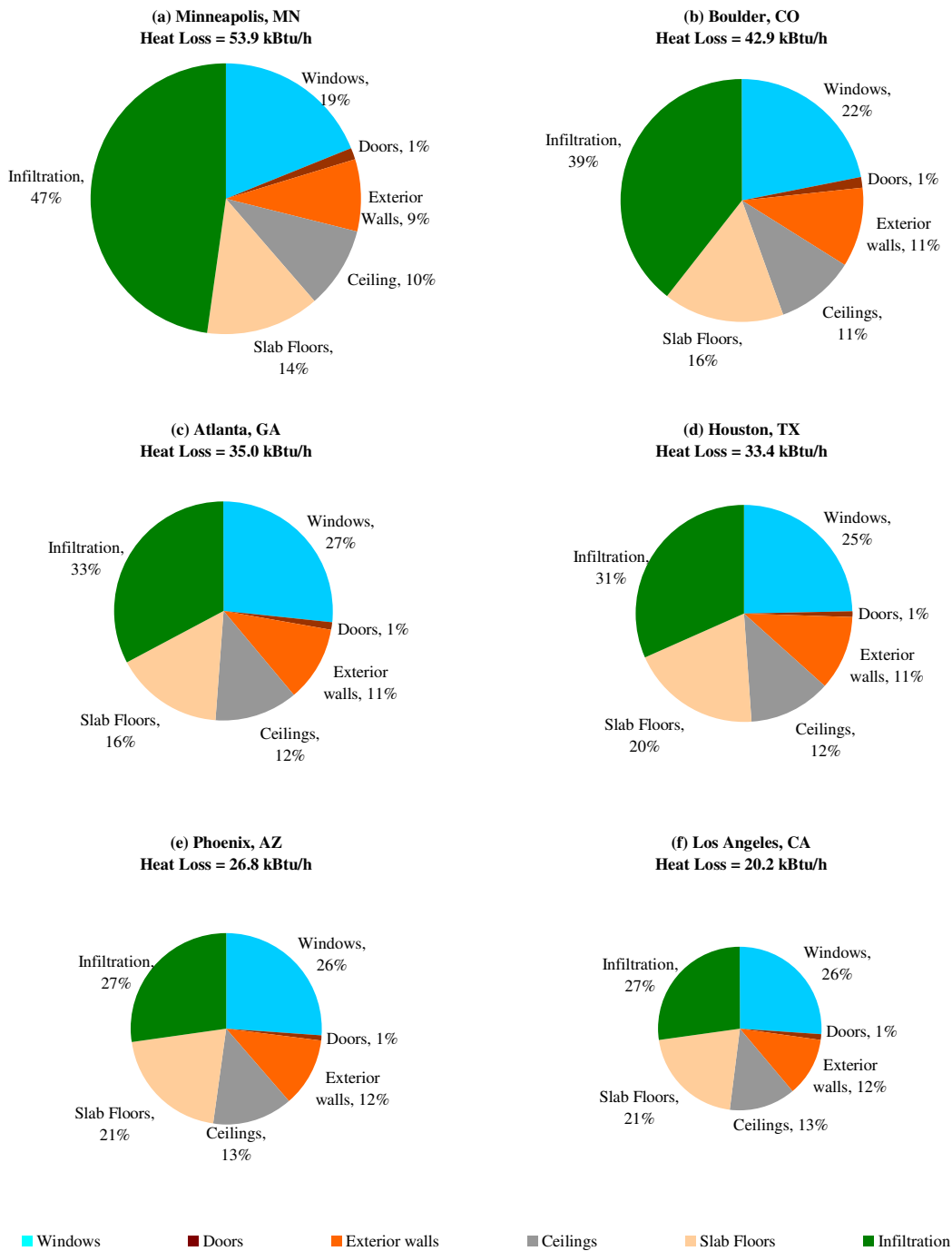


Figure 36 Base-case Peak Heating Load Components in the Six Selected Climate Locations

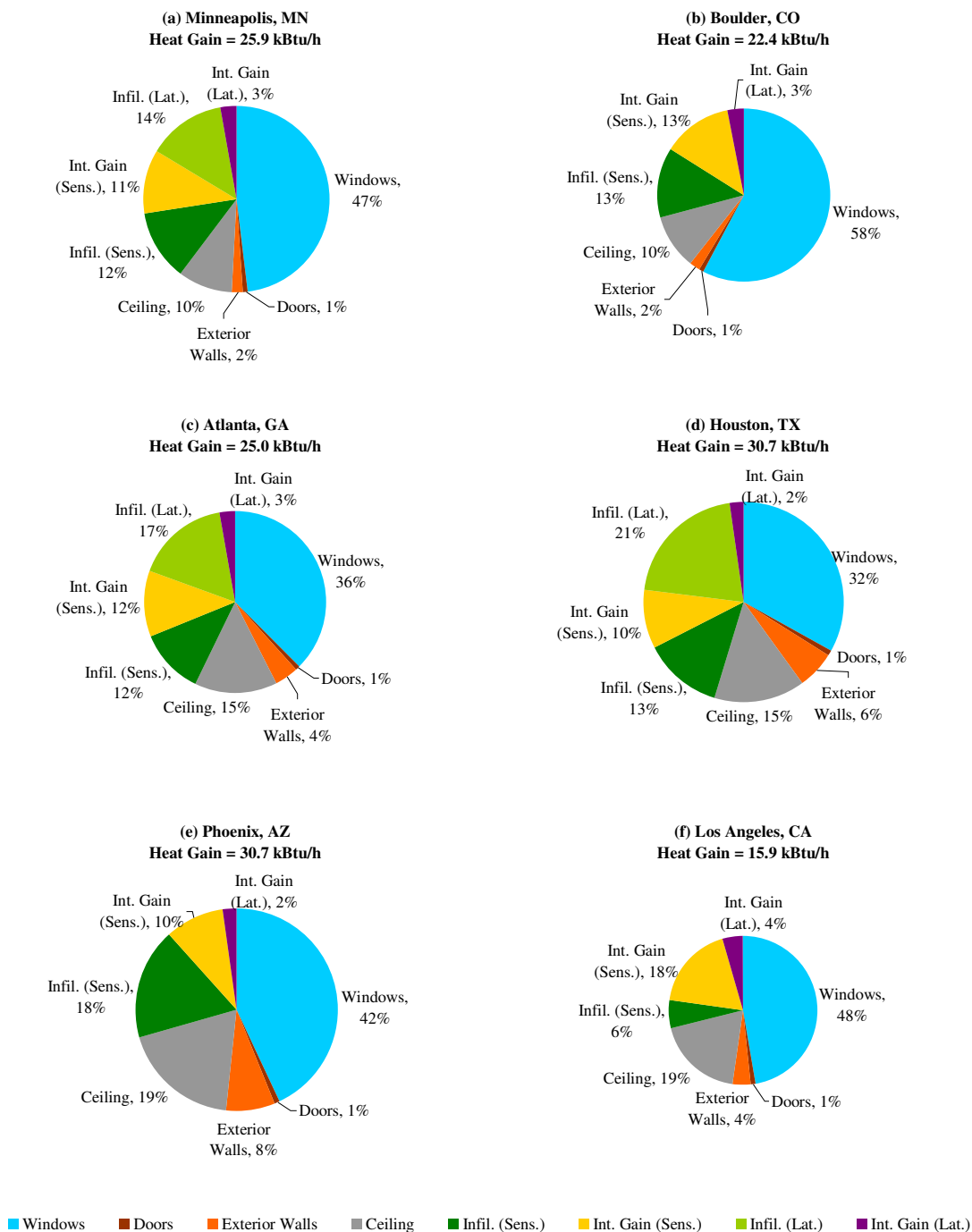


Figure 37 Base-case Peak Cooling Load Components in the Six Selected Climate Locations

3. The windows were the largest contributor to the total heat gain in all climates, which ranged from 30% in the warm climates to up to 60% in the cold climates.
4. Ceiling contributed to 10% of the total heat gain in Minneapolis, 15% in Houston and Atlanta, and 19% in Phoenix and Los, Angeles.
5. Exterior walls and doors (combined) contributed to 3% of the total heat gain in the cold climates to upto 9% in the hot climates.
6. The contribution of sensible infiltration gain was 12-13% of the total heat gain in most locations, except 18% in Phoenix, and 6% in Los Angeles. Latent gains from infiltration ranged from 14-17% in locations with humid summer, with higher contribution in warm climate locations.
7. Internal gains ranged from 12% to 22% of the total heat gain, with higher values associated with locations having smaller total heat gains.

### 5.3.3. Selection of Energy-efficiency Measures

The analysis of building energy needs and the peak heating and cooling load components helped with the understanding of the interactions between the building components, indoor conditions, and climate parameters. The selection of energy-efficiency measures was aimed to minimize the base-case building energy needs for the peak months and peak days. As described in Section 4.5.3, first the potential energy-efficiency measures, which reduce both the heating and cooling energy use, were selected. These include: high insulation levels for roof and walls, air-tight construction, windows with a low U-value, high-efficiency HVAC systems, lighting and equipment. For the lighting and equipment, the same measures were considered for all climates, as shown in Table 8. The climate-specific measures selected for each location are described in the following sections.

*Table 8 Energy-efficiency Measures for Lighting and Appliances*

End Use	Base Case (kWh/yr)	Proposed Measures (kWh/yr)
Hardwired Lighting <sup>8</sup>	1,964	713
Refrigerator	669	452
Clothes Washer (3 ft <sup>3</sup> )	123	109
Clothes Dryer (Electric)	974	770
Dishwasher (8 place)	240	180
Range (Electric)	706	626
Variable Miscellaneous Electrical Loads	2,797	1,738
Fixed Miscellaneous Electrical Loads	808	485
Plug-in lighting	491	178
Annual Total Equipment Electricity Use	6,808	4,538
Average Equipment Electricity Use (kW)	0.78	0.52

<sup>8</sup> Base case: 86% Incandescent, 14% Fluorescent; Proposed House: 90% Fluorescent, 10% Incandescent

#### 5.3.3.1. *Minneapolis, MN*

Minneapolis is located in a very cold climate region with very cold temperatures during the winter, high solar radiation in the summer and high wind speeds. In Minneapolis, the space heating energy use during the winter was the largest end use to be reduced. Figure 36(a) and Figure 37(a) show 53.9 kBtu/h peak heat loss and 25.9 kBtu/h peak heat gain in Minneapolis, with infiltration contributing to 40% of the heat loss and 26% of the heat gain. This indicates the need to have a very airtight construction. Furthermore, the windows were identified as the next largest contributor responsible for 19% of the heat loss and 47% of the heat gain. This indicates the need to have windows with lower U-factors, moveable night insulation for the windows, a window distribution favoring south, and overhangs designed for blocking the summer sun. For minimizing the heat gain and loss from opaque envelope components (i.e., exterior walls, roof and floor each contributing 10-15% to the total heat gain and loss), a compact design with a minimum building heat-loss coefficient (building UA) (i.e., high insulation on exterior walls, floor and roof/ceiling) would be desired. Considering the code-specified high ceiling insulation requirements of the base-case, adding more insulation may have diminished returns. Therefore, a compact two-story house (i.e., 50% reduced ceiling area), and maximum windows facing the south was considered for the maximum energy efficiency configuration in Minneapolis. A high-efficiency lighting and equipment were considered to reduce the electricity use. In addition to these measures, a heat recovery ventilator would minimize the energy use for conditioning the outdoor air from mechanical ventilation, which would be required for a house with very airtight construction considered for this location.

#### 5.3.3.2. *Boulder, CO*

Boulder is located in a cold climate region with low temperatures in the winter, high solar radiation in the winter and summer. Due to a high average annual wind speed, natural ventilation in the summer at night is possible but not included in this study. The heating and cooling needs are smaller and the harvestable solar and wind energy in Boulder is higher compared to Minneapolis. Figure 36(b) and Figure 37(b) show 42.9 kBtu/h heat loss and 22.4 kBtu/h heat gain in Boulder, with infiltration contributing to 39% of the heat loss and 26% of the heat gain, and windows contributing to 22% of the heat loss and 58% of the heat gain. This indicates the need to consider measures similar to those for Minneapolis, i.e., an airtight construction, compact configuration and high insulation. However, in Boulder, window solar gains in the summer need more attention. Like Minneapolis, high-efficiency lighting and equipment, and mechanical ventilation with heat recovery ventilators would be beneficial.

#### 5.3.3.3. *Atlanta, GA*

Atlanta is located in a mixed-humid climate region with moderate heating and cooling loads. Figure 36(c) and Figure 37(c) show 35 kBtu/h heat loss and 25 kBtu/h heat gain in Atlanta. Infiltration contributed to 33% of the total heat loss in the winter and 29% heat gain (including 17% as latent portion)



in the summer, indicates that airtight construction is a potential measure. The high average dew-point temperature prevents natural ventilation in Atlanta in the summer. Windows contributing to 27% of the heat loss and 36% of the heat gain indicating the need for a lower U-value, lower SHGC, and properly sized window overhangs. Ceilings contributed to 12% of the heat loss and 15% of the heat gain. Therefore, ceiling insulation with a higher R-value would reduce the conduction heat gain through ceiling. In addition, high-efficiency lighting, equipment and cooling system were considered.

#### 5.3.3.4. *Houston, TX*

Houston is located in hot-humid climate region with lower heating and higher cooling loads compared to Atlanta. Figure 36(d) and Figure 37(d) show 33.4 kBtu/h heat loss and 30.7 kBtu/h heat gain in Houston. Infiltration contributed over 30% of the heat loss and gain (including 17% as latent portion). The high average dew-point temperature prevents natural ventilation in Houston in the summer. Windows contribute to 25% heat loss and 32% heat gain. Thus, the most important considerations in Houston would be minimizing the infiltration, higher R-values for ceiling and wall insulation, and having lower U-value and lower SHGC windows. In addition, high-efficiency lighting, equipment and cooling system were considered.

#### 5.3.3.5. *Phoenix, AZ*

Phoenix is located in hot-dry climate region with smaller heating and much higher cooling loads compared to Houston. Figure 36(e) and Figure 37(e) show 26.8 kBtu/h heat loss and 30.7 kBtu/h heat gain in Phoenix. The large heat gain is mostly from the windows and ceiling, which would be the most important factors to be reduced. This would require providing low SHGC windows, additional ceiling insulation and large overhangs. In addition, high-efficiency lighting, equipment and cooling system were considered. Due to the lower dew-point temperatures in Phoenix, evaporative cooling is a potential strategy, which is not considered in this study.

#### 5.3.3.6. *Los Angeles, CA*

Los Angeles is located in marine climate with similar heating and yet smaller cooling loads, when compared to Phoenix. Figure 36(f) and Figure 37(f) show 20.2 kBtu/h heat loss and 15.9 kBtu/h heat gain in Los Angeles. Of these small loads, windows and infiltration contributes over 25% each to the heat loss. The heat gain is mostly from the windows (48%) and the ceiling (19%). This would require providing low SHGC windows, and higher ceiling insulation. In addition, high-efficiency lighting, equipment and cooling system are also important considerations.

In summary, for each site, the measures considered in this study included: a well insulated, airtight building envelope; high-performance windows; energy-efficient lighting and appliances, high-efficiency HVAC system; HVAC unit and ducts located in the conditioned space (i.e., within the building's thermal envelope). Passive cooling strategies such as natural ventilation and evaporative

cooling were not considered for this study. These measures were applied in combination in a set of parametric simulation, to determine the most favorable building configuration, which could result in minimized overall building UA and accommodate more south-facing windows, and an optimum shading overhang depth and window distribution in order to maximize passive solar gain, while minimizing cooling season heat gain.

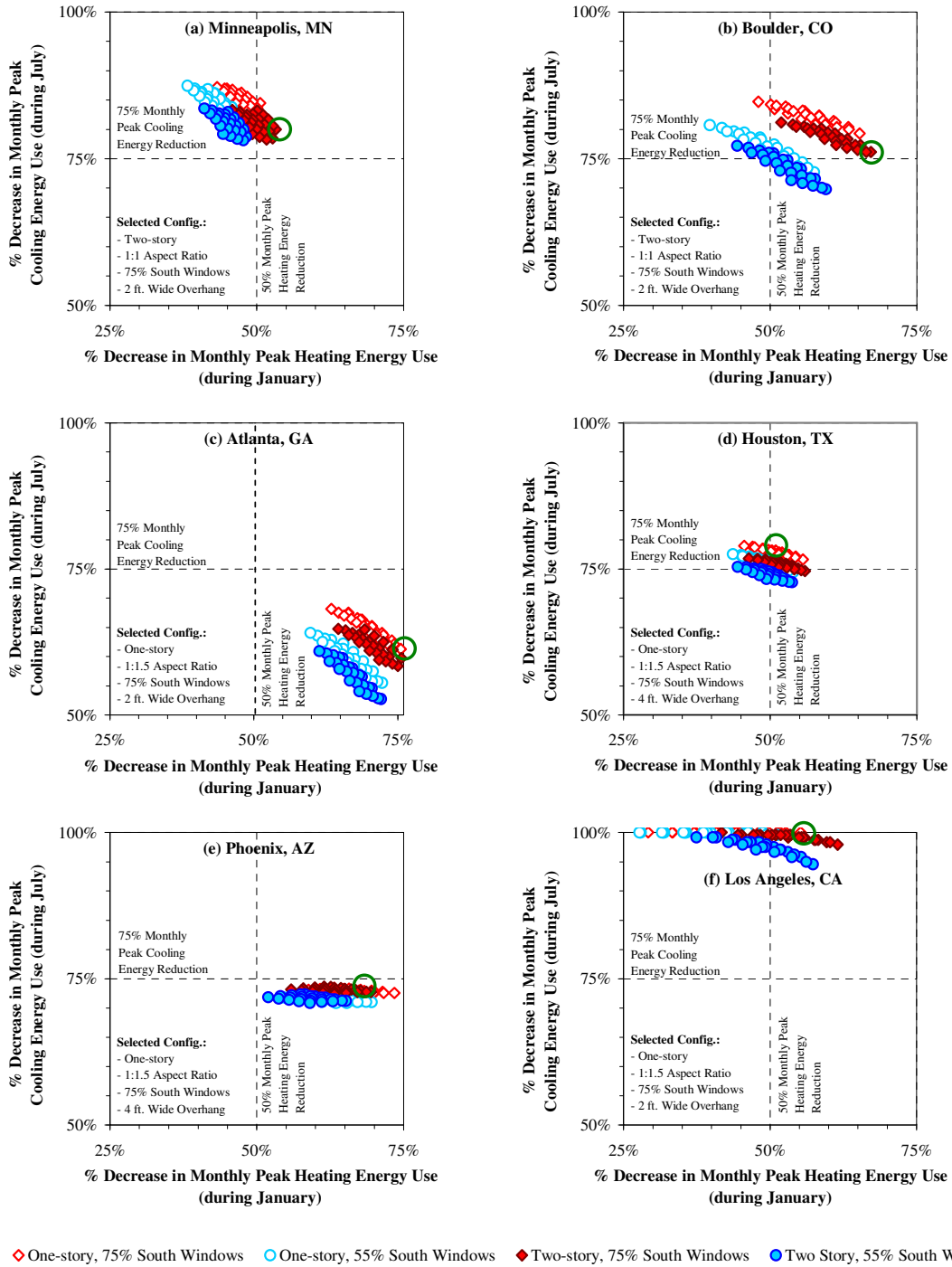
#### 5.3.4. *Determination of the Optimum Building Configuration*

Certain energy-efficiency strategies related to the building geometry (which determines the area of the thermal boundary surfaces of the building) and fenestration system (such as the overhang depth, window distribution on different orientations, and solar heat gain coefficient), which result in a reduction in heating energy use in the winter, may result in an increase in cooling energy use in the summer. Therefore, an optimum combination of these strategies was sought for each location using parametric simulations. To accomplish this, the proposed house with the energy-efficiency measures selected in Section 3 for each location was simulated for all possible configurations formed by incrementally changing the building's north-south to east-west aspect ratio – from 1: 1 to 1: 3, window distribution – from 55% to 75% on the south<sup>9</sup>, overhang depth – from 2 ft. to 4 ft., and number of floors from one to two story. From the DOE-2.1e output for the base-case and proposed house configurations, the monthly peak heating energy use (i.e., for January) was obtained from the SS-A report, and the monthly peak cooling electricity use (i.e., for July) was obtained from the PS-E report. Finally, the percent decrease in the monthly peak heating energy use for the proposed house configurations with respect to the base case versus the percent decrease in cooling electricity use were compared for selecting the optimum building configuration for each location.

Figure 38 and Figure 39 show the results of the parametric simulations for the six selected locations on the xy-scatter plots. In these plots, the x-axis represents the percent decrease in monthly peak heating energy use and the y-axis represents the percent decrease in monthly peak cooling electricity use. In Figure 38, the scale of the x-axis and the y-axis was kept the same across all six plots in order to illustrate the comparison among the six locations. In Figure 39 an expanded scale was used in order to better identify the final configurations used in the analysis for each site. In each figure, the unfilled markers represent one-story configuration and filled markers represent two-story configurations. In Figure 38, the red square markers correspond to 75% windows on the south and blue circular markers correspond to 55% windows on the south, which shows that for each location providing more windows on the south results in higher heating and cooling energy savings. In Figure 39, the results for 75% windows on the south are plotted using a larger scale in order to understand the impact of the variation in the window

---

<sup>9</sup> The window redistribution was accomplished by changing the east and west window area, and keeping the north window area fixed to 15% of the total window area.



EW-to-NS Aspect Ratio: varied from 1:1 to 1:3 in 0.5 increments; Overhang Width: varied from 2 ft. to 4 ft. in 0.5 ft. increments

Figure 38 Impact of the Building and Window Configuration on the Monthly Peak Heating and Cooling Energy Use of the Proposed Design in the Six Selected Climate Locations

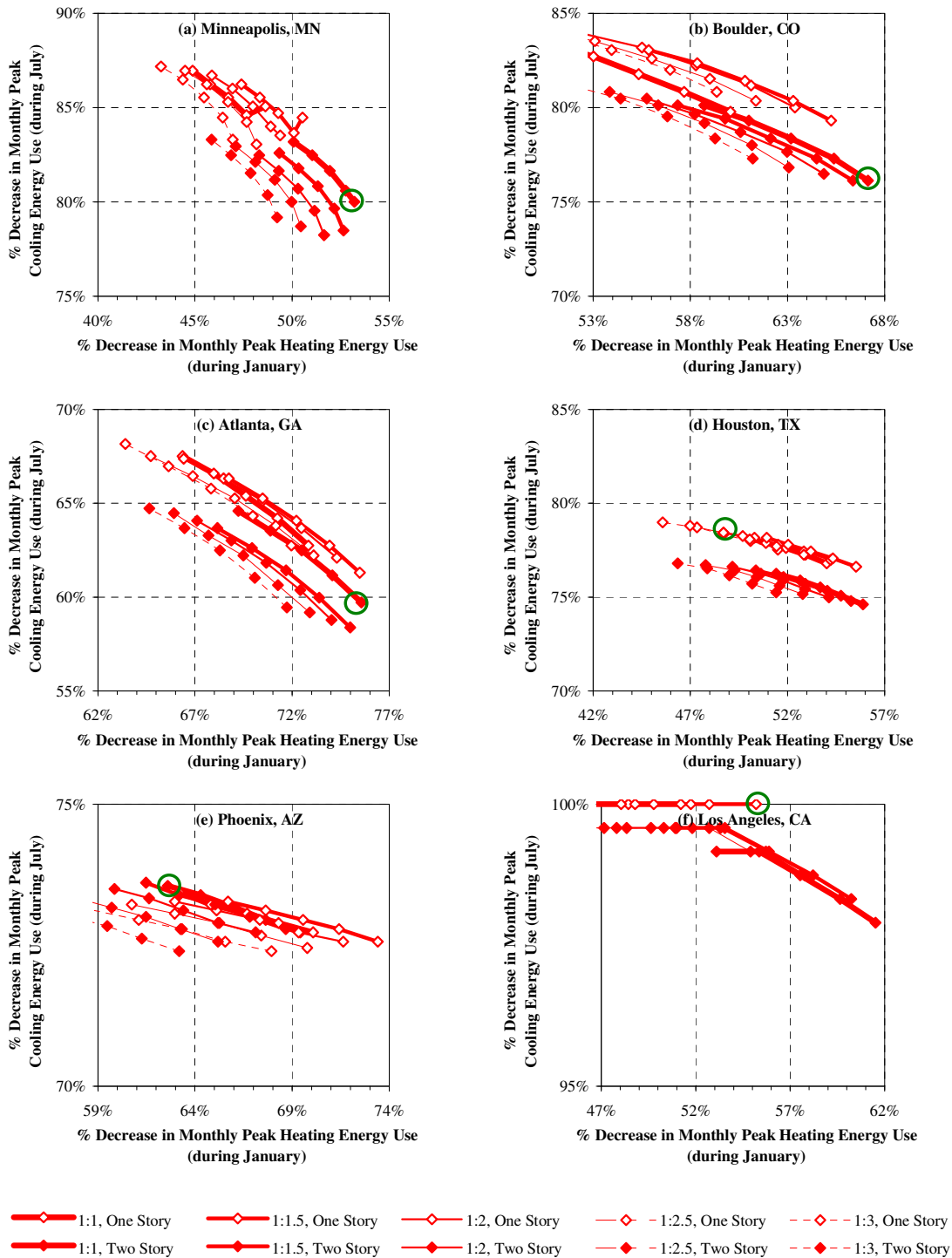


Figure 39 Impact of the Building Aspect Ratio and Overhang Depth on the Monthly Peak Heating and Cooling Energy Use of the Proposed Design in the Six Selected Climate Locations

Table 9 Measures for Achieving Maximum Energy-efficiency in the Six Selected Locations

Building Characteristics	Minneapolis, MN		Boulder, CO		Atlanta, GA		Houston, TX		Phoenix, AZ		Los Angeles, CA	
	Base-case	Energy-efficient	Base-case	Energy-efficient	Base-case	Energy-efficient	Base-case	Energy-efficient	Base-case	Energy-efficient	Base-case	Energy-efficient
Building Configuration	Aspect Ratio	1:1	1:1	1:1	1:1.5	1:1.5	1:1	1:1.5	1:1	1:1.5	1:1	1:1.5
	Number of Floors	1	2	1	1	1	1	1	1	1	1	1
Lighting and Equipment	Lighting kW	0.22	0.08	0.22	0.08	0.22	0.08	0.22	0.08	0.22	0.08	0.08
	Equipment kW	0.78	0.52	0.78	0.52	0.78	0.52	0.78	0.52	0.78	0.52	0.52
HVAC System	Duct Location	Attic	Room	Attic	Room	Attic	Room	Attic	Room	Attic	Room	Attic
	HVAC System Efficiency	SEER 13 7.7 HSPF	SEER 15 9.0 HSPF	SEER 13 7.7 HSPF	SEER 15 9.0 HSPF	SEER 13 7.7 HSPF	SEER 15 9.0 HSPF	SEER 13 7.7 HSPF	SEER 15 9.0 HSPF	SEER 13 7.7 HSPF	SEER 15 9.0 HSPF	SEER 13 7.7 HSPF
Building Envelope	Infiltration (Specific Leakage Area)	0.00057	0.00036	0.00057	0.00036	0.00057	0.00036	0.00057	0.00036	0.00057	0.00036	0.00036
	Radiant Barrier	None	None	None	None	None	None	None	None	None	None	None
	Ceiling R-value	38	57	37	57	27	57	23	57	22	57	22
	Wall R-value <sup>10</sup>	11+7.5	26	11+5.5	26	11+2	26	11	26	11	26	11
	Slab Perimeter R-value	6	10	5	10	4	10	0	0	0	0	0
	Wall Absorbance	0.75	0.75	0.75	0.75	0.75	0.75	0.75	0.25	0.75	0.25	0.75
	Roof Absorbance	0.75	0.9	0.75	0.9	0.75	0.75	0.75	0.5	0.75	0.5	0.5
	Window U-value	0.28	South:0.2 Other: 0.13	0.3	South:0.2 Other: 0.13	0.44	South:0.2 Other: 0.13	0.47	0.14	0.47	0.14	0.47
	Window SHGC	0.68	South:0.52 Other: 0.19	0.68	South:0.52 Other: 0.19	0.4	South:0.52 Other: 0.19	0.4	0.16	0.4	0.16	0.4
	Frame Type	Wood	Vinyl	Wood	Vinyl	Wood	Vinyl	Aluminum	Vinyl	Aluminum	Vinyl	Aluminum
Fenestration System	Window Distribution	Equal	S: 75% N: 15% E: 5% W: 5%	Equal	S: 75% N: 15% E: 5% W: 5%	Equal	S: 75% N: 15% E: 5% W: 5%	Equal	S: 75% N: 15% E: 5% W: 5%	Equal	S: 75% N: 15% E: 5% W: 5%	
	Exterior Shading (Overhang Depth)	None	2 ft.	None	2 ft.	None	2 ft.	None	4 ft.	None	4 ft.	2 ft.
Interior Shading <sup>11</sup>	Interior Shading <sup>11</sup>	0.9/0.7	0.9/0.7	0.9/0.7	0.9/0.7	0.9/0.7	0.9/0.7	0.9/0.7	0.9/0.25	0.9/0.7	0.9/0.25	0.9/0.25
	Moveable Night Insulation	None	R-21	None	R-21	None	R-21	None	None	None	None	None

<sup>10</sup> The base-case wall assembly was simulated as a wood frame wall with an R-11 cavity insulation and a continuous insulation to achieve the 2000/2001 standard reference design requirements. For the proposed design, SIP walls were simulated as an R-26 continuous insulation.

<sup>11</sup> The interior shading value for the energy efficient option is 0.25 in the summer, which was simulated as automatic drapes that activate for a maximum direct radiation of 30 Btu/h-ft<sup>2</sup> on the window plane.

overhang depth and aspect ratio. In this figure, the markers connected with the bold line represent a 1:1 aspect ratio. The markers connected with the fine dotted lines represent a 1:3 aspect ratio. On each line, markers on the right represent a two feet overhang and markers on the left represent a four feet overhang. For each location, an optimum combination was sought based on the priority for reducing peak heating versus peak cooling energy use.

After the preferred level of reduction in the heating versus cooling energy use was identified, the corresponding building and window configuration was then used for the proposed off-grid, off-pipe building design. For the six locations, the preferred configurations are:

1. A 1:1 two-story house with 75% of the windows on the south and a two feet overhang depth (which is the minimum overhang depth considered for the proposed design) for Minneapolis and Boulder,
2. A 1: 1.5 north-south to east-west aspect ratio, one-story house with 75% of the windows on the south and a two feet overhang depth in Atlanta and Los Angeles;
3. A 1: 1.5 north-south to east-west aspect ratio, one-story house with 75% of the windows on the south and a four feet overhang depth in Houston and Phoenix.

In this manner, the simulation results of the selected final configuration for each location was identified and used for further investigation. Table 9 lists all the measures considered for each location including the optimized configurations as determined above.

### 5.3.5. *Reduced Energy Use*

For the proposed design, the impact of combined measures was investigated using the same procedures as the base case (i.e., using the Manual J Average Load Procedure<sup>12</sup> for the peak heating and cooling load components, and investigation of the DOE-2.1e simulation output for building thermal energy and electricity use). The calculations for the Manual J Average Load Procedure are included in Appendix C, and the results of the calculations are shown in Figure 40 through Figure 42. Figure 40 shows a comparison of the peak heating and cooling load components for both the base case and the proposed design for the six locations. It shows that the selected measures reduced the peak cooling loads by 30-60% and peak heating loads by 30-40% in different locations. The contribution of the load components to the total heat gain/loss for the proposed design in each location was investigated using relatively-sized pie-charts of the heating and cooling load components as shown in Figure 41 and Figure 42, respectively. A comparison of Figure 41 with Figure 36 (i.e., for the base case house) shows that for Minneapolis and Boulder, the contribution of peak heating load components to the total heating load for the proposed designed was approximately the same as the base case. On the other hand, for other locations, the

---

<sup>12</sup> The Manual J Average Load Procedure is applicable to single zone applications with adequate exposure diversity. For designs that do not benefit from adequate exposure diversity (such as the proposed design with window distribution favoring the south), a Peak Load Procedure is recommended. However, considering that the proposed house was simulated as a single zone unit, the analysis of peak load components was performed using the Average Load Procedure.

contribution of windows was reduced and slab-on-grade floor increased for the proposed design, since slab-on-grade floor perimeter insulation was not considered for these locations due to a high termite infestation probability. This shows that there is a need for improved methods for providing slab-on-grade perimeter insulation, which could provide energy use reduction, at the same time, prevent termite infestation. A comparison of Figure 42 with Figure 37(i.e., for the base case house) shows that, for all locations, the contribution of all building envelope components to the total heat gain was smaller in the proposed design. This includes the highest reductions from the fenestration system improvements, especially, in the warm climates. On the other hand, contribution of infiltration and internal gain increased for the proposed designs.

For investigation of loads for the sizing the renewable energy systems, the results of the DOE-2.1e simulations are shown in Figure 43 through Figure 48. Figure 43 and Figure 44 compare the annual electricity use and thermal energy use for the six locations for the base-case and proposed design. Figure 45 and Figure 46 show the electricity use and thermal energy use by month for each location. Figure 47 and Figure 48 show the hourly electricity use for a peak winter day and hourly thermal energy use for a peak summer day for each location. In these figures, the base-case energy use is also shown for a reference to determine the impact of energy-efficiency measures on annual, monthly and peak day energy use.

The comparison of annual energy use shows that 40-60% of the thermal energy needs and 45-60% of the electricity needs could be reduced in all locations. On a monthly basis, energy use for peak summer and winter months were compared. In Minneapolis, a 50% reduction in peak winter monthly energy use and a 44% reduction in peak summer monthly electricity use were achieved. In Boulder, the peak monthly savings were 61% and 42% for the winter and summer, respectively. All other locations showed approximately a 55-70% reduction in peak monthly electricity use in the winter. The peak monthly electricity use reduction in the summer for these locations varied from 42% to 45%. A comparison of the peak daily energy use of the base case and the proposed house showed approximately a 50% reduction in the peak daily electricity and thermal energy use in Minneapolis, Boulder and Atlanta. Higher reductions of up to 60-70% were observed in all other locations.

These comparisons show that the application of the available measures along with the carefully selected design strategies can produce more than 50% reductions in all locations, which is very important for an off-grid house where the sizing, usability and cost-effectiveness of renewable systems is largely impacted by small changes in the peak energy use.

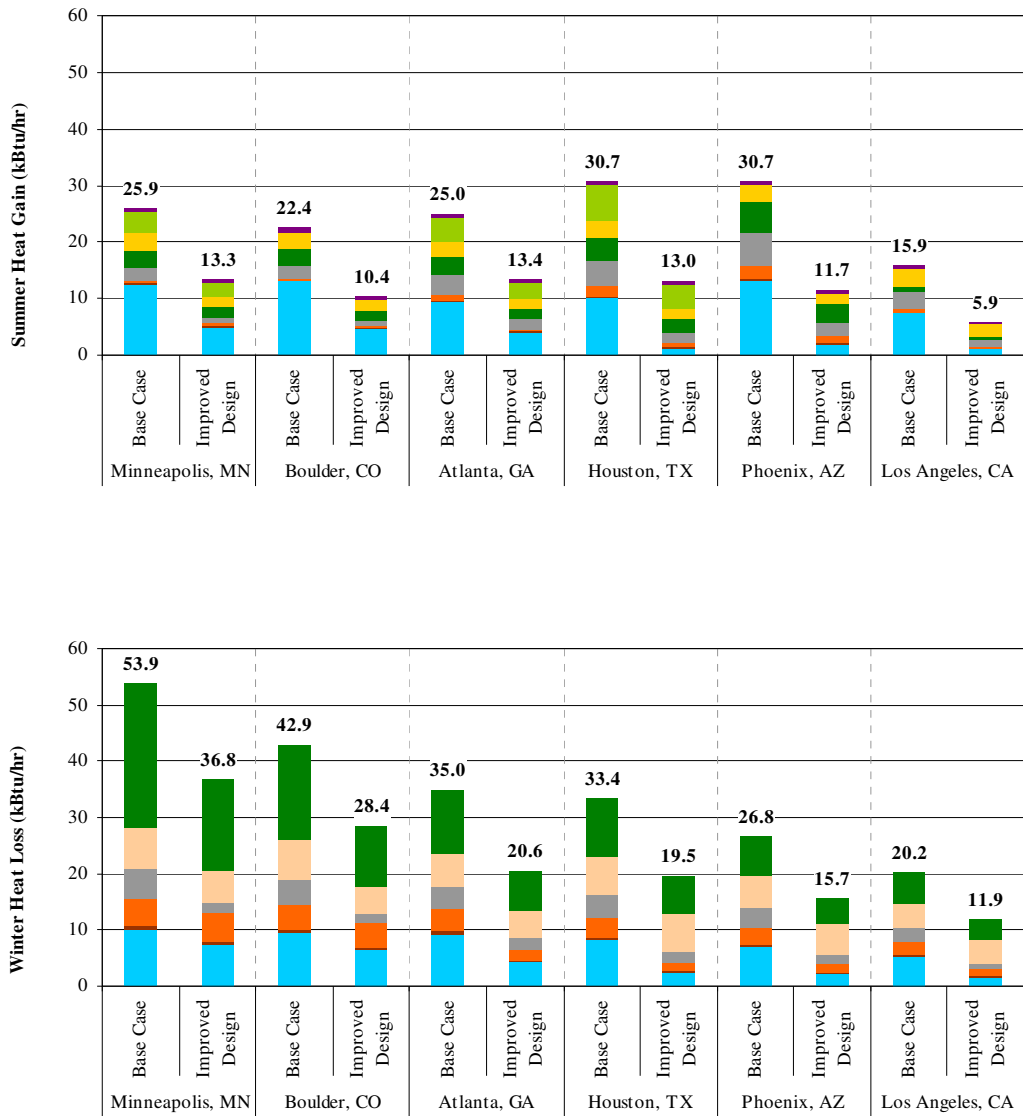


Figure 40 Peak Load Components of the Base-case House and Proposed Design in the Six Selected Locations



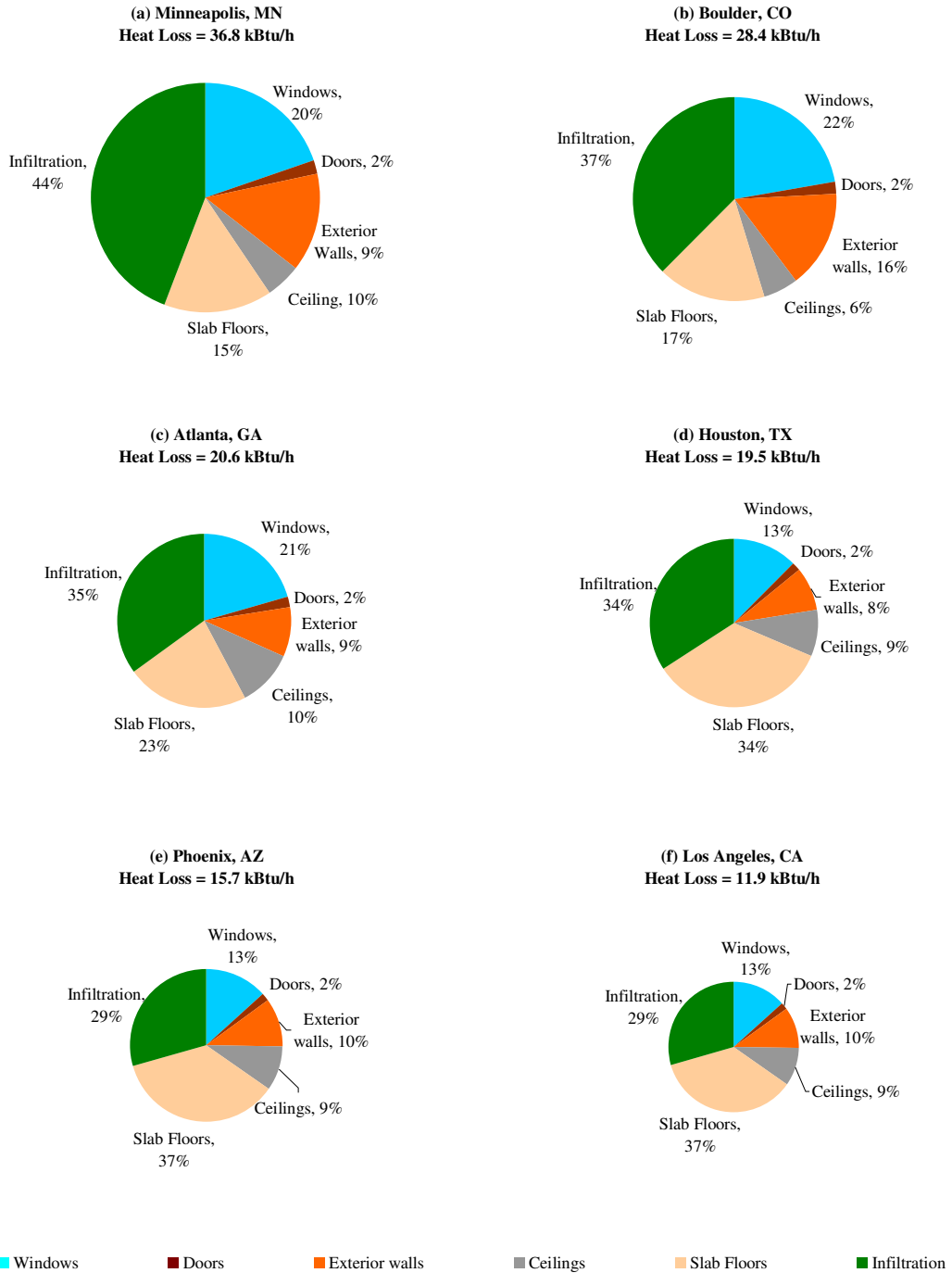


Figure 41 Peak Heating Load Components of the Proposed Design for the Six Selected Climate Locations

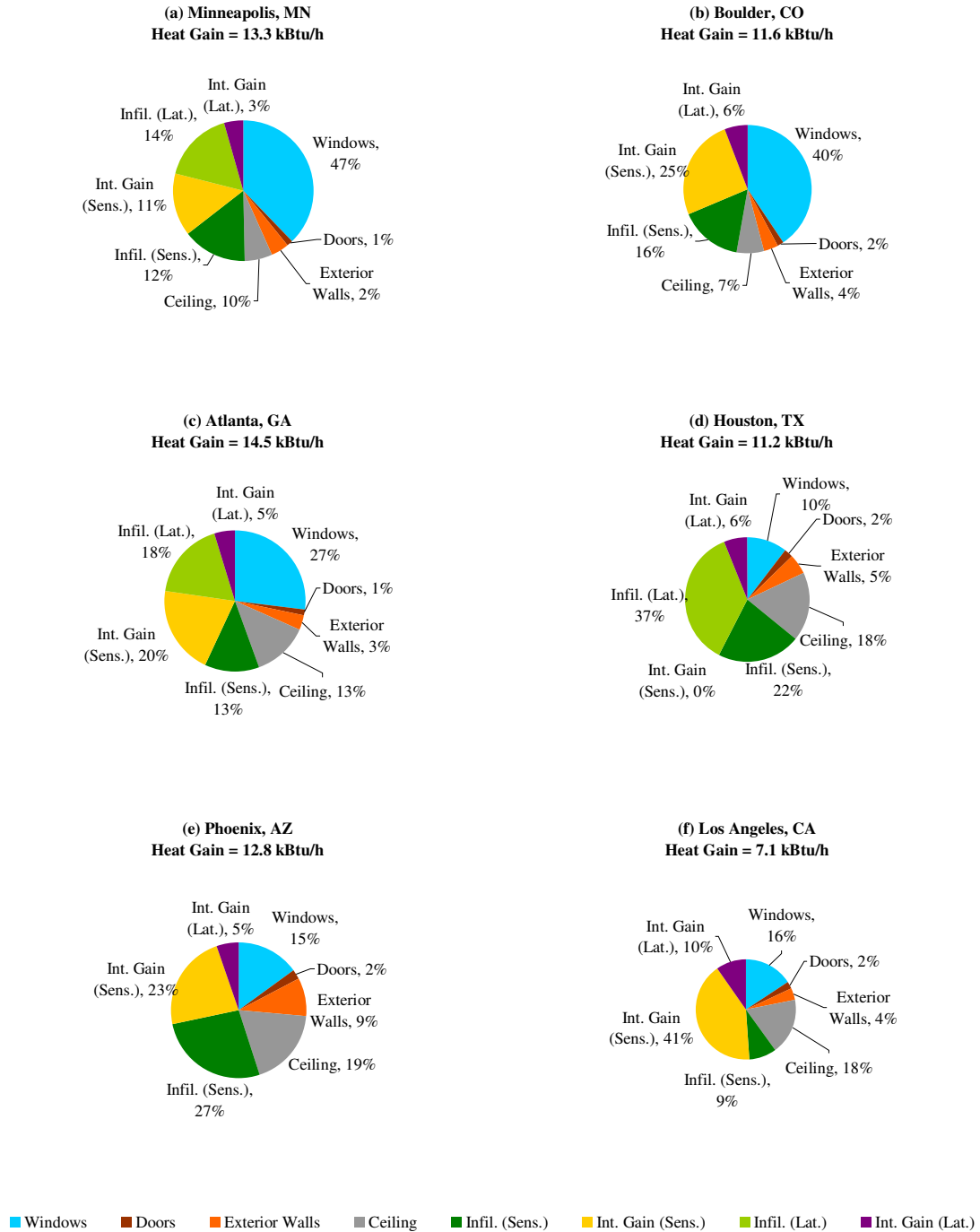


Figure 42 Peak Cooling Load Components of the Proposed Design for the Six Selected Climate Locations

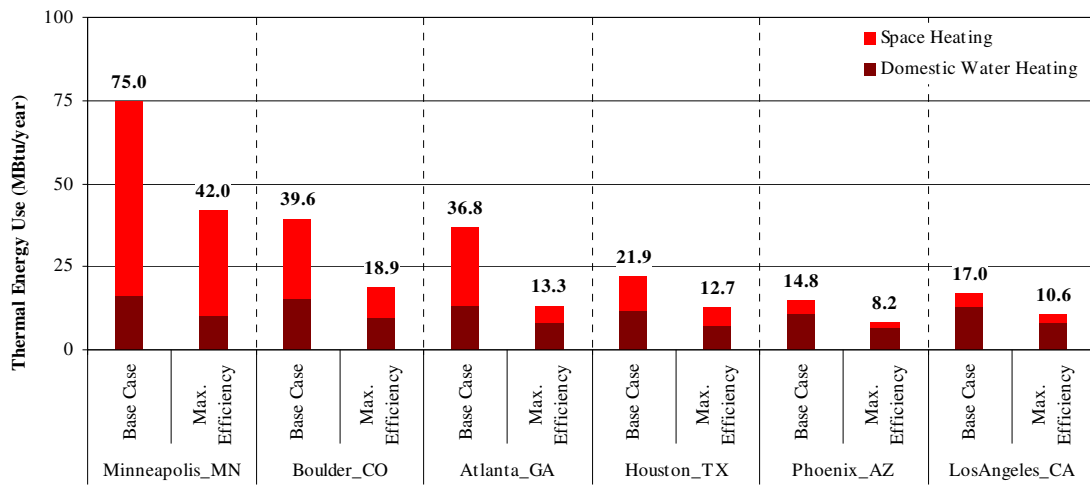


Figure 43 Minimized Annual End-use Thermal Energy Use in the Six Selected Climate Locations

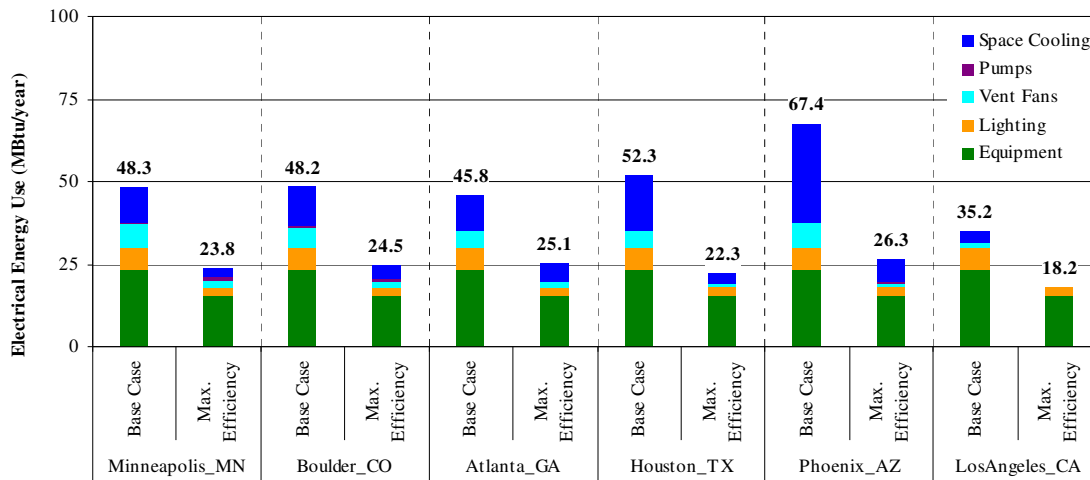


Figure 44 Minimized Annual End-use Electricity Use in the Six Selected Climate Locations

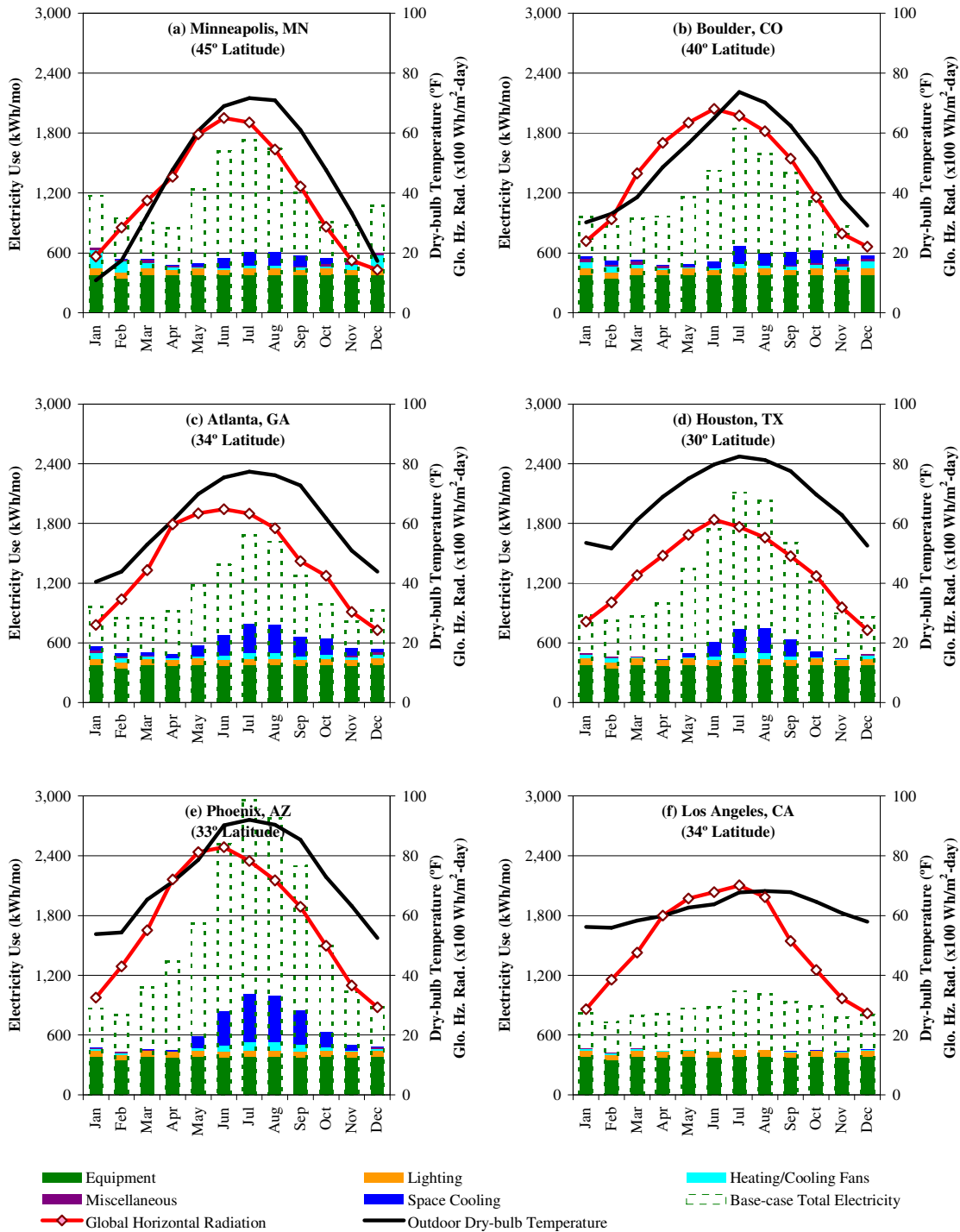


Figure 45 Minimized Monthly End-use Electricity Use in the Six Selected Climate Locations

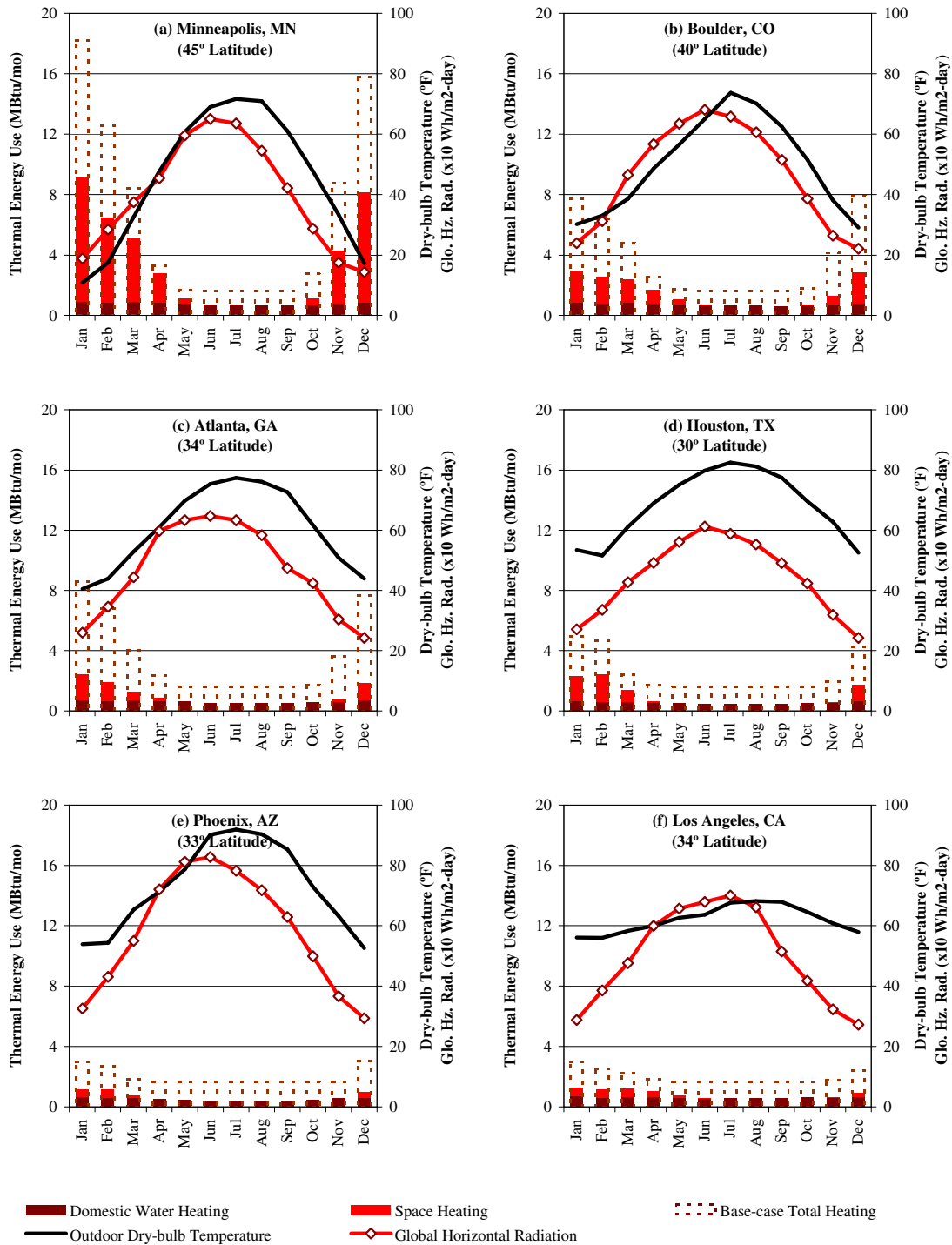


Figure 46 Minimized Monthly End-use Thermal Energy Use in the Six Selected Climate Locations

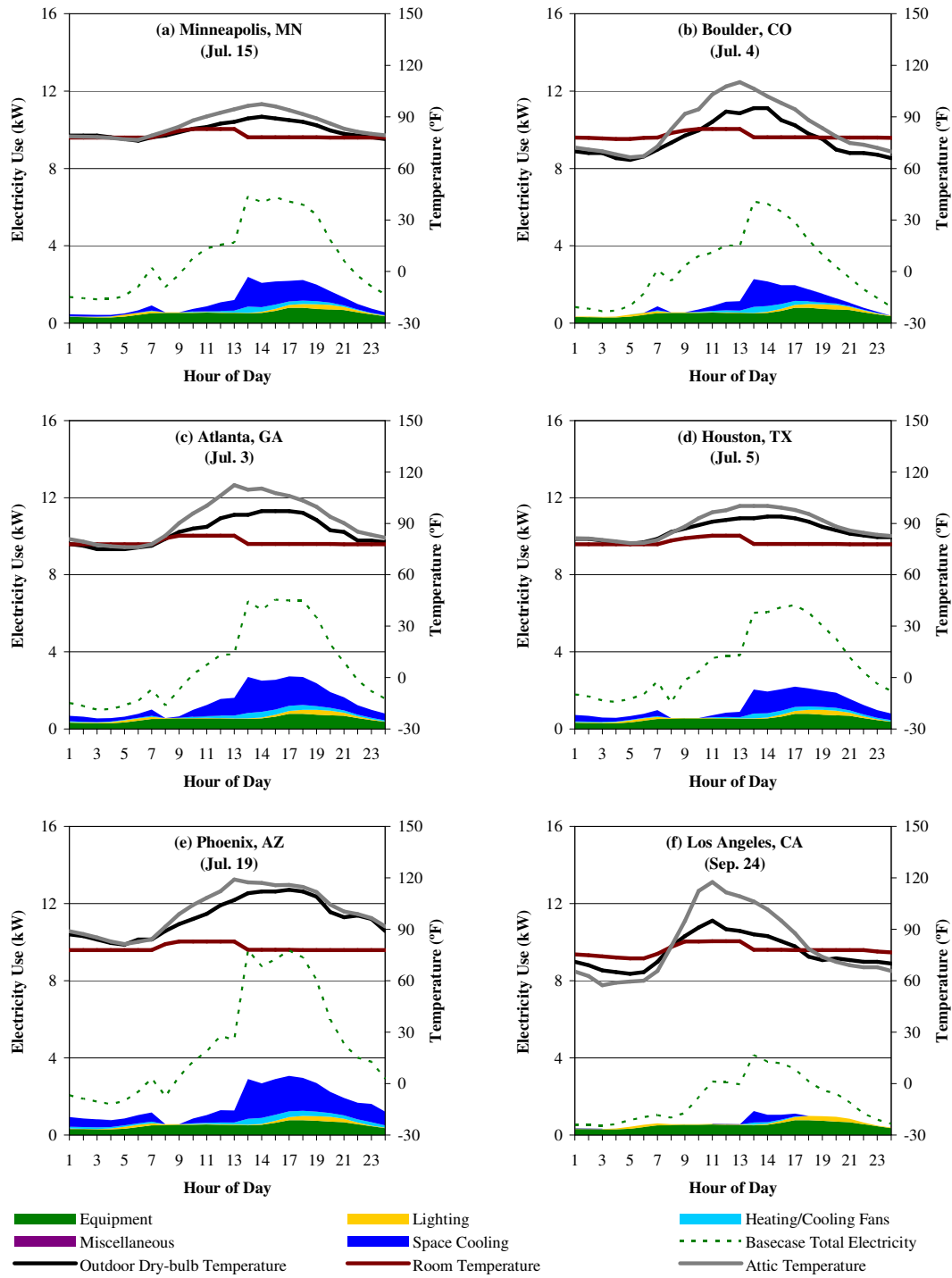


Figure 47 Minimized Peak Summer Day Hourly End-use Electricity Use in the Six Selected Climate Locations

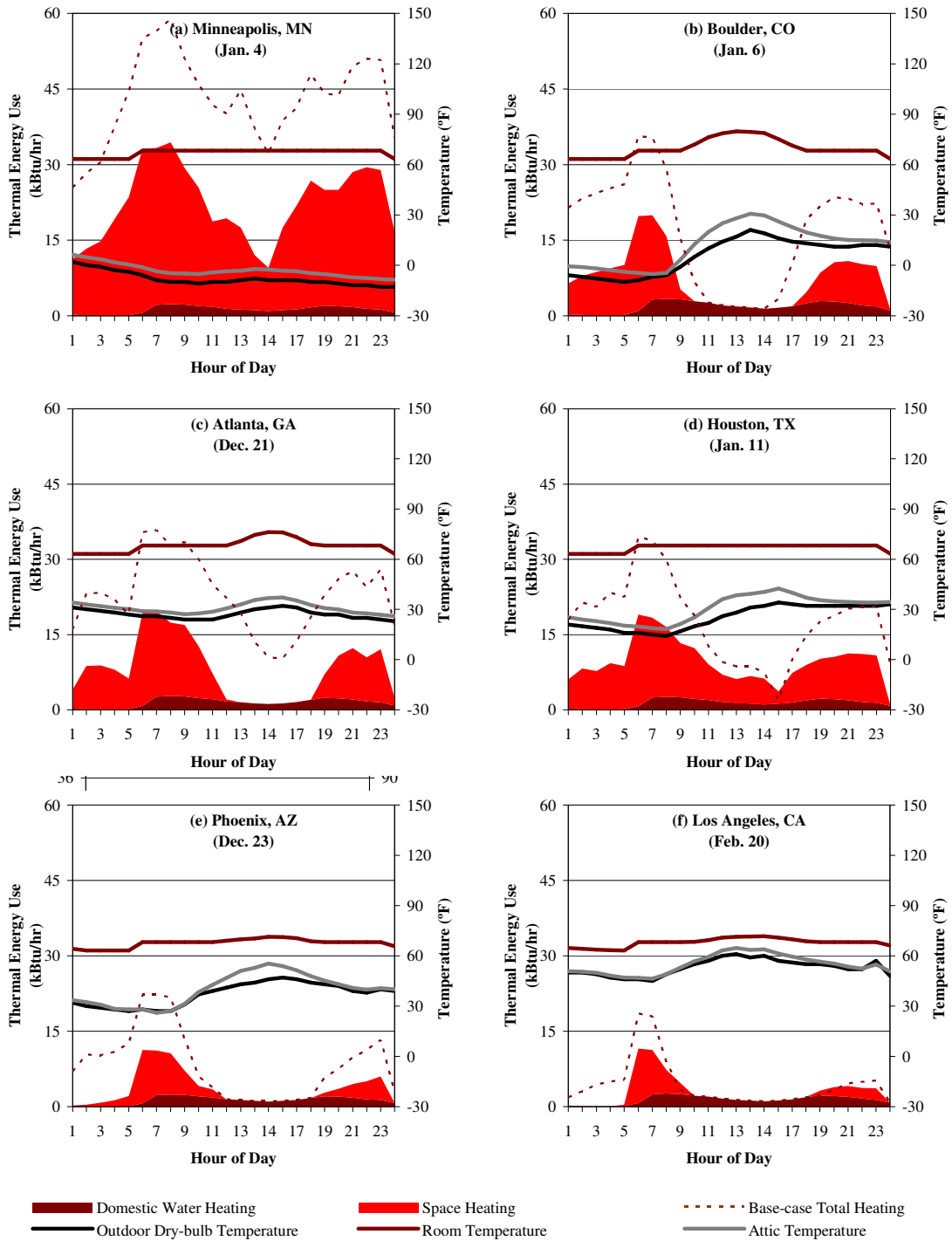


Figure 48 Minimized Peak Winter Day Hourly End-use Thermal Energy Use in the Six Selected Climate Locations

#### 5.4. Quantification of On-site Harvestable Renewable Resources

In the following sections, the analysis for quantifying the performance of the active solar thermal system, photovoltaic system and wind power system, and for the determination of the normalized system sizing parameters for the rainwater harvesting system for the six selected climate locations is presented. The results of the analysis were used with the reduced building energy and water needs determined in Section 5.5 to perform the system sizing for achieving self-sufficiency.

##### 5.4.1. *Analysis of the Solar Thermal System*

The performance of solar thermal systems was analyzed using the procedure described in Section 4.6.1. First a flat plate collector and an evacuated tube collector with a higher performance rating were selected from the SRCC collector database (SRCC 2008). Then, the monthly output from a solar thermal system with these collectors was quantified in each location for varying areas and tilts using the F-CHART program.

##### 5.4.1.1. *Selection of Solar Thermal Collectors*

To select high performance solar thermal collectors, the collector performance ratings (i.e., the collector test intercept ( $F_R\tau\alpha$ ) and test slope ( $F_RU_L$ )) for several commercially available collectors were obtained from the SRCC (2008) and plotted on an x-y scatter plot. In addition, the collector test intercept and test slope corresponding to the F-CHART default flat plate collector and the evacuated tube collector were placed on the same plot. Figure 49(a) shows the xy-scatter plot of collector test slope on the x-axis versus the test intercept on the y-axis. On this plot, the most efficient collectors have a high test intercept and a low test slope. The square markers represent flat plate collectors, circular markers represent evacuated tube collectors. Among the flat plate collectors, the unfilled markers represent collectors with air as the heat transfer fluid and filled markers represent collectors with water as the heat transfer fluid. Among the evacuated tube collectors, the unfilled marker represents a concentrating parabolic collector. The black square and circular markers represent the F-CHART default flat plate collector and evacuated tube collector, respectively.

Figure 49(a) shows that the flat plate collectors are available with a wide range of collector efficiency and test slope. On the other hand, evacuated tube collectors have a narrower range of test slope and a wide range of the test intercept. For certain evacuated tube collectors, the test intercept is comparable to that of flat plate collectors. The F-CHART default collector parameters represent high performance collectors in each category. Using this plot, two flat plate collectors (including F1, with the highest test intercept, and F2, with the smallest test slope among all flat plate collectors) and two evacuated tube collectors (including E1, with the highest test intercept, and E2, with the smallest test slope among all evacuated tube collectors) were selected for further comparison.



Figure 49(b) shows the performance curve for six collectors including: three flat plate collectors (F0, F1 and F2) and three evacuated tube collectors (E0, E1 and E2). Figure 50 shows the incident angle modifiers for the flat plate collectors, and Figure 51 shows the transverse and longitudinal incident angle modifiers for the evacuated tube collectors<sup>13</sup>. To investigate the impact of incident angle modifiers on the collector efficiency at a varying angle of incidence, the product of test slope ( $F_R(\tau\alpha)_n$ ) and incident angle modifiers  $(\tau\alpha)_\theta/(\tau\alpha)_n$  was plotted in Figure 51. It shows the combined effect of the two parameters and provided a better indicator of the collector heat gain. Finally, collector F2 and E1 were selected for analyzing the performance of solar thermal collectors using the F-CHART.

#### 5.4.1.2. Determination of the F-CHART Input Parameters

The F-CHART input parameters, which include weather parameters, system parameters and collector parameters, were determined using the procedure described in Section 4.6.1.2. Among these, the system parameter - building UA, and the weather parameter – the balance point temperature for space heating, were determined from the slope and intercept of the linear curve-fit of the monthly average hourly thermal energy use (obtained from DOE-2.1e results) versus monthly average dry-bulb temperatures. Figure 52 shows the linear curve-fits for the base case and proposed house on the xy-scatter plots for the six selected locations. Each curve-fit equation expresses the monthly average hourly space heating energy use (y) as a linear function of outdoor dry-bulb temperature (x). The slope of the linear curve-fit (-m) represents the building UA, and the x-intercept (-m/c) represents the balance point temperature for space heating. The resulting values and other climate-specific F-CHART input parameters are listed in Table 10. The collector parameters for the two selected collectors are listed in Table 11. The common F-CHART collector and system parameters, which were the same for all climate locations and both collector types, are listed in Table 12 for the base case and the proposed house. Using these inputs, the monthly solar thermal system output from a 64 ft<sup>2</sup>, a 128 ft<sup>2</sup>, 192 ft<sup>2</sup> and a 256 ft<sup>2</sup> collector areas for the two selected collector types were obtained using the procedure described in Section 4.6.1.3.

---

<sup>13</sup> It was noted that the F-CHART default incident angle modifiers are the same irrespective of the collector type and the direction of incident angle perpendicular or parallel to the evacuated tube axis, and are therefore representative of high-performance flat plate collectors.

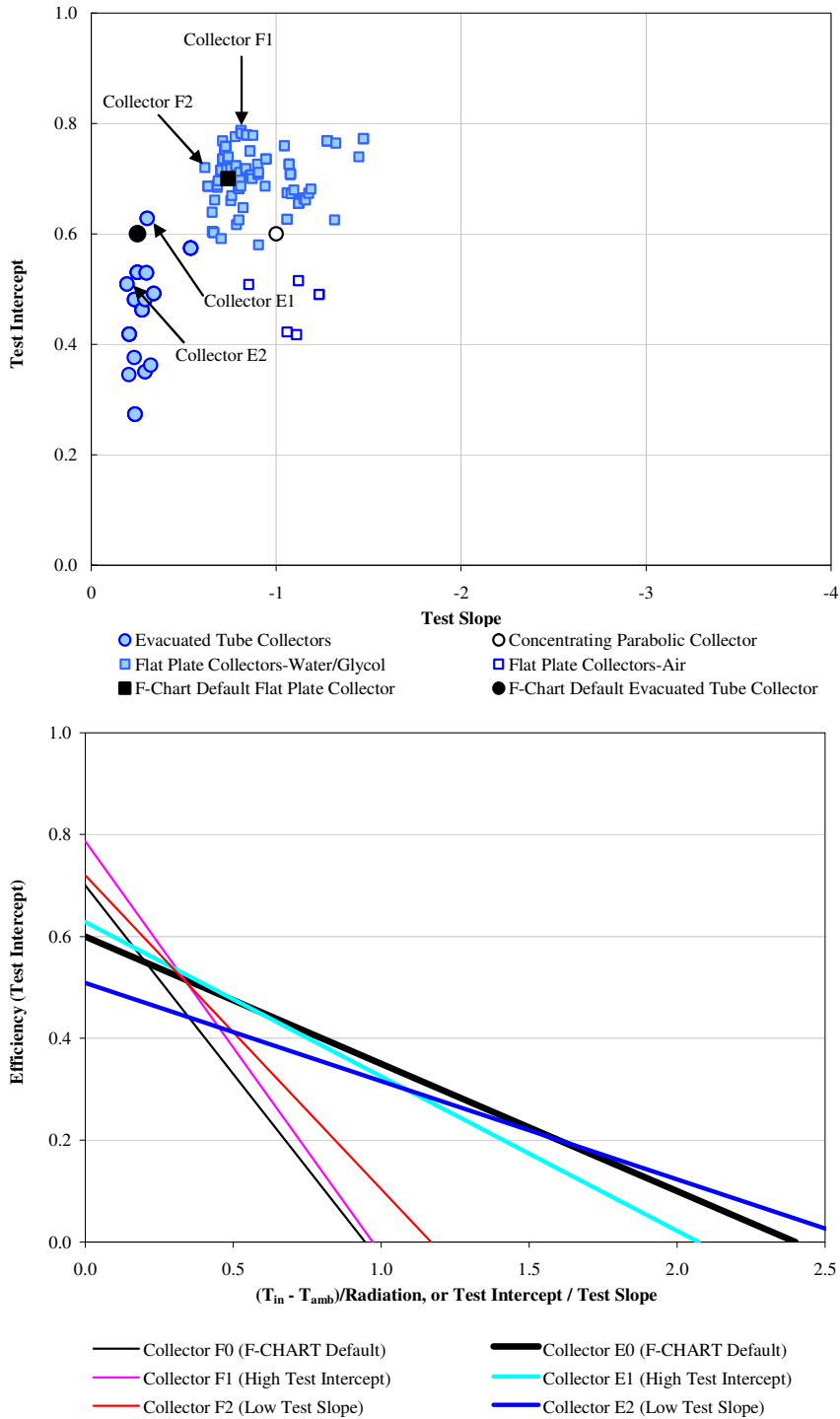


Figure 49 Test Slope ( $F_R U_L$ ) and Test Intercept ( $F_R \tau \alpha$ ) for: (a) All Solar Thermal Collectors on an x-y Scatter Plot, and (b) Selected Solar Thermal Collectors using Collector Efficiency Curves

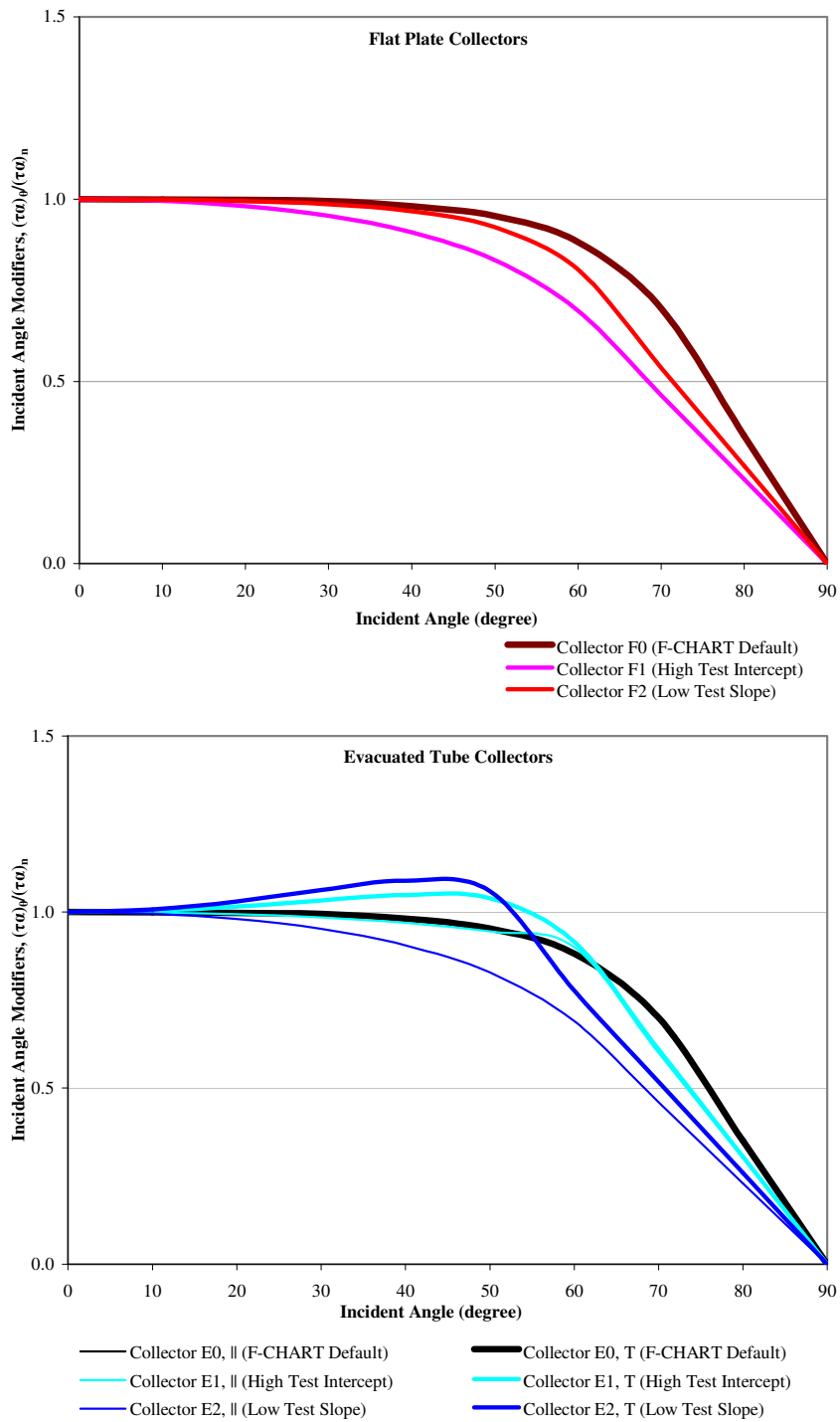


Figure 50 Incident Angle Modifiers  $K_\theta$  for: (a) Flat Plate Collectors, (b) Evacuated Tube Collectors

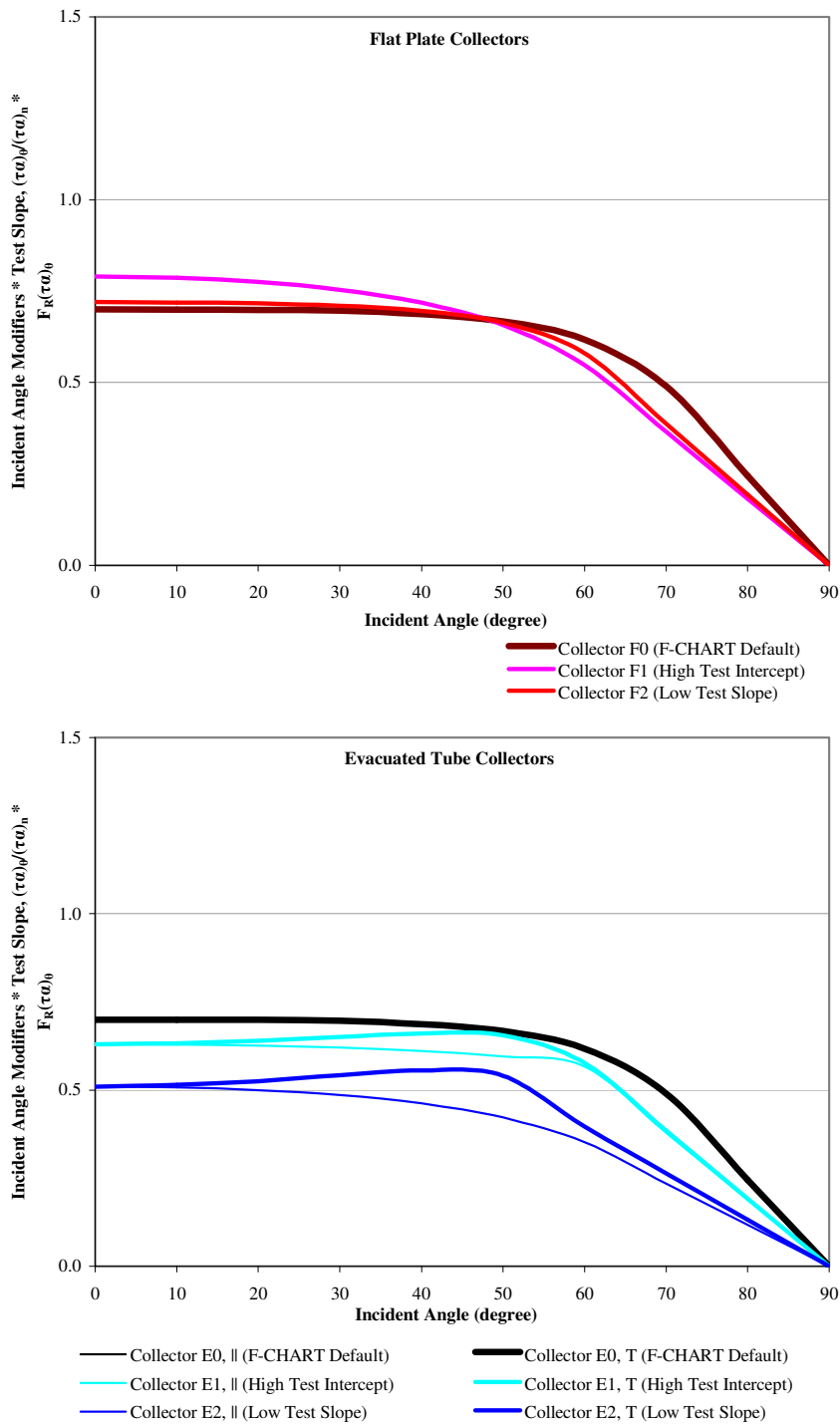


Figure 51 Product of Test Slope and Incident Angle Modifiers  $K_0$  for: (a) Flat Plate Collectors, (b) Evacuated Tube Collectors

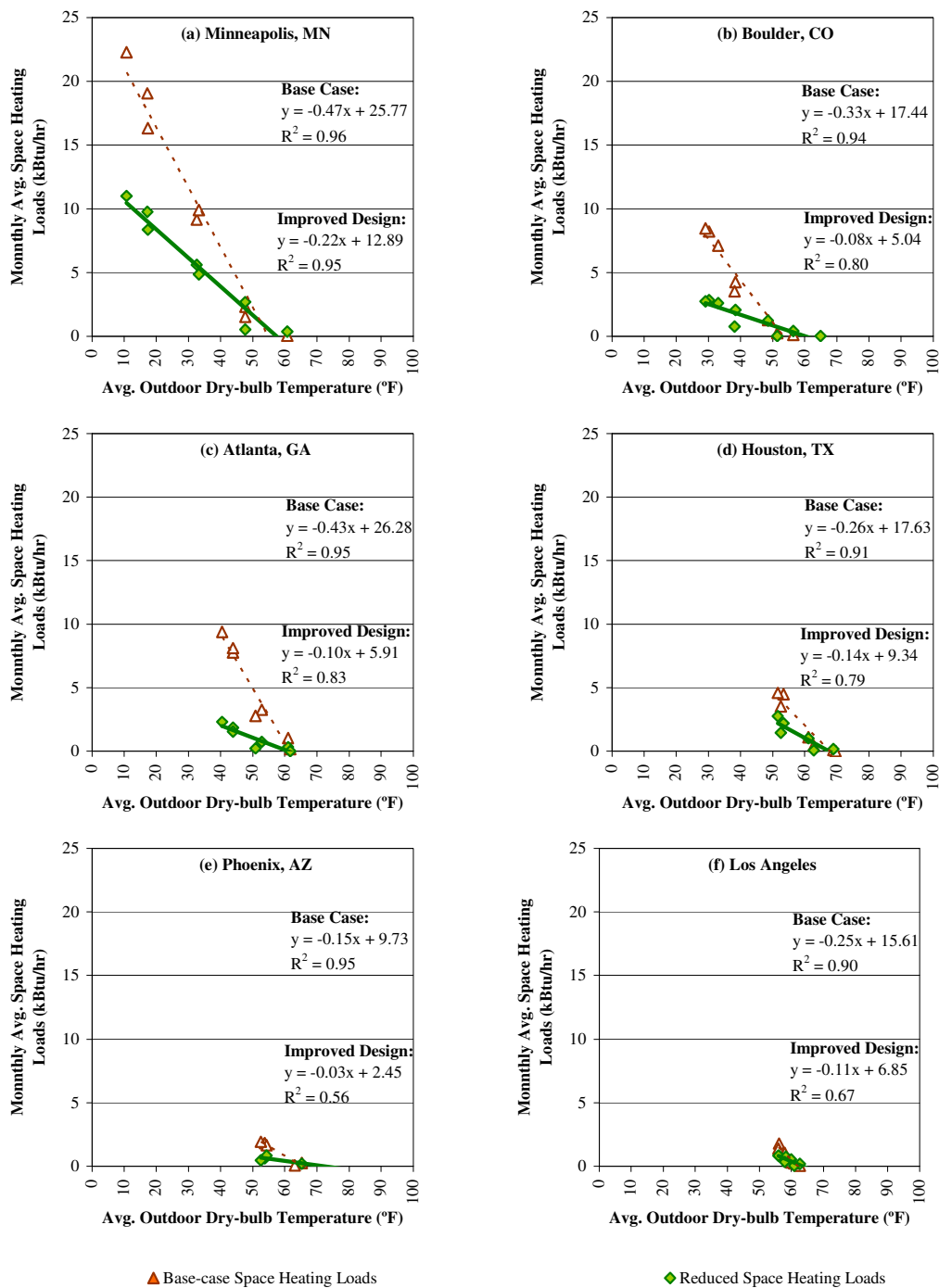


Figure 52 Determination of Building UA and  $T_{bal}$  for the Six Selected Climate Locations

Table 10 Climate Location Specific F-CHART Input Parameters

	Minneapolis, MN	Boulder, CO	Atlanta, GA	Houston, TX	Phoenix, AZ	Los Angeles, CA
LOCATION AND WEATHER PARAMETERS (for January – the Peak Winter Month)						
Latitude ( $\phi$ )	45°	40°	34°	30°	33°	34°
Degree-day Base (°F)	51.6	51.7	63.4	68.1	66.5	63.6
Heating Degree-day <sup>14</sup> (°F-days)	1,631	1,058	745	389	335	265
Solar Radiation <sup>14</sup> (kWh/m <sup>2</sup> .day)	1.88	2.39	2.60	2.71	3.25	2.87
Dry-bulb Temperature <sup>14</sup> (°F)	10.8	30.2	40.5	53.4	53.8	56.1
Water Mains Temperature <sup>14</sup> (°F)	40.1	46.9	56.7	64.4	65.1	64.6
Ground Reflectance <sup>14</sup> ( $\rho_g$ )	0.39	0.28	0.1	0.14	0.17	0.06
COLLECTOR PARAMETERS						
Collector Slope <sup>15</sup> ( $\beta$ )	71°	64°	53°	49°	57°	54°
Collector Fluid Specific Heat (Btu/lb.°F)	0.8	0.8	0.8	1.0	1.0	1.0
SYSTEM PARAMETERS						
Building UA (Btu/h.°F)	195.4	76.2	159.2	159.6	74.8	103.6
Avg. Daily Hot Water Usage <sup>16</sup> (gal/day)	50.1	49.3	47.9	46.4	46.2	46.4
Collector-Storage Heat Exchanger	Yes	Yes	No	No	No	No

Table 11 Collector-specific F-CHART Input Parameters

COLLECTOR PARAMETERS (SRCC 2009)	Flat Plate Collectors	Evacuated Tube Collectors
Collector Type	Flat Plate	Evacuated Tube
Test Slope ( $F_R U_L$ )	0.81	0.30
Test Intercept ( $F_R \tau \alpha$ )	0.79	0.63
Incidence Angle Modifiers <sup>17</sup> ( $K_{\tau\alpha} = 1 + b_1[1/\cos\theta - 1] + b_2[1/\cos\theta - 1]^2$ )		
Coefficients $b_1$ and $b_2$ (Perpendicular)	-0.29, -0.01	+0.27, -0.35
Coefficients $b_1$ (Parallel)	-	-0.10
Test Collector Flow rate per Area (gpm/ft <sup>2</sup> )	14.5	14.9
Test Collector Fluid Specific Heat (Btu/lb.°F)	1.0	1.0

<sup>14</sup> Values for the peak winter month (i.e., January) are listed here.

<sup>15</sup> Collector slope is optimized for January, for all locations.

<sup>16</sup> Reduced domestic hot water use for January is listed here, which is estimated as 38% less than the base case, for all climate locations.

<sup>17</sup> Angular dependent values of incident angle modifiers were used (as shown in Figure 50).

Table 12 Common F-CHART Input Parameters (for All Climate Locations and Collector Types)

COLLECTOR PARAMETERS	
Collector Panel Area ( $A_c$ , ft <sup>2</sup> )	Varied
Collector Azimuth ( $\gamma$ )	South
Receiver Orientation (for Evacuated Tube Collectors)	North-South
Collector Flow rate per Area (gpm/ft <sup>2</sup> )	Same as Test Collector Specifications
SYSTEM PARAMETERS	
Water Volume / Collector Area (gal/ft <sup>2</sup> )	1.85
Fuel <sup>18</sup>	Electric
Efficiency of Fuel Usage (%)	100%
Domestic Hot Water	Yes
Water Set Temperature	120 °F
Environmental Temperature	68 °F
UA of Auxiliary Storage Tank (Btu/h.°F)	11.2
Pipe Heat Loss	No
Supply Pipe UA (Btu/h.°F)	-
Return Pipe UA (Btu/h.°F)	-
Relative Load Heat Exchanger Size	0.5

#### 5.4.1.3. F-CHART Output

The results of the solar thermal system analysis are shown in Figure 53 for the six selected locations. The monthly thermal loads are shown as orange bars. The output of the flat plate and evacuated tube collectors are shown as square and circular markers, respectively, which indicate the fraction of combined space heating and domestic water heating loads met by the solar thermal energy. The collector tilt was optimized for the winter peak month. For such a tilt, the solar radiation incident on the collector plane is shown as the brown line. In addition, the global horizontal radiation is indicated as the dotted brown line for a reference. For each location, the tilted collector surface increased the wintertime thermal collection and decreased the summertime thermal collection which improve the overall performance. In this analysis, the useful monthly solar thermal energy from the varying collector areas were compared with the thermal loads. The unmet loads, if any, were converted to electrical loads for sizing the electricity generation system.

<sup>18</sup> These parameters are required only for economics calculations.

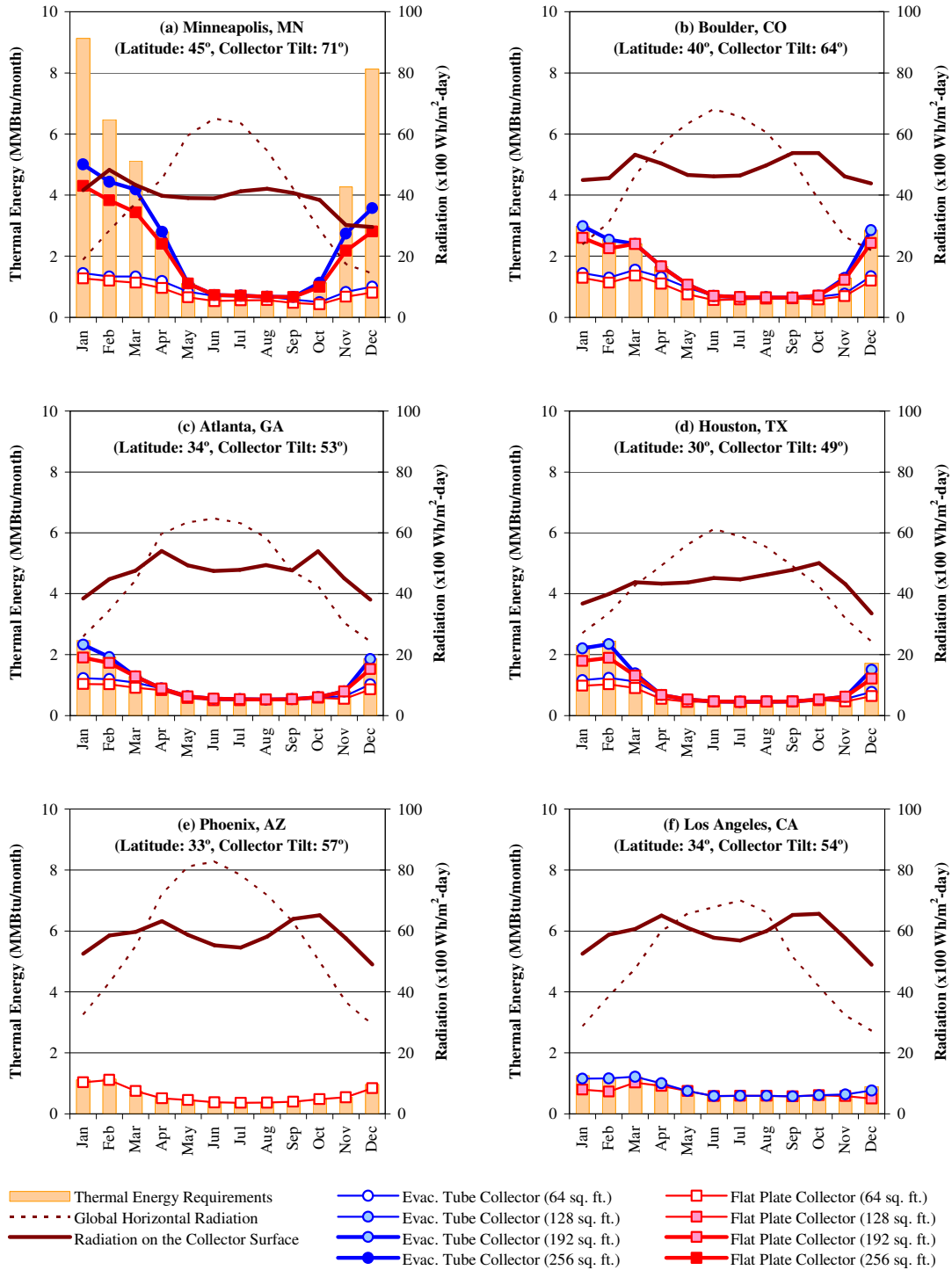


Figure 53 Performance of Flat Plate and Evacuated Tube Collectors in the Six Selected Climate Locations



#### 5.4.2. *Performance of the Photovoltaic System*

The performance of photovoltaic system in different climates was analyzed using the procedure described in Section 4.6.2. The performance of a photovoltaic system depends on the panel reference efficiency, temperature coefficient, and cell temperature at NOCT conditions. A higher reference efficiency, a lower temperature coefficient, and a lower cell temperature are desirable for increased output. In this analysis both, mono-crystalline PV panels, which have higher reference efficiency and a higher temperature coefficient, and thin-film PV panels, which have a lower reference efficiency and a lower temperature coefficient, were considered. For this study, a mono-crystalline panel with 18.5% efficiency and 0.0038 per °C of temperature coefficient, and a thin-film PV panels with 6.67% efficiency and 0.0021 per °C of temperature coefficient were selected for the analysis. The analysis was performed using the PV F-CHART program with TMY2 weather data for each location.

The PV F-CHART system inputs for the two selected PV panel types are listed in Table 13. Since the analysis was based on an equal capacity of both types of PV panels the array area of the thin-film PV panel was approximately three-times larger than that of mono-crystalline PV panels. For both PV panel types, the same efficiency for the power tracking electronics and the power conditioning electronics was used. Table 14 lists the climate location specific PV F-CHART input including the latitude, annual average solar radiation, dry-bulb temperature, ground reflectance and the array tilt. For each location, an array tilt of latitude + 15°, latitude, and latitude – 15° were used for the analysis, which correspond to the optimum tilt for the winter season, entire year, and summer season, respectively. The optimum tilt for a location was then determined by comparing the monthly electricity output at these tilts versus the building electricity loads for the PV system.

##### 5.4.2.1. *PV F-CHART Results*

The PV F-CHART output includes: solar radiation incident on the array surface ( $H_T$ ), electricity conversion efficiency of the PV array at the installed conditions ( $\eta$ ), and the electricity output (in kWh). From the PV F-CHART output, the ratio of installed efficiency and reference efficiency of the PV array (i.e.,  $\eta/\eta_{ref}$ ) and the ratio of electricity output and installed capacity (in kWh/kWp) were calculated for each location.

Figure 54 shows the ratio of installed efficiency and reference efficiency for the six locations. The dark green curves correspond to the mono-crystalline PV array and the light green curves correspond to thin-film PV array, oriented at the latitude tilt. It also shows the two climate parameters including solar radiation as the red line and ambient dry bulb temperature as the black line. Figure 54 shows that all locations receive similar amounts of solar radiation, except Phoenix, AZ, which receives 30% more solar radiation compared to other locations. For locations with higher ambient temperatures, the increased PV cell temperature results in thin-film PV cells performing slightly better in summer compared to mono-crystalline PV cells. Therefore, for warm climate locations, the reduced performance of mono-crystalline

cells favor the use of thin-film PV panels of the same capacity. However, this would triple the array area requirement.

Figure 55 shows the ratio of electricity output and installed capacity (in kWh/kWp) for the mono-crystalline PV array (as dark green lines) and the thin-film PV array (as light green lines), tilted at latitude + 15° (as dotted lines), latitude (as bold lines), and latitude – 15° (as thin lines) for each location. It shows the monthly variation in the PV electricity output due to array tilt. This profile would be used with the monthly electricity output for sizing the PV system for the six locations.

*Table 13 Photovoltaic Panel Specific PV F-CHART Input Parameters*

SYSTEM PARAMETERS	Mono-crystalline PV Panels (3.7 kW)	Thin-film PV Panels (3.7 kW)
Array Area	20 m <sup>2</sup>	55 m <sup>2</sup>
Cell Temperature at NOCT Conditions	48.5 °C	46 °C
Array Reference Efficiency	18.5 %	6.67 %
Array Reference Temperature	25 °C	25 °C
Array Temperature Coefficient	0.0038 per °C	0.0021 per °C
Power Tracking Efficiency	0.88	0.88
Power Conditioning Efficiency	0.90	0.90

*Table 14 Climate Location Specific PV F-CHART Input Parameters*

	Minneapolis, MN	Boulder, CO	Atlanta, GA	Houston, TX	Phoenix, AZ	Los Angeles, CA
LOCATION AND WEATHER PARAMETERS						
Latitude ( $\phi$ )	45°	40°	34°	30°	33°	34°
Global Horizontal Solar Radiation <sup>20</sup> (kWh/m <sup>2</sup> -day)	1.88	2.39	2.60	2.71	3.25	2.87
Dry-bulb Temperature <sup>Error! Bookmark not defined.</sup> (°F)	10.8	30.2	40.5	53.4	53.8	56.1
Ground Reflectance <sup>Error! Bookmark not defined.</sup> ( $\rho_g$ )	0.39	0.28	0.1	0.14	0.17	0.06
SYSTEM PARAMETERS						
Array Slope ( $\beta$ )	30°, 45°, 60°	25°, 40°, 55°	29°, 34°, 49°	15°, 30°, 45°	30°, 33°, 48°	29°, 33°, 49°

<sup>20</sup> Values for the peak winter month (i.e., January) are listed here.

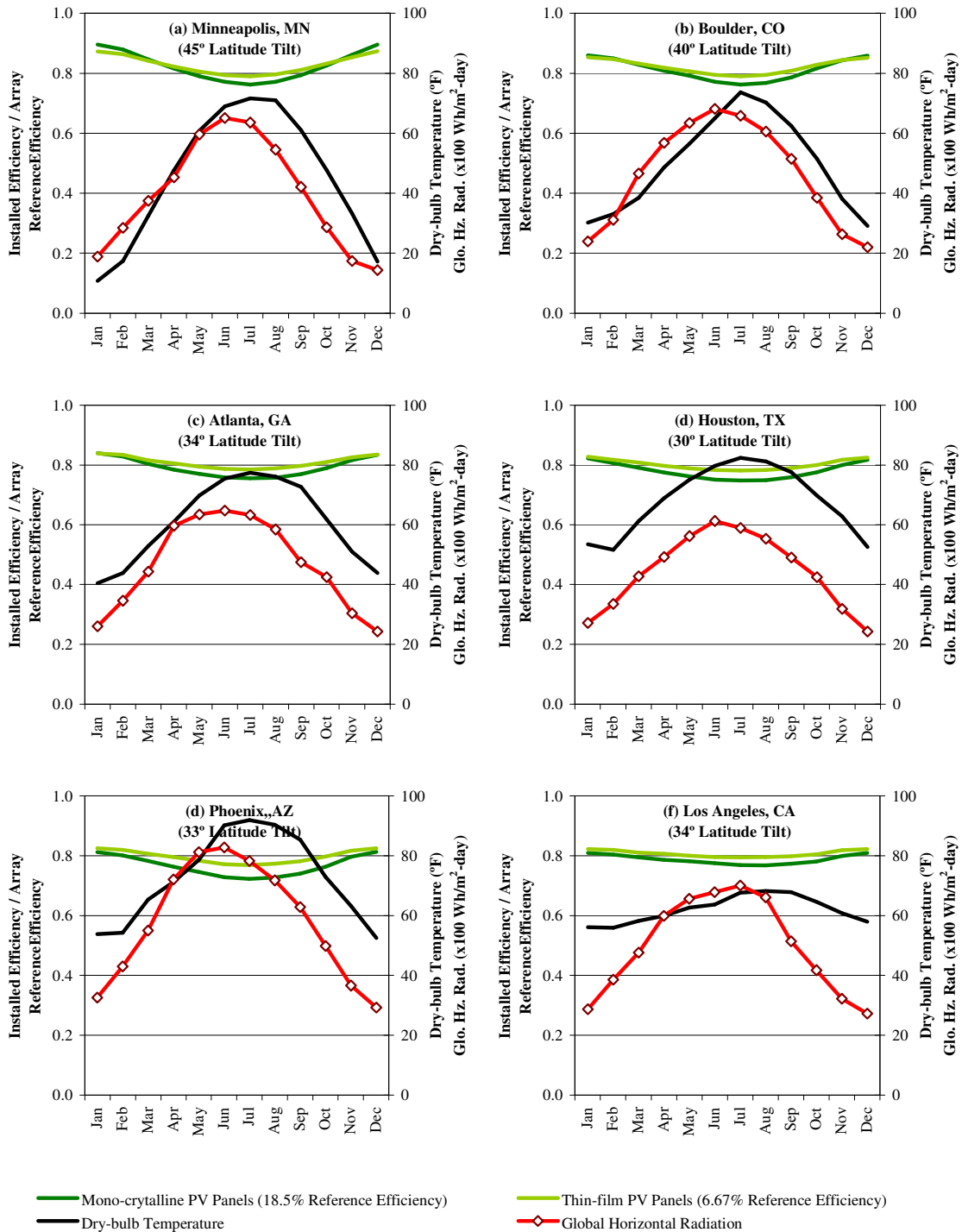


Figure 54 Performance of Mono-crystalline and Thin-film PV Arrays in the Six Selected Climate Locations

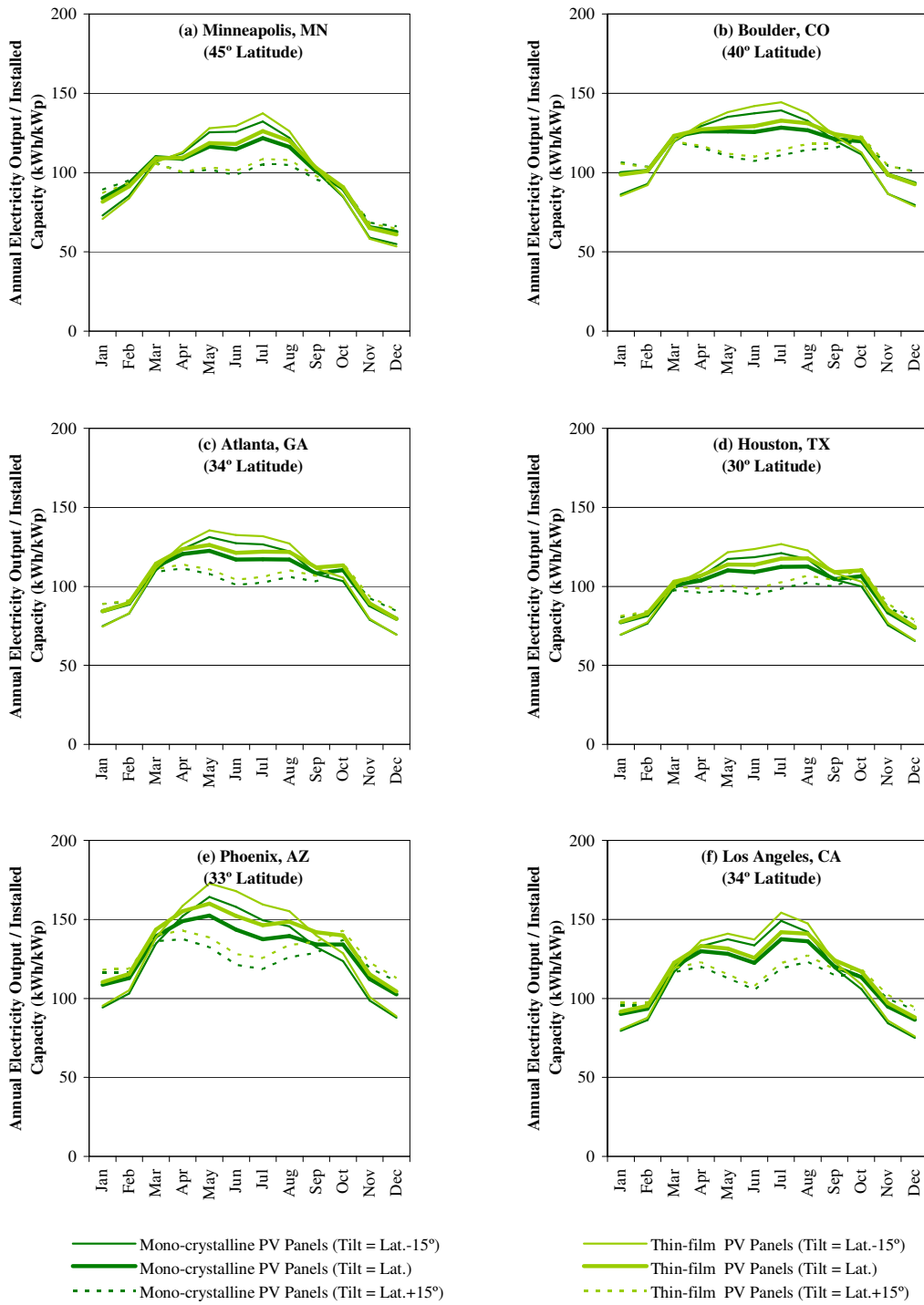


Figure 55 Electricity Output from Mono-crystalline and Thin-film PV Arrays at Varying Tilts in the Six Selected Climate Locations

### 5.4.3. *Performance of Wind Turbines*

The performance of wind turbines was analyzed using the procedure described in Section 4.6.3. First, four residential wind turbines of different rated capacities were selected, which include: a 7.5 kW turbine (Bergey 2009), a 3 kW turbine (Southwest Wind Power 2009a), a 2.5 kW turbine (Wind energy Solutions 2009), and a 2.4 kW turbine (Southwest Wind Power 2009b). For these turbines, the product specifications and power curves were obtained from the manufacturer's product data sheets. Table 15 shows the specifications and Figure 56 shows the power curves for the selected wind turbines.

Table 15 *Wind Turbine Specifications*

Specifications	Wind Turbine 1	Wind Turbine 2	Wind Turbine 3 <sup>21</sup>	Wind Turbine 4
Rated Capacity	7.5 kW	3 kW	2.5 kW	2.4 kW
Rated Wind Speed	31 mph	24 mph	20 mph	29 mph
Rotor Diameter	23 ft.	15 ft.	16 ft.	12 ft.
Start-up/Cut-in Speed	8 mph	7.5 mph	6.7 mph	8 mph
Cut-out Speed	None (Furling at 36 mph)	60 mph	45 mph	60 mph
Maximum Design Wind Speed	125 mph	120 mph	135 mph	140 mph
Tower Height	60 -120 ft.	30 -70 ft.	40 ft.	30-70 ft.

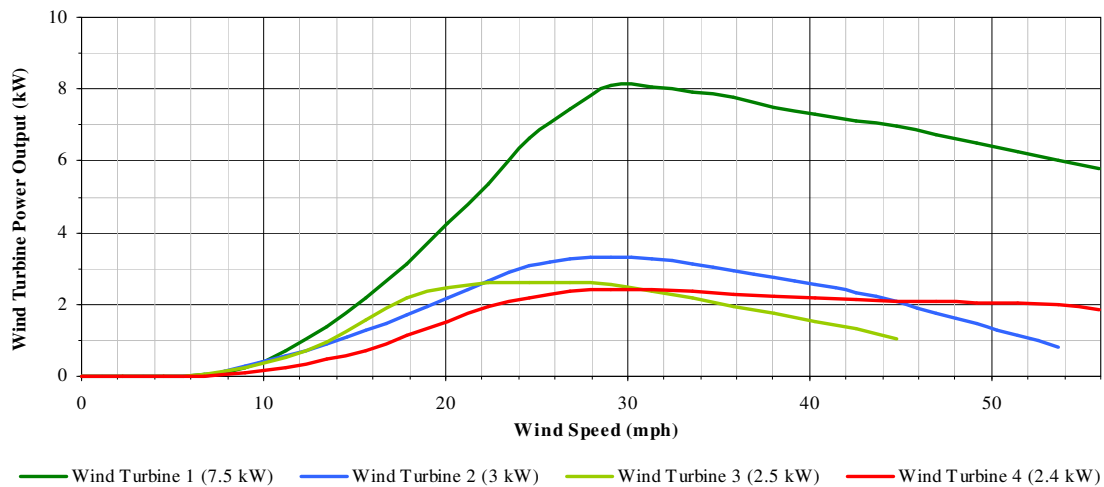


Figure 56 *Wind Turbine Power Curves*

<sup>21</sup> Suitable for grid-connection.

Figure 56 and Table 15 show that the 7.5 kW turbine has the highest electricity output at low wind speeds. It can be installed on a 60 ft. to 120 ft. high tower, where the wind speed would be higher. However, it has a rated wind speed of 31mph, which is less likely to achieve for a residential application (i.e., in a suburban terrain and at a lower tower height). The 2.5 kW wind turbine has the lowest rated wind speed, lowest cut-in wind speed, and a higher electricity output at lower wind speeds, compared to other wind turbines of similar size. However, it is available only with a 40 ft. tower height. The 3 kW and 2.4 kW wind turbines are available with up to 70 ft. high tower, but their performance at low wind speeds is lower than the 2.5 kW turbine. Considering that low wind speeds are more likely to occur at suburban locations, a 7.5 kW turbine at a 60 ft. tower height and a 2.5 kW turbine at a 40 ft. tower height were selected for further analysis in the six selected locations. For these two wind turbines, the wind power generation was estimated using the corresponding power curves with NOAA hourly wind speed data.

Figure 57 shows the wind speed distribution at the NOAA meteorological station for twelve years (1997-2008), the manufacturer's power curves for the two selected turbines, and the turbine output for the critical year for the six locations. In each figure, the x-axis shows the wind speed bins (in mph). The wind speed distribution (i.e., the frequency of occurrence of wind at different speeds) for the twelve years is plotted as grey markers with respect to the left hand y-axis showing the frequency of wind speed (in hours per year). The critical year (i.e., when the frequency of occurrence of higher wind speeds is the lowest) is highlighted with black markers. The power curves of the 7.5 kW and 2.5 kW wind turbines are shown as the thin dark green and light green thin lines, respectively, with respect to the left hand y-axis showing the turbine power output (time 10 W unit). The electricity output (in kWh) from these turbines during the critical year are plotted as a dark green curve (for the 7.5 kW wind turbine) and a light green curve (for the 2.5 kW wind turbine) with respect to the right y-axis showing the electricity generation (in kWh). The area under these curves represents the annual electricity output (as shown on the figures) from the two wind turbines during the critical year, installed in a flat, open terrain at a 33 ft. tower height.

Figure 58 shows the wind speed distribution (as dark grey and light grey markers) and the turbine power output (as dark green and light green curves with bold lines) for the critical year calculated at 60 ft. and 40 ft. height, respectively, from the ground in a suburban terrain, which correspond to the tower heights of the two selected turbines installed at a site located in a suburban area. These corrected wind speeds were calculated using the procedure described in Section 4.6.3, which were 82% and 75% of the measured wind speed at the NOAA weather station. In addition, for a reference, the critical year wind speed distribution at a 33 ft. height in a flat, open terrain (from Figure 57) is plotted as black markers, and the corresponding power output from the two turbines (from Figure 57) are plotted as dark green and light green, dotted line curves. A comparison of the electricity output from the two turbines over the year is shown in Table 16 as: i) the annual electricity output (kWh/yr), and ii) the ratio annual electricity output and the turbine capacity (kWh/kWp).

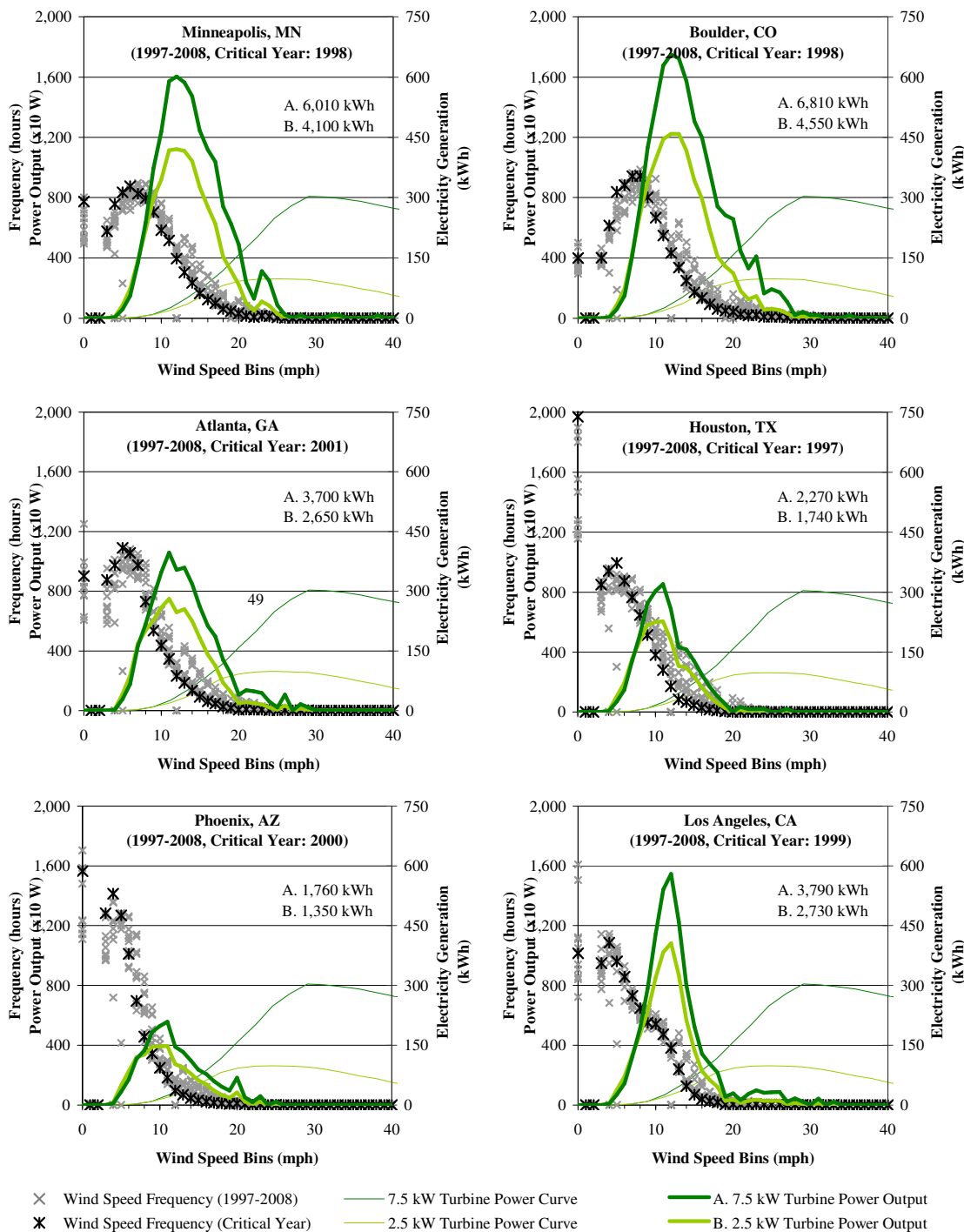


Figure 57 Twelve-year Wind Speed Distribution and Turbine Power Output at the NOAA Weather Station in the Six Selected Climate Locations

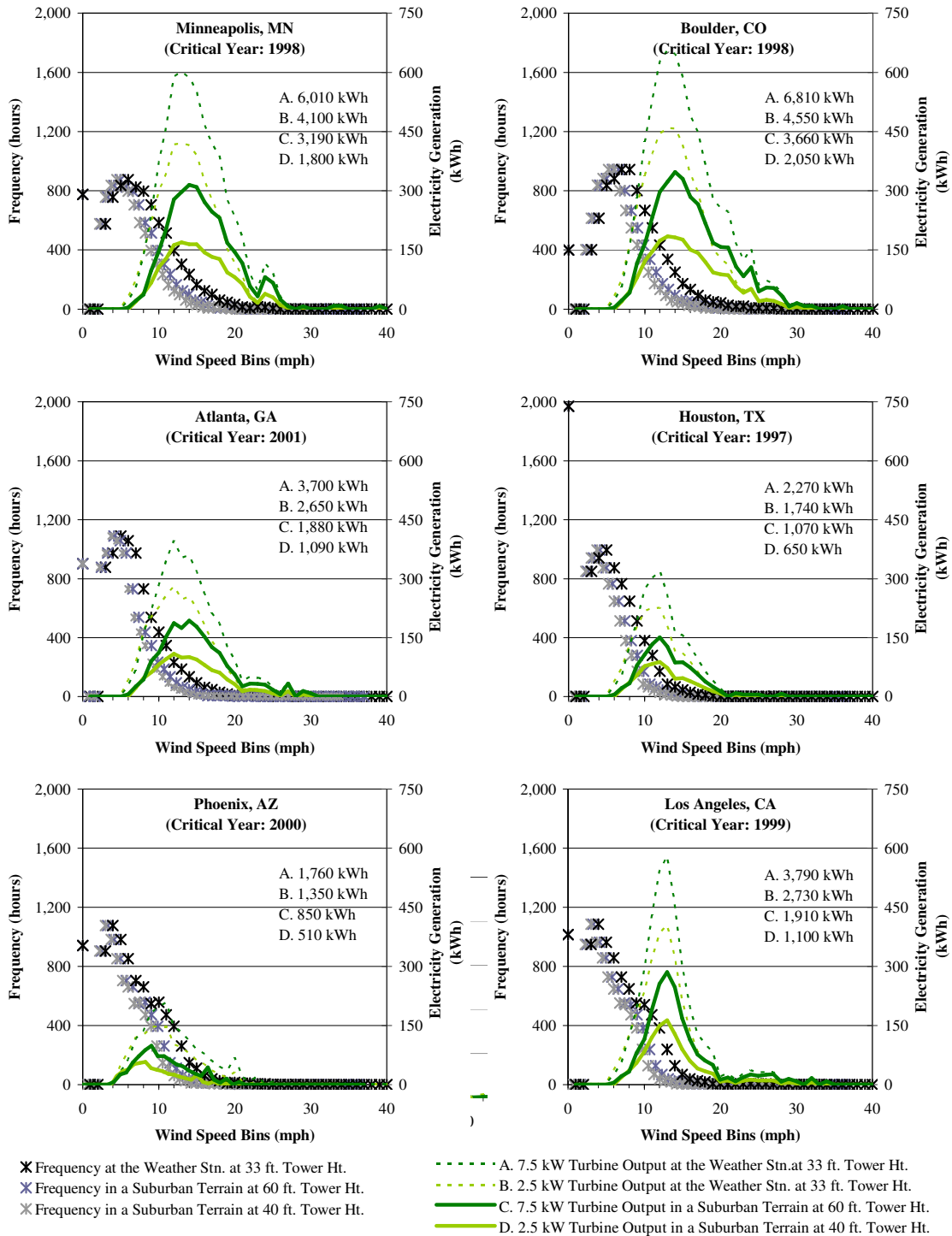


Figure 58 Critical Year Wind Speed Distribution and Turbine Power Output in a Suburban Terrain at the Tower Height in the Six Selected Climate Locations



Table 16 Wind Turbine Electricity Output

Climate Location	At NOAA Weather Station (Open, Flat Terrain)				At Local Suburban Terrain			
	From 7.5 kW Wind Turbine at 33 ft. Height		From 2.5 kW Wind Turbine at 33 ft. Height		From 7.5 kW Wind Turbine at 60 ft. Height		From 2.5 kW Wind Turbine at 40 ft. Height	
	kWh/yr	kWh/kWp	kWh/yr	kWh/kWp	kWh/yr	kWh/kWp	kWh/yr	kWh/kWp
Minneapolis, MN	6,010	800	4,100	1,640	3,190	547	1,800	720
Boulder, CO	6,810	908	4,500	1,820	3,660	607	2,050	820
Atlanta, GA	3,700	493	2,650	1,060	1,880	353	1,090	436
Houston, TX	2,270	303	1,740	696	1,070	232	650	260
Phoenix, AZ	1,760	235	1,350	540	850	180	510	204
Los Angeles, CA	3,790	505	2,730	1,092	1,910	364	1,100	440

From Figure 57, Figure 58 and Table 16, the following conclusions about the wind speed characteristics<sup>22</sup> and wind power potential can be made<sup>23,24</sup>:

1. **Prevailing Wind Speed:** Using the measured wind speed at the NOAA weather stations, the prevailing wind speed (i.e., the wind speed with the highest frequency) for the critical year was 8 mph in Boulder, 6 mph in Minneapolis, 5 mph in Atlanta and Houston, and 4 mph in Phoenix and Los Angeles, which occurred for only 10% to 12% of the hours per year at all locations. It is worth noticing that the prevailing wind speed in all locations was less than the cut-in wind speed of the two selected turbine. Therefore, there is a need for a newer class of wind turbines with very low cut-in speeds.
2. **Most Productive Wind Speed:** The most productive wind speed (i.e., for which the product of the frequency and turbine power output was the highest) ranged between 11 mph to 13 mph for all locations, which occurred for only 2% to 5% of the hours during the critical year.
3. **Peak Wind Speed:** The peak wind speed versus the maximum design wind speed is an important consideration for a safe operation of the wind power system. The peak wind speed, obtained from the measured wind speed data (i.e., averaged over the most recent two-minute period prior to the observation time), ranged from 30 mph to 33 mph in Minneapolis, Boulder and Los Angeles (which is close to the rated wind speed for the 7.5 kW wind turbine) and was less than 25 mph in Houston and Phoenix (which is close to the rated wind speed of the 2.5 kW wind turbine). On the other hand, the

<sup>22</sup> Using the wind speed corrected for the local terrain and tower height, the above conclusions about the prevailing wind speed, most productive wind speed and peak wind speed in each location would be scaled down by 82% for the 7.5 kW and by 75% for the 2.5 kW wind turbine.

<sup>23</sup> The observations are based on the measured hourly wind speed data obtained from the NOAA weather stations. It is to be noted that the recorded wind speed is the average wind speed for the most recent two-minute period prior to the observation time, calculated from a series of 24 five-second average values. Therefore, it may not accurately predict its interaction with the wind turbine.

<sup>24</sup> The conclusions accounting for the effect of the local site terrain assume that off-grid, off-pipe house in each location was on a suburban terrain, and are not representative of other terrain types.

wind gusts recorded during these period indicate that, for certain months, the wind gusts were significantly higher than those recorded hourly as two-minute averages. Furthermore, among all locations, Boulder experiences up to 100 mph wind gusts during the winter (NOAA 2009), which was not reflected in the measured hourly two-minute averages. Since, the peak wind speed at most of the locations was very low compared to the maximum design wind speed (except for Boulder, for which the peak wind speed was lower but close to the maximum design wind speed) shown in Table 15, it shows that the operation of a wind turbine system would be safe in these locations. However, for Boulder, additional provisions for the safe installation of wind turbine is must. On the other hand, since the wind speed at these locations achieves the rated wind speed of the wind turbine only for a few hours in a year, it shows that the wind turbines would reach their rated output only for a few hours of the year.

4. Hours with No Wind Power Potential: The degree of utilization of the wind turbine in each location was determined from the hours with no wind power potential .e., wind speed below the turbine cut-in speed). During the critical year, the hours with no wind power potential were 44% of the hours in a year in Minneapolis, 36% in Boulder, 56% in Atlanta, 64% in Houston, 75% in Phoenix, and 56% in Los Angeles. These include hours with no wind (shown as markers crossing the y-axis), which ranged between 6-10% in Minneapolis, 3-5% in Boulder, 7-14% in Atlanta, 13-22% in Houston, 13-19% in Phoenix, and 8-18% in Los Angeles. Using the wind speed corrected for the suburban terrain and tower height, there were more hours with no wind power potential, which were 47% in Minneapolis, 53% in Boulder, 67% in Atlanta, 73% in Houston, 83% in Phoenix, and 64% in Los Angeles. This shows a significant reduction in the utilization of the wind turbines considering the local site terrain.
5. Annual Electricity Output: A comparison of the annual electricity output from the 7.5 kW and 2.5 kW wind turbines at the NOAA weather station height and site terrain in Table 16 shows that the smaller turbine (which is one-third of the size of the larger turbine) produced 67% of the electricity output from the larger turbine in Minneapolis and Boulder, 72% in Atlanta and Los Angeles, and 77% in Houston and Phoenix. This indicates that the installation of more than one smaller turbines might be more advantageous than a single large turbine of equivalent capacity (for the same installation conditions). For the assumed installation conditions (i.e., suburban terrain and respective tower heights), the electricity output from the two wind turbines was about 53% and 45% of those obtained using the uncorrected wind speed in Minneapolis and Boulder, 50% and 40% in Atlanta and Los Angeles, and 48% and 38% in Houston and Phoenix. These values approximately match with the simplified estimate of 55.5% and 42.5%, as mentioned in Section 4.6.3.
6. Annual Electricity Output per unit installed Capacity: A comparison of the annual electricity output per unit installed capacity (in kWh/kWp) of the 7.5 kW and 2.5 kW turbines in Table 16 shows that using the measured wind speed at the NOAA weather station height and site terrain, the output of

smaller turbine was more than twice of that from the larger turbine. On the other hand, considering the assumed installation conditions, the relative output of the smaller turbine was only 10% to 30% more (i.e., 1.1 to 1.3 times) than that from the larger turbine.

From the above discussion, it can be concluded that wind is a potentially large renewable energy resource in Minneapolis and Boulder, and a modest resource in Atlanta and Los Angeles. The wind turbine output is significantly affected by the wind speed. Therefore, the potential for wind power generation can be realized more effectively by using the maximum tower height (i.e., available/permitted by the local regulations), which also requires minimum obstructions at a site. In addition, if the tower height is not a limitation for the smaller wind turbines at the maximum permitted tower height, the installation of one or more smaller turbine(s) might be more advantageous than a single larger turbine.

#### 5.4.4. *Determination of Sizing Parameters for the Rainwater Harvesting System*

The sizing parameters for the rainwater harvesting system were determined using the procedure described in Section 4.6.4, which include: calculations for the unit catchment area, a calculation for the unit daily water demand, and the determination of normalized system sizing parameters.

To begin with, first the rainfall characteristics for the six selected locations were investigated. Figure 59 shows the rainfall characteristics for the six selected locations based on twelve years (1997-2008) of measured daily rainfall data. For each location, it shows: (i) measured annual rainfall (in inches per day) shown as twelve stacked bars, where each stacked bar shows the monthly rainfall during a year using the color index at the bottom of the figures, (ii) the number of days of rainfall occurrence, shown as blue markers, and (iii) the frequency of occurrence of first-flush days (i.e., when rainfall occurs after a period longer than three days, requiring a certain amount of rainwater to be diverted before collection can begin), shown as red markers. The twelve-year averages for these variables are shown as horizontal lines across the graph including: a black line for annual rainfall, a blue line for days of rainfall occurrence and a red line for days requiring first-flush diversion.

For each location in this figure, the measured annual rainfall indicates the size of the catchment area requirement to meet the water demand; or conversely, the degree of water use reduction required to ensure that the reduced demand is fulfilled from available catchment area. The monthly distribution of rainfall, shown as stacked bars, indicates the scale of rainwater storage requirement. The number of first-flush days indicates the amount of first-flush rainwater, if collected separately, available for site irrigation during dry periods. The annual rainfall versus the frequency of rainfall occurrence indicates the average rainfall intensity (i.e., the amount of rainfall per rainfall event), which would determine the sizing requirements of the rainwater conveyance system. A comparison of the annual averages (i.e., the horizontal lines) with the year-to-year variation in these variables indicates the degree of utilization of the rainwater harvesting system over a period of twelve years. The lower values of these variables indicate the critical rainfall conditions for which the sizing of rainwater harvesting system would be performed.

Since the lower limits for these variables do not always occur during the same year, normalized parameters were derived which could represent the extreme rainfall conditions for a location and be used for a comparison of rainwater harvesting potential across different climate locations. Figure 60 shows the minimum, maximum and average values for several rainwater system sizing parameters in the six selected locations, including: (a) rainfall intensity per unit of catchment area (i.e., ratio of annual rainfall and number of days of rainfall), (b) first-flush volume to be diverted per unit of catchment area, (c) catchment area requirement per unit of average daily water demand, and (d) rainwater storage volume requirement per unit of average daily water demand. These ranges were derived from the rainfall data shown in Figure 59. The higher limits of the rainfall intensity, catchment area requirement and storage requirement indicate the critical rainfall conditions for which the sizing of rainfall harvesting system was performed. The lower limits of the first flush volume indicate the rainwater harvestable for outdoor use. From these figures, the following conclusions can be made:

1. Figure 60(a) shows that the maximum rainfall intensity in Houston was the highest for all locations, (i.e., 0.36 gal per ft<sup>2</sup>/day), followed closely by 0.3 gal per ft<sup>2</sup>/day in Atlanta and Los Angeles, 0.22 gal per ft<sup>2</sup>/day in Minneapolis, and 0.15 gal per ft<sup>2</sup>/day in Boulder and Phoenix. These estimates combined with the required catchment area determined the sizing of the rainwater conveyance system.
2. Figure 60(b) shows that in Minneapolis, Boulder, Atlanta, and Houston, approximately 0.23 gallons of the rainwater per square foot of catchment area, diverted as the first flush, can be collected for the outdoor use. For Phoenix and Los Angeles, the minimum available first-flush volume for outdoor use was only 0.11 and 0.07 gallons per square foot of catchment area, respectively. These estimates combined with the required catchment area and rainfall distribution over the year would determine the rainwater availability for outdoor use and the sizing requirement of the additional storage tank.
3. Figure 60(c) shows that the catchment area requirement per unit of daily water demand could be as high as 15 ft<sup>2</sup>/gal in Atlanta, 23 ft<sup>2</sup>/gal in Houston, 32 ft<sup>2</sup>/gal in Minneapolis, 90 ft<sup>2</sup>/gal in Boulder, 125 ft<sup>2</sup>/gal in Los Angeles and 235 ft<sup>2</sup>/gal in Phoenix. These estimates indicate that minimizing the water demand and providing a large catchment area, possibly with custom-designed catchment surfaces, are very important for Los Angeles and Phoenix.
4. Figure 60(d) shows that the primary rainwater storage requirement per gallon of daily water demand could be as high as 93 gallons for Atlanta, 105 gallons for Houston, 168 gallons for Boulder, 176 gallons for Minneapolis, 198 gallons for Phoenix, and 293 gallons for Los Angeles. These estimates indicate the impact of rainfall distribution on the storage requirement (i.e., locations with more uniform rainfall distribution over the year require smaller storage).

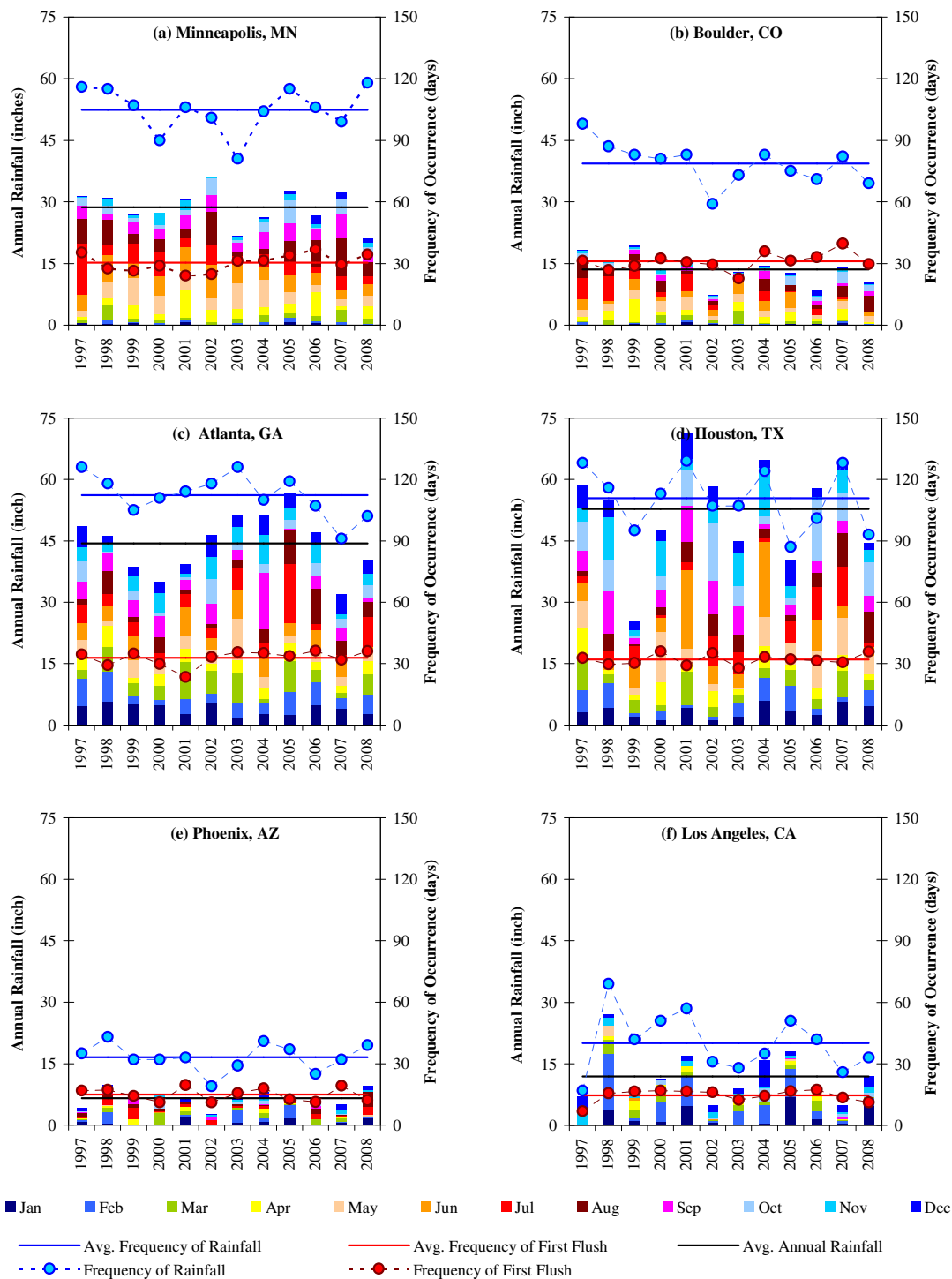


Figure 59 Rainfall Characteristics in the Six Selected Climate Locations

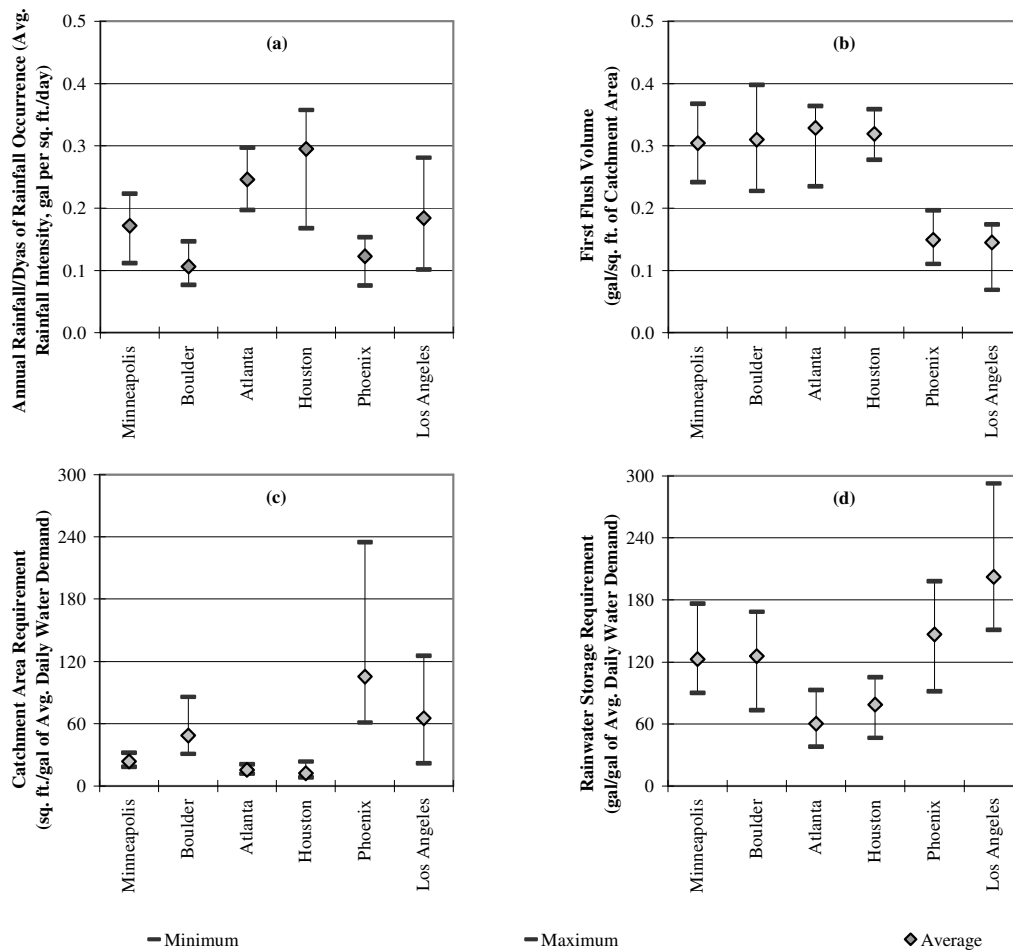


Figure 60 Rainfall Harvesting Potential in the Six Selected Climate Locations Indicated by: (a) Rainfall Intensity per Unit Catchment Area, (b) First-flush Volume per Unit Catchment Area, (c) Catchment Area Requirement per Unit Daily Water Demand, and (d) Rainwater Storage Requirement per Unit Daily Water Demand

## 5.5. Sizing of Systems for Self-sufficiency

The sizing of renewable energy and rainwater harvesting systems was performed for the monthly needs of the proposed house. The performance of the systems analyzed in the previous section was used for sizing the systems.

### 5.5.1. Solar Thermal System for Heating Needs

The sizing of solar thermal system was performed to provide the building's space heating and domestic hot water requirements. To accomplish this, the monthly thermal energy needs of the building was compared with the monthly thermal energy output for varying collector area. The monthly thermal

energy needs were obtained from DOE-2.1e results. The performance of a solar thermal system with flat plate collectors and evacuated tube collectors of varying area at a winter-optimized tilt for the six selected climate locations was obtained from Section 5.4.1. Figure 61 shows the comparison of the building energy needs and solar thermal system output with the preferred collector area. The unmet thermal loads (in Minneapolis) were carried over to electricity loads for sizing PV/wind electricity generation system.

#### 5.5.2. *Photovoltaic and Wind Power System for Electricity Needs*

The combined renewable electricity generating system was designed to provide the building's electricity needs for space cooling, unmet space heating and domestic water heating loads, heating/cooling fan electricity use, lighting and equipment, the solar thermal pump and the water supply pressurization pump. The space cooling, HVAC fans, lighting and equipment electricity use were obtained from the DOE-2.1e output. The unmet space heating loads were obtained from the F-CHART results combined with the building's thermal loads, obtained in the previous section. The solar thermal pump energy use was determined using the procedure described in Section 5.4.1. For locations with wind speeds useful for electric power generation, a 7.5 kW wind turbine was selected and the monthly electricity generation was calculated for the critical year using the manufacturer's wind turbine power curve with measured hourly wind data, as shown in Figure 62. The monthly electricity generation was then compared with monthly electricity loads to evaluate the possibility of installing multiple turbines, and to determine the unmet monthly electricity loads for sizing the PV system.

Figure 62 shows that the locations with a more uniform wind energy resource are Minneapolis, Boulder and Los Angeles. The consistent power output from the selected wind turbine offsets at least 30% of electricity loads for a month. Thus, for these locations, the potential of installing two or three smaller wind turbines could greatly reduce or eliminate the need for the more expensive PV system. However, depending on the available solar radiation, locations with a higher potential of PV electricity generation can have wind power system supplemented by a PV system or vice-versa. For the unmet electricity needs, the sizing of PV system was performed for the panel type selected in Section 5.4.2 using PV F-CHART with TMY2 weather data. Using the PV panel parameters of the selected type, the panel tilt and area were adjusted iteratively to meet the unmet electricity needs, as shown in Figure 63.

For other locations including Houston and Phoenix, Figure 62 shows that the months with the highest electricity needs have the least power output from the wind turbine. Thus, for these locations, a wind turbine cannot offset the PV system sizing requirement. The PV F-CHART analysis for these locations in Figure 63 showed that PV panels tilted at an angle optimized for summer were able to meet winter electricity needs. On the other hand, in Atlanta, the PV panels tilted for maximum output in summer were not able to provide winter electricity needs. Since, the wind turbine in Atlanta was useful for providing electricity during peak winter months, it allowed PV panels to be tilted at an angle optimum for summer months, thereby, minimizing the PV panel area for the peak summer months.

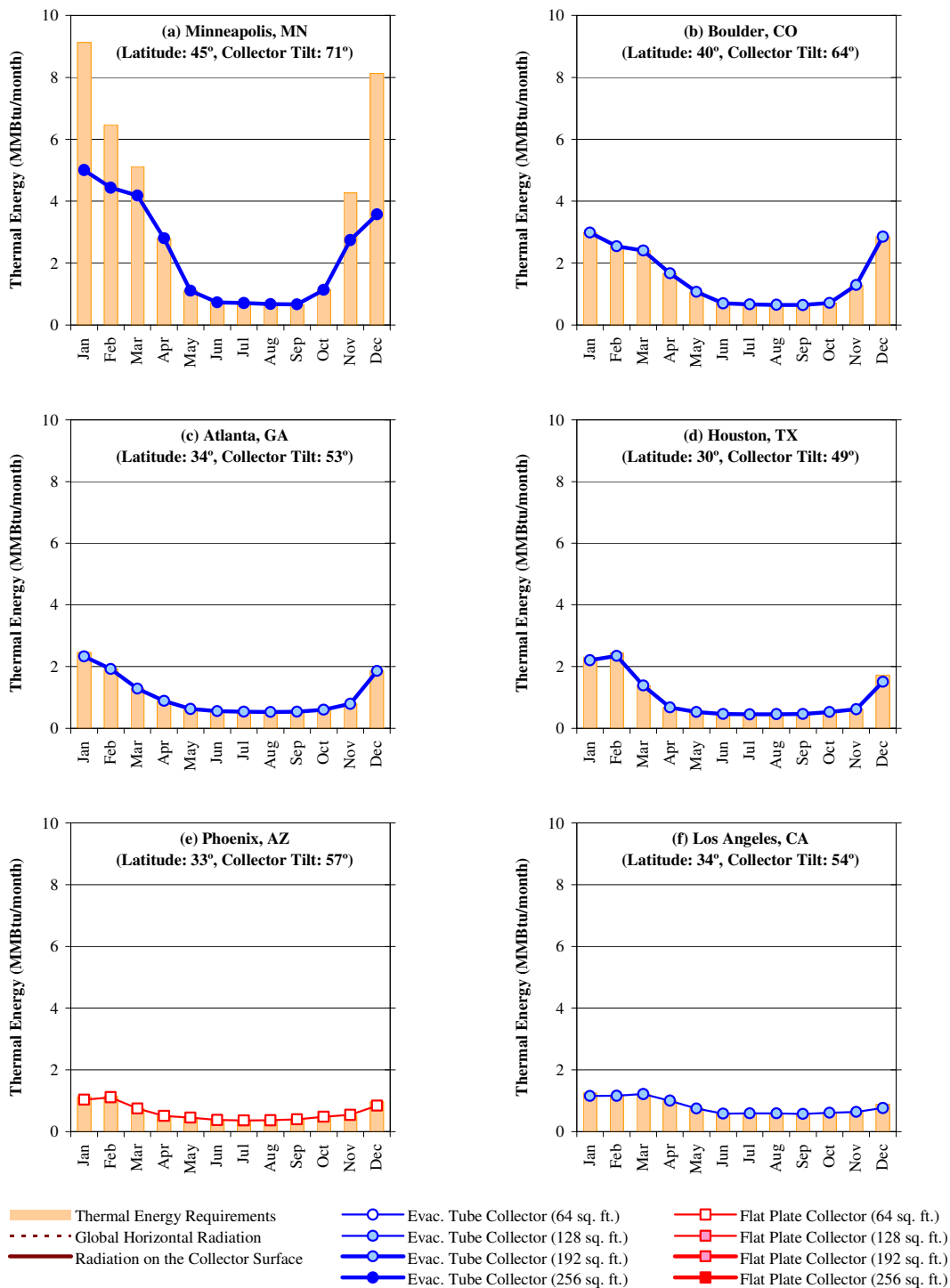


Figure 61 Sizing of the Solar Thermal System in the Six Selected Climate Locations



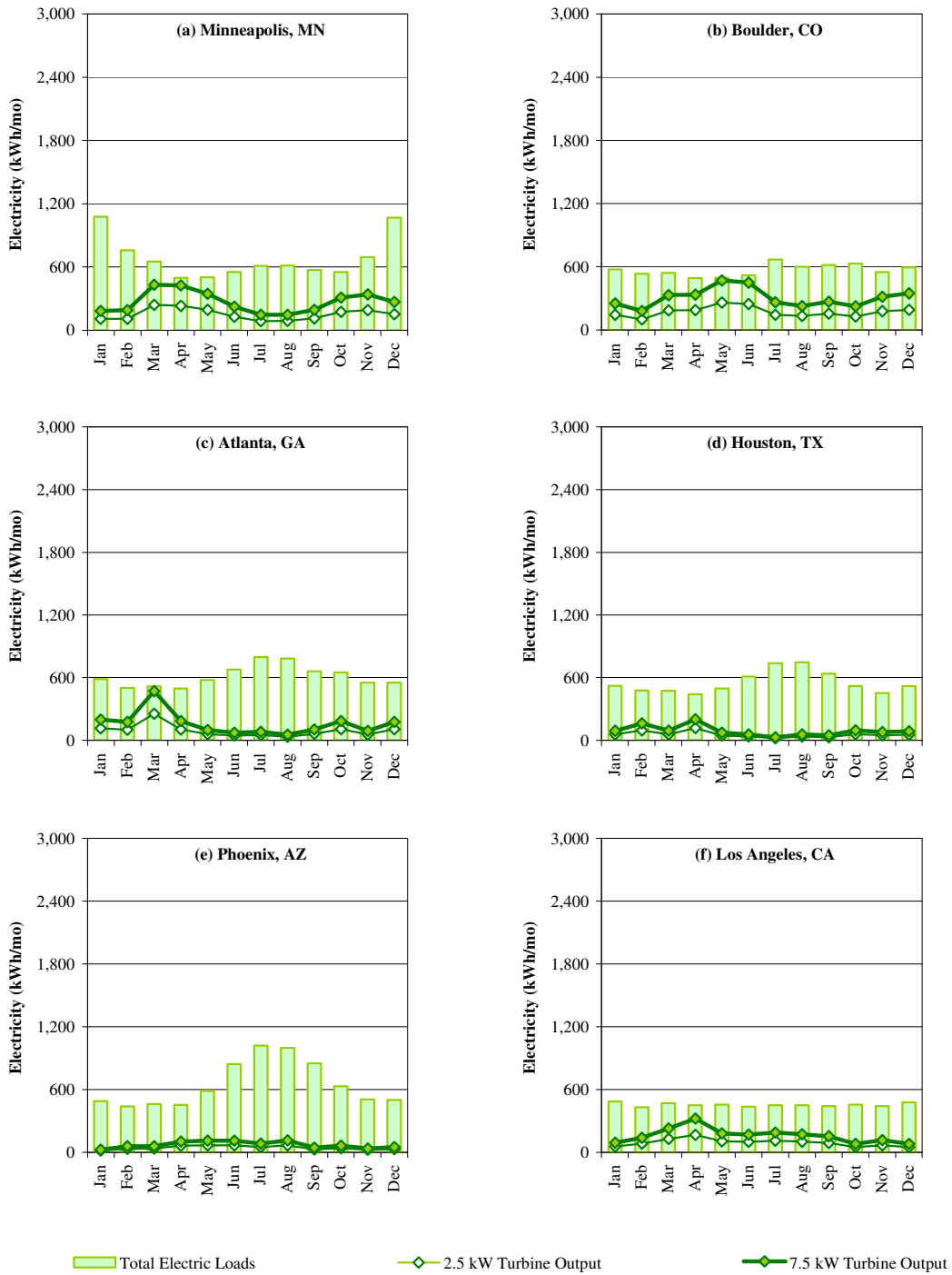


Figure 22 Monthly Wind Turbine Electricity Output versus Monthly Electricity Needs in the Six Selected Climate Locations

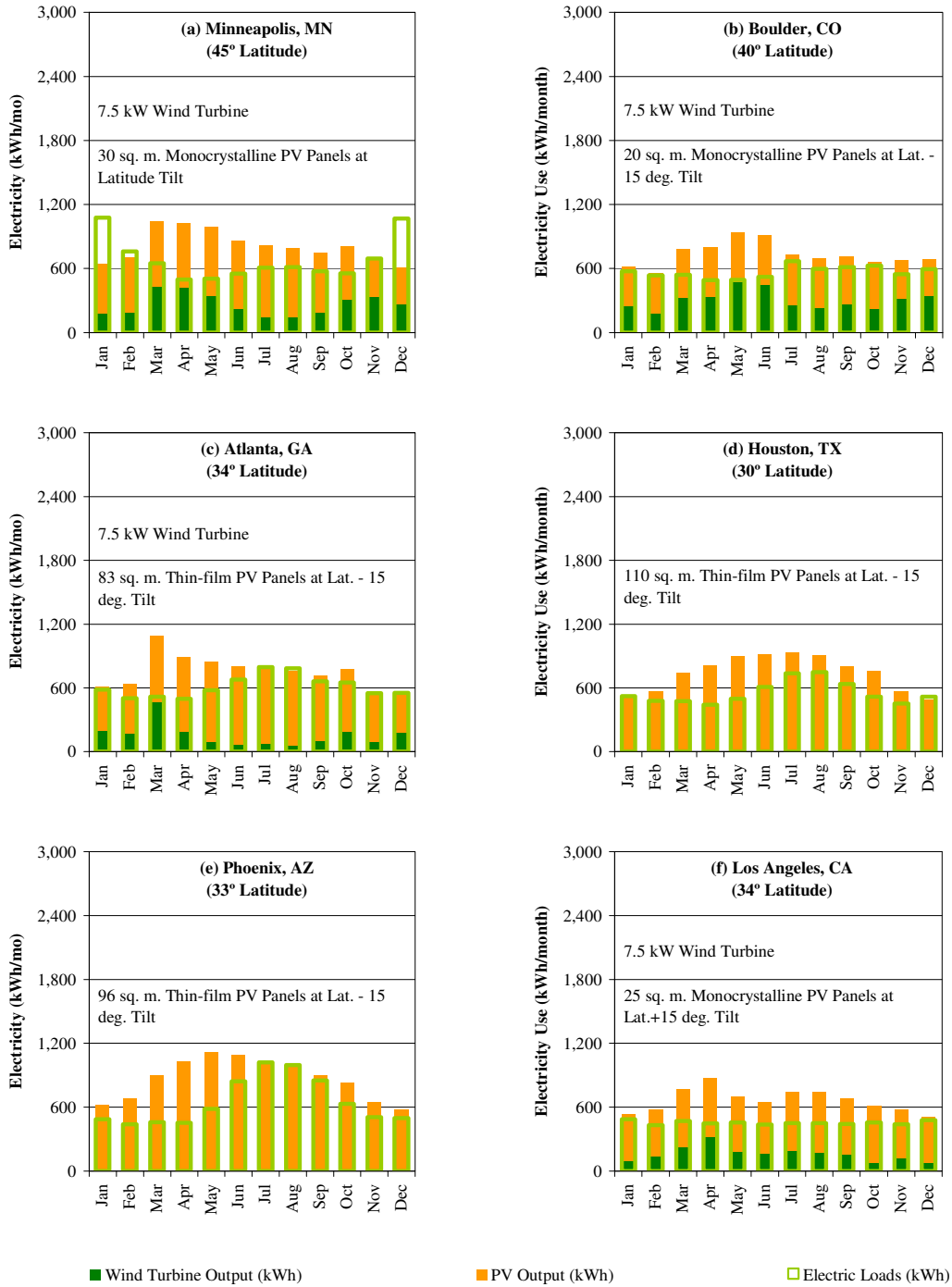


Figure 63 Sizing of the Photovoltaic and Wind Power Systems in the Six Selected Climate Locations

### 5.5.3. *Electricity Storage System*

For the sizing of the electricity storage system, (i) the minimum available insolation in 7, 14, 21, and a month-long consecutive-day periods and resulting equivalent number of NO-SUN days, and (ii) the available surplus insolation over 7, 14, 21, and a month-long consecutive-day periods (and resulting equivalent number of EXTRA SUN days) were obtained from NASA (2008). The equivalent number of NO SUN days and EXTRA SUN days are plotted in Figure 64 and Figure 65, respectively.

In order for the electricity storage system to be able to provide the cumulated electricity needs over a period when there was not sufficient insolation, the maximum of the NO-SUN days was multiplied by the monthly average building electricity needs obtained from DOE-2 output (shown as line graph in Figure 64) to determine the cumulative electricity needs for each month (shown as a bold line graph in Figure 64). The largest of the 12 monthly values was used as the storage capacity required to provide electricity during NO-SUN days for that location.

Furthermore, the electricity storage system should be able to store excess electricity generated when the insolation exceeds the electricity needs accumulated over a period. For this, the maximum of the EXTRA-SUN days was multiplied by the monthly average electricity generated (shown as a line graph in Figure 65) obtained from the PV F-CHART output, to determine the cumulative electricity storage for each month that the batteries could provide (shown as a bold line graph in Figure 65). The largest of the 12 monthly values was then used as the storage capacity required to store electricity during EXTRA-SUN days.

Finally, the larger of the two storage capacities calculated for NO-SUN days or EXTRA-SUN days was used as the required electricity storage capacity. Figure 64 and Figure 65 show an effective storage capacity of 140 kWh for Minneapolis, 117 kWh in Boulder, 160 kWh for Atlanta, 218 kWh for Houston, 128 kWh for Houston, and 102 kWh for Los Angeles. The large storage requirements for all these locations are due to the occurrence of 8-10 days of equivalent NO SUN or EXCESS SUN periods, combined with the high electricity use during peak winter (cloudy) days or late summer (less clear) days with high electricity use. For locations with good potential for wind power, the availability of electricity during periods with less/no useful radiation would greatly reduce the electricity storage sizing requirement. However, statistics of extended periods without harvestable wind was not available from current NOAA records.

For the electricity storage system, a battery bank was considered. In addition to the effective storage capacity requirements, other parameters considered for selecting the type and sizing of the battery system include: battery efficiency due to charge/discharge cycle, allowable depth of discharge, performance of the batteries as affected by the extreme winter conditions, battery voltage and system voltage.

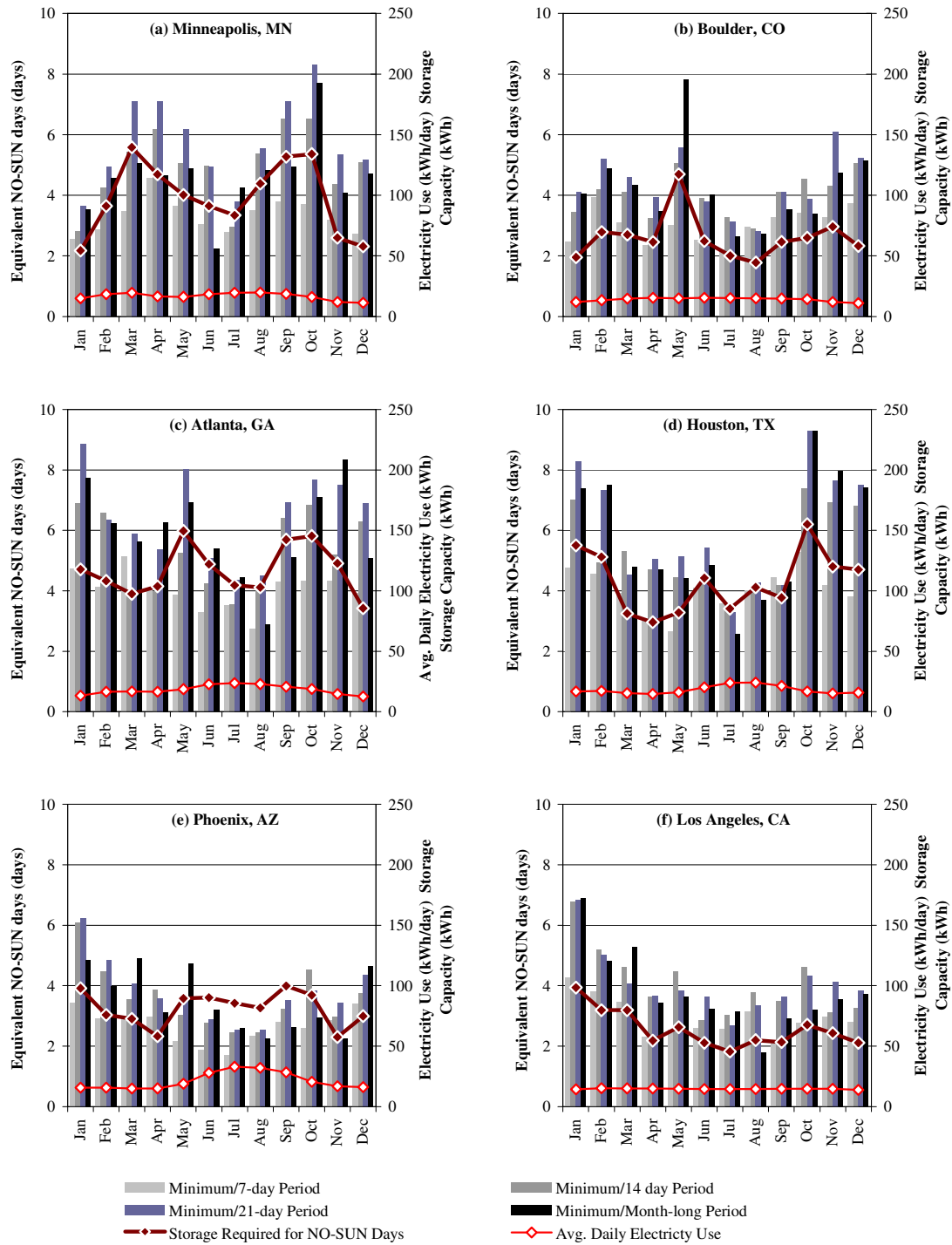


Figure 64 Determination of the Electricity Storage Requirements for NO-SUN days in the Six Selected Climate Locations

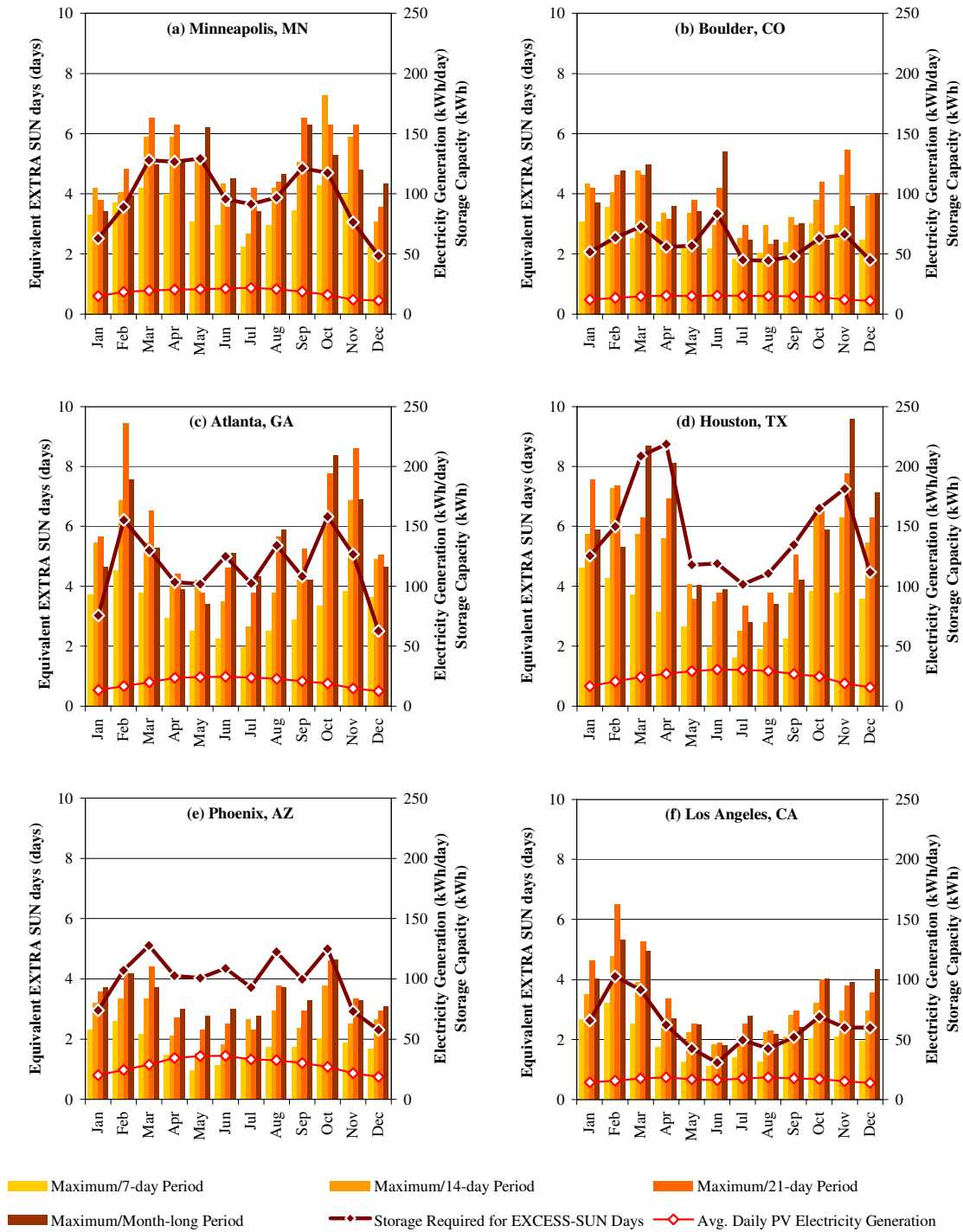


Figure 65 Determination of the Electricity Storage Requirement for EXTRA SUN Days in the Six Selected Climate Locations

#### 5.5.4. Rainwater Harvesting System for Indoor Water Use

The sizing of rainwater harvesting system was performed for critical conditions in terms of the amount of rainfall and length of dry period. The normalized system sizing parameters (i.e., the catchment area and rainwater storage volume requirements per unit of daily water demand) were derived in Section 5.4.4 and the reduced indoor water use from water-efficiency measures estimated previously were used for determining the required level of water use reduction, and the sizing requirements for the catchment area and rainwater storage tank volume. Table 17 shows the results of the analysis for all six locations.

First, the maximum required catchment area per unit of daily demand and maximum required storage volume per unit of daily demand were obtained from Figure 60 of Section 5.4.4, which represent the critical rainfall conditions in terms of the amount of rainfall and length of dry period, respectively. Next, considering the catchment area requirement per unit of daily water demand, the level of water-efficiency measures was selected and the resulting reduced indoor water use was obtained from Table 6 of Section 5.2. Using this information, the catchment area and the rainwater storage volume requirements were calculated, which would provide the reduced indoor water use throughout the year with critical rainfall conditions. The total first flush volume of water was then calculated in order to determine the potential of treating and using it for domestic use requiring non-potable water as compared to greywater recycling and reuse. Finally, the dimensions of the available roof catchment area (and additional roof/ground catchment area, if needed) and the storage tank were determined.

Table 17 shows that the catchment area requirement in Atlanta, Houston and Minneapolis is 20 ft<sup>2</sup> to 30 ft<sup>2</sup> per unit gal/day water demand. On the other hand, Boulder, Phoenix and Los Angeles require 86 ft<sup>2</sup>, 125 ft<sup>2</sup> and 235 ft<sup>2</sup> per unit gal/day water demand. The building configuration selected for Minneapolis and Boulder was two-story, which would provide only up to 1,650 ft<sup>2</sup> roof catchment area including the roof eaves. The roof catchment area in Houston, Phoenix and Los Angeles was 2,900 sq. ft. to 3,300 ft<sup>2</sup> including the roof eaves. Thus, it is evident that additional catchment area of 925 ft<sup>2</sup> in Minneapolis, 4,095 ft<sup>2</sup> in Boulder, 12,398 ft<sup>2</sup> in Phoenix and 5,450 ft<sup>2</sup> in Los Angeles would be required. The additional area provided above grade (e.g., the roof) with an adequate slope would have 0.75 – 0.9 run-off coefficient, which would collect sufficient rainwater. However, the area provided as ground catchment area would have much smaller run-off coefficient (approx. 0.35, for a slightly sloped surface and specially designed ground catchment surface). Considering this, the additional area requirement would be up to 2.5 times the calculated additional catchment area.

For the reduced water demand, a rainwater storage tank volume of 11,000 to 13,000 gallons would be adequate for all locations except Minneapolis and Los Angeles, which require up to 15,600 gallons and 19,500 gallons storage tank due to long dry-periods throughout the summer. The dimensions of the storage tank were determined considering the site-conditions.

Finally, the additional need for catchment area was determined, which combined with roof catchment area could provide for the reduced water needs. The amount of harvestable rainwater was calculated after deducting the first-flush volume (one gal per 100 ft<sup>2</sup>) diverted from the catchment. This estimate was used to calculate the monthly and cumulative rainwater supply and average demand fulfilled. The sizing of the storage tank was then determined by comparing the cumulative demand and rainwater supply.

*Table 17 Sizing of the Rainwater Harvesting System*

System Sizing	Minneapolis, MN	Boulder, CO	Atlanta, GA	Houston, TX	Phoenix, AZ	Los Angeles, CA
Max. Req. Catchment Area per unit Daily Demand (ft <sup>2</sup> /gal per day)	29	86	19	23	235	125
Max. First-flush Volume to be Diverted per unit Catchment Area (gal/ ft <sup>2</sup> )	0.37	0.40	0.36	0.36	0.20	0.17
Max. Req. Storage Volume per unit Daily Demand (gal/gal per day)	176	168	93	105	198	293
Proposed Level of Water-efficiency	Level 2	Level 3	Level 1	Level 1	Level 3	Level 3
Resulting Indoor Water-use (gal per day)	88.8	66.8	121.6	121.6	66.8	66.8
Catchment Area Required (ft <sup>2</sup> )	2,575	5,745	2,310	2,797	15,698	8,350
First-flush Volume to be Diverted (gal)	953	2,298	832	1,007	3,140	1,420
Storage Volume Required (gal)	15,629	11,223	11,309	12,768	13,226	19,572
Available Roof Catchment Area (ft <sup>2</sup> ) <sup>25</sup>	1,250+400	1,250+400	2,500+400	2,500+800	2,500+800	2,500+400
Additional Effective Catchment Area Needed (ft <sup>2</sup> )	925	4,095	0	0	12,398	5,450

#### 5.5.5. *Septic System for Sewage Disposal*

The need for sewage disposal is proportional to the indoor water use in a residence. Considering this, the amount of sewage generated in six locations was estimated to account for the reduced indoor water use. Septic tank size requirements or minimum design flows should be determined from onsite codes (US EPA 2002). In general, codes typically specify design flows of 100 gallons per bedroom per day with a peak flow of 5 to 10 gpm (NSFC 1995). This is close to the value calculated for the base-case house, based on the amount of indoor water use and a safety factor of two (considering a maximum instantaneous peak discharge rate of up to 5 gpm for water-efficient fixtures). This resulted into 1,200-gallon septic tank size. Next, after consideration of the level of water efficiency measures for selected locations, the reduced design flows were calculated, and the septic tank size was determined, as listed in Table 18.

<sup>25</sup> This considers roof area, and the number of floors, and includes an extended roof area for eaves/roof overhang for window shading.

Table 18 Sizing of the Septic System

	Minneapolis, MN	Boulder, CO	Atlanta, GA	Houston, TX	Phoenix, AZ	Los Angeles, CA
Proposed Level of Water-efficiency	Level 3	Level 3	Level 1	Level 1	Level 3	Level 3
Resulting Indoor Water-use and Waste-water generation (gal per day) <sup>26</sup>	88.8	66.8	121.6	121.6	66.8	66.8
Peak Instantaneous Flow (gal per min)	5	5	5	5	5	5
Septic Tank Size Required (gal)	750	750	1,000	1,000	750	750
Absorption Field Area Requirement (ft <sup>2</sup> ) <sup>27-28</sup>	750	750	1,000	1,000	750	750
Leaching Field Area Requirement (ft <sup>2</sup> ) <sup>29</sup>	1,500	1,500	2,000	2,000	1,500	1,500

<sup>26</sup> The estimates of the reduced water use and wastewater generation are based on the level of water-efficiency measures considered for each location, as shown in Table 17.

<sup>27</sup> Soil percolation rates may range between less than 10 to 120 min per inch, which requires 150 to 600 sq. ft. per bedroom absorption field area for a typical single-family house.

<sup>28</sup> This assumes an average soil percolation rate of 46 to 60 min per inch. For such soil, backfill above the infiltration barrier shall be sand, loamy sand, or sandy loam, when available. Two to four inches of loamy soil shall be used to cap the sandy backfill to keep rainwater from entering the system (Schultheis 1997).

<sup>29</sup> This assumes a 3 ft. wide absorption trench with 3 ft. wide spacing. For future expansion, a larger spacing to accommodate additional trenches or expansion to the adjacent site area, if available, can be considered.



## **CHAPTER VI**

### **SUMMARY AND CONCLUSIONS**

This chapter summarizes this dissertation, discusses the findings and limitations, presents the conclusions and offers recommendations for future research. The summary reviews the objectives, research methodology and the results of the analysis. The discussion includes the key finding of the analysis, climate location specific opportunities and challenges, building and system design priorities, recommended architectural applications for an integrated design, and the limitations of the methodology encountered in this dissertation. The overall research outcome is presented in the conclusions. Finally, based on the limitations of this study, the recommendations for future research are presented.

#### **6.1. Summary of Research Objectives**

This purpose of this study was to investigate the feasibility of off-grid, off-pipe design approach for single-family detached residences in six different climate regions across the U.S. to achieve self-sufficiency using only on-site renewable resources, and to formulate a procedure for an integrated analysis and design of such homes. This was accomplished by investigating the base-case energy, water and sewage disposal needs of a 2000/2001 IECC standard house in six U.S. climate locations; identifying the potential and critical availability periods for the renewable energy and water resources in the selected locations; minimizing the base-case needs, using the energy and water efficiency measures presented in this dissertation; and sizing the renewable systems to ensure self-sufficiency for energy, water and sewage disposal needs of the house. The methodology used in this study provided the basis for formulating a general procedure for designing off-grid, off-pipe homes.

#### **6.2. Summary of the Methodology**

The methodology used in this study utilizes a number of existing software programs and analysis tools with several sources of weather data for each of the six locations. These include: the DOE-2.1e simulation program using TMY2 hourly weather data for the analysis of whole-building energy use; F-CHART and PV-F-CHART programs with TMY2 average monthly weather data for the analysis of active solar thermal and photovoltaic systems, respectively; the use of wind turbine power curves with twelve years of measured hourly wind data for the analysis of wind power generation; NASA solar energy datasets for monthly extreme insolation conditions for the sizing of electricity storage system; cumulative supply versus demand analysis using twelve years of measured daily rainfall data for the sizing of rainwater harvesting system; and the US EPA design manual for the sizing of sewage disposal system.

This study used a 2000/2001 IECC standard reference design of a single-family detached house as the base case in each location. Other characteristics of the base-case house were determined from the U.S. Census Housing Survey Data and the Building America Research Benchmark Definition. The

analysis was performed in six climate locations across the U.S. with dissimilar base-case building energy requirements and the availability of renewable resources (i.e., solar radiation, wind and rainwater). These included: Minneapolis, MN (very cold climate), Boulder, CO (cold climate), Atlanta, GA (mixed-humid climate), Houston, TX (hot and humid climate), Phoenix, AZ (hot-dry climate), and Los Angeles, CA (marine climate). For each location, the base-case building energy use was determined using the DOE-2.1e energy simulation program. The indoor water use and sewage disposal needs were estimated using the results of a 1999 empirical study by the American Water Works Association (Mayer and DeOreo 1999), with revisions by Vickers (2001) to account for the federal maximum water use requirements for plumbing fixtures and appliances, established by the 1992 U.S. Energy Policy Act.

For each location, energy and water efficiency measures were analyzed in a combined application to reduce the base-case building energy and indoor water use. The energy-efficiency measures included: building configuration; improved airtightness and thermal properties of the exterior walls and roof; improved thermal properties of the windows, window distribution on the four sides, and the use of overhangs and moveable insulation; high-efficiency HVAC and DHW systems; and energy-efficient lighting and appliances. The reductions in indoor water use were estimated for three levels of water-efficiency measures including: (i) the use of water-efficient plumbing fixtures and appliances, (ii) greywater reuse for toilet flushing, and (iii) greywater recycling for non-potable uses (including toilets and clothes washing). The selection of energy and water efficiency measures was made to minimize the monthly peak energy use and average daily indoor water use.

Next, the harvestable on-site renewable resources were quantified at each location, which included: solar thermal energy for providing space heating and domestic water heating, wind power and solar radiation for electricity generation, and rainwater for indoor water use. For this, the performance of the renewable energy systems with different types/capacities of active solar thermal collectors, photovoltaic panels and wind turbines was analyzed for varying system and installation configurations. In addition, normalized system sizing parameters (i.e., per unit of daily water use) were derived for the rainwater harvesting system.

The estimates of reduced building energy and water needs combined with the estimates of harvestable on-site renewable resources for varying system and installation configurations were used for the sizing of renewable energy, rainwater harvesting and sewage disposal systems, which provided all household energy and water needs, and facilitated on-site sewage disposal. In this manner, the integrated analysis procedure, developed for this dissertation, was used to analyze and design off-grid, off-pipe homes, in six U.S. climate locations.

### **6.3. Summary of Analysis and Results**

The summary of analysis and results is presented for the six selected climate locations in terms of the energy use for the base-case and the proposed house in each climate location, and the sizing of systems

for self-sufficiency including: solar thermal system, wind power system, photovoltaic system, electricity storage system, rainwater harvesting system, and sewage disposal system.

### 6.3.1. *Energy Use for the Base-case and Proposed House*

#### 6.3.1.1. *Annual Energy Use*

The analysis showed that the base-case annual thermal energy and electricity use was 75.0 MMBtu (thermal) and 48.3 MMBtu (electric) in Minneapolis, 39.6 MMBtu and 48.2 MMBtu in Boulder, 36.8 MMBtu and 45.8 MMBtu in Atlanta, 21.9 MMBtu and 52.3 MMBtu in Houston, and 14.8 MMBtu and 67.4 MMBtu in Phoenix and 17.0 MMBtu and 35.2 MMBtu in Los Angeles, respectively. Using the energy-efficiency measures, described in this dissertation, the annual thermal energy and electricity use were reduced by 44% (thermal) and 51% (electric) in Minneapolis, 52% and 49% in Boulder, 64% and 45% in Atlanta, 42% and 57% in Houston, 45% and 61% in Phoenix and 38% and 48% in Los Angeles.

#### 6.3.1.2. *Monthly Energy Use*

The peak winter monthly thermal energy use was reduced as follows for each location: 18 MMBtu (base case) to 9.1 MMBtu (proposed design, resulting in 50% reduction) in Minneapolis, 7.7 MMBtu to 3 MMBtu (62% reduction) in Boulder, 8.6 MMBtu to 2.5 MMBtu (71% reduction) in Atlanta, 5.0 MMBtu to 2.3 MMBtu (54% reduction) in Houston, 3 MMBtu to 1.1 MMBtu (62% reduction) in Phoenix, and 3 MMBtu to 1.3 MMBtu (57% reduction) in Los Angeles, respectively.

The peak summer monthly electricity use was reduced as follows for each location: 1,733 kWh to 604 kWh (65% reduction) in Minneapolis, 1,844 kWh to 664 kWh (64% reduction) in Boulder, 1,681 kWh to 792 kWh (53% reduction) in Atlanta, 2,105 kWh to 734 kWh (65% reduction) in Houston, 2,963 kWh to 1,017 kWh (66% reduction) in Phoenix, and 1,037 kWh to 446 kWh (57% reduction) in Los Angeles, respectively.

#### 6.3.1.3. *Peak Day Energy Use*

The peak winter daily thermal energy use was reduced as follows for each location: 1,031 kBtu to 534 kBtu (48% reduction) in Minneapolis, 410 kBtu to 175 kBtu (57% reduction) in Boulder, 549 kBtu to 195 kBtu (65% reduction) in Atlanta, 425 kBtu to 230 kBtu (46% reduction) in Houston, 200 kBtu to 84 kBtu (58% reduction) in Phoenix, and 103 kBtu to 69 kBtu (33% reduction) in Los Angeles, respectively. The reduced loads were then used to calculate the hot water storage tank size obtained from the analysis of the solar thermal system.

The peak summer daily electricity use was reduced as follows for each location: 81.7 kWh to 27.1 kWh (67% reduction) in Minneapolis, 68.6 kWh to 23.8 kWh (65% reduction) in Boulder, 78.9 kWh to 33.5 kWh (58% reduction) in Atlanta, 82.1 kWh to 27.8 kWh (66% reduction) in Houston, 113.2 kWh to 38.0 kWh (67% reduction) in Phoenix, and 43.5 kWh to 16.1 kWh (63% reduction) in Los Angeles,

respectively. The reduced loads were then combined with the NO-SUN days over a consecutive period to determine the cumulative electricity storage needs for extended periods of less insolation.

### 6.3.2. *Sizing of Systems for Self-sufficiency*

#### 6.3.2.1. *Solar Thermal System Sizing*

The analysis of solar thermal system was performed using the F-CHART program for a flat plate and evacuated tube type collectors in the selected locations. In order to obtain the building heat loss coefficient required for the F-CHART input, the DOE-2.1e building monthly space heating loads were plotted against the average monthly temperature to calculate the slope of the change-point linear curve. After the application of the energy-efficiency measures, described in the dissertation, the building UA for each location was reduced from 470 Btu/h.°F to 224 Btu/h.°F (52% reduction) in Minneapolis, 327 Btu/h.°F to 84 Btu/h.°F in Boulder (74% reduction), 427 to 97 Btu/h.°F in Atlanta (77% reduction), 260 to 138 Btu/h.°F in Houston (47% reduction), 147 to 34 Btu/h.°F in Phoenix (77% reduction), and 252 to 108 Btu/h.°F in Los Angeles (57% reduction). The reduced building thermal loads were then used to provide the smaller sizing needs for the solar thermal system.

For the determination of the solar thermal collector type and area, the thermal loads of the house were compared with the solar thermal system output for a flat plate collector and an evacuated tube collector with varying collector areas. The type and area required to meet the peak winter thermal loads was then selected (except for Minneapolis, for which the unmet thermal loads were transferred to the electricity loads). The analysis showed the preferred collector type for all locations was evacuated tube collector, except for flat plate collectors for Phoenix. The selected collector areas were 256 ft<sup>2</sup> in Minneapolis, 192 ft<sup>2</sup> in Boulder, 160 ft<sup>2</sup> in Atlanta and Houston, 64 ft<sup>2</sup> in Phoenix, and 96 ft<sup>2</sup> in Los Angeles.

#### 6.3.2.2. *Wind Power System Sizing*

The wind speed and power output from a 7.5 kW and a 2.5 kW wind turbine were analyzed for each location. The results showed a significant impact as a result of the tower height and terrain parameters. The results indicated that, compared to a flat, open terrain, a suburban terrain results in a 28% reduction in wind speed and 50% reduction in power output at a 60 ft. tower height, and a 25% reduction in wind speed and a 40% reduction in power output at a 40 ft. tower height. The reduced output due to the terrain characteristics can be offset to some extent by increasing the tower height. The analysis of wind power output for the selected locations showed that wind is a large energy resource for Minneapolis and Boulder, and a modest resource in Los Angeles and Atlanta. Further analysis on a monthly basis showed that wind energy can offset a significant portion of the electricity needs throughout the year in Boulder, during the spring and fall in Minneapolis and Atlanta, and during the spring and summer in Los Angeles.

For all these locations (except Houston, and Phoenix), a 7.5 kW wind turbine was selected which is available with a higher tower.

#### 6.3.2.3. *Photovoltaic System Sizing*

The electrical output from an 18.5% efficient mono-crystalline PV array and a 6.7% efficient thin-film PV array of equal capacity (i.e., the area of the thin-film PV panel was twice the area of the mono-crystalline panel) were analyzed in each climate location. The results showed a considerable impact from the different temperature coefficients, resulting in a smaller output from mono-crystalline PV panels in the summer, especially in Phoenix and Houston. For locations with a higher wind power potential, PV panels were provided to complement the wind turbine output and the sizing was performed for the larger of the remaining monthly electricity needs. For other locations, the sizing was performed to ensure that the peak summer and winter electricity needs are met. A minimum tilt of 15 degrees was considered in order to minimize the reduction in the performance or need for a more frequent cleaning due to dust accumulation on the panels. With these criteria, the required PV panel area for the six locations were 30 m<sup>2</sup>, 20 m<sup>2</sup> and 25 m<sup>2</sup> of mono-crystalline PV panels in Minneapolis, Boulder and Los Angeles, respectively; and 83 m<sup>2</sup>, 110 m<sup>2</sup> and 96 m<sup>2</sup> of thin-film PV panels in Atlanta, Houston and Phoenix.

#### 6.3.2.4. *Battery Storage System*

The sizing of battery storage system was performed for the larger of the cumulative energy needs during the longest equivalent NO-SUN period and the cumulative electricity generation during the longest equivalent SURPLUS-SUN period. The selected locations had approximately 8-10 days of equivalent NO SUN or EXCESS SUN periods. The NO-SUN periods with high electricity needs occurred during peak winter (cloudy days) or late summer (less clear day and high electricity use) period. For most location, the EXCESS-SUN period occurred in the spring or the fall, which were characterized by days with clear sky and smaller electricity needs compared to the summer period. With these estimates, the effective storage capacity of 140 kWh for Minneapolis, 117 kWh in Boulder, 160 kWh for Atlanta, 218 kWh for Houston, 128 kWh for Houston, and 102 kWh for Los Angeles was required. Considering other battery sizing parameters including: the 40-50% maximum depth of discharge limitation, the 3% degradation due to extreme temperatures in cold climates and the 2% loss due to the charge/discharge cycle for all locations, the required battery bank size would be about twice the calculated effective storage capacity.

#### 6.3.2.5. *Rainwater Harvesting System*

The sizing of rainwater harvesting system was performed for the critical rainfall conditions in terms of the amount of rainfall and the length of the dry-periods that occurred during the last 12 years (1997-2008). Using the measured daily rainfall data for each location, two parameters representing critical rainfall conditions were derived, which include: the maximum required catchment area per unit of daily demand, and the maximum required storage volume per unit of daily demand. Based on these parameters,

the level (i.e., the amount) of water efficiency measures required to achieve the needed water use reductions were determined. Finally, for the reduced water use, catchment area and storage volume were calculated. Following these steps, the estimated daily water use in the selected locations were 121.6 gal/day using high-efficiency fixtures and appliances (Level 1) for Atlanta and Houston, 88.8 gal/day considering Level 1 with greywater reuse for flushing toilets (Level 2) for Minneapolis, and 66.8 gal/day for Boulder, Phoenix and Los Angeles considering Level 1 with greywater recycle for non-potable end-use including toilet flushing and clothes washing. For these daily water demands, the catchment area requirements were 2,300 to 2,800 ft<sup>2</sup> in Minneapolis, Atlanta and Houston, 5,700 ft<sup>2</sup> in Boulder, 8,400 ft<sup>2</sup> in Los Angeles and 15,700 ft<sup>2</sup> in Phoenix. The storage requirements were 11,000 to 13,000 gallons for all locations, except 15,600 gallons in Minneapolis and 19,600 gallons in Los Angeles.

#### 6.3.2.6. *Sewage Disposal System*

The need for sewage disposal was estimated from the reduced water use: 121.6 gal/day for Atlanta and Houston, 88.8 gal/day for Minneapolis, and 66.8 gal/day for Boulder, Phoenix and Los Angeles. By choosing water-efficient fixtures and appliances, a reduced peak instantaneous flow of 5 gpm can be achieved, which results in a septic tank of 750 gallons or less in all locations, which is the minimum size specified in the codes. Assuming an average soil percolation rate of 46 to 60 min per inch, absorption field of a 750 ft<sup>2</sup> area would be needed, requiring a 1,500 ft<sup>2</sup> of leaching field with 3 ft. wide trenches spaced 3 ft. apart.

### 6.4. Discussion

To begin with, first the criteria used for the analysis of energy and water use and the sizing of the systems for self-sufficiency were determined, which forms the basis of this study and the discussion. Next, the opportunities and challenges in designing the off-grid, off-pipe homes in the selected climate locations was presented, which indicate some common trends among the opportunities in all locations and some climate-specific challenges for achieving self-sufficiency for the building energy needs, indoor water use and sewage disposal. Based on these criteria, the priorities for the building and system design were discussed and a general approach for making design decisions was laid out.

In addition to these criteria, several other factors were identified that contributed to the successful design and implementation of off-grid, off-pipe designs as an architectural policy. These include considerations for the integration of the building, site and systems on a micro or individual house scale, as well as for the overall feasibility of this approach on a macro or community scale. A number of these considerations are recommended as efficient architectural policy. Finally, the limitations of the analysis procedure used in this study are recognized, which formed the basis of the recommendations for future research.

#### 6.4.1. *Criteria for the Analysis Procedure*

The following are the general criteria used for the analysis of energy and water use and sizing of systems for self-sufficiency:

1. The monthly peak energy consumption was identified as the main criteria for energy use reduction. The daily peak energy consumption was observed, simultaneously, to assess the scale of the impact of energy efficiency measures.
2. The energy-efficiency measures, which reduced either or both of the building heating and cooling energy use were considered first. With these measures applied to the base-case house, the optimum combination of building shape and fenestration properties was sought using a parametric analysis.
3. Water-efficiency measures were determined depending of the availability of harvestable rainwater at each site. At a minimum, the use of high-efficiency plumbing fixtures and water conserving appliances was considered for all locations. The resulting reductions in the domestic hot water use were then accounted for in the energy analysis.
4. The critical periods were defined as periods when the availability of renewable resources was less than the building needs, and therefore required storage.
5. The tilt and area of solar thermal collectors and photovoltaic systems were determined in order to maximize the usable energy output during the months with peak thermal and electricity loads. The type of systems were determined based on the severity of winter or summer climate.
6. The output from two wind turbines of different size and tower heights was quantified, which favor the use of more than one smaller turbine versus one large turbine. After this was performed, the sizing of PV system was then determined to provide for the remaining building electricity needs.
7. For the rainwater harvesting system, the year with the minimum rainfall did not always coincide with the year having the longest dry period. Therefore, these two normalized system-sizing parameters were used to indicate the critical rainfall conditions from the twelve years of measured daily rainfall data. These two parameters then guided the selection of water efficiency and conservation level required to reduce the demand to a level that could utilize the available catchment area.

#### 6.4.2. *Opportunities*

The results of the analysis identified the following opportunities for the energy and water use reductions, and on-site harvesting of renewable resources available in the selected climate locations, which could be generalized to other locations with similar climate characteristics.

1. In all climates, 50-70% peak month and peak day energy savings were possible.
2. Indoor water use reductions of up to 33% could be achieved from easy-to-implement water-efficiency measures (i.e., high efficiency plumbing fixtures and water using appliances). Further reductions of up to 63% could be achieved from additional more stringent water-efficiency measures (greywater reuse/recycling).

3. Depending on the building's thermal loads, the annual thermal energy collection of 150-300 kBtu/ ft<sup>2</sup> was achievable in all locations.
4. In all locations, an annual electricity production of 1,100-1,600 kWh/kWp from solar radiation was achievable.
5. In locations with high average wind speeds, the annual electricity production of at least 700 kWh/kWp (using coefficients reflective of the suburban local terrain) to up to 1,800 kWh/kWp (for flat, open terrain) was achievable from wind turbines. In locations with low average wind speeds, an annual electricity output of only approximately 200 kWh/kWp was achievable.
6. For locations with more than 40 inches of annual rainfall, it was possible to provide daily indoor water use (122 gal/day) only from the roof as the catchment area (up to 3,000 ft<sup>2</sup>) with minimal water efficiency measures.
7. For sewage disposal, a 1,000 gallon septic tank was required with 2,000 ft<sup>2</sup> of leaching field area, assuming minimal water use reductions in all locations.

#### 6.4.3. *Challenges*

Although, the energy and water use reductions were in the same range for all climate locations, meeting the reduced loads with only the renewable systems was found to be very challenging in some climates. For example:

1. Due to the seasonal and year-to-year variations in the resource availability, the criteria of sizing for the critical periods for achieving self-sufficiency necessitated large size and reduced average utilization of collection and storage systems.
2. In a very cold climate, meeting the building thermal energy needs with only the solar thermal system was found to be very difficult, resulting in the need for back-up heating using biomass or biofuel, which could be grown and harvested on-site. This requires additional considerations for the on-site harvesting/production, storage and utilization of biomass and/or biofuel, which were not pursued in this study.
3. For the utilization of a wind power system, the site area and surroundings must be suitable (i.e., preferably an unobstructed area on the windward side for at least 150 ft. from the tower).
4. The annual electricity production from the combined PV/wind renewable electric systems could be fully utilized to provide the electricity needs throughout the year, only if there is sufficient electricity storage capacity (i.e., 100-200 kWh, depending on the cumulative electricity needs during unfavorable days for renewable electricity generation).
5. In certain climate locations (i.e., Phoenix and Los Angeles), providing the indoor water supply from rainwater harvested only from the roof of the house was found to be very difficult. For these locations, the need for additional custom-designed catchment surfaces was identified. In addition, for locations



with only seasonal rainfall, the need for a large storage tank and additional considerations for ensuring safe and clean potable water from such a storage was identified.

6. For the sewage disposal system, the soil conditions should be suitable, or the site area should be large enough to accommodate a larger leaching field required for poor soil with lower percolation rates. Considering such challenges, the design priorities for each location should be determined.

#### 6.4.4. *Building and System Design Priorities*

Performing the analysis for the different climate locations revealed some conflicting design priorities when the design decision favoring the performance of one system impacted the performance of another system in an opposite manner, or impacted different energy end-use in opposite ways. These cases required re-evaluation of alternative design strategies, energy-efficiency measures, and system sizing. From such instances, a general approach for the determination of the building and system design priorities can be laid out, as follows:

1. The building dimensions/ geometry, window distribution and shading strategies tend to impact the heating and cooling energy use in an opposite manner. In such cases, the availability of harvestable renewable energy resources (i.e., passive solar) versus the building energy use during other periods should be evaluated to determine the most critical energy end-use to be reduced.
2. In a very cold climate location with a lower potential of rainwater harvesting, the priority for a compact building design (i.e., two-story house) for minimizing the peak thermal energy use would result in a smaller roof area for rainwater harvesting, which might conflict with the design priority for providing a large catchment area. In such cases, first the energy-efficiency and water efficiency measures should be reevaluated to assess the possibility of further reduction in the building energy/water needs, and then the need for or ease of increasing the sizing of the building systems should be reevaluated/compared.
3. In general, a compact building plan with a 1: 1 and 1: 1.5 aspect ratio was found optimum. However, such configuration allows limited wall area available for southern windows (unless windows with a higher lintel height or a lower sill height are considered). Considering that the other sides of the building have smaller window areas, taller south windows allow more daylighting penetration preferred in a square-shape building layout. On the other hand, for a fixed wall height, the effectiveness of providing fixed overhangs for allowing winter sun and blocking summer sun through taller windows is reduced. In such cases, retractable or flexible-tilt exterior shades and awnings should be considered.
4. For locations with a high availability of solar radiation, the system installation criteria can be relaxed to some extent, and more traditional architectural designs of the buildings can be considered for making integrated design decision that integrates renewable system design with regional architecture.

#### 6.4.5. *Recommended Architectural Policy*

In regard to architectural policy, there are several other factors that can contribute to the successful design and implementation of off-grid, off-pipe design approach. These include: considerations for the integration of the building, site and systems on a micro (or building) scale, as well as for the overall feasibility of this approach on a macro (or community) scale.

##### 6.4.5.1. *Considerations for the Integration of the Building, Site, and Systems*

The methodology developed for this study allows flexibility in selecting the system size and installation conditions according to the design of the building, to a certain extent. However, in order to ensure that the systems are installed for maximized performance, the building design, site and landscaping should accommodate the systems at their best performance, without compromising the functionality, livability, and structural integrity of the building. With these concerns, the specific considerations for an integrated design of the building and systems should include:

1. **Surroundings:** The surroundings of the building including the neighboring built structures and trees should ensure no shading of the solar collectors and PV array, and should not obstruct the wind turbine. In case the horizon elevated due to the topography of the site, a lower tilt of the solar collector and PV array may be needed.
2. **Building Site and Landscaping:** The building site should accommodate systems for sewage disposal, provision for water recycling, custom designed catchment surfaces, and a rainwater storage tank. With an innovative design approach, these system components can be camouflaged/integrated into the site landscape or building structure.
3. **Building Design:** The design of the building should ensure sufficient roof area for mounting solar collectors and PV arrays, and a self-maintained roof catchment surface for rainwater harvesting, proper tilt(s) for the installation of building-mounted system components; sufficient space for the installation, monitoring, and maintenance of equipment, and storage for biomass and batteries. The structure of the building should be designed to be able to support the building mounted system components. The layout of indoor and outdoor spaces, building entrance, and location of the windows with respect to the positioning of system components, and vice versa, should ensure avoidance of noise, undisturbed vision, and clear access.
4. **Safety Consideration:** The installation of all systems including the PV/wind electric system, batteries, and solar thermal system must comply with safety codes. Access to the system components must be protected, as needed. The rainwater harvesting system should be designed with proper considerations for providing safe and clean portable water. The back-up biomass system should ensure safe and clean combustion.

#### 6.4.5.2. *Considerations for the Overall Feasibility*

This study assessed the feasibility of off-grid, off-pipe single-family detached homes in six different U.S. locations from the viewpoint of whether or not it could be achieved, as well as to determine system sizing requirements. In other words, it performed a quantitative analysis to learn if it is possible to achieve self-sufficiency from on-site renewable resources to provide the building energy use, water use and sewage disposal needs. To accomplish this, certain energy and water efficiency measures were identified and the systems for the harvesting on-site available renewable resources were considered. The overall feasibility of such a design approach on a macro (or community) scale, which would determine its merit for implementing as an architectural policy for the benefit of the environment and society, depends on the existing support systems in terms of the technology (for the cost-effective design and implementation of this approach), policies (such as financial incentives, building codes and regulations, and community planning), society (in terms of public perception and acceptance of this approach), and logistics (i.e., specialized, well-coordinated resources including: human resources, process resources, and natural resources). An explanation of these support systems, their interdependence and significance in the framework of off-grid, off-pipe design approach is included in Section 1.2.

#### 6.4.6. *Limitations of the Analysis Procedure Specific to This Study*

The application of the proposed methodology presented many limitations, which can be grouped in three general categories: i) a lack of design weather data for sizing renewable systems; ii) inherent limitations of individual analysis programs, analysis tools and analysis methods used for this study; and iii) limitations of the integration process.

##### 6.4.6.1. *Weather Data*

Currently, there is no single consistent weather data source that can be used for an integrated analysis for energy-efficiency, water-efficiency, and renewable measures. Therefore, weather data from several different sources were used. Unfortunately, there are several concerns with using different weather data sources, which include: i) the use of non-coincident meteorological data for the analysis of building energy use and renewable energy systems, and ii) the use of typical year weather data for building energy and solar system analysis, and extreme years for the wind electric, rainwater and electricity storage system sizing. Achieving complete self-sufficiency would also require considering extreme weather years with higher than typical building energy use and lower than typical solar system output, which are usually two different periods.

In this study, the effect of hourly incompatibility was reduced to some extent by integrating the results to a monthly basis. However, in order to perform a consistent analysis, one design weather year should be created for the analysis of energy use and the sizing of different systems including: the active solar, PV, wind power and rainwater harvesting systems.

#### 6.4.6.2. *Potential Alternative Systems*

This study is limited to the capabilities of the analysis program and methods used, and the available weather data resources. This choice excluded the analysis of a number of viable energy-efficiency and renewable energy strategies including passive solar strategies, active solar cooling systems, ground source heat pumps, radiant floor heating system, energy recovery systems, daylighting and natural ventilation. In addition, it allowed only an approximate estimation of energy and water savings from water efficiency strategies. Furthermore, it excluded the analysis of other potential electricity storage methods such as hydrogen for use in fuel cells. For a more thorough design of off-grid, off-pipe houses, some of these systems may have a higher potential for success, but would require using other analysis programs which could simulate these systems.

#### 6.4.6.3. *Analysis and Integration Methodology*

In this study, the inputs across different methods/tools used for this study were synchronized to a limited extent. For example, converting the space heating loads from the DOE-2.1e output to building UA for the F-CHART program, and converting the unmet thermal loads to electricity loads while taking into account the operating efficiency of the heat pump. Also the interaction among several systems and components were not taken into account. For example, the thermal impacts of roof mounted PV panels and/or solar thermal collectors on the building energy use were not considered. Furthermore, auxiliary energy end uses were determined approximately using simple estimation/assumptions. For example, the operation of the pump required for the solar thermal system was based on a simple estimation of period of collector operation and assumed pumping power per unit of collector area ( $\text{W}/\text{m}^2$ ), and the operation of pressurization pump for the water supply system was based on an assumption from a reputable source (in Wh per gallon). In the future, in order to perform an integrated analysis, a truly integrated analysis program would be needed that could simulate the interaction among all energy and water systems and components of the building.

The time step for the analysis of building energy use and of the different systems was not the same. For example, the analysis of the energy use was based on hourly weather records, whereas, for the solar system output, monthly average weather data was used. The performance of the wind electric systems was also based on the monthly total output. The design of the rainwater harvesting system was based on the annual rainwater supply and water demand. This integration method, based on monthly or annual data, is applicable only for the full utilization of the resources during the analysis period. To take into account the actual performance of the systems, the use of analysis tools with a detailed hourly modeling capability is recommended.

This methodology utilized an iterative method to arrive at an optimal combination of energy efficiency strategies and system configuration. The use of an optimization programs might help at arriving

these solutions in a more efficient way. However, the optimization criteria for such analysis should use peak or critical conditions in terms of energy use or resource availability.

### 6.5. Conclusions

This study developed an integrated analysis method for the design and analysis of off-grid, off-pipe homes in different climates, using the analysis tools and methods selected for this study. This procedure was demonstrated using six different U.S. climatic locations. Figure 66 reiterates the steps proposed for the integration procedure, with the analysis steps pertaining to building, occupancy and site under consideration. First, a preliminary climate and site analysis should be performed. This would require obtaining weather data from several sources as well as assessing the microclimate conditions. Next, the energy use of the proposed house should be simulated and analyzed for peak winter and summer

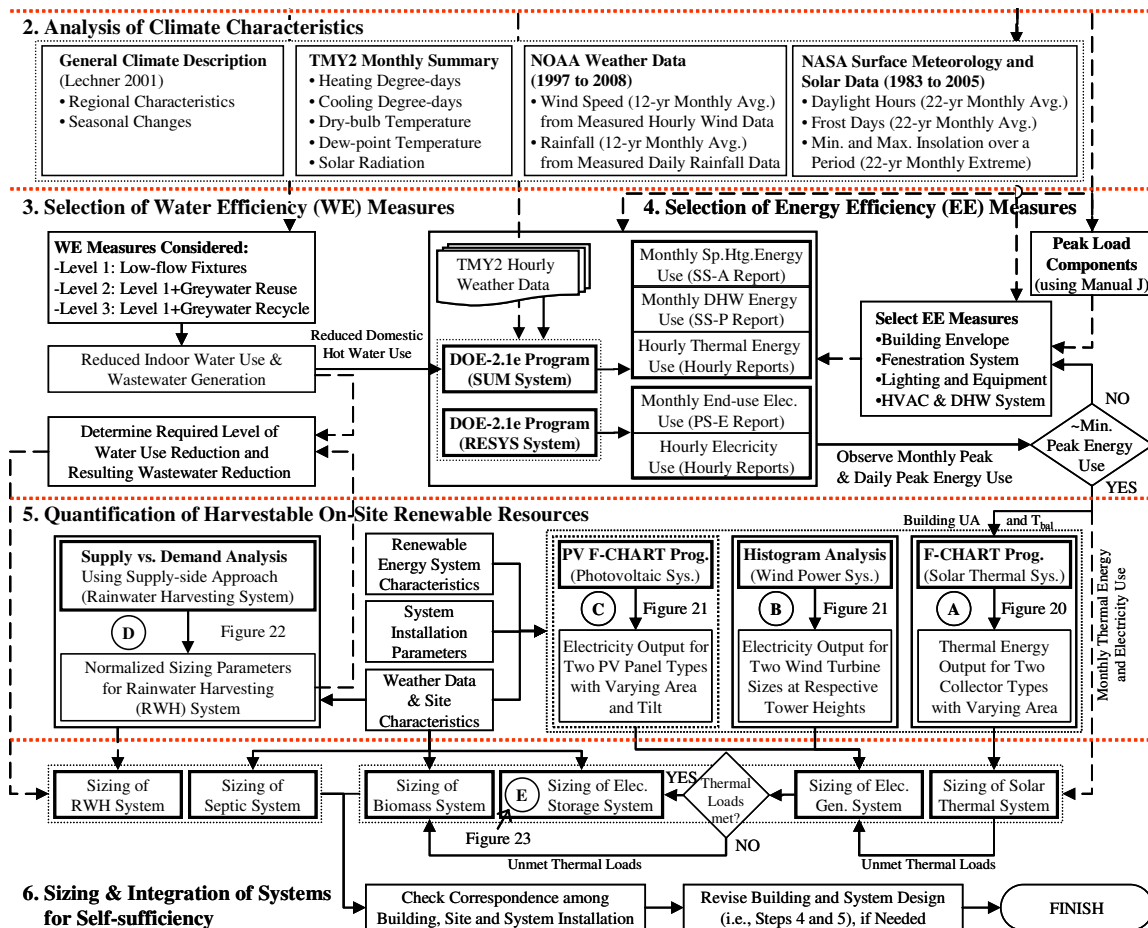


Figure 66 Procedure for an Integrated Analysis of Off-grid, Off-pipe Homes

months. By investigating the potential load components, the selection of energy efficiency measures should be made and the reduced energy use for the proposed house should be determined. Next the performance of renewable energy systems should be determined with varying system parameters, which could be scaled to meet the peak building loads. For the sizing of rainwater harvesting system, normalized sizing parameters should be calculated, which determine the level of water use reduction and the sizing of the rainwater harvesting system. Next, the sizing of systems for self-sufficiency should be performed to meet the reduced building needs. Finally, the integration of building, site and systems should be checked for any required adjustment. Figure 67 shows a schematic design of the proposed off-grid, off-pipe residence with the systems required for achieving self sufficiency.

Using these steps for the six selected climate locations showed that achieving self-sufficiency for energy, water and sewage disposal is possible provided the systems for the collection and storage of renewable resources are large. On the other hand, in most cases, the utilization of these systems was small, especially, in location with a high year-to-year and seasonal variations in the weather conditions. For increased utilization of these systems, the minimization of the peak building needs, the utilization of harvested energy for secondary purposes, and considering alternative systems for such applications would be preferred.

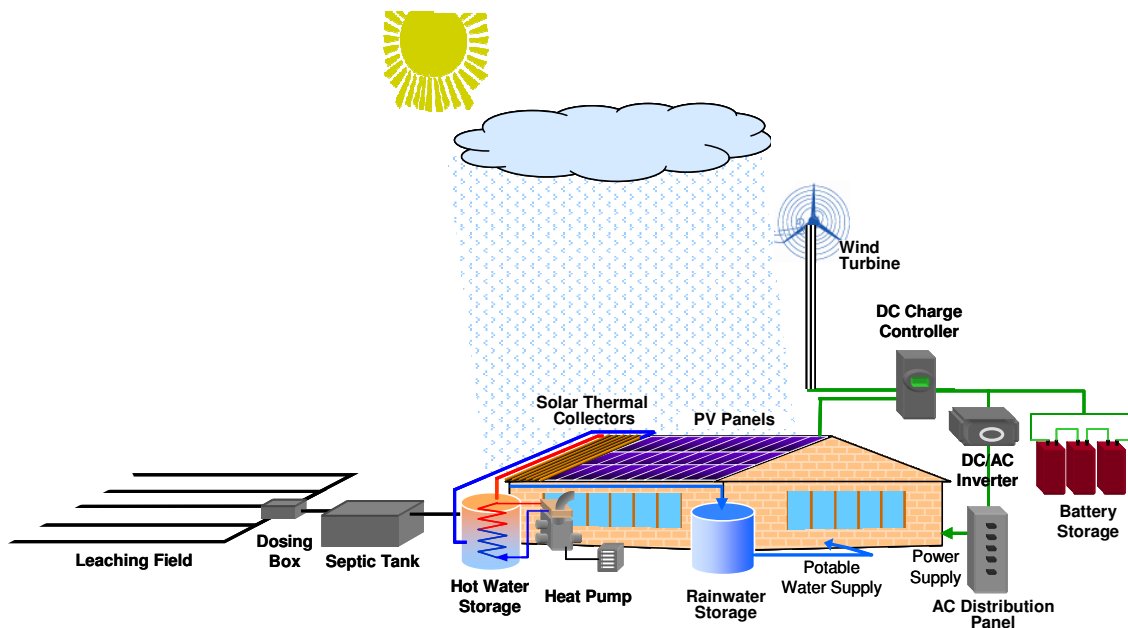


Figure 67 Schematic Design of the Proposed Off-grid, Off-pipe Residence

## 6.6. Recommendations for Future Research

The limitation of this study were recognized earlier in this chapter. In order to improve the usefulness of the analysis procedure for the design of off-grid, off-pipe homes, as discussed in Section 6.4.6, the recommendations for further research can be summarized as follows:

1. Development of improved design weather data: For the sizing of systems for self-sufficiency, design weather data are needed, which could represent the extreme weather conditions for a location in terms of the building energy use as well as the availability of harvestable renewable resources. This may require development of multiple years of design weather data representing extreme conditions for all relevant climate parameters. In addition, the currently used data recording procedure for wind data at meteorological weather station records an average wind speed for the most recent two-minute period prior to the observation time (calculated from a series of 24 five-second average values), which is intended for aviation purposes. The data recording for wind data measurement should be hourly-averaged wind speed, which would provide a better estimate of the hourly average wind power. In addition, improved low wind speed data is expected as new ultrasonic wind sensors are used to replace traditional contact anemometers. This will improve the measurement of wind speeds below the certain speed of the contact anemometer (i.e., 2-5 mph).
2. Analysis of more appropriate building systems: For the analysis for self-sufficiency using renewable resources, an integrated simulation capability of several alternative measures and systems such as, solar thermal cooling systems, radiant heating systems, ground source heat pumps, energy recovery systems, hydrogen storage and hydrogen-based space heating and electric power generation systems, would be beneficial.
3. Development of integrated analysis programs with customized optimization criteria: Considering that the analysis procedure requires multiple parametric analysis, the use of optimization programs with customized optimization criteria would be beneficial.

In addition, in order to assess the overall feasibility of this approach in different parts of the world (including those selected for this study), further research is needed to investigate the political and social support systems, and the state-of-the-art technology as the technical and logistical support systems required to maintain the building systems. These are pre-requisites for the wide-scale implementation the proposed off-grid, off-pipe design approach as an architecture policy. Within these domains, the following aspects related to the off-grid, off-pipe design approach are potential areas for future investigation:

1. Investigation of Innovative Design and Construction Methods: This study focused on the selection of energy-efficiency measures and sizing of systems for achieving self-sufficiency, using commercially available technologies. Further investigation for more appropriate design concepts, cost-effective building materials, construction methods, and structural systems for the building and system integration would be beneficial for establishing the overall feasibility of this approach.

2. Evaluation of Codes and Regulations: An investigation of the existing building codes and regulations is required to identify the barriers and propose necessary revisions, which could address the additional considerations for the off-grid, off-pipe design and credit for the benefits of such approach.
3. Evaluation of Existing Design Guidelines: The approach for determining the building design for this study was focused on minimizing the envelope loads of a building - mechanically conditioned and thermostatically controlled throughout the year, with a highly insulated envelope and several other energy-efficiency measures. On the other hand, a reverse procedure might be followed for an alternative approach, where the cost-effective level of insulation and energy efficiency measures are sought and the passive strategies for daylighting and natural ventilation are considered. For such a case, the climate-specific building design guidelines such as those proposed in Lechner (2001) pertinent to each climate zone would need to be evaluated against the system design priorities dictated by the analysis of renewable energy systems.
4. Evaluation of the Application of Off-grid, Off-pipe Design Approach at the Community-level: Although this study is focused on individual sustenance of an off-grid, off-pipe house, it is recognized in Section 2.1.2 that the barriers of existing living concepts, codes and regulations, and affordability faced by such development in different parts of the world, are easier to overcome on a community scale. Therefore, an evaluation of this approach on a community scale from the viewpoints of architectural design and planning as well as the selection and sizing of systems are potential areas for future research.



## REFERENCES

- ACEEE. 2007. *Consumer Guide to Home Energy Savings*. 9th ed. Washington, DC: American Council for an Energy Efficient Economy.
- A Global Overview of Renewable Energy Sources (AGORES). 2009. Sources of Renewable Energy: Biomass. Hoeilaart (Brussels), Belgium: LIOR International. <http://www.agores.org/SECTORS/BIO/default.htm> (accessed July 30, 2009).
- AIA Research Corporation. 1978. *Regional Guidelines for Building Passive Energy Conserving Homes*. Washington, DC: U.S. Government Printing Office.
- Alexander, K.V., and E.P. Giddens. 2008. Microhydro: Cost-effective, Modular Systems for Low Heads. *Renewable Energy* 33(6):1379-1391.
- Alter, L. 2007a. Clivus Multrum at the Bronx Zoo. *Treehugger: Design & Architecture (Bathroom)*. [http://www.treehugger.com/files/2007/03/clivus\\_multrum\\_at\\_the\\_bronx\\_zoo.php](http://www.treehugger.com/files/2007/03/clivus_multrum_at_the_bronx_zoo.php) (accessed July 30, 2009).
- Alter, L. 2007b. Grey Water Guerrillas. *Treehugger: Science & Technology (Water)*. [http://www.treehugger.com/files/2007/05/grey\\_water\\_guer.php](http://www.treehugger.com/files/2007/05/grey_water_guer.php) (accessed July 30, 2009).
- Alter, L. 2008. Vancouver Office Building Goes "Off-Pipe". *TreeHugger: Science & Technology (Water)*. <http://www.treehugger.com/files/2008/09/office-building-has-composting-toilets.php> (accessed July 30, 2009).
- American Ground Water Trust (AGWT). 2008. Septic Systems for Waste Water Disposal. <http://www.agwt.org/info/septicssystems.htm> (accessed July 30, 2009).
- American Wind Energy Association (AWEA). 2009. Wind Energy Basics. [http://www.awea.org/faq/wwt\\_basics.html](http://www.awea.org/faq/wwt_basics.html) (accessed July 30, 2009).
- Anker, P. 2005. The Ecological Colonization of Space. *Environmental History* 10(2):239-268.
- Aresteh, D., S. Selkowitz, J. Apte, and M. LaFrance. 2006. Zero Energy Windows. *Proceedings of the 2006 ACEEE Summer Study on Energy Efficiency in Buildings* 3:1-14.
- Arney, M., P. Seward, and J.F. Kreider. 1981. P-chart - a Passive Solar Design Method. *Energy Engineering* 78(3):41-50.
- ASHRAE. 2004. *ANSI/ASHRAE Standard 152-2004 - Method of Test for Determining the Design and Seasonal Efficiencies of Residential Thermal Distribution Systems*. Atlanta, GA: American Society of Heating, Refrigerating, and Air-Conditioning Engineers.
- ASHRAE. 2005. *ASHRAE Handbook - Fundamentals*. Atlanta, GA: American Society of Heating, Refrigerating, and Air-Conditioning Engineers.
- ASHRAE. 2007. *ASHRAE Handbook - HVAC Applications*. Atlanta, GA: American Society of Heating, Refrigerating, and Air-Conditioning Engineers.
- ASHRAE. 2008. *ASHRAE Handbook - HVAC Systems and Equipment*. Atlanta, GA: American Society of Heating, Refrigerating, and Air-Conditioning Engineers.

- Balcomb, J.D., D. Barley, R. McFarland, J. Perry, Jr., W. Wray, and S. Noll. 1980. *Passive Solar Design Handbook. Volume Two of Two Volumes: Passive Solar Design Analysis*. Los Alamos, NM: Los Alamos Scientific Laboratory.
- Balcomb J.D., S.J. Hayter and N.L. Weaver. 2001. ENERGY-10 PV: Photovoltaics, A New Capability. NREL/CP-550-29637. Golden, CO: National Renewable Energy Laboratory.
- Baldwin, J.D. 1996. *Bucky Works: Buckminster Fuller's Ideas for Today*. New York, NY: John Wiley & Sons, Inc.
- Barnhart, E. 2007. *Bioshelter Guidebook: Bioshelter Research by New Alchemy Institute (1971-1991)*. Cape Cod, MA: New Alchemy Institute.
- Bergey. 2009. BWC EXCEL Wind Turbine: Detailed Technical Description of the Excel-R Turbine and Specification Sheets. <http://www.bergey.com/Products/Excel.html> (accessed July 30, 2009).
- Briggs, R.S., R.G. Lucas, and Z.T. Taylor. 2003. *ASHRAE 4610/4611 - Climate Classification for Building Energy Codes and Standards*. Atlanta, GA: American Society of Heating, Refrigerating, and Air-Conditioning Engineers.
- Building Energy Codes Program (BECP). 2008. Residential State Codes. U.S. Department of Energy. [http://www.energycodes.gov/implement/state\\_codes/state\\_status\\_full .php](http://www.energycodes.gov/implement/state_codes/state_status_full.php) (accessed July 30, 2009).
- Chang, M., M.W. McBroom, and R.S. Beasley. 2004. Roofing as a Source of Nonpoint Water Pollution. *Journal of Environmental Management* 73(4):307-315.
- Chen, S., C. Chu, M. Cheng, and C. Lin. 2009. The Autonomous House: A Bio-Hydrogen Based Energy Self-Sufficient Approach. *International Journal of Environmental Research and Public Health* 6(4):1515-1529.
- Christensen, C., S. Horowitz, R. Anderson, and S. Barker. 2005. BEopt: Software for Identifying Optimal Building Designs on the Path to Zero Net Energy. NREL/CP-550-37733. Golden, CO: National Renewable Energy Laboratory.
- Clark, D.R., S.A. Klein, and W.A. Beckman. 1983. Algorithm for Evaluating Hourly Radiation Utilizability Function. *ASME Journal of Solar Energy Engineering* 105(3):281-287.
- Clark, D.R., S.A. Klein, and W.A. Beckman. 1984. A Method for Estimating the Performance of Photovoltaic Systems. *Solar Energy* 33(6):551-555.
- Clarke, J.A. 2001. *Energy Simulation in Building Design*. 2nd ed. Oxford, UK: Butterworth-Heineman.
- Crawley, D.B., J.W. Hand, M. Kummert, and B.T. Griffith. 2008. Contrasting the Capabilities of Building Energy Performance Simulation Programs. *Building and Environment* 43(4):661-673.
- Crawley, D.B., L.K. Lawrie, C.O. Pedersen, F.C. Winkelmann, M.J. Witte, R.K. Strand, R.J. Liesen, W.F. Buhl, Y.J. Huang, R.H. Henniger, J. Glazer, D.E. Fisher, D.B. Shirey, III, B.T. Griffith, P.G. Ellis, and L. Gu. 2004. EnergyPlus: New, Capable, and Linked. *Journal of Architectural and Planning Research* 21(4):292-302.
- Crawley, D.B., L.K. Lawrie, F.C. Winkelmann, W.F. Buhl, Y.J. Huang, C.O. Pedersen, R.K. Strand, R.J. Liesen, D.E. Fisher, M.J. Witte, and J. Glazer. 2001. EnergyPlus: Creating a New-generation Building Energy Simulation Program. *Energy and Buildings* 33(4):319-331.

- Cummings, J.B., J.J. Tooley, Jr., and N. Moyer. 1991. Investigation of Air Distribution System Leakage and Its Impacts in Central Florida Homes. FSEC-CR-397-91. Cocoa, FL: Florida Solar Energy Center.
- Cunningham, P., and I. Woofenden. 2007. Microhydro-Electric Systems Simplified. *Home Power Magazine* 117:40-45.
- Dahl, T. 2008. Photovoltaic Power Systems: Technology White Paper. CH2M Hill Polar Services. [http://www.polarpower.org/static/docs/PVWhitePaper1\\_31.pdf](http://www.polarpower.org/static/docs/PVWhitePaper1_31.pdf) (accessed July, 30, 2009).
- Davis Energy Group, Inc. 2006. Measure Information Template - PEX Parallel Piping Hot Water Distribution Systems. 2008 California Building Energy Efficiency Standards. [http://www.energy.ca.gov/title24/2008standards/prerulemaking/documents/2006-05-18\\_workshop/2006-05-11\\_PEX.PDF](http://www.energy.ca.gov/title24/2008standards/prerulemaking/documents/2006-05-18_workshop/2006-05-11_PEX.PDF) (accessed July 30, 2009).
- Davis, S. 2003. *Microhydro: Clean Power from Water*. Gabriola Island, BC, Canada: New Society Publishers.
- Department of General Services (DGS). 2007. Title 24 Overview. The State of California. <http://www.dsa.dgs.ca.gov/Code/title24.htm> (accessed July 30, 2009).
- Dixon, A., D. Butler, and A. Fewkes. 1999. Water Saving Potential of Domestic Water Reuse Systems Using Greywater and Rainwater in Combination. *Water Science and Technology* 39(5):25-32.
- Duffie, J.A. and W.A. Beckman. 2006. *Solar Engineering of Thermal Processes*. 3rd ed. Hoboken, NJ: John Wiley & Sons, Inc.
- Earthship Biotecture. 2009. Earthship Village Ecologies. <http://www.earthship.net/buildings/44-communities/557-earthship-village-ecologies.html> (accessed October 30, 2009).
- Eiffert, P., and G.J. Kiss. 2000. *Building Integrated Photovoltaic Designs for Commercial and Institutional Structures: A Sourcebook for Architects*. Springfield, VA: U.S. Department of Commerce.
- Elliott, D.L., C.G. Holladay, W.R. Barchet, H.P. Foote and W.F. Sandusky. 1986. Wind Energy Resource Atlas of the United States. DOE/CH 10093-4. Golden, CO: Solar Energy Research Institute.
- Energy Systems Research Unit (ESRU). 2002. *The ESP-r System for Building Energy Simulation, User Guide Version 10 Series*. Glasgow, Scotland: University of Strathclyde.
- EnergyGauge USA. 2009. EnergyGauge USA: Energy and Economic Analysis Software. <http://www.energygauge.com/usares/>.
- Erbs, D.G., S.A. Klein, and W.A. Beckman. 1983. The Estimation of Degree Days and Ambient Temperature Bin Data from Monthly Average Temperatures. *ASHRAE Journal* 25(6):60-65.
- Evans, D.L., W.A. Facinelli, and R.T. Otterbein. 1978. Combined Photovoltaic/Thermal System Studies. SAND 78-7031. Tempe, AZ: Arizona State University.
- Fewkes, A. 2000. Modelling of Performance of Rainwater Collection System: Towards a Generalized Approach. *Urban Water* 1(4):323-333.
- Fewkes, A., and D. Butler. 2000. Simulating the Performance of Rainwater Collection Systems using Behavioural Models. *Building Services Engineering Research and Technology* 21(2):99-106.

- Fine, H.A., and D.L. McElroy. 1989. Assessment of the Energy Conservation Potential of Active (Variable Thermal Resistance and Switchable Absorptance) Building Thermal Insulation Systems. *Thermal Performance of the Exterior Envelopes of Buildings IV*:639-653.
- Fletcher, S. 2007. CERA: Alternative Energy Sources Remain Hot Industry Topic. *Oil & Gas Journal* 105(8):31-34.
- Fowles, B. 2004. The Quest for 'A Beautiful Act': Meeting Human and Ecological Rights in Creating the Sustainable Built Environment. In A.K. Haugested, and J.D. Wulfhorst (Eds.), *Future as Fairness: Ecological Justice and Global Citizenship* (pp. 139-160). New York, NY: Rodopi.
- Fuentes, M.K. 1985. A Simplified Thermal Model of Photovoltaic Modules. SAND85-0330. Albuquerque, NM: Sandia National Laboratories.
- Geltz, C. 1993. Building an Energy-Efficient Home Office. *Home Energy Magazine* 10(3):35-37.
- German Energy Society. 2008. *Planning and Installing Photovoltaic Systems: A Guide for Installers, Architects and Engineers*. 2nd ed. London, UK; Sterling, VA: Earthscan.
- Gipe, P. 2004. *Wind Power: Renewable Energy for Home, Farm, and Business*. Revised ed. White River Junction, VT: Chelsea Green Publishing Company.
- Givoni, B. 1998. *Climate Considerations in Building and Urban Design*. New York, NY: Van Nostrand Reinhold.
- Gordon, J.M., and Y. Zarmi. 1981a. Analytic Model for Passively-heated Solar Houses -1. Theory. *Solar Energy* 27(4):331-342.
- Gordon, J.M., and Y. Zarmi. 1981b. Analytic Model for Passively-heated Solar Houses -2. Users Guide. *Solar Energy* 27(4):343-347.
- Gould, J., and E. Nissen-Petersen. 1999. *Rainwater Catchment Systems for Domestic Supply: Design Construction and Implementation*. London, UK: Intermediate Technology Publications.
- Haberl, J.S., and S. Cho. 2004a. Literature Review of Uncertainty of Analysis Methods (DOE-2.1e). ESL-TR-04/11-01. College Station, TX: Energy Systems Laboratory, Texas A&M University.
- Haberl, J.S., and S. Cho. 2004b. Literature Review of Uncertainty of Analysis Methods (F-CHART Program). ESL-TR-04/08-04. College Station, TX: Energy Systems Laboratory, Texas A&M University.
- Haberl, J.S., and S. Cho. 2004c. Literature Review of Uncertainty of Analysis Methods (PV F-CHART Program). ESL-TR-04/10-02. College Station, TX: Energy Systems Laboratory, Texas A&M University.
- Hastings, R., and M. Wall. 2007a. *Sustainable Solar Housing, Volume 1: Strategies and Solutions*. Sterling, VA: Earthscan.
- Hastings, R., and M. Wall. 2007b. *Sustainable Solar Housing, Volume 2: Exemplary Buildings and Technologies*. Sterling, VA: Earthscan.
- Hay, H.R., and J.I. Yellott. 1970. A Naturally Air Conditioned Building. *Mechanical Engineering* 92(1):19-25.

- Hendron, R. 2008. Building America Research Benchmark Definition, Updated December 19, 2008. NREL/TP-550-44816. Golden, CO: National Renewable Energy Laboratory.
- Herbertson, A.J. 1905. The Major Natural Regions: An Essay in Systematic Geography. *The Geographical Journal* 25(3):300-310.
- Hirsch, J. 2006. DOE2.com: Weather Data & Weather Data Processing Utility Programs. <http://www.doe2.com/Download/Weather/TMY2/> (accessed July 30, 2009).
- Hittle, D.C. 1977. *The Building Loads Analysis and System Thermodynamics Program, BLAST*. Champaign, IL: U.S. Army Construction Engineering Research Laboratory.
- Hittle, D.C. 1979a. *The Building Loads Analysis and System Thermodynamics (BLAST) Program, Version 2.0. Users Manual, Volume I*. Champaign, IL: Army Construction Engineering Research Lab.
- Hittle, D.C. 1979b. *The Building Loads Analysis and System Thermodynamics (BLAST) Program, Version 2.0. Users Manual, Volume II*. Champaign, IL: Army Construction Engineering Research Lab.
- Huang, J., J. Hanford, and F. Yang. 1999. Residential Heating and Cooling Load Components Analysis. LBNL-44636. Berkeley, CA: Lawrence Berkeley National Laboratory.
- Hunn, B.D., J.W. Jones, M.M. Grasso, and D.D. Hitzfelder. 1990. Effect of Shading Devices on Building Energy Use and Peak Demand in Minnesota. PB-93-159010/XAB. Austin, TX: University of Texas.
- Intergovernmental Panel on Climate Change (IPCC). 2007. Summary for Policymakers. In B. Metz, O.R. Davidson, P.R. Bosch, R. Dave, L.A. Meyer (Eds.), *Climate Change 2007: Mitigation of Climate Change* (pp. 1-24). New York, NY: Cambridge University Press.
- Intermediate Technology Development Group (ITDG). 2008. Rainwater Harvesting: Technical Note. Intermediate Technology Development Group. [http://www.itdg.org/html/technical\\_enquiries/docs/rainwater\\_harvesting.pdf](http://www.itdg.org/html/technical_enquiries/docs/rainwater_harvesting.pdf) (accessed July, 30, 2009).
- International Code Council (ICC). 1999. *2000 International Energy Conservation Code*. Falls Church, VA: International Code Council, Inc.
- International Code Council (ICC). 2001. *2001 Supplement to the International Energy Conservation Code*. Falls Church, VA: International Code Council, Inc.
- International Code Council (ICC). 2003. *2003 International Energy Conservation Code*. Country Club Hills, IL: International Code Council, Inc.
- International Code Council (ICC). 2004. *2004 Supplement to the International Energy Conservation Code*. Country Club Hills, IL: International Code Council, Inc.
- International Code Council (ICC). 2006. *2006 International Energy Conservation Code*. Country Club Hills, IL: International Code Council, Inc.
- Johnson, D., and E. Wyatt. 1997. Dampers, Reclaimers and Pumps-Oh My!. *Home Energy Magazine* 14(4):31-35.
- Jones, R.W. (ed.), J.D. Balcomb, C.E. Kosiewicz, G.S. Lazarus, R.D. McFarland, and W.O. Wray. 1982. *Passive Solar Design Handbook, Volume 3. Passive Solar Design Analysis*. Los Alamos, NM: Los Alamos National Laboratory.

- Judkoff, R., and J. Neymark. 1995. International Energy Agency Building Energy Simulation Test (BESTEST) and Diagnostic Method. NREL/TP-472-6231. Golden, CO: National Renewable Energy Laboratory.
- Kim, R., S. Lee, and J. Kim. 2005. Application of a Metal Membrane for Rainwater Utilization: Filtration Characteristics and Membrane Fouling. *Desalination* 177(1-3):121-132.
- King, D.L., J.K. Dudley, and W.E. Boyson. 1996. PVSIM: A Simulation Program for Photovoltaic Cells, Modules, and Arrays. *Proceedings of the 25th IEEE Photovoltaic Specialists Conference*:1295-1297.
- Kissock, J.K., J.S. Haberl, and D.E. Claridge. 2003. Inverse Modeling Toolkit: Numerical Algorithms. *ASHRAE Transactions* 109(2):424-434.
- Klein, S.A. 1973. TRNSYS - A Transient Simulation Program. Rept. 3. Madison, WI: Solar Energy Laboratory, University of Wisconsin-Madison.
- Klein, S.A. 1976. A Design Procedure for Solar Heating Systems. Ph.D. Dissertation, University of Wisconsin-Madison.
- Klein, S.A., and W.A. Beckman. 1983. *PV F-Chart User's Manual: DOS Version*. Middletown, WI: F-Chart Software.
- Klein, S.A. and W.A. Beckman. 1993a. F-Chart User's Manual: Windows Version. F-Chart Software. <http://www.fchart.com/>.
- Klein, S.A. and W.A. Beckman. 1993b. PV F-Chart User's Manual: Windows Version. F-Chart Software. <http://www.fchart.com/>.
- Klein, S.A., W.A. Beckman, and J.A. Duffie. 1976. TRNSYS - A Transient Simulation Program. *ASHRAE Transactions* 82(I):623-633.
- Klien, S.A., W.A. Beckman, J.W. Mitchell, J.A. Duffie, N.A. Duffie, T.L. Freeman, J.C. Mitchell, J.E. Braun, B.L. Evans, J.P. Kummer, R.E. Urban, A. Fiksel, J.W. Thornton, N.J. Blair, P.M. Williams, D.E. Bradley, T.P. McDowell, and M. Kummert. 2004. *TRNSYS 16 – A TRAnSient SYstem Simulation Program, User Manual*. Madison, WI: Solar Energy Laboratory, University of Wisconsin-Madison.
- Krauter, S.C.W. 2006. *Solar Electric Power Generation: Photovoltaic Energy Systems*. Berlin, Germany: Springer-Verlag.
- Kreider, J.F., and F. Kreith. 1982. *Solar Heating and Cooling: Active and Passive Design*. 2nd ed. Washington, DC: Hemisphere Publishing Corporation.
- Kusuda, T. 1974. NBSLD - Computer Program for Heating and Cooling Loads in Buildings. NBSIR 74-574. Washington, DC: National Bureau of Standards.
- Kusuda, T. 1976. NBSLD - Computer Program for Heating and Cooling Loads in Buildings. Building Science Series 69. Washington, DC: National Bureau of Standards.
- Kutscher, C.F., ed. 2007. *Tackling Climate Change in the U.S.: Potential Carbon Emissions Reductions from Energy Efficiency and Renewable Energy by 2030*. American Solar Energy Society. [http://ases.org/images/stories/file/ASES/climate\\_change.pdf](http://ases.org/images/stories/file/ASES/climate_change.pdf) (accessed July 30, 2009).
- Lechner, N. 2001. *Heating, Cooling, Lighting: Design Methods for Architects*. 2nd ed. New York, NY: John Wiley & Sons, Inc.

- Liu, B.Y.H., and R.C. Jordan. 1963. The Long-Term Average Performance of Flat-Plate Solar Energy Collectors. *Solar Energy* 7(2):53-74.
- Liu, Z., J. Mukhopadhyay, M. Malhotra, J. Haberl, D. Gilman, C. Montgomery, K. McKelvey, C. Culp, and B. Yazdani. 2008. Methodology for Residential Building Energy Simulations Implemented in the International Code Compliance Calculator (IC3). *Sixteenth Symposium of Improving Building Systems in Hot and Humid Climates*, December 16-17, Dallas/Plano, TX.
- Lstiburek, J. 2000. *Builder's Guide to Hot-Humid Climates*. Westford, MA: Building Science Corporation.
- Lutz, J. 2005. Estimating Energy and Water Losses in Residential Hot Water Distribution Systems. LBNL-57199. Berkeley, CA: Lawrence Berkeley National Laboratory.
- Lutz, J., C.D. Whitehead, A. Lekov, D. Winiarski, and G. Rosenquist. 1998. WHAM: A Simplified Energy Consumption Equation for Water Heaters. *Proceedings of the 1998 ACEEE Summer Study on Energy Efficiency in Buildings* 1:171-183.
- Marion, B., M. Anderberg, and P. Gray-Hann. 2005. Recent Revisions to PVWATTS. NREL/CP-520-38975. Golden, CO: National Renewable Energy Laboratory.
- Mayer, P.W., and W.B. DeOreo. 1999. *Residential End Uses of Water*. Denver, CO: American Water Works Association Research Foundation.
- Mayfield, J., 2000. Snapshots of Shading Options. *Home Energy Magazine* 17(5):20-23.
- Mazria, E., 2003. It's the Architecture, Stupid!. *Solar Today* (May/June):48-50.
- Mazria, E., and K. Kershner. 2008. The 2030 Blueprint: Solving Climate Change Saves Billions. 2030 Inc./Architecture 2030. <http://www.architecture2030.org/pdfs/2030Blueprint.pdf> (accessed July 30, 2009).
- McFarland, R.D. 1978. PASOLE: A General Simulation Program for Passive Solar Energy. LA-7433-MS. Las Alamos, NM: Las Alamos National Laboratory.
- McMahon, T.A., and R.G. Mein. 1978. Preface (Reservoir Capacity and Yield). *Development in Water Science* 9(1978):iii-v.
- Menicucci, D.F. 1985. PVFORM: A New Approach to Photovoltaic System Modeling. *Proceedings of the 18th IEEE Photovoltaic Specialists Conference*:1614-1619.
- Menicucci, D.F., and J. Fernandez. 1988. User's Manual for PVFORM: A Photovoltaic System Simulation Program for Stand-Alone and Grid-Interactive Applications. SAND85-0376. Albuquerque, NM: Sandia National Laboratories.
- Miller, W.A., K.T. Loye, A.O. Desjarlais, and R.P. Blonski. 2002. Cool Roofs with Complex Inorganic Color Pigments. *Proceedings of the 2002 ACEEE Summer Study on Energy Efficiency in Buildings* 1:195-206.
- Mitalas, G.P. and D.G. Stephenson. 1967. Room Thermal Response Factors. *ASHRAE Transactions* 73(2):1-7.
- Moran, P.A.P. 1959. *The Theory of Storage*. London: Methuen.

- Mother Earth News. 1984. Retrofit Catalytic Converters. *Mother Earth News: Do it Yourself*. November/December. <http://www.motherearthnews.com/Do-It-Yourself/1984-11-01/Retrofit-Catalytic-Converters.aspx> (accessed July 30, 2009).
- NASA. 2008. NASA Surface Meteorology and Solar Energy Dataset. <http://eosweb.larc.nasa.gov/sse/> (accessed July, 30, 2009).
- National Oceanic and Atmospheric Administration (NOAA). 2008. Quality Controlled Local Climatological Data. National Climatic Data Center (NCDC). <http://cdo.ncdc.noaa.gov/ulcd/ULCD> (accessed December 15, 2008).
- National Oceanic and Atmospheric Administration (NOAA). 2009. Boulder Wind Info. Earth System Research Laboratory, Physical Science Division. <http://www.esrl.noaa.gov/psd/boulder/wind.html> (accessed July 30, 2009).
- National Renewable Energy Laboratory (NREL). 2003. A Consumer's Guide: Heat Your Water with the Sun. DOE/GO-102003-1824. Washington, DC: U.S. Department of Energy, Energy Efficiency and Renewable Energy.
- National Renewable Energy Laboratory (NREL). 2004. HOMER: The Micropower Optimization Model: Innovation for Our Energy Future. NREL/FS-710-35406. Washington, DC: U.S. Department of Energy, Energy Efficiency and Renewable Energy.
- National Renewable Energy Laboratory (NREL). 2005. Small Wind Electric Systems: A U.S. Consumer's Guide. DOE/GO-102005-2095. Washington, DC: U.S. Department of Energy, Energy Efficiency and Renewable Energy.
- National Renewable Energy Laboratory (NREL). 2007. PVWATTS: A Performance Calculator for Grid-Connected PV Systems. U.S. Department of Energy, Energy Efficiency and Renewable Energy. [http://rredc.nrel.gov/solar/codes\\_algs/PVWATTS/](http://rredc.nrel.gov/solar/codes_algs/PVWATTS/).
- National Renewable Energy Laboratory (NREL). 2008. Dynamic Maps, GIS Data, & Analysis Tools: Solar Maps. <http://www.nrel.gov/gis/solar.html> (accessed July 30, 2009).
- National Small Flow Clearinghouse (NSFC). 1995. Inspections: From the State Regulations. WWPCRG40. Morgantown, WV: National Small Flows Clearinghouse.
- Noll, S., and W.O. Wray. 1978. A Microeconomic Approach to Passive Solar Design - Performance, Cost, Optimal Sizing and Comfort Analysis. *Energy* 4:575-591.
- Nutt, B.B. 1994. The Use and Management of Passive Solar Environments. *Renewable Energy* 5(5-8):1009-1014.
- Pacific Northwest Laboratory (PNL). 2009. Energy Codes Climate Zones. Article #1420. <http://resourcecenter.pnl.gov/cocoon/morf/ResourceCenter/article/1420> (accessed July 30, 2009).
- Pahl, G. 2007. *The Citizen-powered Energy Handbook: Community Solutions to a Global Crisis*. White River Junction, VT: Chelsea Green Publishing Company.
- Peel, M.C., B.L. Finlayson, and T.A. McMahon. 2007. Updated World Map of the Köppen-Geiger Climate Classification. *Hydrology and Earth System Sciences* 11:1633-1644.
- Perez, R. 1984. An Anisotropic Model of Diffuse Solar Radiation with Applications to an Optimization of Compound Parabolic Concentrators. USDOE #DEFG0577ET20182. Albany, NY: Atmospheric Sciences Research Center, State University of New York at Albany.



- Pletzer, R.K., J.W. Jones, and B.D. Hunn. 1988. Effect of Shading Devices on Residential Energy Use in Austin, Texas. PB-89-184428/XAB. Austin, TX: University of Texas.
- PRISM Group. 2006. Precipitation: Annual Climatology (1971-2000). PRISM Group, Oregon State University. <http://prism.oregonstate.edu/products/matrix.phtml?vartype=tmax&view=maps> (accessed July 30, 2009).
- Ramlow, B., and B. Nusz. 2006. *Solar Water Heating: A Comprehensive Guide to Solar Water and Space Heating Systems*. Gabriola Island, BC, Canada: New Society Publishers.
- RESNET. 2007. Procedures for Verification of International Energy Conservation Code Performance Path Calculation Tools. RESNET Publication No. 07-003. Residential Energy Services Network, Inc. <http://www.natresnet.org/standards/iecc/procedures.pdf> (accessed July 30, 2009).
- Reynolds, M.E. 1991. *Earthship: Systems and Components, Vol. 2*. Earthship Biotechnology.
- Roaf, S., M. Fuentes, and S. Thomas. 2007. *Ecohouse: A Design Guide*. 3rd ed. Oxford, UK: Elsevier.
- Rocky Mountain Institute (RMI). 1995. Windows. Home Energy Briefs #2. <http://www.p2pays.org/ref/32/31141.pdf> (accessed July 30, 2009).
- Rocky Mountain Institute (RMI). 2004. Water Heating. Home Energy Briefs #5. [http://www.rmi.org/images/PDFs/HEBs/E04-15\\_HEB5\\_WaterHeat.pdf](http://www.rmi.org/images/PDFs/HEBs/E04-15_HEB5_WaterHeat.pdf) (accessed July 30, 2009).
- Rogers, A. 2009. Do Wind Turbines Really Kill Birds? *Mother Earth News*. <http://www.motherearthnews.com/Renewable-Energy/Do-Wind-Turbines-Kill-Birds.aspx> (accessed July 30, 2009).
- Rosen, N. 2007. *How to Live Off-grid: Jjourney Outside the System*. London, UK: Doubleday.
- Russel, S. 2004. Solar-Electric Systems Simplified. *Home Power Magazine* 104(December/January):72-78.
- Rutkowski, H. 2004. *Manual J: Residential Load Calculation*. 8th ed. Arlington, VA: Air Conditioning Contractors of America.
- Sagrillo, M. 2008. Wind Power: Are Vertical axis Turbines Better? *Mother Earth News* (February/March). <http://www.motherearthnews.com/Renewable-Energy/2008-02-01/Wind-Power-Horizontal-and-Vertical-Axis-Wind-Turbines.aspx> (accessed July 30, 2009).
- Schultheis, R.A. 1997. Septic Tank/Soil Absorption Field Systems: A Homeowner's Guide to Installation and Maintenance. Water Quality Initiative Publication WQ 401. Revised March 15, 1997. University of Missouri Cooperative Extension Service.
- Simmons, G., V. Hope, G. Lewis, J. Whitmore, and W. Gao. 2001. Contamination of Potable Roof-collected Rainwater in Auckland, New Zealand. *Water Research* 35(6):1518-1524.
- Socolow, R.H., and S.W. Pacala. 2006. A Plan to Keep Carbon in Check. *Scientific American* 295(3):50-57.
- Solar Rating and Certification Corporation (SRCC). 2008. Glazed Collector Rating Listings. <http://www.solar-rating.org/ratings/ratings.htm> (accessed July 30, 2009).
- Southwest Wind Power. 2009a. Whisper 500TM Wind Turbine. [http://www.windenergy.com/products/whisper\\_500.htm](http://www.windenergy.com/products/whisper_500.htm) (accessed July 30, 2009).

- Southwest Wind Power. 2009b. Skystream 3.7 Wind Turbine. <http://www.skystreamenergy.com/> (accessed July 30, 2009).
- Stansbury, J., and E. Flattau. 1975. Dream House: Tiny Building with Giant Potential. *The Free Lance-Star* 91(120). Fredericksburg, VA.
- Stein, B., and J.S. Reynolds. 2000. *Mechanical and Electrical Equipment for Buildings*. 9th ed. New York, NY: John Wiley & Sons, Inc.
- Stephenson, D.G., and Mitalas, G.P. 1967. Cooling Load Calculations by Thermal Response Factor Method. *ASHRAE Transactions* 73(1):1-7.
- Structural Insulated Panel Association (SIPA). 2004. Technical Info. <http://www.sips.org/content/technical/index.cfm?pageId=21> (accessed July 30, 2009).
- Sylvester, K.E., and J.S. Haberl. 2001. Analysis of the Benefits of Photovoltaic in High Rise Commercial Buildings. ESL-HH-00-05-49. College Station, TX: Energy Systems Laboratory, Texas A&M University.
- Torcellini, P., and D.B. Crawley. 2006. Understanding Zero-Energy Buildings. *ASHRAE Journal* 48:62-65
- Torcellini, P., S. Pless, M. Deru, and D. Crawley. 2006. Zero Energy Buildings: A Critical Look at the Definition. *Proceedings of the 2006 ACEEE Summer Study on Energy Efficiency in Buildings* 3:275-276.
- U.S. Census Bureau. 2009. Characteristics of New Housing for 2008. <http://www.census.gov/const/www/charindex.html> (accessed July 30, 2009).
- U.S. Department of Agriculture (USDA). 2008. Precipitation: Annual Climatology (1961-1990). USDA-NRCS National Water and Climate Center. <http://www.wcc.nrcs.usda.gov/climate/prism.html> (accessed July 30, 2009).
- U.S. Department of Energy (US DOE). 1999. Codes and Standards: The Model Energy Code. DOE/GO-10099-934. Washington, DC: Energy Information Administration, U.S. Department of Energy.
- U.S. Department of Energy (US DOE). 2000. Advanced Wall Framing. Office of Building Technology, State and Community Programs (BTS) Technology Fact Sheet. DOE/GO-102000-0770. Washington, DC: Energy Information Administration, U.S. Department of Energy.
- U.S. Department of Energy (US DOE). 2006. New World Record Achieved in Solar Cell Technology. *News Archive*. <http://www.energy.gov/news/4503.htm> (accessed July 30, 2009).
- U.S. Department of Energy (US DOE). 2007. High-Performance Home Technologies: Guide to Determining Climate Regions by County. Building America Best Practices Series. Energy Efficiency and Renewable Energy, U.S. Department of Energy. [http://apps1.eere.energy.gov/buildings/publications/pdfs/building\\_america/climate\\_region\\_guide.pdf](http://apps1.eere.energy.gov/buildings/publications/pdfs/building_america/climate_region_guide.pdf).
- U.S. Department of Energy (US DOE). 2008a. Building Tools Directory. Building Technologies Program. [http://www.eere.energy.gov/buildings/tools\\_directory/](http://www.eere.energy.gov/buildings/tools_directory/).
- U.S. Department of Energy (US DOE). 2008b. HBLC. Building Energy Software Tools Directory. [http://apps1.eere.energy.gov/buildings/tools\\_directory/software.cfm/ID=61/pagename=alpha\\_list](http://apps1.eere.energy.gov/buildings/tools_directory/software.cfm/ID=61/pagename=alpha_list) (accessed July 30, 2009).

- U.S. Department of Energy (US DOE). 2008c. EnergyPlus Energy Simulation Software. Weather Data. [http://apps1.eere.energy.gov/buildings/energyplus/cfm/weather\\_data.cfm](http://apps1.eere.energy.gov/buildings/energyplus/cfm/weather_data.cfm) (accessed July 30, 2009).
- U.S. Department of Energy (US DOE). 2009a. Solar Decathlon. <http://www.solardecathlon.org>.
- U.S. Department of Energy (US DOE). 2009b. *Building Energy Databook*. Energy Efficiency and Renewable Energy, U.S. Department of Energy. <http://buildingsdatabook.eren.doe.gov/>.
- U.S. Department of Energy (US DOE). 2009c. Operating Your System Off-grid. U.S. Department of Energy: Energy Efficiency and Renewable Energy. [http://www.energysavers.gov/your\\_home/electricity/index.cfm/mytopic=10610](http://www.energysavers.gov/your_home/electricity/index.cfm/mytopic=10610) (accessed July 30, 2009).
- U.S. Energy Information Administration (US EIA). 1994. Biomass Energy Resource Hierarchy. In *Estimates of U.S. Biomass Energy Consumption 1992*. DOE/EIA-0548(92). Washington, DC: U.S. Department of Energy.
- U.S. Energy Information Administration (US EIA). 2008a. Greenhouse Gases, Climate Change and Energy. DOE/EIA-X012. Washington, DC: Energy Information Administration.
- U.S. Energy Information Administration (US EIA). 2008b. Energy Consumption by Sector. In *Annual Energy Review 2007*. DOE/EIA-0384(2007). Washington, DC: Energy Information Administration.
- U.S. Energy Information Administration (US EIA). 2008c. *Carbon Dioxide Emissions in Emissions of Greenhouse Gases in the United States 2007*. DOE/EIA-0573(2007). Washington, DC: Energy Information Administration.
- U.S. Energy Information Administration (US EIA). 2009. Average Heat Content of Selected Biomass Fuels. In *Renewable Energy Annual, 2007*. [http://www.eia.doe.gov/cneaf/solar.renewables/page/rea\\_data/rea\\_sum.html](http://www.eia.doe.gov/cneaf/solar.renewables/page/rea_data/rea_sum.html) (accessed July 30, 2009).
- U.S. Environmental Protection Agency (US EPA). 2002. *Onsite Wastewater Treatment Systems Manual*. EPA/625/R-00/008. Office of Water, Office of Research and Development.
- U.S. Environmental Protection Agency (US EPA). 2006. Climate Change Glossary: Fossil Fuel Terminology Services. <http://www.epa.gov/trs/> (accessed July 30, 2009).
- Vale, B., and R. Vale. 1975. *The Autonomous House: Design and Planning for Self-sufficiency*. New York, NY: Universe Books.
- Vale, B., and R. Vale. 2000. *The New Autonomous House: Design and Planning for Sustainability*. New York, NY: Thames & Hudson.
- VanderWerf P.A., S.J. Feige, P. Chammas, and L.A. Lemay. 1997. *Insulating Concrete Forms for Residential Design and Construction*. New York, NY: McGraw-Hill.
- Vickers, A. 2001. *Handbook of Water Use and Conservation*, 1st ed. Amherst, MA: WaterPlow Press.
- Vliet, G. 2007. Solar-Based Mechanical Systems for Zero-Energy Buildings. Seminar 52 - ASHRAE and ASES Views on Solar Utilization in Zero-Energy Footprint Buildings. *2007 ASHRAE Winter Meeting*, January 27-31, Dallas, TX.
- Wald, M. L. 2008. For Carbon Emissions, a Goal of Less Than Zero. *The New York Times*. [http://www.nytimes.com/2008/03/26/business/businessspecial2/26negative.html?\\_r=1&adxnnl=1&oref=slogin&adxnnlx=1210842102-UJ0VMnY8gg](http://www.nytimes.com/2008/03/26/business/businessspecial2/26negative.html?_r=1&adxnnl=1&oref=slogin&adxnnlx=1210842102-UJ0VMnY8gg) (accessed July 30, 2009).

- Webb, R. 2005. Sustaining Technology. *Architectural Design* 75(2):70-77.
- Wenham, S.R., M.A. Green, M.E. Watt, and R. Corkish. 2007. *Applied Photovoltaics*. 2nd ed. London; Sterling, VA: Earthscan.
- Wiehagen, J., and J.L.Sikora. 2003. Performance Comparison of Residential Hot Water Systems. NREL/SR-550-32922. Upper Marlboro, MD: NAHB Research Center, Inc.
- Wiles, J. 2001. Photovoltaic Power Systems and the National Electric Code: Suggested Practices. SAND2001-0674. Albuquerque, NM: Sandia National Laboratories.
- Wind Energy Solutions. 2009. WES5 Tulipo Wind Turbine. <http://www.windenergysolutions.nl/products/wes5-tulipo/> (accessed July 30, 2009).
- Winkelmann, F.C., B.E. Birdsall, W.F. Buhl, K.L. Ellington, A.E. Erdem, J.J.Hirsch, and S. Gates. 1993. *DOE-2 Supplement, Version 2.1e*. LBL-34947. Berkeley, CA: Regents of the University of California, Lawrence Berkley Laboratory.
- Woofenden, I. 2005. Wind Electric Systems Simplified. *Home Power Magazine* 110:10-17.
- Woofenden, I. 2007a. Renewable... Priorities: Ordering RE Possibilities. *Home Power Magazine* 122:110-111.
- Woofenden, I. 2007b. Ask the Experts: Off-Grid Appliances. *Home Power Magazine* 118:124-125.
- Yakubu, G.S. 1996. The Reality of Living in Passive Solar Homes: A User-experience Study. *Renewable Energy* 8(1-4):177-181.
- Yde, L. 1996. The Plus-Energy House in Denmark. *Sustainable Energy News* 13(June):14-15.
- Yaziz, M.I., H. Gunting, N. Sapari, and A.W. Ghazali. 1989. Variations in Rainwater Quality from Roof Catchments. *Water Research* 23(6):761-765.
- Zhu, K., L. Zhang, W. Hart, M. Liu, and H. Chen. 2004. Quality Issues in Harvested Rainwater in Arid and Semi-arid Loess Plateau of Northern China. *Journal of Arid Environments* 57(4):487-507.

## **APPENDIX A**

### **SIMULATION CAPABILITIES ADDED TO THE DOE-2.1E INPUT**

For this study, a residential simulation model “RES.INP v3.00.10” developed by the Energy Systems Laboratory (ESL) was used, which simulates a single-family house as a single-zone building. This model uses parameters for various building and system characteristics, which can be assigned different values using external DOE-2 include file (Liu et al. 2008). In order to incorporate additional simulation capabilities for this study, including modeling of : i) night insulation over windows, ii) maximum solar controlled interior shading, and iii) domestic hot water tank standby loss. The night insulation over windows was considered for climates with very low temperatures during the winter night. The maximum solar controlled interior shading was considered for hot climates. The modeling capability of standby losses from the DHW tank was incorporated using the Water Heater Analysis Model (WHAM) (Lutz et al. 1998), in order to have a better estimation of energy use reduction from using a more efficient DHW system for the backup.

## A-1. Night Insulation over Windows

```

$ c19 NIGHT INSULATION OVER WINDOWS, USED WITH TEMP. THRESHOLD TEMP VALUE (FIXED AT 40F)

##SET1 P-NIGHTINS c19

##SET1 WINDOWCON-1 #[1 / #[[1 / P-WINDOWU-1[[]] - 0.197]]]
##SET1 CONDMULT-1 #[1 / #[1 + #[P-NIGHTINS[[]] * WINDOWCON-1[[]]]]]

##SET1 WINDOWCON-234 #[1 / #[[1 / P-WINDOWU-234[[]] - 0.197]]]
##SET1 CONDMULT-234 #[1 / #[1 + #[P-NIGHTINS[[]] * WINDOWCON-234[[]]]]]

COND-SCH1-S = SCHEDULE
             THRU DEC 31 (ALL) (1,24) (CONDMULT-1[[]]) ..

COND-SCH1-EWN = SCHEDULE
              THRU DEC 31 (ALL) (1,5) (CONDMULT-234[[]]) (6,22) (1) (23,24) (CONDMULT-234[[]]) ..

COND-TSCH1-S = SCHEDULE THRU DEC 31 (ALL) (1,24) (40) ..
COND-TSCH1-EWN = SCHEDULE THRU DEC 31 (ALL) (1,24) (40) ..

WINDOW1-1 = WINDOW
           HEIGHT = GLASSHT1-1[[]]
           WIDTH = GLASSWID1-1[[]]
           GLASS-TYPE = GLASS-1
           X = #[WX1-1[[]] + FR-EQW1-1[[]]]
           Y = #[WINDOWY1-1[[]] + FR-EQW1-1[[]]]
           FRAME-WIDTH = FR-EQW1-1[[]]
           CONDUCT-SCHEDULE = COND-SCH1-S
           OVERHANG-A = WX1-1[[]]
           OVERHANG-B = OVERHANGHT1-1[[]]
           OVERHANG-W = OVERHANGWID1-1[[]]
           OVERHANG-D = P-OVERHANGD1-1[[]]
           ..

```

## A-2. Maximum Solar Controlled Interior Shading

```

##SET1 P-INTSHADE s09          $ SWITCH FOR INTERIOR SHADING SCHEDULE
##SET1 P-SOLARCONTROL s10     $ BTU/H-FT2, MAX DIRECT RADIATION OVER WINDOWS TO PULL DRAPES
                                $ TO BE USED WITH SHADING MULTIPLIERS IN DDP

$ MAXSOLARCONTROL (WORKS WITH P-SOLARCONTROL IN BTU/H-FT2 AND SHADING MULTIPLIER VALUES IN DDP)

MAXSOL-SCH1 = SCHEDULE THRU DEC 31 (ALL) (1,24) (P-SOLARCONTROL[]) ..
                                $ MODIFY INTERIOR SHADING VALUES IN DDP FOR SUMMER AND WINTER

SET-DEFAULT FOR WINDOW

##IF #[P-INTSHADE[] EQS Y]
SHADING-SCHEDULE = SH-1          $ SHADING SCHEDULE FOR THE WINDOW SHADE
##ENDIF

MAX-SOLAR-SCH = MAXSOL-SCH1     $ PROVIDES RADIATION FLUX INCIDENT ON THE WINDOW DURING THE YEAR
WIN-SHADE-TYPE = MOVABLE-EXTERIOR
CONDUCT-SCHEDULE = COND-SCH1-EWN
CONDUCT-TMIN-SCH = COND-TSCH1-EWN $ OUTSIDE DBT BELOW WHICH SHADES WILL BE DEPLOYED

```

### A-3. Domestic Water Heater Standby Loss

```

PLANT-1 = PLANT-ASSIGNMENT
        FUNCTION = (*DHWLOSS_FUNCTION*,*NONE*)

FUNCTION NAME = DHWLOSS_FUNCTION ..

ASSIGN  MON=IMO
        DAY=IDAY
        HR=IHR
        DHWEF=P-DHWEF[]
        DHWRE=P-DHWRE[]
        DHWCAP=P-DHWCAP[]
        TDHWAMB=P-DHWAMB[]
T:CONST.TEMP.ENVIRONMENT)
        $ 0:UGSPACE,1:ROOM,2:ATTIC,ELSE
TSUPPLY=120
TTANK=120
TRETURN = XXX24
TATTIC = XXX25
TUGSPACE = XXX28
TMAINST=SCHEDULE-NAME (DHWINLETSCH-1)
TNKSIZE=P-DHW-SIZE[]
DHWGPM=DHW-GAL/MIN
DHSCH=SCHEDULE-NAME (DHSCH-1)
LOSSF=DHW-LOSS
        $ DHW-LOSS IN PLANT ASSIGNMENT (FRACTION OF TANK HEAT STORAGE CAPACITY)
..

CALCULATE ..

C      CALCULATE TANK UA USING WHAM MODEL

        UA1=(1/DHWEF)-(1/DHWRE)
        UA2=67.5*(24/41094-1/(DHWRE*DHWCAP))
        UA=UA1/UA2

C      CALCULATE LOAD AND TANK HEAT STORAGE CAPACITY

        DHWGPH=DHWGPM*DHSCH*60
        DHWLOAD=8.341*DHWGPH*(TSUPPLY-TMAINST)
        TNKCAP=8.341*TNKSIZE*(TSUPPLY-TMAINST)

C      ASSIGN HOURLY DHW AMBIENT TEMPERATURE (ONLY IF, NOT GIVEN AS A CONSTANT TEMPERATURE VALUE)

        IF (TDHWAMB .EQ. 2) TDHWAMB = TATTIC
        IF (TDHWAMB .EQ. 2) GOTO 25

        IF (TDHWAMB .EQ. 1) TDHWAMB = TRETURN
        IF (TDHWAMB .EQ. 1) GOTO 25

        IF (TDHWAMB .EQ. 0) TDHWAMB = TUGSPACE
        IF (TDHWAMB .EQ. 0) GOTO 25

C      CALCULATE HOURLY DHW-LOSS (FRACTION OF TANK HEAT STORAGE CAPACITY)

25     LOSS1=UA*(TTANK-TDHWAMB)
        LOSS2=DHWLOAD/(DHWRE*DHWCAP)
        LOSS3=DHWRE/TNKCAP
        LOSSF=LOSS1*(1-LOSS2)*LOSS3

        PRINT 26,
+ MON, DAY, HR, TDHWAMB, TMAINST, LOSSF
26     FORMAT
+ (3F3.0, ' ',F5.1,' ',F5.1,' ',F5.3)

        CONTINUE
        END

END-FUNCTION ..

```



**APPENDIX B**  
**ESTIMATION OF DOMESTIC HOT WATER ENERGY USE**

First, the base-case domestic hot water use by end-use ( $V_{\text{mixed},N}$ ) was calculated for a four bedroom house, which adds up to a 23.3 gal/day hot water use at 120 °F and a 70.0 gal/day hot water use at 105 °F (as shown in Table B-1). Next, the monthly average water mains temperature ( $T_{\text{mains}}$ ) were calculated for an average day of each month using Equation B-1, which takes into account the impact of location and time of year. Finally, the monthly average daily domestic hot water use ( $V_{\text{supply}}$ ) at 120 °F supply temperature ( $T_{\text{supply}} = 120$  °F), was calculated for each location using Equation B-2. This equation accounts for the use of cold water at mains temperature ( $T_{\text{mains}}$ ) to achieve the required mixed temperature ( $T_{\text{mixed},N}$ ) for various hot water end uses.

*Table B- 1 Domestic Hot Water Consumption by End-use<sup>1</sup>*

End Use	End-Use Water Temperature	Water Usage (gal/day) <sup>2</sup>	Base-case Water Usage <sup>3</sup> (gal/day)	Total ( $V_{\text{mixed},N}$ ) (gal/day)
Clothes Washer	120°F	$7.5 + 2.50 * N_{\text{br}}$ (Hot Only)	17.50	$V_{\text{mixed},120^\circ\text{F}} = 23.3$
Dishwasher	120°F	$2.5 + 0.83 * N_{\text{br}}$ (Hot Only)	5.83	
Shower	105°F	$14.0 + 4.67 * N_{\text{br}}$ (Hot + Cold)	32.68	$V_{\text{mixed},105^\circ\text{F}} = 70.0$
Bath	105°F	$3.5 + 1.17 * N_{\text{br}}$ (Hot + Cold)	8.18	
Sinks	105°F	$12.5 + 4.16 * N_{\text{br}}$ (Hot + Cold)	29.14	

<sup>1</sup> Source: Hendron (2008)

<sup>2</sup>  $N_{\text{br}}$  = Number of bedrooms

<sup>3</sup> Calculated for  $N_{\text{b}} = 4$

$$\text{Equation B- 1: } T_{\text{mains}} = (T_{\text{amb,avg}} + \text{offset}) + \text{ratio} * (\Delta T_{\text{amb,max}} / 2) * \sin(0.986 * (\text{day\#} - 15 - \text{lag}) - 90)$$

$$\text{Equation B- 2: } V_{\text{supply}} = \Sigma [V_{\text{mixed,N}} * (T_{\text{mixed,N}} - T_{\text{mains}}) / (T_{\text{supply}} - T_{\text{mains}})], \text{ summed over } N$$

where

$T_{\text{mains}}$	= mains temperature to domestic hot-water tank (°F)
$T_{\text{amb,avg}}$	= annual average ambient air temperature (°F)
$\Delta T_{\text{amb,max}}$	= maximum difference between monthly average ambient temperatures (°F)
0.986	= degrees/day (360/365)
day#	= Julian day of the year (1-365), or = 30*month# - 15 (for average monthly calculations), where month# = month of the year (1-12)
offset	= 6°F
ratio	= 0.4 + 0.01 ( $T_{\text{amb,avg}} - 44$ )
lag	= 35 - 1.0 ( $T_{\text{amb,avg}} - 44$ )
$T_{\text{supply}}$	= hot water supply temperature from domestic hot-water tank (°F)
$T_{\text{mixed,N}}$	= mixed water temperature for N <sup>th</sup> end-use (°F)
$V_{\text{supply}}$	= hot water supply volume at $T_{\text{supply}}$ from domestic hot-water tank (gal/day)
$V_{\text{mixed,N}}$	= mixed water volume at $T_{\text{mixed,N}}$ used for N <sup>th</sup> end-use (gal/day)

Thus, for  $T_{\text{supply}} = 120$  °F, the monthly average daily domestic hot water use ( $V_{\text{supply,120°F}}$ , in gal/day) and domestic water heating loads ( $Q_{\text{supply,120°F}}$ , in Btu/day) can be calculated using the following equations, where the water mains temperature ( $T_{\text{mains}}$ ) were calculated using Equation B-1 for an average day of each month:

$$\begin{aligned} V_{\text{supply,120°F}} &= 23.3 + 70.0 * (105 - T_{\text{mains}}) / (120 - T_{\text{mains}}) \\ Q_{\text{supply,120°F}} &= \rho V C_p (T_{\text{supply}} - T_{\text{mains}}) \\ &= 8.34 * [23.3 + 70.0 * (105 - T_{\text{mains}}) / (120 - T_{\text{mains}})] * 1 * (120 - T_{\text{mains}}) \\ &= 8.34 * (10,146 - 93.3 * T_{\text{mains}}) \end{aligned}$$

The calculated water mains temperature and hot water supply volume for the six locations are plotted in Figure B-1, which were used for the determining the base-case domestic hot water load.

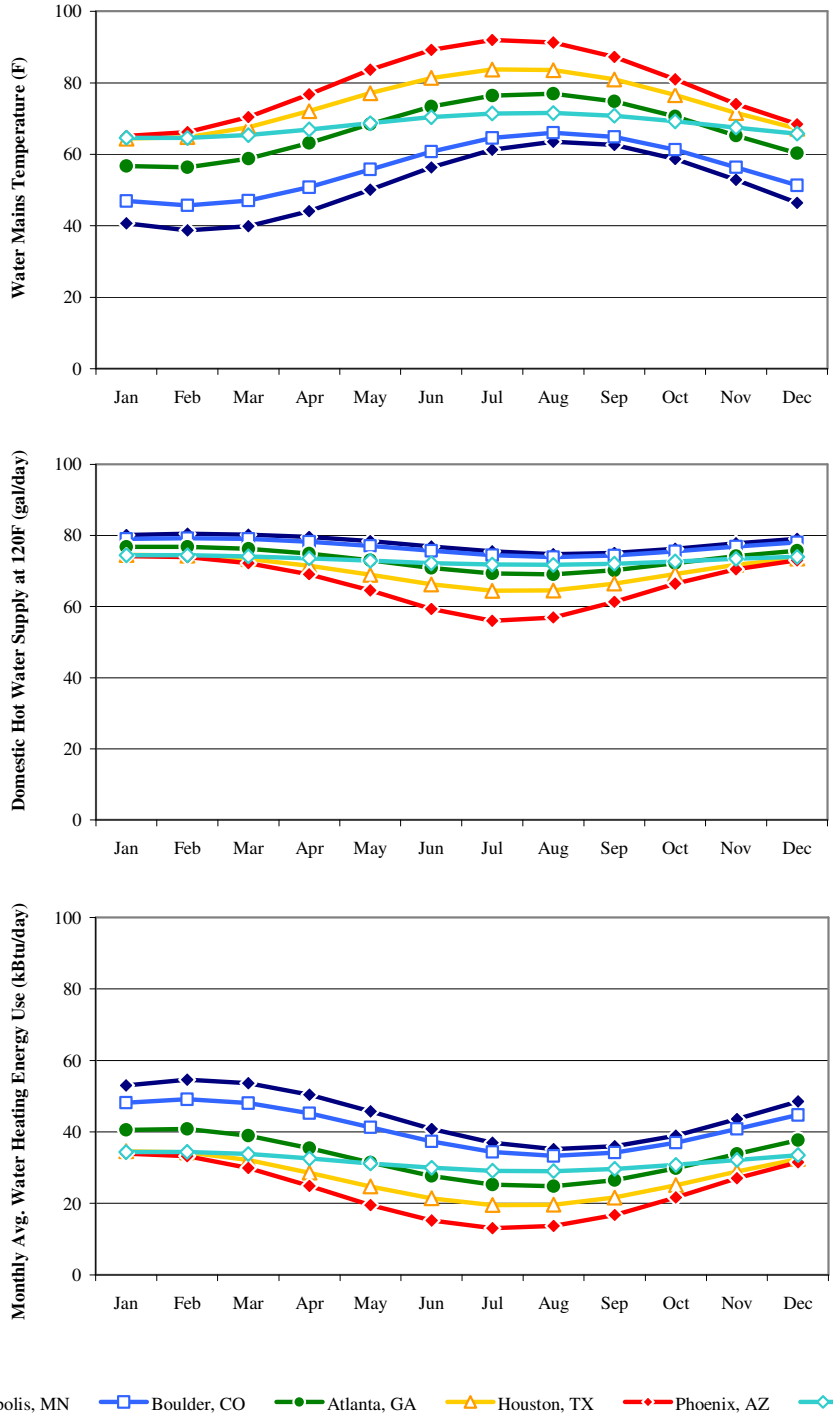


Figure B- 1 Water Mains Temperature ( $T_{mains}$ ), Hot Water Supply Volume ( $V_{supply}$ ) and Monthly Average Daily Energy Use for the Six Locations

**APPENDIX C**  
**DETERMINATION OF HEATING AND COOLING LOAD COMPONENTS**

The building heating and cooling load components were determined using Manual J average load procedure (Rutkowski 2004). The components of the heating and cooling load that were accounted for included: fenestration loads, opaque panel loads (exterior walls, doors, ceiling/roof and slab-on-grade floor), infiltration load, and internal loads. For the fenestration and opaque panel load calculations, the base-case construction characteristics were used. For calculating infiltration loads, the winter air infiltration rate was assumed as 1.2 times and summer air infiltration rate was assumed as 1.6 times the code-specified annual average air infiltration rate (EnergyGauge USA 2009). For the internal loads, the heat gains from the lighting, equipment and occupants including the corresponding sensible and latent fraction, as specified for the base-case house, were considered.

Table C-1 shows the Manual J design outdoor and indoor conditions for the six locations. Table C-2 and Table C-3 show the calculations for the base-case house. Table C-4 and Table C-5 show the calculations for the proposed design.

*Table C-1 Manual J Design Conditions*

	MIN	BOU	ATL	HOU	PHO	LOS	Comments	References
Latitude	44	40	33	29	33	34		
99% Design T	-11	0	23	31	37	45		
1% Design T	88	91	91	94	108	81		
Design grains (50%)	<b>24</b>	<b>-40</b>	<b>37</b>	<b>51</b>	<b>-14</b>	<b>-2</b>	Listed	Table 1A, Manual J
Elevation (ft.)	834	5385	1010	96	1133	97		
Daily Range	M	H	M	M	H	L		
Winter Design T (deg F)	70	70	70	70	70	70	Manual J Default	Section 5-2, Manual J
Summer Design T (deg F)	75	75	75	75	75	75		
Heating Temp. Diff. (HTD, deg F)	81	70	47	39	33	25		
Cooling Temp. Diff. (CTD, deg F)	13	16	16	19	33	6	(Indoor Temp. - Outdoor Temp.) <sub>design</sub>	Section 5-4, Manual J

Table C-2 Heating and Cooling Heat Transfer Multiplier (HTM) Calculations for the Base-case House in the Six Selected Locations

		MIN	BOU	ATL	HOU	PHO	LOS	Comments	References
<b>WINDOWS</b>									
U <sub>windows</sub>		0.28	0.3	0.44	0.47	0.47	0.47		
SHGC		0.68	0.68	0.4	0.4	0.4	0.4		2000/2001 IECC
Peak Solar Factor (PSF)	N	34	35	37	38	37	37	Based on the Latitude	Table 3D-2, Manual J
	E/W	214	216	219	220	219	219		
	S	161	149	116	96	116	121		
Avg. Cooling Load Factor (CLF13)	N	0.29	0.29	0.29	0.29	0.29	0.29	Based on the presence of Internal Shades	Table 3D-3, Manual J
	E/W	0.32	0.32	0.32	0.32	0.32	0.32		
	S	0.18	0.18	0.18	0.18	0.18	0.18		
Interior Shading Coefficient (ISC)		0.7	0.7	0.7	0.7	0.7	0.7	Interior Shading Values for Summer	Table 3D-4, Manual J; 2000 IECC
Heat Transfer Multiplier (HTM)	N	9.03	10.35	10.49	12.48	18.96	6.27	HTM = PSF*CLF*(SHGC/0.87) *ISC + U*CTD	Table 3D-1 Manual J
	E/W	41.11	42.62	29.59	31.59	38.06	25.37		
	S	19.50	19.47	13.76	14.49	22.23	9.83		
Overhang Depth (X, ft.)		All	0	0	0	0	0	Assumes Equal Depth on All Sides	Parametric Simulations
Midsummer Shade Line Multiplier (SLM)	E/W	0.8	0.81	0.82	0.83	0.82	0.82	Midsummer Shade Line Multiplier Values	Table 3E-1, Manual J
	S	2.05	2.6	3.9	5.4	4.28	3.9		
HTM Adjustment for Overhang (HTM <sub>OH</sub> )	E/W	41.11	42.62	29.59	31.59	38.06	25.37	HTM <sub>OH</sub> = 1/H*[X*SLM-Y]*HTM <sub>N</sub> + (H+Y-X*SLM)*HTM <sub>S</sub>	
	S	19.50	19.47	13.76	14.49	22.23	9.83		
Cooling HTM (Weighted Avg.)		27.69	28.77	20.86	22.54	29.33	16.71	For Equal Windows on S, N, E&W	Parametric Simulations
Heating HTM		22.68	21.00	20.68	18.33	15.51	11.75	Heating HTM = U*HTD	Section 6-3, Manual J
<b>OPAQUE SURFACES</b>									
Doors	U <sub>doors</sub>	0.20	0.20	0.20	0.20	0.20	0.20	Fixed to base-case	2000 IECC
	CLTD	24	22	27	30	39	19.6	Based on Const. and Daily Temp. Range	Table 4A (Const. No. 11), Manual J
	Cooling HTM	4.8	4.4	5.4	6	7.8	3.93	Cooling HTM = U*CLTD	Table 4A, Manual J
	Heating HTM	16.2	14	9.4	7.8	6.6	5	Heating HTM = U*HTD	
Walls	U <sub>walls</sub>	0.052	0.058	0.076	0.085	0.085	0.085	Based on Const. (2x4 Wood Frame with Cavity and Continuous Insulation) and Daily Temp. Range	2000/2001 IECC
	Wall Group	K	K	J	I	I	I		Table 4A (Const. No. 14) and 4B, Manual J
	CLTD	8.6	6.6	12.4	20	25	6.76		
	Cooling HTM	0.4472	0.3828	0.9424	1.7	2.125	0.5746	Cooling HTM = U*CLTD	Table 4A, Manual J
	Heating HTM	4.212	4.06	3.572	3.315	2.805	2.125	Heating HTM = U*HTD	
Ceiling	U <sub>ceiling</sub>	0.026	0.0261	0.036	0.04167	0.04368	0.04274	I	2000/2001 IECC
	CLTD	38	36	41	44	53	28	Based on Const. and Daily Temp. Range	Table 4A (Const. No. 16), Manual J
	Cooling HTM	0.988	0.9396	1.476	1.83348	2.31504	1.19672	Cooling HTM = U*CLTD	Table 4A, Manual J
	Heating HTM	2.106	1.827	1.692	1.62513	1.44144	1.0685	Heating HTM = U*HTD	
Slab	F <sub>2, slab</sub>	0.456	0.491	0.604	0.836	0.836	0.836	Based on R-10 and R-0	Assumed, Winkelmann 2002
	Heating HTM	36.936	34.37	28.388	32.604	27.588	20.9	Heating HTM = F2*HTD	Table 4A, Manual J
<b>INFILTRATION</b>									
Altitude Correction Factor (ACF)		0.98	0.83	0.97	1	0.97	1	Altitude Correction Factor	Table 10A, Manual J
Airchange per Hour (ACH)	Annual ACH	0.55	0.50	0.43	0.46	0.39	0.38	ACH = Normalized Leakage * Weather factor; NL = 0.57	2000 IECC, ASHRAE Standard 136
	Heating (ACH <sub>heat</sub> )	0.88	0.79	0.68	0.74	0.62	0.60	ACH <sub>heat</sub> = 1.6 x ACH	EnergyGauge User Manual
	Cooling (ACH <sub>cool</sub> )	0.66	0.60	0.51	0.55	0.47	0.45	ACH <sub>cool</sub> = 1.2 x ACH	
Infiltration CFM	Heating (ICFM <sub>heat</sub> )	295	264	228	246	207	201	ICFM <sub>heat</sub> = ACH <sub>heat</sub> x Vol./60	Section 8-1, Manual J
	Cooling (ICFM <sub>cool</sub> )	221	198	171	185	155	150	ICFM <sub>cool</sub> = ACH <sub>cool</sub> x Vol./60	
Infiltration Load (Btu/h)	Heating	25,683	16,903	11,421	10,564	7,279	5,518	1.1*ACF*ICFM <sub>heat</sub> *HTD	Section 8-7, Manual J
	Sensible Cooling	3,091	2,898	2,916	3,860	5,459	993	1.1*ACF*ICFM <sub>cool</sub> *CTD	
	Latent Cooling	3,528	-4,478	4,168	6,405	-1,432	-205	0.68*ACF*ICFM <sub>cool</sub> *(Grains Diff.)	

Table C- 3 Heating and Cooling Load Components for the Base-case House in the Six Selected Locations

Minneapolis, MN	Total Area	Heating HTM	Cooling HTM	COMPONENTS	HEAT LOSS (Btu/h)	HEAT GAIN (Btu/h)	
						Sensible	Latent
1:1, One-story, Equal	450 sq. ft.	22.7	27.7	Windows	10,206	12,459	-
Windows on All Sides,	40 sq. ft.	16.2	4.8	Doors	648	192	-
No Overhang	1,110 sq. ft.	4.2	0.4	Exterior walls	4,675	496	-
	2,550 sq. ft.	2.1	1.0	Ceilings	5,265	2,470	-
	200 ft.	36.9	-	Slab Floors	7,387	-	-
				Infiltration	25,683	3,091	3,528
				Internal Gains	-	2,931	686
				TOTAL	53,864	21,640	4,214
						25,854	
Boulder, CO	Total Area	Heating HTM	Cooling HTM	COMPONENTS	HEAT LOSS (Btu/h)	HEAT GAIN (Btu/h)	
						Sensible	Latent
1:1, One-story, Equal	450 sq. ft.	21.0	28.8	Windows	9,450	12,944	-
Windows on All Sides,	40 sq. ft.	14.0	4.4	Doors	560	176	-
No Overhang	1,110 sq. ft.	4.1	0.4	Exterior walls	4,507	425	-
	2,550 sq. ft.	1.8	0.9	Ceilings	4,568	2,349	-
	200 ft.	34.4	-	Slab Floors	6,874	-	-
				Infiltration	16,903	2,898	0
				Internal Gains	-	2,931	686
				TOTAL	42,861	21,723	686
						22,409	
Atlanta, GA	Total Area	Heating HTM	Cooling HTM	COMPONENTS	HEAT LOSS (Btu/h)	HEAT GAIN (Btu/h)	
						Sensible	Latent
1:1, One-story, Equal	450 sq. ft.	20.7	20.9	Windows	9,306	9,387	-
Windows on All Sides,	40 sq. ft.	9.4	5.4	Doors	376	216	-
No Overhang	1,110 sq. ft.	3.6	0.9	Exterior walls	3,965	1,046	-
	2,550 sq. ft.	1.7	1.5	Ceilings	4,230	3,690	-
	200 ft.	28.4	-	Slab Floors	5,678	-	-
				Infiltration	11,421	2,916	4,168
				Internal Gains	-	2,931	686
				TOTAL	34,975	20,186	4,854
						25,041	
Houston, TX	Total Area	Heating HTM	Cooling HTM	COMPONENTS	HEAT LOSS (Btu/h)	HEAT GAIN (Btu/h)	
						Sensible	Latent
1:1, One-story, Equal	450 sq. ft.	18.3	22.5	Windows	8,249	10,141	-
Windows on All Sides,	40 sq. ft.	7.8	6.0	Doors	312	240	-
No Overhang	1,110 sq. ft.	3.3	1.7	Exterior walls	3,680	1,887	-
	2,550 sq. ft.	1.6	1.8	Ceilings	4,063	4,584	-
	200 ft.	32.6	-	Slab Floors	6,521	-	-
				Infiltration	10,564	3,860	6,405
				Internal Gains	-	2,931	686
				TOTAL	33,387	23,643	7,091
						30,733	
Phoenix, AZ	Total Area	Heating HTM	Cooling HTM	COMPONENTS	HEAT LOSS (Btu/h)	HEAT GAIN (Btu/h)	
						Sensible	Latent
1:1, One-story, Equal	450 sq. ft.	15.5	29.3	Windows	6,980	13,199	-
Windows on All Sides,	40 sq. ft.	6.6	7.8	Doors	264	312	-
No Overhang	1,110 sq. ft.	2.8	2.1	Exterior walls	3,114	2,359	-
	2,550 sq. ft.	1.4	2.3	Ceilings	3,604	5,788	-
	200 ft.	27.6	-	Slab Floors	5,518	-	-
				Infiltration	7,279	5,459	0
				Internal Gains	-	2,931	686
				TOTAL	26,757	30,047	686
						33,733	
Los Angeles, CA	Total Area	Heating HTM	Cooling HTM	COMPONENTS	HEAT LOSS (Btu/h)	HEAT GAIN (Btu/h)	
						Sensible	Latent
1:1, One-story, Equal	450 sq. ft.	11.8	16.7	Windows	5,288	7,521	-
Windows on All Sides,	40 sq. ft.	5.0	3.9	Doors	200	157	-
No Overhang	1,110 sq. ft.	2.1	0.6	Exterior walls	2,359	638	-
	2,550 sq. ft.	1.1	1.2	Ceilings	2,671	2,992	-
	200 ft.	20.9	-	Slab Floors	4,180	-	-
				Infiltration	5,518	993	0
				Internal Gains	-	2,931	686
				TOTAL	20,215	15,232	686
						15,918	

Table C- 4 Heating and Cooling Heat Transfer Multiplier (HTM) Calculations for the Proposed Design in the Six Selected Locations

		MIN	BOU	ATL	HOU	PHO	LOS	Comments	References
<b>WINDOWS</b>									
U <sub>windows</sub>		0.20	0.20	0.20	0.14	0.14	0.14	Heat Mirror Glazing, Vinyl Frames	Southwall Technologies
SHGC		0.52	0.52	0.52	0.16	0.16	0.16		
Peak Solar Factor (PSF)	N	34	35	37	38	37	37	Based on the Latitude	Table 3D-2, Manual J
	E/W	214	216	219	220	219	219		
	S	161	149	116	96	116	121		
Avg. Cooling Load Factor (CLF13)	N	0.29	0.29	0.29	0.29	0.29	0.29	Based on the presence of Internal Shades	Table 3D-3, Manual J
	E/W	0.32	0.32	0.32	0.32	0.32	0.32		
	S	0.18	0.18	0.18	0.18	0.18	0.18		
Interior Shading Coefficient (ISC)		0.7	0.7	0.7	0.7	0.7	0.7	Interior Shading Values for Summer	Table 3D-4, Manual J; 2000 IECC
Heat Transfer Multiplier (HTM)	N	6.73	7.45	7.69	4.08	6.00	2.22	HTM = PSF*CLF*(SHGC/0.87) *ISC + U*CTD	Table 3D-1 Manual J
	E/W	31.3	32.1	32.5	11.7	13.6	9.9		
	S	14.7	14.4	11.9	4.9	7.3	3.6		
Overhang Depth (X, ft.)		All	2	2	2	4	4	Assumes Equal Depth on All Sides	Parametric Simulations
Midsummer Shade Line Multiplier (SLM)	E/W	0.8	0.81	0.82	0.83	0.82	0.82	Midsummer Shade Line Multiplier Values	Table 3E-1, Manual J
	S	2.05	2.6	3.9	5.4	4.28	3.9		
HTM Adjustment for Overhang (HTM <sub>OH</sub> )	E/W	28.31	29.06	29.34	8.18	10.16	8.88	HTM <sub>OH</sub> = 1/H*[(X*SLM-Y) *HTM <sub>N</sub> +(H+Y-X*SLM)*HTM <sub>D</sub> ]	Parametric Simulations
	S	9.77	8.56	6.16	1.56	3.10	1.71		
Cooling HTM (Weighted Avg.)		11.2	10.4	8.71	2.60	4.24	2.50	For 75:15:5:5 Windows on S, N, E&W	Parametric Simulations
Heating HTM		16.20	14.00	9.40	5.46	4.62	3.50	Heating HTM = U*HTD	Section 6-3, Manual J
<b>OPAQUE SURFACES</b>									
Doors	U <sub>doors</sub>	0.20	0.20	0.20	0.20	0.20	0.20	Fixed to base-case	2000 IECC
	CLTD	24	22	27	30	39	19.6	Based on Const. and Daily Temp. Range	Table 4A (Const. No. 11), Manual J
	Cooling HTM	4.8	4.4	5.4	6	7.8	3.93	Cooling HTM = U*CLTD	Table 4A, Manual J
	Heating HTM	16.2	14	9.4	7.8	6.6	5	Heating HTM = U*HTD	Table 4A, Manual J
Walls	U <sub>walls</sub>	0.036	0.036	0.036	0.036	0.036	0.036	Based on R-26	Assumed
	Wall Group	K	K	K	K	K	K	Based on Const. (SIP) and Daily Temp. Range	Table 4A (Const. No. 14) and 4B, Manual J
	CLTD	8.6	6.6	11.6	14.6	23.6	5.6	Cooling HTM = U*CLTD	Table 4A, Manual J
	Cooling HTM	0.31	0.24	0.42	0.53	0.85	0.205		
Heating HTM	2.92	2.52	1.69	1.40	1.19	0.9	Heating HTM = U*HTD	Table 4A, Manual J	
Ceiling	U <sub>ceiling</sub>	0.018	0.018	0.018	0.018	0.018	0.018	Based on R-57	Assumed
	CLTD	38	36	41	44	53	28	Based on Const. and Daily Temp. Range	Table 4A (Const. No. 16), Manual J
	Cooling HTM	0.68	0.65	0.74	0.79	0.95	0.50	Cooling HTM = U*CLTD	Table 4A, Manual J
	Heating HTM	1.46	1.26	0.85	0.70	0.59	0.45	Heating HTM = U*HTD	
Slab	F <sub>2, slab</sub>	0.49	0.49	0.49	0.836	0.836	0.836	Based on R-10 and R-0	Assumed, Winkelmann 2002
	Heating HTM	39.7	34.3	23.0	32.6	27.6	20.9	Heating HTM = F2*HTD	Table 4A, Manual J
<b>INFILTRATION</b>									
Altitude Correction Factor (ACF)		0.98	0.83	0.97	1	0.97	1	Altitude Correction Factor	Table 10A, Manual J
Airchange per Hour (ACH)	Annual ACH	0.35	0.31	0.27	0.29	0.24	0.24	ACH = Normalized Leakage * Weather factor; NL = 0.36	2000 IECC, ASHRAE Standard 136
	Heating (ACH <sub>heat</sub> )	0.56	0.50	0.43	0.47	0.39	0.38	ACH <sub>heat</sub> = 1.6 x ACH	EnergyGauge User Manual
	Cooling (ACH <sub>cool</sub> )	0.42	0.38	0.32	0.35	0.29	0.29	ACH <sub>cool</sub> = 1.2 x ACH	
Infiltration CFM	Heating (ICFM <sub>heat</sub> )	186	167	144	156	131	127	ICFM <sub>heat</sub> = ACH <sub>heat</sub> x Vol./60	Section 8-1, Manual J
	Cooling (ICFM <sub>cool</sub> )	140	125	108	117	98	95	ICFM <sub>cool</sub> = ACH <sub>cool</sub> x Vol./60	
Infiltration Load (Btu/h)	Heating	16,221	10,676	7,213	6,672	4,597	3,485	1.1*ACF*ICFM <sub>heat</sub> *HTD	Section 8-7, Manual J
	Sensible Cooling	1,952	1,830	1,842	2,438	3,448	627	1.1*ACF*ICFM <sub>cool</sub> *CTD	
	Latent Cooling	2,228	-2,828	2,633	4,045	-904	-129	0.68*ACF*ICFM <sub>cool</sub> *(Grains Diff.)	

Table C- 5 Heating and Cooling Load Components for the Proposed Design in the Six Selected Locations

Minneapolis, MN	Total Area	Heating HTM	Cooling HTM	COMPONENTS	HEAT LOSS (Btu/h)	HEAT GAIN (Btu/h)	
						Sensible	Latent
1:1, Two-story, 75%	450 sq. ft.	16.2	11.2	Windows	7,290	5,024	
Windows on the South,	40 sq. ft.	16.2	4.8	Doors	648	192	
2 ft. Wide Overhang	1,773 sq. ft.	2.9	0.3	Exterior walls	5,170	549	
	1,250 sq. ft.	1.5	0.7	Ceilings	1,823	855	
	142 ft.	39.7		Slab Floors	5,616		
				Infiltration	16,221	1,952	2,228
				Internal Gains		1,899	588
				TOTAL	36,767	10,471	2,816
						13,287	
Boulder, CO	Total Area	Heating HTM	Cooling HTM	COMPONENTS	HEAT LOSS (Btu/h)	HEAT GAIN (Btu/h)	
						Sensible	Latent
1:1, Two-story, 75%	450 sq. ft.	14.0	10.4	Windows	6,300	4,700	
Windows on the South,	40 sq. ft.	14.0	4.4	Doors	560	176	
2 ft. Wide Overhang	1,773 sq. ft.	2.5	0.2	Exterior walls	4,468	421	
	1,250 sq. ft.	1.3	0.6	Ceilings	1,575	810	
	142 ft.	34.3		Slab Floors	4,853		
				Infiltration	10,676	1,830	0
				Internal Gains		2,931	686
				TOTAL	28,432	10,869	686
						11,555	
Atlanta, GA	Total Area	Heating HTM	Cooling HTM	COMPONENTS	HEAT LOSS (Btu/h)	HEAT GAIN (Btu/h)	
						Sensible	Latent
1:1.5, One-story, 75%	450 sq. ft.	9.4	8.7	Windows	4,230	3,919	
Windows on the South,	40 sq. ft.	9.4	5.4	Doors	376	216	
2 ft. Wide Overhang	1,143 sq. ft.	1.7	0.4	Exterior walls	1,934	477	
	2,500 sq. ft.	0.8	0.7	Ceilings	2,115	1,845	
	204 ft.	23.0		Slab Floors	4,698		
				Infiltration	7,213	1,842	2,633
				Internal Gains		2,931	686
				TOTAL	20,566	11,230	3,319
						14,548	
Houston, TX	Total Area	Heating HTM	Cooling HTM	COMPONENTS	HEAT LOSS (Btu/h)	HEAT GAIN (Btu/h)	
						Sensible	Latent
1:1.5, One-story, 75%	450 sq. ft.	5.5	2.6	Windows	2,457	1,171	
Windows on the South,	40 sq. ft.	7.8	6.0	Doors	312	240	
4 ft. Wide Overhang	1,143 sq. ft.	1.4	0.5	Exterior walls	1,605	601	
	2,500 sq. ft.	0.7	0.8	Ceilings	1,755	1,980	
	204 ft.	32.6		Slab Floors	6,651		
				Infiltration	6,672	2,438	4,045
				Internal Gains		4	686
				TOTAL	19,452	6,434	4,731
						11,165	
Phoenix, AZ	Total Area	Heating HTM	Cooling HTM	COMPONENTS	HEAT LOSS (Btu/h)	HEAT GAIN (Btu/h)	
						Sensible	Latent
1:1.5, One-story, 75%	450 sq. ft.	4.6	4.2	Windows	2,079	1,907	
Windows on the South,	40 sq. ft.	6.6	7.8	Doors	264	312	
4 ft. Wide Overhang	1,357 sq. ft.	1.2	0.8	Exterior walls	1,612	1,153	
	2,500 sq. ft.	0.6	1.0	Ceilings	1,485	2,385	
	204 ft.	27.6		Slab Floors	5,628		
				Infiltration	4,597	3,448	0
				Internal Gains		2,931	686
				TOTAL	15,665	12,136	686
						12,822	
Los Angeles, CA	Total Area	Heating HTM	Cooling HTM	COMPONENTS	HEAT LOSS (Btu/h)	HEAT GAIN (Btu/h)	
						Sensible	Latent
1:1.5, One-story, 75%	450 sq. ft.	3.5	2.5	Windows	1,575	1,127	
Windows on the South,	40 sq. ft.	5.0	3.9	Doors	200	157	
2 ft. Wide Overhang	1,357 sq. ft.	0.9	0.2	Exterior walls	1,221	274	
	2,500 sq. ft.	0.5	0.5	Ceilings	1,125	1,260	
	204 ft.	20.9		Slab Floors	4,264		
				Infiltration	3,485	627	0
				Internal Gains		2,931	686
				TOTAL	11,870	6,376	686
						7,062	



## APPENDIX D SYSTEMS PERFORMANCE DATA

This appendix includes product data for the glazing type, solar thermal collectors, photovoltaic panels, and wind turbines analyzed in this study.

*Table D-1 Performance Data of Heat Mirror Glazing*

Product	Glazing Configuration		Thickness		Outside Dimension	U-factor		Solar Heat Gain Performance		Transmission and Reflectance				
	Glass Type	Gas Fill	IP	SI		IP Units	SI Units	SC	SHGC	Tsol	Tvis	Rvis Ext.	Rvis Int.	Tuv
HM 88	Bronze/LowE	Krypton	1/8in.	3mm	1in	0.11	0.65	0.41	0.35	0.23	0.46	0.11	0.12	0.005
HM 88	Clear/Clear	Krypton	1/8in.	3mm	1-1/2in	0.19	1.08	0.68	0.59	0.48	0.72	0.19	0.19	0.012
HM SC75	Gray/LowE	Krypton	1/4in.	6mm	1-1/2in	0.11	0.63	0.24	0.21	0.12	0.26	0.08	0.15	0.003
HM TC88	Clear/Clear	Krypton	1/8in.	3mm	1-1/2in	0.13	0.76	0.59	0.51	0.38	0.65	0.14	0.15	0.014

*Table D-2 Performance Data of Solar Thermal Collectors*

COLLECTOR PARAMETERS (SRCC 2009)	Flat Plate Collectors		Evacuated Tube Collectors	
	Solene-Corona SLCO-32	Viessmann Vitosol 200F	Beijing Sunda SEIDO 2-16	Viessmann Vitosol 300T
Collector Type	Flat Plate	Flat Plate	Evacuated Tube	Evacuated Tube
Test Slope ( $F_R U_L$ )	0.81	0.62	0.30	0.19
Test Intercept ( $F_R \tau \alpha$ )	0.79	0.72	0.63	0.51
Incidence Angle Modifier ( $K_{am} = 1 + b_1[1/\cos\theta - 1] + b_2[1/\cos\theta - 1]^2$ )				
Coefficients $b_1$ and $b_2$ (Perpendicular)	-0.29, -0.01	-0.07, -0.12	+0.27, -0.35	+0.52, -0.74
Coefficients $b_1$ (Parallel)	-	-	-0.10	-0.31
Test Collector Flow rate per Area (gpm/ft <sup>2</sup> )	14.5	14.6	14.9	15.2
Test Collector Fluid Specific Heat (Btu/lb.°F)	1.0	0.8	1.0	0.8

*Table D-3 Performance Data of Photovoltaic Panels*

System Characteristics	Sunpower 230 (Monocrystalline Silicon)	Unisolar PNL-144 (Amorphous Silicon)
Cell Temperature at NOCT Conditions	48.5 °C	46 °C
Array Reference Efficiency	18.5 %	6.67 %
Array Reference Temperature	25 °C	25 °C
Array Temperature Coefficient	0.0038 per °C	0.0021 per °C

*Table D- 4 Performance Data of Wind Turbines*

Specifications	BWC Excel-R (7.5 kW)	Whisper 500 (3 kW)	WES <sup>5</sup> Tulipo (2.5 kW) <sup>1</sup>	Skystream 3.7 (2.4 kW)
Rated Capacity	7.5 kW	3 kW	2.5 kW	2.4 kW
Rated Wind Speed	31 mph	24 mph	20 mph	29 mph
Rotor Diameter	23 ft.	15 ft.	16 ft.	12 ft.
Start-up/Cut-in Speed	8 mph	7.5 mph	6.7 mph	8 mph
Cut-out Speed	None (Furling at 36 mph)	60 mph	45 mph	60 mph
Maximum Design Wind Speed	125 mph	120 mph	135 mph	140 mph
Tower Height	60 -120 ft.	30 -70 ft.	40 ft.	30-70 ft.

---

<sup>1</sup> Suitable for grid-connection.

## APPENDIX E

### ANALYSIS OF SOLAR THERMAL SYSTEM

The analysis of active solar thermal system with flat plate collectors and evacuated tube collectors was performed using the F-CHART program with TMY2 weather data. In F-CHART, the calculations are performed for an average day of each month and summed for the number of days of the month. For each month, first the collector parameters (tilt and azimuth) are used with the location and weather data (i.e., latitude, solar radiation and ground reflectance ) to determine daily incident radiation on the collector plane (HT). Then, the system parameters are used with weather data to determine the monthly total thermal loads on the system (L). These include: i)\_space heating loads, ii)\_domestic water heating loads, and iii)\_DHW auxiliary tank standby losses. Next, the collector test slope (FRUL) and test intercept ( $FR\tau\alpha$ ) are modified to take into account the installation factors, which include: i)\_heat transfer fluid characteristics ( $C_p$  and  $\dot{m}$ ), if different from the collector test conditions, and ii)\_hot water supply and return pipe UA. In addition, other correction factors are calculated, which include: iii)\_FR'/FR, for collector-storage heat exchanger, if present, iv)\_ $(\tau\alpha)/(\tau\alpha)_n$ , for collector incident angle modifiers, v)\_hot water storage volume per unit of collector area, if different from the F-CHART standard assumption (i.e., 75 liters per square meter of collector area), and vi)\_load heat exchanger effectiveness ( $\epsilon_L$ , if different from F-CHART standard assumption)<sup>1</sup>. Next, the dimensional variables X and Y are calculated using the collector area, loads, average incident radiation, dry-bulb temperature, and all the correction factors. Finally, the fraction of loads met by solar f, is obtained from correlations between the variables X and Y.

An example calculation for the F-CHART program is presented in the following tables. Table E-1 shows the F-CHART input parameters. Table E-2 summarizes the algorithm used in the F-CHART program, including the reference from Duffie and Beckman (2001). The monthly calculation steps of the F-CHART are shown in Table E-3 through Table E-6.

---

<sup>1</sup> The f-chart for liquid system was developed with  $\epsilon_L * C_{min}/(UA)_h = 2$ , where  $(UA)_h$  is building UA and  $C_{min}$  is the minimum fluid-capacitance rate  $(mC_p)_{min}$  in the load heat exchanger, generally that of the air.

Table E-1 F-CHART Input Parameters

## Weather Parameters

Month	Radiation kJ/m <sup>2</sup>	Temp. C	Humidity kg/kg	Mains C	Reflect.	HDD C-days
Jan	6409	-10.9	0.001	4.8	0.39	905
Feb	9807	-7.6	0.0013	3.7	0.39	726
Mar	13511	-0.5	0.0024	4.4	0.23	584
Apr	16989	8	0.0039	6.7	0.12	313
May	20568	15.1	0.0063	10	0.12	126
Jun	22511	20.4	0.0095	13.5	0.12	31
Jul	22830	23.2	0.0115	16.2	0.12	11
Aug	19455	21.4	0.0108	17.5	0.12	23
Sep	14636	15.8	0.0079	17	0.12	106
Oct	10057	9.4	0.0049	14.8	0.12	283
Nov	6125	0.7	0.0029	11.6	0.18	528
Dec	4977	-7.6	0.0014	8	0.3	803

## System Parameters

Water Storage House Heating System		
Location	MINNEAPOLIS	MN
Water volume / collector area	75	liters/m <sup>2</sup>
Building UA (0 if only DHW)	274	W/C
Fuel	Elec	
Efficiency of fuel usage	100	%
Domestic hot water)	Yes	
Daily hot water usage	300	liters
Water set temperature	60	C
Environmental temperature	20	C
UA of auxiliary storage tank	4	W/C
Pipe heat loss	No	
Inlet pipe UA	2.64	W/C
Outlet pipe UA	2.64	W/C
Relative load heat exchanger size	1	
Collector-store heat exchanger	No	
Tank-side flow rate/area	0.015	kg/sec-m <sup>2</sup>
Heat exchanger effectiveness	0.5	

## Collector Parameters

Evacuated Tubular Collector		
Number of collector panels	2	
Collector panel area	2.97	m <sup>2</sup>
FR*UL (Test slope)	1.419	W/m <sup>2</sup> -C
FR*TAU*ALPHA (Test intercept)	0.6	
Collector slope	33	degrees
Collector azimuth (South=0)	0	degrees
Receiver orientation	NS	
Incidence angle modifier (Perpendicular)	Ang Dep	
Incidence angle modifier (Parallel)	Ang Dep	
Collector flow rate/area	0.015	kg/sec-m <sup>2</sup>
Collector fluid specific heat	4.19	kJ/kg-C
Modify test values	Yes	
Test collector flow rate/area	0.015	kg/sec-m <sup>2</sup>
Test fluid specific heat	4.19	kJ/kg-C

Table E- 2 F-CHART Calculation Steps

			Reference	EQUATIONS	
	Latitude	$\Phi = 44.9$	14.77		
	Collector slope	$\beta = 70.0$	11.57		
		$\Phi - \beta = -25.1$			
	Surface azimuth	$\gamma = 0$			
Radiation calculations	Day of year	$n =$ (mo.)	Tb 1.6.1		
	Declination for avg. day of month	$\delta =$ (mo.)	1.6.1a	$\delta = 23.45 \sin[360(284+n)/365]$	
	Sunset hour angle	$\omega_s =$ (mo.)	1.6.10	$\omega_s = \cos^{-1}\{-\tan \Phi \cdot \tan \delta\}$	
		$\omega_{s1} =$ (mo.)	2.19.3	$\omega_{s1} = \cos^{-1}\{-\tan(\Phi - \beta) \cdot \tan \delta\}$	
	Sunset hour angle for mean day of the month	$\omega_s' =$ (mo.)		$\omega_s' = \min[\cos^{-1}\{-\tan \Phi \cdot \tan \delta\}, \cos^{-1}\{-\tan(\Phi - \beta) \cdot \tan \delta\}] = \min[\omega_s, \omega_{s1}]$	
	Avg. daily beam rad. on (tilted surface / hz. surface)	$R_b =$ (mo.)		$R_b = [\cos(\Phi - \beta) \cdot \cos \delta \cdot \sin \omega_s' + (\pi/180) \cdot \omega_s' \cdot \sin(\Phi - \beta) \cdot \sin \delta] / [\cos \Phi \cdot \cos \delta \cdot \sin \omega_s + (\pi/180) \cdot \omega_s \cdot \sin \Phi \cdot \sin \delta]$	
	Monthly avg. daily horizontal Radiation	$H =$ (mo.) MJ/m <sup>2</sup>			
	Ground. Refl.	$\rho_g =$ (mo.)			
	Solar constant	$G_{sc} = 1367$ W/m <sup>2</sup>	Sec 1.2	$G_{sc} = 1367$ W/m <sup>2</sup>	
	Monthly avg. daily extraterrestrial rad.	$H_o =$ (mo.) MJ/m <sup>2</sup>	1.10.3	$H_o = (24 \times 3600 / \pi) \cdot G_{sc} \cdot [1 + 0.033 \cos(360n/365)] \cdot [\cos \Phi \cdot \cos \delta \cdot \sin \omega_s + (\pi/180) \cdot \omega_s \cdot \sin \Phi \cdot \sin \delta]$	
	Monthly average clearness index	$K_T =$ (mo.)	2.9.1	$K_T = H / H_o$	
	Ration of Monthly avg. daily diffuse and total hz. rad.	$H_d / H =$ (mo.)	2.12.1	$H_d / H = 1.391 - 3.560 K_T + 4.189 K_T^2 - 2.137 K_T^3$ , for $\omega_s \leq 81.4^\circ$ and $0.3 \leq K_T \leq 0.8$ $H_d / H = 1.311 - 3.022 K_T + 3.427 K_T^2 - 1.821 K_T^3$ , for $\omega_s > 81.4^\circ$ and $0.3 \leq K_T \leq 0.8$	
Monthly avg. daily rad. on the collector plane	$H_T =$ (mo.) MJ/m <sup>2</sup>	2.19.1	$H_T = H \cdot \{ [1 - (H_d/H)] \cdot R_b + (H_d/H) \cdot [(1 + \cos \beta)/2] + \rho_g \cdot [(1 - \cos \beta)/2] \}$		
Loads calculations	Space Heating Loads	Monthly avg. ambient temperature	$T_a =$ (mo.) °C		
		Balance point temp.	$T_{bal} = 18.3$ °C		
		Heating degree days base 18.3°C	(mo.) °C-days		
		Bldg. overall heat loss coefficient	BldgUA = (mo.) W/°C		
		Space heating loads	$Q_{space} =$ (mo.) GJ/day	$Q_{space} = \text{BldgUA} \cdot \text{HDD}_{\text{month}} \cdot 24 \cdot 3600 / 10^9$	
	Total Water Heating Loads	Domestic Water Heating Loads	Water mains temperature	$T_{\text{mains}} =$ (mo.) °C	$Q_{\text{HW}} = V \cdot \text{Cp} \cdot (T_{\text{supply}} - T_{\text{mains}})$
			Daily hot water use (at Tsupply)	$V_{\text{HW}} =$ (mo.) L/month	
			Water Set T	$T_{\text{supply}} =$ (mo.) °C	
			Domestic Water Heating load	$Q_{\text{HW}} =$ (mo.) GJ/month	
		Standby Losses	Environmental temp. (for tank)	$T_{\text{amb}} =$ (mo.) °C	
	UA for auxiliary storage tank	$UA_{\text{tank}} = 4.0$ W/°C			
	Standby loss from aux. storage tank	$Q_{\text{stby}} =$ (mo.) GJ/month			
	Total (DHW Loads + Standby Losses)	$Q_{\text{DHW}} =$ (mo.) GJ/month			
	Total thermal loads (space heating + water heating)	$L =$ (mo.) GJ/month			
Collector and System calculations	Collector Type	Type = Flat Plate/Evac. Tube			
	Collector Test Slope	$F_R U_L = 4.200$ W/m <sup>2</sup> ·°C			
	Collector Test Intercept	$F_R(\tau\alpha)_n = 0.700$			
	Installed Collector area	$A_c = 3.00$ m <sup>2</sup>			
	Corrections for $F_R U_L$ and $F_R(\tau\alpha)_n$	Corrections for flow rate	Collector flow rate/area	$(m/Ac)_{\text{use}} = 0.011$ kg/sec·m <sup>2</sup>	6.20.4 $F'U_L = -(mCp/Ac) \cdot \text{Ln}[1 - (F_R U_L A_c / mCp)]$
			Collector fluid specific heat	$(Cp)_{\text{use}} = 4.190$ kJ/kg·°C $(mCp)_{\text{use}} = 0.138$ kW/°C	
	Ex 10.8.1 (p.441)		Test collector flow rate/area	$(m/Ac)_{\text{test}} = 0.015$ kg/sec·m <sup>2</sup>	6.20.3 $r = [(mCp/Ac) \cdot \{1 - \exp(-AcF'U_L/mCp)\}]_{\text{use}} / [F_R U_L]_{\text{test}}$
			Test collector fluid sp. heat	$(Cp)_{\text{test}} = 4.190$ kJ/kg·°C $(F'U_L)_{\text{test}} = 4.347$ W/m <sup>2</sup> ·°C $r = 0.988$	
			$F_R U_L = 4.148$ W/m <sup>2</sup> ·°C	Ex 10.8.1	$F_R U_L = r \cdot F_R U_L$
			$F_R(\tau\alpha)_n = 0.691$		$F_R(\tau\alpha)_n = r \cdot F_R(\tau\alpha)_n$

Table E- 2 (Cont.)

		Reference		EQUATIONS	
Final Calculations	Corrections for pipe losses	Inlet Pipe UA	$UA_i = 0 \text{ (W/}^\circ\text{C)}$	10.3.9	$(\tau\alpha)' / (\tau\alpha)_n = 1/[1 + UA_i/(mCp)_c]$
		Outlet Pipe UA	$UA_o = 0 \text{ (W/}^\circ\text{C)}$	10.3.10	$U_i/U_L = [1 - \{UA_i/(mCp)_c\} + \{UA_i + UA_o\}/(mCp)_c] / [1 + UA_i/(mCp)_c]$
			$(\tau\alpha)/(\tau\alpha)_n = 1.000$	Ex 10.8.1	$F_R U_L' = F_R U_L \cdot U_i/U_L$
			$U_i/U_L = 1.000$		
			$F_R U_L' = 4.15$		
			$F_R(\tau\alpha)_n' = 0.691$		$F_R(\tau\alpha)_n' = F_R(\tau\alpha)_n \cdot [(\tau\alpha)' / (\tau\alpha)_n]$
	Corrections for collector-storage HX Ex 10.8.1 (p.441)	Tank side flow rate/area	$(m/A_c)_{\text{tank}} = 0.015 \text{ kg/sec-m}^2$		
		Tank fluid (water) sp. heat	$(C_p)_{\text{tank}} = 4.19 \text{ kJ/kg}^\circ\text{C}$ $(mC_p)_{\text{tank}} = 0.189 \text{ kW/}^\circ\text{C}$		
		Collector-storage HX eff.	$\epsilon = 0.5$		
		Coll. HX heat removal factor $F_R/F_R = 1.00$		10.2.3	$F_R/F_R = [1 + \{A_c \cdot F_R \cdot U_L / (mCp)_c\} \cdot \{(mCp)_c / (\epsilon(mCp)_{\text{min}} - 1)\}]^{-1}$
	For IAM corrections	Hour Angle, 2.5 h from noon $\omega =$	$37.500$	Sec 5.10	$\cos\theta = \sin\delta \cdot \sin\Phi \cdot \cos\beta - \sin\delta \cdot \cos\Phi \cdot \sin\beta \cdot \cos\gamma + \cos\delta \cdot \cos\Phi \cdot \cos\beta \cdot \cos\omega + \cos\delta \cdot \sin\Phi \cdot \sin\beta \cdot \cos\gamma \cdot \cos\omega + \cos\delta \cdot \sin\beta \cdot \sin\gamma \cdot \sin\omega$
		Incident angle $\theta =$	(mo.)	1.6.2	
		Zenith Angle $\theta_z =$	(mo.)	1.6.5	$\cos\theta_z = \cos\delta \cdot \cos\Phi \cdot \cos\omega + \sin\delta \cdot \sin\Phi$
		Solar azimuth angle $\gamma_s =$	(mo.)	1.6.6	$\gamma_s = \text{sign}(\omega) \cdot \cos^{-1}[(\cos\theta_s \cdot \sin\Phi - \sin\delta) / \sin\theta_s \cdot \cos\Phi]$
		Incident angle (parallel comp.) $\theta_1 =$	(mo.)	McIntire and Reed (1983)	$\tan^2\theta_1 = \tan^2\theta_i + \tan^2\theta_2$ ; $\tan\gamma_s = \tan\theta_1 / \tan\theta_2$ or $\tan\theta_1 = \cos\gamma_s \cdot \tan\theta_2$ ; and $\tan\theta_2 = \sin\gamma_s \cdot \tan\theta_1$
	Incident angle (perp. Comp.) $\theta_2 =$	(mo.)			
	IAM coefficients (perp.) $b_{01}(t) =$	$0.000$			
	$b_{02}(t) =$	$0.000$			
	IAM coefficient (parallel) $b_0(l) =$	NA			
	IAM (Flat plate) $K_{\tau\alpha}(\theta) =$	(mo.)	6.17.10	$K_{\tau\alpha}(\theta) = 1 + b_{01} \cdot (1/\cos\theta - 1) + b_{02} \cdot (1/\cos\theta - 1)^2$	
	IAM (perpendicular) $K_{\tau\alpha}(\theta) =$	(mo.)		$K_{\tau\alpha}(\theta) = 1 + b_{01} \cdot (1/\cos\theta - 1) + b_{02} \cdot (1/\cos\theta - 1)^2$	
	IAM (parallel) $K_{\tau\alpha}(\theta) =$	(mo.)		$K_{\tau\alpha}(\theta) = 1 + b_{01} \cdot (1/\cos\theta - 1)$	
	IAM (Evacuated tube) $K_{\tau\alpha}(\theta) \cdot K_{\tau\alpha}(\theta) =$	(mo.)	6.17.12		
	Coll. $\tau\alpha$ for (mo. avg./ normal incidence) $(\tau\alpha) / (\tau\alpha)_n =$	(mo.)	6.17.8	$(\tau\alpha) / (\tau\alpha)_n = K_{\tau\alpha}(\theta)$ for flat-plate collector; $(\tau\alpha) / (\tau\alpha)_n = K_{\tau\alpha}(\theta) \cdot K_{\tau\alpha}(\theta)$ for evacuated tube collector	
X (Ref. collector loss/Heating Load)		$X =$	(mo.)	20.2.3	$X = F_R U_L (100 - T_a) \cdot \Delta t \cdot A_c / L$ ; where $\Delta t = N \cdot 24 \cdot 3600 \text{ sec/month}$ (from Ex 20.2.1, p.677)
	Water volume/collector area $V/A_c =$	$75.00 \text{ L/m}^2$			
	$X_c =$	(mo.)	20.3	$X_c = X \cdot [(V/A_c) / 75]^{-0.25}$	
Y (Absorbed solar energy/heating load)		$Y =$	(mo.)	20.2.4	$Y = F_R'(\tau\alpha)_n \cdot (\tau\alpha) / (\tau\alpha)_n \cdot H_T \cdot N \cdot A_c / L$
	$T_{hi} =$	(mo.) $^\circ\text{C}$			
	$T_{co} =$	$48.9 \text{ }^\circ\text{C}$ (=120F)			
	$T_{ci} =$	$20.0 \text{ }^\circ\text{C}$ (=68F)			
	$\epsilon_L =$	(mo.)	3.17.5	$\epsilon_L = (T_{co} - T_{ci}) / (T_{hi} - T_{ci})$	
	$m_{\text{air}} =$	(mo.)/L/sec			
	$\epsilon_{\text{std}} =$	(mo.)	20.3.3	$\epsilon_{\text{std}} = UA/C_{\text{min}}$ , where $C_{\text{min}} = (mCp)_{\text{air}}$	
	Relative load HX size $\epsilon_L / \epsilon_{\text{std}} =$	(mo.)	20.3.3	$Y_c = Y \cdot \{0.39 + 0.65 \cdot \text{Exp}\{-0.139(UA)_f / (\epsilon_L \cdot C_{\text{min}})\}\}$	
	$Y_c =$	(mo.)	20.3.3		
F (fraction of loads met by solar)		$f =$	(mo.)	20.3.1	$f = 1.029Y - 0.065X - 0.245Y^2 + 0.0018X^2 + 0.0215Y^3$ (fraction of monthly load L met by monthly solar)
		$F =$	(Annual)	20.2.5	$F = [\Sigma(fL)] / [\Sigma L]$ , $\Sigma =$ summation for 12 months

Table E- 3 F-CHART Calculations for Incident Solar Radiation

Month	N	n	$\delta$	$\sin \delta$	$\cos \delta$	$\tan \delta$	$\omega_s$	$\sin \omega_s$	$\omega_{s1}$	$\omega_s'$	$\sin \omega_s'$	$R_b$	H	$\rho_g$	$H_o$	$K_T$	$H_o/H$	$H_d/H$	$H_a/H$	$H_r$
													MJ/m2		MJ/m2					
Jan	31	17	-20.92	-0.36	0.93	-0.38	67.64	0.92	100.33	67.64	0.92	3.05	6.4	0.39	12.2	0.52	0.37	0.41	0.37	14.77
Feb	28	47	-12.95	-0.22	0.97	-0.23	76.76	0.97	96.19	76.76	0.97	2.14	9.8	0.39	17.7	0.55	0.34	0.38	0.34	17.35
Mar	31	75	-2.42	-0.04	1.00	-0.04	87.59	1.00	91.13	87.59	1.00	1.41	13.5	0.23	25.1	0.54	0.36	0.39	0.39	16.12
Apr	30	105	9.41	0.16	0.99	0.17	99.50	0.99	85.54	85.54	1.00	0.88	17.0	0.12	33.2	0.51	0.38	0.42	0.42	14.18
May	31	135	18.79	0.32	0.95	0.34	109.80	0.94	80.82	80.82	0.99	0.61	20.6	0.12	39.2	0.52	0.37	0.41	0.41	13.90
Jun	30	162	23.09	0.39	0.92	0.43	115.11	0.91	78.47	78.47	0.98	0.51	22.5	0.12	41.8	0.54	0.35	0.39	0.39	13.83
Jul	31	198	21.18	0.36	0.93	0.39	112.69	0.92	79.53	79.53	0.98	0.56	22.8	0.12	40.4	0.56	0.33	0.37	0.37	14.56
Aug	31	228	13.45	0.23	0.97	0.24	103.78	0.97	83.56	83.56	0.99	0.76	19.5	0.12	35.5	0.55	0.35	0.38	0.38	14.84
Sep	30	258	2.22	0.04	1.00	0.04	92.21	1.00	88.96	88.96	1.00	1.17	14.6	0.12	28.0	0.52	0.37	0.41	0.41	14.72
Oct	31	288	-9.60	-0.17	0.99	-0.17	80.31	0.99	94.55	80.31	0.99	1.87	10.1	0.12	19.9	0.51	0.38	0.42	0.38	14.56
Nov	30	318	-18.91	-0.32	0.95	-0.34	70.06	0.94	99.25	70.06	0.94	2.78	6.1	0.18	13.5	0.45	0.44	0.47	0.44	11.72
Dec	31	344	-23.05	-0.39	0.92	-0.43	64.94	0.91	101.51	64.94	0.91	3.40	5.0	0.3	10.8	0.46	0.43	0.47	0.43	11.57

Table E- 4 F-CHART Calculations for Thermal Loads

Month	$T_a$	HDD	BldgUA	$Q_{space}$	$T_{mains}$	$V_{hw}$	$T_{supply}$	$Q_w$	$T_{amb}$	$Q_{sby}$	$Q_{dhw}$	L/month
	°C	°C-days	W/°C	GJ	°C	L/month	°C	GJ	°C	GJ	GJ	GJ
Jan	-10.9	905	274	21.425	4.8	300	60	2.149	20	0.429	2.577	24.002
Feb	-7.6	726	274	17.187	3.7	300	60	1.980	20	0.429	2.408	19.595
Mar	-0.5	584	274	13.825	4.4	300	60	2.164	20	0.429	2.593	16.418
Apr	8	313	274	7.410	6.7	300	60	2.008	20	0.429	2.437	9.846
May	15.1	126	274	2.983	10	300	60	1.946	20	0.429	2.375	5.358
Jun	20.4	31	274	0.734	13.5	300	60	1.752	20	0.429	2.180	2.914
Jul	23.2	11	274	0.260	16.2	300	60	1.705	20	0.429	2.134	2.394
Aug	21.4	23	274	0.544	17.5	300	60	1.655	20	0.429	2.083	2.628
Sep	15.8	106	274	2.509	17	300	60	1.620	20	0.429	2.049	4.558
Oct	9.4	283	274	6.700	14.8	300	60	1.760	20	0.429	2.188	8.888
Nov	0.7	528	274	12.500	11.6	300	60	1.823	20	0.429	2.252	14.752
Dec	-7.6	803	274	19.010	8	300	60	2.024	20	0.429	2.453	21.463
				105.087				22.586		5.143	27.729	132.816

Table E- 5 F-CHART Calculations for Incident Angle Modifiers

Month	$\theta$	$\cos \theta$	$\tan \theta$	$\theta_z$	$\sin \theta_z$	$\cos \theta_z$	$\gamma_s$	$\sin \gamma_s$	$\cos \gamma_s$	$\theta_1$	$\cos \theta_1$	$\theta_t$	$\cos \theta_t$	$K(\theta_1)$	$K(\theta_t)$	$K(\theta_1) \cdot K(\theta_t)$	$K(\theta)$	$(\tau\alpha) / (\tau\alpha)_n$
	Jan	34.66	0.82	0.69	74.14	0.96	0.27	44.23	0.70	0.72	26.35	0.90	25.75	0.90	NA	NA	NA	0.96
Feb	37.33	0.80	0.76	67.06	0.92	0.39	51.79	0.79	0.62	25.25	0.90	30.93	0.86	NA	NA	NA	0.96	1.00
Mar	42.65	0.74	0.92	57.86	0.85	0.53	63.54	0.90	0.45	22.32	0.93	39.51	0.77	NA	NA	NA	0.96	1.00
Apr	50.27	0.64	1.20	47.93	0.74	0.67	80.69	0.99	0.16	11.02	0.98	49.90	0.64	NA	NA	NA	0.96	1.00
May	57.10	0.54	1.55	40.58	0.65	0.76	99.38	0.99	-0.16	-14.14	0.97	56.75	0.55	NA	NA	NA	0.96	1.00
Jun	60.38	0.49	1.76	37.45	0.61	0.79	110.47	0.94	-0.35	-31.60	0.85	58.75	0.52	NA	NA	NA	0.96	1.00
Jul	58.92	0.52	1.66	38.81	0.63	0.78	105.29	0.96	-0.26	-23.63	0.92	58.00	0.53	NA	NA	NA	0.96	1.00
Aug	53.15	0.60	1.33	44.69	0.70	0.71	88.01	1.00	0.03	2.65	1.00	53.13	0.60	NA	NA	NA	0.96	1.00
Sep	45.47	0.70	1.02	53.90	0.81	0.59	69.63	0.94	0.35	19.49	0.94	43.62	0.72	NA	NA	NA	0.96	1.00
Oct	38.83	0.78	0.80	64.10	0.90	0.44	55.27	0.82	0.57	24.63	0.91	33.48	0.83	NA	NA	NA	0.96	1.00
Nov	35.20	0.82	0.71	72.35	0.95	0.30	46.06	0.72	0.69	26.08	0.90	26.93	0.89	NA	NA	NA	0.96	1.00
Dec	34.19	0.83	0.68	76.05	0.97	0.24	42.32	0.67	0.74	26.67	0.89	24.58	0.91	NA	NA	NA	0.96	1.00

Table E- 6 F-CHART Final Calculations for Fraction of Loads Met by Solar

Month	T <sub>hi</sub> °C	ε <sub>L</sub>	m <sub>air</sub> L/sec	ε <sub>stnd</sub>	ε <sub>L</sub> / ε <sub>stnd</sub>	X	Y	X <sub>c</sub>	Y <sub>c</sub>	f	fL
Jan	80	0.48	1180	0.23	1	0.15	0.04	0.15	0.04	0.03	0.726
Feb	80	0.48	1180	0.23	1	0.17	0.05	0.17	0.05	0.04	0.811
Mar	80	0.48	1180	0.23	1	0.20	0.06	0.20	0.06	0.05	0.830
Apr	80	0.48	1180	0.23	1	0.30	0.09	0.30	0.09	0.07	0.694
May	80	0.48	1180	0.23	1	0.53	0.17	0.53	0.17	0.13	0.699
Jun	80	0.48	1180	0.23	1	0.88	0.30	0.88	0.29	0.23	0.659
Jul	80	0.48	1180	0.23	1	1.07	0.39	1.07	0.39	0.30	0.712
Aug	80	0.48	1180	0.23	1	1.00	0.36	1.00	0.36	0.28	0.731
Sep	80	0.48	1180	0.23	1	0.60	0.20	0.60	0.20	0.16	0.721
Oct	80	0.48	1180	0.23	1	0.34	0.11	0.34	0.10	0.08	0.741
Nov	80	0.48	1180	0.23	1	0.22	0.05	0.22	0.05	0.04	0.532
Dec	80	0.48	1180	0.23	1	0.17	0.03	0.17	0.03	0.02	0.525
										ΣfL =	8.382
										F =	0.063



## APPENDIX F

### ANALYSIS OF PHOTOVOLTAIC SYSTEM

The analysis of photovoltaic system was performed using the PV F-CHART program with TMY2 weather data. In PV F-CHART, the calculations are performed for each hour for an average day of each month and summed for the number of days of the month. For each hour, first the PV panel installation parameters (tilt and azimuth) are used with the location and monthly weather data (i.e., latitude, solar radiation and ground reflectance ) to synthesize hourly incident solar radiation on the collector plane ( $I_T$ ). Then, the panel and system parameters (i.e., array area and efficiency, array temperature coefficient, cell temperature at NOCT conditions, and efficiency of maximum power-point electronics and power-conditioning electronics) are used with the weather parameters to determine the array efficiency and electricity output at installed conditions. Next, the general utilizability is calculated for each hour using the electricity loads on the system. Finally, the fraction of loads met by solar “ $f$ ” is calculated. Combining the fraction of load met by solar electricity with the electricity loads on the system, useful electricity output from the system can be calculated.

An example calculation for the PV F-CHART program is presented in the following tables. Table F-1 shows the PV F-CHART input parameters and Table F-2 shows the annual summary of the PV F-CHART output.

Table F- 1 PV F-CHART Input Parameters

Weather Parameters				
Month	Radiation kJ/m <sup>2</sup>	Temp. °C	Hum kg/kg	Ground Reflectance
Jan	6409	-10.9	0.0010	0.39
Feb	9807	-7.6	0.0013	0.39
Mar	13511	-0.5	0.0024	0.23
Apr	16989	8.0	0.0039	0.12
May	20568	15.1	0.0063	0.12
Jun	22511	20.4	0.0095	0.12
Jul	22830	23.2	0.0115	0.12
Aug	19455	21.4	0.0108	0.12
Sep	14636	15.8	0.0079	0.12
Oct	10057	9.4	0.0049	0.12
Nov	6125	0.7	0.0029	0.18
Dec	4977	-7.6	0.0014	0.3

## System Parameters

City	MINNEAPOLIS	MN
Cell temperature at NOCT conditions	48.5	°C
Array reference efficiency	0.185	
Array reference temperature	25	°C
Array temperature coefficient * 1000	3.8	1/°C
Power tracking efficiency	0.88	
Power conditioning efficiency	0.9	
% standard deviation of load	Monthly	%
Array area (no. of panels X panel area)		m <sup>2</sup>
Array slope	Latitude	degrees
Array azimuth(South=0)	0	degrees

Table F- 2 PV F-CHART Output

Months	Solar [kW-hrs]	Efficiency [%]	Load [kW-hrs]	f [%]	Sell [kW-hrs]	Buy [kW-hrs]
Jan	2,078	16.55	0	100	309.6	0
Feb	2,352	16.26	0	100	344.1	0
Mar	2,881	15.65	0	100	405.8	0
Apr	2,960	15.08	0	100	401.8	0
May	3,275	14.61	0	100	430.5	0
Jun	3,305	14.26	0	100	424.3	0
Jul	3,548	14.09	0	100	450.0	0
Aug	3,349	14.25	0	100	429.7	0
Sep	2,821	14.67	0	100	372.5	0
Oct	2,423	15.26	0	100	332.7	0
Nov	1,692	15.93	0	100	242.5	0
Dec	1,551	16.55	0	100	231.0	0
Yr	32,235	0	0	100	4,375.0	0

## **APPENDIX G**

### **ANALYSIS OF WIND POWER SYSTEM**

The analysis of wind turbine output was performed to determine the monthly electricity output from wind turbines of different sizes taking into account their installation conditions. To accomplish this, measured hourly wind speed data for twelve years (1997-2008) was obtained from the NOAA weather stations in the six selected locations, and arranged to determine the monthly and annual wind speed frequency distribution for each year. The annual wind speed frequency distribution was then combined with the manufacturer's wind turbine power curves to determine the annual electricity output for the twelve years. The year with minimum annual electricity output was termed as the critical year. For the critical year, first the measured wind speed obtained from NOAA weather stations was corrected to take into account the impact of local terrain and tower height. Finally, the monthly electricity output was determined using the monthly, corrected wind speed frequency distribution with the turbine power curves. Table G-1 through Table G-18 show the analysis for the critical year for the six selected locations. For each location, three tables are included, which include:

1. Wind Speed Frequency at the NOAA Weather Station for the Critical Year,
2. Electricity Output for the Critical Year using the Measured Wind Speed Data from the NOAA Weather Stations; and
3. Electricity Output for the Critical Year using the Wind Speed Corrected for the Local Terrain and Tower Height

*Table G-1 Wind Speed Frequency at the NOAA Weather Station for the Critical Year (1998) in Minneapolis, MN*

Wind Speed		Wind Speed Frequency											
knots	mph	Jan	Feb	Mar	Apr	May	Jun	Jul	Aug	Sep	Oct	Nov	Dec
0	0.00	61	74	34	76	56	59	90	71	80	49	61	63
1	1.15	0	0	0	0	0	0	0	0	0	0	0	0
2	2.30	0	0	0	0	0	0	0	0	0	0	0	0
3	3.45	53	64	31	38	48	44	67	76	51	27	31	45
4	4.60	61	77	44	47	50	71	99	70	69	40	53	75
5	5.75	80	75	56	63	74	76	78	74	76	53	74	55
6	6.90	98	64	61	44	66	76	72	83	80	73	69	89
7	8.06	75	69	71	58	68	66	55	73	71	75	60	83
8	9.21	86	47	55	52	71	66	77	73	62	83	60	64
9	10.36	58	43	67	47	57	60	66	68	50	70	48	70
10	11.51	42	41	75	40	54	55	38	53	47	65	34	39
11	12.66	35	28	53	47	49	35	27	37	43	67	56	37
12	13.81	30	33	37	38	24	47	28	24	32	31	43	29
13	14.96	26	17	36	41	34	14	21	18	12	36	29	20
14	16.11	17	9	30	35	19	16	11	10	13	23	32	18
15	17.26	5	7	21	22	21	12	6	9	10	15	23	13
16	18.41	6	7	20	25	10	7	3	2	13	8	13	10
17	19.56	9	4	18	15	8	9	5	1	4	9	10	6
18	20.71	1	2	10	10	16	0	0	1	3	5	6	7
19	21.86	1	3	10	6	7	3	1	1	2	3	6	3
20	23.02	0	4	4	4	4	0	0	0	1	3	5	7
21	24.17	0	0	4	1	3	0	0	0	1	1	3	1
22	25.32	0	1	2	0	2	0	0	0	0	1	0	1
23	26.47	0	2	2	6	1	1	0	0	0	2	1	1
24	27.62	0	0	2	4	1	1	0	0	0	1	1	2
25	28.77	0	1	0	0	0	1	0	0	0	0	1	1
26	29.92	0	0	1	0	0	0	0	0	0	0	0	0
27	31.07	0	0	0	0	0	0	0	0	0	0	0	0
28	32.22	0	0	0	0	0	0	0	0	0	1	0	0
29	33.37	0	0	0	0	0	0	0	0	0	0	0	0
30	34.52	0	0	0	0	0	0	0	0	0	0	0	0
31	35.67	0	0	0	0	0	0	0	0	0	0	0	0
32	36.82	0	0	0	1	0	0	0	0	0	0	0	0
33	37.98	0	0	0	0	1	0	0	0	0	0	0	0
34	39.13	0	0	0	0	0	0	0	0	0	0	0	0
35	40.28	0	0	0	0	0	0	0	0	0	0	0	0
36	41.43	0	0	0	0	0	0	0	0	0	0	0	0
37	42.58	0	0	0	0	0	0	0	0	0	0	0	0
38	43.73	0	0	0	0	0	1	0	0	0	0	0	0
39	44.88	0	0	0	0	0	0	0	0	0	0	0	0
40	46.03	0	0	0	0	0	0	0	0	0	0	0	0
41	47.18	0	0	0	0	0	0	0	0	0	0	0	0
42	48.33	0	0	0	0	0	0	0	0	0	0	0	0
43	49.48	0	0	0	0	0	0	0	0	0	0	0	0
44	50.63	0	0	0	0	0	0	0	0	0	0	0	0
45	51.79	0	0	0	0	0	0	0	0	0	0	0	0
Hours Data Available		744	672	744	720	744	720	744	744	720	741	719	739
Missing Data		0.00%	9.68%	0.00%	3.23%	0.00%	3.23%	0.00%	0.00%	3.23%	0.40%	3.36%	0.67%





Table G- 4 Wind Speed Frequency at the NOAA Weather Station for the Critical Year (1998) in Denver, CO (Used for Boulder, CO)

Wind Speed		Wind Speed Frequency											
knots	mph	Jan	Feb	Mar	Apr	May	Jun	Jul	Aug	Sep	Oct	Nov	Dec
0	0.00	49	57	23	23	27	17	40	48	11	29	48	27
1	1.15	0	0	0	0	0	0	0	0	0	0	0	0
2	2.30	0	0	0	0	0	0	0	0	0	0	0	0
3	3.45	34	42	24	28	35	30	33	36	31	38	29	40
4	4.60	61	66	36	41	33	48	69	60	40	55	49	56
5	5.75	77	87	62	70	65	58	78	62	66	85	72	55
6	6.90	74	71	71	71	53	59	85	76	75	90	80	76
7	8.06	86	77	81	68	66	71	85	92	80	95	68	73
8	9.21	77	53	95	80	74	68	90	81	96	87	63	79
9	10.36	63	40	76	72	66	71	59	72	78	78	62	63
10	11.51	54	42	55	69	49	60	53	60	66	53	56	49
11	12.66	38	39	45	40	58	44	44	46	51	40	47	56
12	13.81	37	16	37	46	44	35	27	41	35	26	39	49
13	14.96	27	13	30	30	34	33	24	29	30	22	23	40
14	16.11	19	5	19	28	40	29	18	13	22	12	23	21
15	17.26	19	6	17	7	25	22	8	6	14	10	17	21
16	18.41	15	8	21	10	16	11	8	7	8	9	11	9
17	19.56	9	3	8	7	18	18	6	6	3	2	9	3
18	20.71	1	1	4	8	10	10	3	2	5	5	5	7
19	21.86	1	2	4	4	10	11	2	2	3	1	8	2
20	23.02	1	2	3	9	7	9	4	0	2	1	3	2
21	24.17	0	2	3	1	4	5	2	4	0	1	1	3
22	25.32	0	0	3	2	2	4	0	0	1	1	3	2
23	26.47	1	3	1	3	2	2	1	1	3	1	2	1
24	27.62	0	1	0	0	2	1	0	0	0	1	1	2
25	28.77	0	0	1	1	2	0	2	0	0	1	0	2
26	29.92	1	0	0	0	1	3	1	0	0	1	1	0
27	31.07	0	1	0	1	1	1	1	0	0	0	0	0
28	32.22	0	0	0	0	0	0	0	0	0	0	0	1
29	33.37	0	1	0	0	0	0	0	0	0	0	0	1
30	34.52	0	0	0	0	0	0	0	0	0	0	0	1
31	35.67	0	0	1	0	0	0	0	0	0	0	0	0
32	36.82	0	0	0	0	0	0	0	0	0	0	0	0
33	37.98	0	0	0	0	0	0	0	0	0	0	0	0
34	39.13	0	0	0	0	0	0	0	0	0	0	0	0
35	40.28	0	0	0	0	0	0	1	0	0	0	0	0
36	41.43	0	0	0	0	0	0	0	0	0	0	0	0
37	42.58	0	0	0	0	0	0	0	0	0	0	0	0
38	43.73	0	0	0	0	0	0	0	0	0	0	0	0
39	44.88	0	0	0	0	0	0	0	0	0	0	0	0
40	46.03	0	0	0	0	0	0	0	0	0	0	0	0
41	47.18	0	0	0	0	0	0	0	0	0	0	0	0
42	48.33	0	0	0	0	0	0	0	0	0	0	0	0
43	49.48	0	0	0	0	0	0	0	0	0	0	0	0
44	50.63	0	0	0	0	0	0	0	0	0	0	0	0
45	51.79	0	0	0	0	0	0	0	0	0	0	0	0
Hours Data Available		744	744	638	720	719	744	720	744	744	720	744	720
Missing Data		0.00%	0.00%	14.25%	3.23%	3.36%	0.00%	3.23%	0.00%	0.00%	3.23%	0.00%	3.23%







Table G- 7 Wind Speed Frequency at the NOAA Weather Station for the Critical Year (2001) in Atlanta, GA

Wind Speed		Wind Speed Frequency											
knots	mph	Jan	Feb	Mar	Apr	May	Jun	Jul	Aug	Sep	Oct	Nov	Dec
0	0.00	51	58	40	82	88	90	110	98	80	97	73	34
1	1.15	0	0	0	0	0	0	0	0	0	0	0	0
2	2.30	0	0	0	0	0	0	0	0	0	0	0	0
3	3.45	40	71	49	89	100	81	69	105	67	68	81	56
4	4.60	63	64	50	92	117	83	85	110	94	65	99	52
5	5.75	80	70	59	96	99	126	103	109	87	76	95	89
6	6.90	88	76	63	75	90	97	95	99	103	88	80	102
7	8.06	119	72	72	69	76	89	81	80	76	75	80	84
8	9.21	66	51	72	43	44	46	78	53	70	69	63	74
9	10.36	60	51	39	50	31	31	46	37	48	35	47	61
10	11.51	38	32	47	23	26	31	32	20	36	46	49	57
11	12.66	38	39	44	26	25	17	21	20	21	29	21	45
12	13.81	20	25	41	13	20	13	9	6	14	22	10	40
13	14.96	28	18	32	16	8	8	9	5	5	29	13	15
14	16.11	19	21	34	6	10	3	1	1	6	11	5	17
15	17.26	7	14	23	11	5	2	3	0	3	14	1	9
16	18.41	16	4	16	8	1	2	0	1	3	7	2	3
17	19.56	6	1	20	4	3	0	1	0	2	6	1	3
18	20.71	2	1	7	6	0	0	0	0	4	6	0	2
19	21.86	1	1	10	3	1	0	0	0	0	1	0	1
20	23.02	0	0	3	2	0	1	0	0	1	0	0	0
21	24.17	0	0	7	1	0	0	0	0	0	0	0	0
22	25.32	0	1	4	2	0	0	0	0	0	0	0	0
23	26.47	0	2	2	2	0	0	0	0	0	0	0	0
24	27.62	0	0	2	1	0	0	0	0	0	0	0	0
25	28.77	0	0	1	0	0	0	0	0	0	0	0	0
26	29.92	0	0	5	0	0	0	0	0	0	0	0	0
27	31.07	0	0	0	0	0	0	0	0	0	0	0	0
28	32.22	0	0	1	0	0	0	1	0	0	0	0	0
29	33.37	0	0	1	0	0	0	0	0	0	0	0	0
30	34.52	0	0	0	0	0	0	0	0	0	0	0	0
31	35.67	0	0	0	0	0	0	0	0	0	0	0	0
32	36.82	0	0	0	0	0	0	0	0	0	0	0	0
33	37.98	0	0	0	0	0	0	0	0	0	0	0	0
34	39.13	0	0	0	0	0	0	0	0	0	0	0	0
35	40.28	0	0	0	0	0	0	0	0	0	0	0	0
36	41.43	0	0	0	0	0	0	0	0	0	0	0	0
37	42.58	0	0	0	0	0	0	0	0	0	0	0	0
38	43.73	0	0	0	0	0	0	0	0	0	0	0	0
39	44.88	0	0	0	0	0	0	0	0	0	0	0	0
40	46.03	0	0	0	0	0	0	0	0	0	0	0	0
41	47.18	0	0	0	0	0	0	0	0	0	0	0	0
42	48.33	0	0	0	0	0	0	0	0	0	0	0	0
43	49.48	0	0	0	0	0	0	0	0	0	0	0	0
44	50.63	0	0	0	0	0	0	0	0	0	0	0	0
45	51.79	0	0	0	0	0	0	0	0	0	0	0	0
Hours Data Available		742	672	744	720	744	720	744	744	720	744	720	744
Missing Data		0.27%	9.68%	0.00%	3.23%	0.00%	3.23%	0.00%	0.00%	3.23%	0.00%	3.23%	0.00%





*Table G- 10 Wind Speed Frequency at the NOAA Weather Station for the Critical Year (1997) in Houston, TX*

Wind Speed		Wind Speed Frequency											
knots	mph	Jan	Feb	Mar	Apr	May	Jun	Jul	Aug	Sep	Oct	Nov	Dec
0	0.00	95	77	121	102	166	228	292	229	202	138	127	191
1	1.15	0	0	0	0	0	0	0	0	0	0	0	0
2	2.30	0	0	0	0	0	0	0	0	0	0	0	0
3	3.45	66	38	65	40	83	81	117	66	72	73	76	72
4	4.60	71	51	72	52	80	85	111	75	82	87	95	79
5	5.75	102	66	88	63	97	77	79	82	74	88	99	79
6	6.90	80	74	94	75	57	78	49	87	59	74	83	63
7	8.06	83	75	68	72	70	59	27	73	50	60	61	67
8	9.21	59	66	81	60	52	36	30	43	42	68	53	56
9	10.36	55	61	59	59	47	28	14	35	24	52	46	32
10	11.51	40	45	36	52	41	12	10	21	10	36	37	40
11	12.66	26	43	27	41	20	12	7	11	18	26	17	31
12	13.81	16	22	16	33	10	6	1	11	8	21	12	14
13	14.96	8	14	3	18	4	6	2	6	5	7	4	7
14	16.11	5	9	4	21	2	6	1	2	5	5	2	4
15	17.26	4	6	4	12	3	3	2	0	0	6	2	3
16	18.41	2	3	4	6	1	1	1	1	1	2	2	4
17	19.56	0	4	1	5	1	1	0	2	0	1	1	0
18	20.71	0	4	0	1	0	1	1	0	0	0	2	0
19	21.86	0	2	0	1	1	0	0	0	0	0	0	0
20	23.02	0	0	0	0	0	0	0	0	0	0	0	0
21	24.17	0	1	0	0	0	0	0	0	0	0	1	0
22	25.32	0	0	0	1	0	0	0	0	0	0	0	0
23	26.47	0	0	0	1	0	0	0	0	0	0	0	0
24	27.62	0	0	0	1	0	0	0	0	0	0	0	0
25	28.77	0	0	0	0	0	0	0	0	0	0	0	0
26	29.92	0	0	0	0	0	0	0	0	0	0	0	0
27	31.07	0	1	0	0	0	0	0	0	0	0	0	0
28	32.22	0	0	0	0	0	0	0	0	0	0	0	0
29	33.37	0	0	0	0	0	0	0	0	0	0	0	0
30	34.52	0	0	0	0	0	0	0	0	0	0	0	0
31	35.67	0	0	0	0	0	0	0	0	0	0	0	0
32	36.82	0	0	0	0	0	0	0	0	0	0	0	0
33	37.98	0	0	0	0	0	0	0	0	0	0	0	0
34	39.13	0	0	0	0	0	0	0	0	0	0	0	0
35	40.28	0	0	0	0	0	0	0	0	0	0	0	0
36	41.43	0	0	0	0	0	0	0	0	0	0	0	0
37	42.58	0	0	0	0	0	0	0	0	0	0	0	0
38	43.73	0	0	0	0	0	0	0	0	0	0	0	0
39	44.88	0	0	0	0	0	0	0	0	0	0	0	0
40	46.03	0	0	0	0	0	0	0	0	0	0	0	0
41	47.18	0	0	0	0	0	0	0	0	0	0	0	0
42	48.33	0	0	0	0	0	0	0	0	0	0	0	0
43	49.48	0	0	0	0	0	0	0	0	0	0	0	0
44	50.63	0	0	0	0	0	0	0	0	0	0	0	0
45	51.79	0	0	0	0	0	0	0	0	0	0	0	0
Hours Data Available		712	662	743	716	735	720	744	744	652	744	720	742
Missing Data		4.30%	11.02%	0.13%	3.76%	1.21%	3.23%	0.00%	0.00%	12.37%	0.00%	3.23%	0.27%





Table G- 13 Wind Speed Frequency at the NOAA Weather Station for the Critical Year (2000) in Phoenix, AZ

Wind Speed		Wind Speed Frequency											
knots	mph	Jan	Feb	Mar	Apr	May	Jun	Jul	Aug	Sep	Oct	Nov	Dec
0	0.00	223	159	144	95	102	87	76	87	127	148	139	171
1	1.15	0	0	0	0	0	0	0	0	0	0	0	0
2	2.30	0	0	0	0	0	0	0	0	0	0	0	0
3	3.45	164	105	123	75	83	85	82	103	122	123	102	111
4	4.60	128	104	130	117	97	89	118	102	140	134	119	131
5	5.75	91	102	102	115	100	106	124	97	105	87	120	114
6	6.90	61	65	86	92	107	88	91	92	74	70	93	89
7	8.06	38	41	56	61	72	62	70	70	58	59	61	46
8	9.21	12	23	33	46	51	52	61	51	31	35	31	29
9	10.36	9	24	26	34	29	46	51	40	16	31	21	17
10	11.51	4	7	14	19	32	36	31	40	22	15	20	9
11	12.66	4	13	10	26	28	27	17	18	11	12	6	10
12	13.81	3	12	2	9	15	14	8	13	5	9	2	4
13	14.96	0	7	4	10	6	10	4	8	5	10	1	4
14	16.11	1	2	6	6	7	6	1	8	0	4	3	3
15	17.26	1	4	2	6	3	2	2	5	1	2	0	3
16	18.41	2	1	1	0	2	4	0	5	3	4	1	0
17	19.56	2	1	2	1	0	2	4	1	0	1	1	0
18	20.71	0	1	1	2	4	0	1	0	0	0	0	1
19	21.86	0	0	0	2	2	0	1	1	0	0	0	1
20	23.02	0	1	2	3	2	2	2	0	0	0	0	0
21	24.17	0	0	0	1	1	0	0	1	0	0	0	0
22	25.32	0	0	0	0	0	1	0	0	0	0	0	0
23	26.47	0	0	0	0	0	1	0	1	0	0	0	1
24	27.62	0	0	0	0	0	0	0	0	0	0	0	0
25	28.77	0	0	0	0	0	0	0	1	0	0	0	0
26	29.92	0	0	0	0	0	0	0	0	0	0	0	0
27	31.07	0	0	0	0	0	0	0	0	0	0	0	0
28	32.22	0	0	0	0	0	0	0	0	0	0	0	0
29	33.37	0	0	0	0	0	0	0	0	0	0	0	0
30	34.52	0	0	0	0	0	0	0	0	0	0	0	0
31	35.67	0	0	0	0	0	0	0	0	0	0	0	0
32	36.82	0	0	0	0	0	0	0	0	0	0	0	0
33	37.98	0	0	0	0	0	0	0	0	0	0	0	0
34	39.13	0	0	0	0	0	0	0	0	0	0	0	0
35	40.28	0	0	0	0	0	0	0	0	0	0	0	0
36	41.43	0	0	0	0	0	0	0	0	0	0	0	0
37	42.58	0	0	0	0	0	0	0	0	0	0	0	0
38	43.73	0	0	0	0	0	0	0	0	0	0	0	0
39	44.88	0	0	0	0	0	0	0	0	0	0	0	0
40	46.03	0	0	0	0	0	0	0	0	0	0	0	0
41	47.18	0	0	0	0	0	0	0	0	0	0	0	0
42	48.33	0	0	0	0	0	0	0	0	0	0	0	0
43	49.48	0	0	0	0	0	0	0	0	0	0	0	0
44	50.63	0	0	0	0	0	0	0	0	0	0	0	0
45	51.79	0	0	0	0	0	0	0	0	0	0	0	0
Hours Data Available		743	672	744	720	743	720	744	744	720	744	720	744
Missing Data		0.13%	9.68%	0.00%	3.23%	0.13%	3.23%	0.00%	0.00%	3.23%	0.00%	3.23%	0.00%







Table G- 16 Wind Speed Frequency at the NOAA Weather Station for the Critical Year (1999) in Los Angeles, CA

Wind Speed		Wind Speed Frequency											
knots	mph	Jan	Feb	Mar	Apr	May	Jun	Jul	Aug	Sep	Oct	Nov	Dec
0	0.00	104	83	67	58	73	60	60	90	71	124	128	97
1	1.15	0	0	0	0	0	0	0	0	0	0	0	0
2	2.30	0	0	0	0	0	0	0	0	0	0	0	0
3	3.45	88	87	80	60	59	71	57	93	67	94	86	106
4	4.60	114	93	70	64	74	77	81	93	98	102	90	129
5	5.75	97	71	99	61	70	71	101	63	69	83	84	93
6	6.90	93	56	62	72	79	70	65	55	78	74	74	79
7	8.06	68	53	54	67	73	61	55	51	56	64	48	79
8	9.21	56	48	56	58	70	41	49	53	51	49	59	57
9	10.36	30	40	57	56	40	54	60	37	53	54	37	34
10	11.51	32	43	44	65	48	52	44	62	46	37	46	22
11	12.66	20	36	55	37	57	58	56	44	38	36	27	8
12	13.81	17	21	33	34	44	64	50	49	33	14	9	14
13	14.96	12	15	21	21	25	30	37	26	21	7	14	9
14	16.11	1	7	12	15	17	7	17	16	19	4	7	5
15	17.26	8	2	10	13	8	2	8	6	8	1	1	2
16	18.41	2	4	8	4	5	1	3	4	2	0	3	2
17	19.56	1	4	4	7	1	1	1	1	1	0	1	4
18	20.71	1	6	4	4	0	0	0	1	1	0	0	1
19	21.86	0	1	0	1	1	0	0	0	0	0	1	0
20	23.02	0	0	0	2	0	0	0	0	0	0	3	0
21	24.17	0	0	1	1	0	0	0	0	0	0	0	0
22	25.32	0	0	1	2	0	0	0	0	0	0	1	0
23	26.47	0	0	2	2	0	0	0	0	0	0	1	0
24	27.62	0	1	1	2	0	0	0	0	0	0	0	0
25	28.77	0	0	1	3	0	0	0	0	0	0	0	0
26	29.92	0	0	1	3	0	0	0	0	0	0	0	0
27	31.07	0	0	0	1	0	0	0	0	0	0	0	0
28	32.22	0	0	0	2	0	0	0	0	0	0	0	0
29	33.37	0	0	1	0	0	0	0	0	0	0	0	0
30	34.52	0	0	0	0	0	0	0	0	0	0	0	0
31	35.67	0	0	0	2	0	0	0	0	0	0	0	0
32	36.82	0	0	0	0	0	0	0	0	0	0	0	0
33	37.98	0	0	0	1	0	0	0	0	0	0	0	0
34	39.13	0	0	0	0	0	0	0	0	0	0	0	0
35	40.28	0	0	0	0	0	0	0	0	0	0	0	0
36	41.43	0	0	0	0	0	0	0	0	0	0	0	0
37	42.58	0	0	0	0	0	0	0	0	0	0	0	0
38	43.73	0	0	0	0	0	0	0	0	0	0	0	0
39	44.88	0	0	0	0	0	0	0	0	0	0	0	0
40	46.03	0	0	0	0	0	0	0	0	0	0	0	0
41	47.18	0	0	0	0	0	0	0	0	0	0	0	0
42	48.33	0	0	0	0	0	0	0	0	0	0	0	0
43	49.48	0	0	0	0	0	0	0	0	0	0	0	0
44	50.63	0	0	0	0	0	0	0	0	0	0	0	0
45	51.79	0	0	0	0	0	0	0	0	0	0	0	0
Hours Data Available		744	671	744	718	744	720	744	744	712	743	720	741
Missing Data		0.00%	9.81%	0.00%	3.49%	0.00%	3.23%	0.00%	0.00%	4.30%	0.13%	3.23%	0.40%





**APPENDIX H**  
**ANALYSIS OF RAINWATER HARVESTING SYSTEM**

The analysis of rainwater harvesting system was performed to determine the normalized system sizing parameters (i.e., the catchment area and storage size requirements per unit gallon of average daily water demand). To accomplish this, first daily rainfall data for twelve years (1997-2008) from the NOAA weather stations for the six selected locations were obtained. For each year, monthly calculations were first performed for a unit catchment area to obtain average daily demand fulfilled (gal per day/sq. ft. of catchment area) and storage requirements (gal/sq. ft. of catchment area), assuming full utilization of the harvested rainwater. Finally, these calculations for the twelve years were used for determining the system sizing requirements per unit daily demand. Table H- 1 shows an example monthly calculation using one year of daily rainfall data (1997) for Minneapolis, MN. Table H- 2 through Table H- 7 show the final calculations for determining the normalized system sizing parameters for the six selected locations, which are based on the twelve years of monthly calculations.

*Table H- 1 Example Monthly Calculations for a Year for Determining System Sizing Requirements per Unit Catchment Area*

Month	Monthly Rainfall Statistics					Analysis (per Unit Catchment Area)						
	Monthly Rainfall		Occurrence days	Number of Days Requiring First Flush		First- flush Volume gal/sqft	Harvestable Rainwater gal/sqft	Avg. Daily Demand gpd/sqft	Cumulative Supply gal/sqft	Cumulative Demand gal/sqft	Cum. Supply - Cum. Demand gal/sqft	
	inch	gal/sqft		days	days							%
	{1}	{2}	{3}={2}*7.48/12	{4}	{5}	{6}={5}/({4})	{7}	{8}	{9}=Σ{8}/Σn	{10}=Cum.{8}	{11}=Cum.({9}*n)	{12}={10}-{11}
Jan	0.60	0.37		11	3.6	32.9%	0.04	0.34	0.053	0.34	1.63	-1.30
Feb	0.07	0.04		3	2.6	87.4%	0.03	0.02	0.053	0.36	3.11	-2.75
Mar	0.46	0.29		7	3.0	42.9%	0.03	0.26	0.053	0.61	4.74	-4.13
Apr	0.97	0.60		10	3.6	36.2%	0.04	0.57	0.053	1.18	6.32	-5.14
May	1.65	1.03		13	3.0	23.1%	0.03	1.00	0.053	2.18	7.95	-5.78 (Max. Deficit)
Jun	3.70	2.31		11	3.6	32.9%	0.04	2.27	0.053	4.45	9.53	-5.09
Jul	12.44	7.75		19	3.0	15.8%	0.03	7.72	0.053	12.17	11.17	1.01
Aug	6.01	3.75		12	2.0	16.7%	0.02	3.73	0.053	15.90	12.80	3.10
Sep	3.21	2.00		10	3.0	30.0%	0.03	1.97	0.053	17.87	14.38	3.49 (Max. Surplus)
Oct	2.03	1.27		8	3.6	45.3%	0.04	1.23	0.053	19.10	16.01	3.09
Nov	0.15	0.09		6	1.6	27.1%	0.02	0.08	0.053	19.18	17.59	1.58
Dec	0.12	0.07		6	2.6	43.7%	0.03	0.05	0.053	19.23	19.23	0.00
<b>TOTAL</b>	<b>31.41</b>	<b>19.58</b>		<b>116</b>	<b>35.4</b>	<b>30.5%</b>	<b>0.35</b>	<b>19.2</b>		<b>Storage Size Requirement</b>		<b>9.27</b>

*Table H- 2 Calculations for the Normalized Rainwater Harvesting System Sizing Parameters for Minneapolis, MN*

Annual Rainfall Statistics (from Monthly Statistics)						System Sizing (per Unit Catchment Area)						System Sizing (per Unit Daily Demand)	
Year	Annual Rainfall		Occurrence	Number of Days Requiring First Flush		First- flush Volume	Harvestable Rainwater	Avg. Daily Demand	Max. Surplus Volume	Max. Deficit Volume	Storage Requirement	Catchment Area Requirement	Storage Requirement
	inch	gal/sqft		days	days								
[1]	[2]	[3]	[4]	[5]	[6]	[7]	[8]	[9]=[8]/N	[10]=max{12}mo	[13]=1/[9]	[14] = [12]/[9]	[13]=1/[9]	[14] = [12]/[9]
1997	31.4	19.6	116	35.4	30.5%	0.35	19.2	0.053	3.49	5.78	9.27	10.1	50
1998	30.9	19.2	115	27.5	23.9%	0.27	19.0	0.052	3.24	2.37	5.62	10.8	103
1999	27.0	16.8	107	26.5	24.8%	0.26	16.5	0.045	3.17	3.13	6.30	23.4	88
2000	27.3	17.0	90	29.0	32.2%	0.29	16.7	0.046	1.81	3.90	5.71	12.5	77
2001	30.9	19.3	106	24.1	22.8%	0.24	19.0	0.052	2.37	3.55	5.93	8.3	72
2002	36.1	22.5	101	24.9	24.6%	0.25	22.3	0.061	3.60	5.20	8.80	10.2	95
2003	21.7	13.5	81	31.4	38.7%	0.31	13.2	0.036	2.67	2.28	4.95	13.2	87
2004	26.3	16.4	104	31.5	30.3%	0.31	16.1	0.044	1.95	2.53	4.48	9.1	88
2005	32.6	20.3	115	34.0	29.6%	0.34	20.0	0.055	2.03	3.35	5.39	14.7	60
2006	26.7	16.7	106	36.7	34.7%	0.37	16.3	0.045	2.06	2.69	4.76	10.2	105
2007	32.2	20.1	99	29.5	29.8%	0.29	19.8	0.054	2.45	4.61	7.06	9.2	46
2008	21.1	13.2	118	34.4	29.1%	0.34	12.8	0.035	0.98	2.18	3.16	13.4	71
Avg.	28.7	17.9	105	30.4	29.2%	0.30	17.6	0.048	2.5	3.5	6.0	12.1	79
Min.	21.1	13.2	81	24.1	22.8%	0.24	12.8	0.035	1.0	2.2	3.2	8.3	46
Max.	36.1	22.5	118	36.7	38.7%	0.37	22.3	0.061	3.6	5.8	9.3	23.4	105

*Table H- 3 Calculations for the Normalized Rainwater Harvesting System Sizing Parameters for Boulder, CO (Using the Rainfall Data from the NOAA Weather Station in Denver, CO)*

Annual Rainfall Statistics (from Monthly Statistics)						System Sizing (per Unit Catchment Area)						System Sizing (per Unit Daily Demand)	
Year	Annual Rainfall		Occurrence	Number of Days Requiring First Flush		First- flush Volume	Harvestable Rainwater	Avg. Daily Demand	Max. Surplus Volume	Max. Deficit Volume	Storage Requirement	Catchment Area Requirement	Storage Requirement
	inch	gal/sqft		days	days								
[1]	[2]	[3]	[4]	[5]	[6]	[7]	[8]	[9]=[8]/N	[10]=max{12}mo	[13]=1/[9]	[14] = [12]/[9]	[13]=1/[9]	[14] = [12]/[9]
1997	18.4	11.5	98	31.4	32.0%	0.31	11.2	0.031	1.74	2.42	4.16	32.7	136
1998	15.9	9.9	87	26.9	30.9%	0.27	9.7	0.026	1.71	1.71	3.42	37.8	129
1999	19.5	12.2	83	28.9	34.8%	0.29	11.9	0.033	2.69	2.55	5.24	30.7	161
2000	13.7	8.5	81	32.5	40.1%	0.32	8.2	0.022	1.20	1.08	2.28	44.6	102
2001	15.1	9.4	83	30.7	37.0%	0.31	9.1	0.025	2.29	0.74	3.04	40.1	122
2002	7.3	4.6	59	29.5	50.0%	0.29	4.3	0.012	0.65	0.63	1.29	85.8	110
2003	13.0	8.1	73	22.7	31.2%	0.23	7.9	0.022	2.64	0.98	3.62	46.5	168
2004	14.5	9.1	83	36.0	43.4%	0.36	8.7	0.024	1.43	1.91	3.34	42.1	141
2005	12.8	8.0	75	31.5	42.0%	0.31	7.7	0.021	1.09	1.35	2.44	47.6	116
2006	8.7	5.4	71	33.1	46.6%	0.33	5.1	0.014	0.00	1.02	1.02	71.8	73
2007	13.9	8.6	82	39.7	48.5%	0.40	8.2	0.023	1.00	1.22	2.22	44.3	98
2008	10.3	6.4	69	29.7	43.1%	0.30	6.1	0.017	0.81	1.67	2.48	60.0	149
Avg.	13.6	8.5	79	31.1	40.0%	0.31	8.2	0.022	1.4	1.4	2.9	48.7	125
Min.	7.3	4.6	59	22.7	30.9%	0.23	4.3	0.012	0.0	0.6	1.0	30.7	73
Max.	19.5	12.2	98	39.7	50.0%	0.40	11.9	0.033	2.7	2.5	5.2	85.8	168

Table H- 4 Calculations for the Normalized Rainwater Harvesting System Sizing Parameters for Atlanta, GA

Annual Rainfall Statistics (from Monthly Statistics)						System Sizing (per Unit Catchment Area)						System Sizing (per Unit Daily Demand)	
Year	Annual Rainfall		Occurrence	Number of Days Requiring First Flush		First-flush Volume	Harvestable Rainwater	Avg. Daily Demand	Max. Surplus Volume	Max. Deficit Volume	Storage Requirement	Catchment Area Requirement	Storage Requirement
	inch	gal/sqft		days	days								
[1]	[2]	[3]	[4]	[5]	[6]	[7]	[8]	[9]=[8]/N	[10]=max{12}mo	[13]=1/[9]	[14] = [12]/[9]	[13]=1/[9]	[14] = [12]/[9]
1997	48.5	30.2	126	34.5	27.4%	0.34	29.9	0.082	2.24	0.89	3.14	12.2	38
1998	46.3	28.8	118	29.2	24.8%	0.29	28.5	0.078	5.64	0.00	5.64	12.8	72
1999	38.6	24.1	105	34.9	33.2%	0.35	23.7	0.065	1.71	0.75	2.46	15.4	38
2000	35.0	21.8	111	29.7	26.8%	0.30	21.5	0.059	1.19	1.71	2.91	17.0	49
2001	39.3	24.5	114	23.5	20.6%	0.23	24.3	0.066	5.80	0.35	6.15	15.1	93
2002	46.3	28.9	118	33.2	28.2%	0.33	28.5	0.078	1.16	3.81	4.97	12.8	64
2003	51.2	31.9	126	35.6	28.3%	0.36	31.6	0.086	5.29	1.73	7.02	11.6	81
2004	51.5	32.1	110	35.1	31.9%	0.35	31.7	0.087	0.00	6.72	6.72	11.5	78
2005	56.6	35.3	119	33.7	28.4%	0.34	35.0	0.096	6.26	2.03	8.29	10.4	87
2006	47.1	29.4	107	36.4	34.0%	0.36	29.0	0.080	1.77	1.67	3.45	12.6	43
2007	31.9	19.9	91	31.9	35.0%	0.32	19.5	0.054	0.88	1.30	2.18	18.7	41
2008	40.4	25.2	102	36.1	35.4%	0.36	24.8	0.068	1.99	0.59	2.58	14.7	38
Avg.	44.4	27.7	112	32.8	29.5%	0.33	27.3	0.075	2.8	1.8	4.6	13.7	60
Min.	31.9	19.9	91	23.5	20.6%	0.23	19.5	0.054	0.0	0.0	2.2	10.4	38
Max.	56.6	35.3	126	36.4	35.4%	0.36	35.0	0.096	6.3	6.7	8.3	18.7	93

Table H- 5 Calculations for the Normalized Rainwater Harvesting System Sizing Parameters for Houston, TX

Annual Rainfall Statistics (from Monthly Statistics)						System Sizing (per Unit Catchment Area)						System Sizing (per Unit Daily Demand)	
Year	Annual Rainfall		Occurrence	Number of Days Requiring First Flush		First-flush Volume	Harvestable Rainwater	Avg. Daily Demand	Max. Surplus Volume	Max. Deficit Volume	Storage Requirement	Catchment Area Requirement	Storage Requirement
	inch	gal/sqft		days	days								
[1]	[2]	[3]	[4]	[5]	[6]	[7]	[8]	[9]=[8]/N	[10]=max{12}mo	[13]=1/[9]	[14] = [12]/[9]	[13]=1/[9]	[14] = [12]/[9]
1997	58.5	36.4	128	32.7	25.6%	0.33	36.1	0.099	3.88	1.08	4.96	10.1	50
1998	54.8	34.1	116	29.6	25.5%	0.30	33.9	0.093	0.82	8.70	9.52	10.8	103
1999	25.5	15.9	95	30.2	31.8%	0.30	15.6	0.043	2.78	0.99	3.77	23.4	88
2000	47.7	29.7	113	36.0	31.8%	0.36	29.4	0.080	1.85	4.31	6.17	12.5	77
2001	71.3	44.4	129	29.1	22.6%	0.29	44.2	0.121	1.95	6.77	8.72	8.3	72
2002	58.3	36.3	107	35.1	32.8%	0.35	36.0	0.099	0.42	8.91	9.33	10.2	95
2003	44.9	28.0	107	27.7	25.9%	0.28	27.7	0.076	0.52	6.09	6.61	13.2	87
2004	64.8	40.4	124	33.2	26.8%	0.33	40.0	0.109	7.83	1.80	9.64	9.1	88
2005	40.3	25.1	87	32.1	36.9%	0.32	24.8	0.068	2.26	1.84	4.10	14.7	60
2006	57.9	36.1	101	31.5	31.2%	0.31	35.8	0.098	4.18	6.11	10.29	10.2	105
2007	64.4	40.1	128	30.6	23.9%	0.31	39.8	0.109	2.54	2.52	5.06	9.2	46
2008	44.6	27.8	93	35.9	38.6%	0.36	27.4	0.075	1.72	3.58	5.30	13.4	71
Avg.	52.7	32.9	111	32.0	29.5%	0.32	32.5	0.089	2.6	4.4	7.0	12.1	79
Min.	25.5	15.9	87	27.7	22.6%	0.28	15.6	0.043	0.4	1.0	3.8	8.3	46
Max.	71.3	44.4	129	36.0	38.6%	0.36	44.2	0.121	7.8	8.9	10.3	23.4	105



Table H- 6 Calculations for the Normalized Rainwater Harvesting System Sizing Parameters for Phoenix, AZ

Annual Rainfall Statistics (from Monthly Statistics)						System Sizing (per Unit Catchment Area)						System Sizing (per Unit Daily Demand)	
Year	Annual Rainfall		Occurrence	Number of Days Requiring First Flush		First-flush Volume	Harvestable Rainwater	Avg. Daily Demand	Max. Surplus Volume	Max. Deficit Volume	Storage Requirement	Catchment Area Requirement	Storage Requirement
	inch	gal/sqft		days	days								
[1]	[2]	[3]	[4]	[5]	[6]	[7]	[8]	[9]=[8]/N	[10]=max{12}mo	[13]=1/[9]	[14] = [12]/[9]	[13]=1/[9]	[14] = [12]/[9]
1997	4.3	2.6	35	16.9	48.2%	0.17	2.5	0.007	0.46	0.34	0.79	147.1	117
1998	9.9	6.1	43	17.2	40.1%	0.17	6.0	0.016	1.19	0.30	1.49	61.1	91
1999	6.6	4.1	32	14.2	44.5%	0.14	3.9	0.011	0.99	1.13	2.12	92.6	196
2000	7.5	4.7	32	11.1	34.7%	0.11	4.6	0.012	0.71	0.98	1.69	80.3	136
2001	6.7	4.2	33	19.6	59.5%	0.20	4.0	0.011	1.38	0.19	1.57	91.6	144
2002	2.7	1.7	19	11.0	57.9%	0.11	1.6	0.004	0.04	0.68	0.72	234.8	169
2003	6.3	4.0	29	15.6	53.9%	0.16	3.8	0.010	1.67	0.00	1.67	96.2	161
2004	8.0	5.0	41	17.9	43.6%	0.18	4.8	0.013	0.85	0.55	1.40	76.3	107
2005	7.0	4.4	37	12.6	34.1%	0.13	4.3	0.012	2.31	0.00	2.31	85.6	198
2006	5.5	3.4	25	11.2	45.0%	0.11	3.3	0.009	0.52	0.68	1.20	111.1	133
2007	5.1	3.1	32	19.2	60.1%	0.19	3.0	0.008	0.29	0.93	1.22	123.5	151
2008	9.6	6.0	39	12.1	31.1%	0.12	5.8	0.016	1.07	1.45	2.53	62.6	158
Avg.	6.6	4.1	33	14.9	46.1%	0.15	4.0	0.011	1.0	0.6	1.6	105.2	147
Min.	2.7	1.7	19	11.0	31.1%	0.11	1.6	0.004	0.0	0.0	0.7	61.1	91
Max.	9.9	6.1	43	19.6	60.1%	0.20	6.0	0.016	2.3	1.5	2.5	234.8	198

Table H- 7 Calculations for the Normalized Rainwater Harvesting System Sizing Parameters for Los Angeles, CA

Annual Rainfall Statistics (from Monthly Statistics)						System Sizing (per Unit Catchment Area)						System Sizing (per Unit Daily Demand)	
Year	Annual Rainfall		Occurrence	Number of Days Requiring First Flush		First-flush Volume	Harvestable Rainwater	Avg. Daily Demand	Max. Surplus Volume	Max. Deficit Volume	Storage Requirement	Catchment Area Requirement	Storage Requirement
	inch	gal/sqft		days	days								
[1]	[2]	[3]	[4]	[5]	[6]	[7]	[8]	[9]=[8]/N	[10]=max{12}mo	[13]=1/[9]	[14] = [12]/[9]	[13]=1/[9]	[14] = [12]/[9]
1997	6.9	4.3	17	6.9	40.4%	0.07	4.2	0.012	0.00	3.40	3.40	86.1	293
1998	27.0	16.8	69	15.6	22.6%	0.16	16.7	0.046	8.80	0.00	8.80	21.9	193
1999	7.1	4.4	42	16.6	39.5%	0.17	4.2	0.012	2.30	0.00	2.30	86.2	198
2000	11.3	7.0	51	17.0	33.3%	0.17	6.9	0.019	3.80	0.06	3.86	53.4	206
2001	17.0	10.6	57	16.6	29.1%	0.17	10.4	0.029	5.78	0.00	5.78	35.1	203
2002	5.0	3.1	31	16.1	52.0%	0.16	3.0	0.008	0.20	1.54	1.74	122.7	213
2003	8.9	5.5	28	12.5	44.6%	0.12	5.4	0.015	1.78	0.45	2.23	67.5	151
2004	15.8	9.8	35	14.4	41.0%	0.14	9.7	0.026	1.51	3.66	5.17	37.8	195
2005	17.9	11.2	51	16.7	32.8%	0.17	11.0	0.030	6.82	0.00	6.82	33.2	226
2006	9.2	5.7	42	17.4	41.3%	0.17	5.6	0.015	2.83	0.00	2.83	65.6	186
2007	4.9	3.0	26	13.5	51.9%	0.13	2.9	0.008	0.23	0.99	1.21	125.3	152
2008	12.0	7.5	33	11.2	34.1%	0.11	7.4	0.020	3.01	1.23	4.24	49.7	211
Avg.	11.9	7.4	40	14.5	38.6%	0.15	7.3	0.020	3.1	0.9	4.0	65.4	202
Min.	4.9	3.0	17	6.9	22.6%	0.07	2.9	0.008	0.0	0.0	1.2	21.9	151
Max.	27.0	16.8	69	17.4	52.0%	0.17	16.7	0.046	8.8	3.7	8.8	125.3	293

## APPENDIX I

### SPREADSHEETS FOR THE INTEGRATION OF RESULTS

The spreadsheets used for the calculations and analysis are presented here. It contains six sets of tables for each climate location. Each set consists of the following eight tables. Table I-2 through I-8 demonstrate an example for the integration of results for the sizing of renewable energy systems.

1. Weather Parameters (including Design Parameters)
2. Simulated Monthly and Peak Day Hourly Energy Use
3. Calculation of BuildingUA and  $T_{bal}$
4. Harvestable Renewable Energy
5. Selection/Sizing of Renewable Energy Systems
6. Sizing of Battery Storage System
7. Sizing of Rainwater harvesting System

#### **I.1. Weather Parameters**

These tables list monthly summary of weather data and monthly values for design parameters determined from weather parameters, which include:

1. Monthly heating degree-day (HDD65°F), cooling degree-day (CDD50°F), average dry bulb temperature (°F), diurnal temperature range (°F), relative humidity (%), global horizontal radiation (kWh/m<sup>2</sup>-day)
2. Average wind speed (mph) and daily average precipitation (inch/day) calculated from measured data obtained from NOAA
3. Daylight hours (for estimating operating hours of solar thermal pumps), number of frost days (for determining the impact on solar thermal system and battery storage system performance), minimum available insolation and available surplus insolation over consecutive day periods of 7 days, 14 days, 21 days and one month (as percent of average monthly insolation) based on 22-year period (1983-1995) obtained from NASA data.
4. HVAC system operation mode (heating or cooling on) and interior shade multipliers (0.85 for heating season and 0.7 for cooling season)
5. Indoor water use (gal/day), water mains temperature (°F), and domestic hot water use (gal/day) for the base case and the off-grid, off-pipe house.

#### **I.2. Simulated Monthly and Peak Days Hourly Energy Use**

These tables list the monthly and peak day hourly thermal energy and electricity use obtained from DOE-2 simulation output for the basecase house and the off-grid, off-pipe house. The thermal energy use include space heating energy loads obtained from SS-A report and domestic water heating loads

obtained from SS-P report. The electricity use include lighting, equipment, heating and cooling fans, and miscellaneous for the base case, and the additional auxiliary electricity use for operating solar thermal pump and indoor water supply pressurization pump. The monthly space heating loads was obtained from SS-A, domestic water heating loads from SS-P, and electricity end-use from PS-E reports. The hourly loads for peak days were obtained from HOURLY-REPORTS in SYSTEMS, VARIABLE-TYPE = END-USE, and in PLANT, VARIABLE-TYPE = PLANT-ASSIGNMENT. In addition, outdoor dry-bulb temperature and space temperatures (conditioned space and attic) were also obtained from HOURLY-REPORTS in SYSTEMS.

*Table I- 1: Sources for Monthly and Hourly End-use Energy Use*

	Monthly Loads	Peak Day Hourly Loads		
	DOE-2 Report	Location	VARIABLE-TYPE	VARIABLE-LIST
Outdoor Drybulb Temperature	-		GLOBAL	8
Room Temperature	-	LOADS	RM-1 (Name of Space)	1
Attic Temperature	-		ATTIC-1 (Name of Space)	1
Space Heating Loads	SS-A	SYSTEMS	<Name of PLANT- ASSIGNMENT>	2
Domestic Water Heating Loads	SS-P			131
Lighting				1
Equipment				3
Space Cooling Loads	PS-E	SYSTEMS	END-USE	6
Miscellaneous				8
Heating and Cooling Fans				9
Solar Thermal Pumps	Estimated		Estimated	
Water Supply Pressurization Pumps				

### **I.3. Calculation of BuildingUA and $T_{bal}$**

In order to calculate Building UA and  $T_{bal}$  for F-CHART input for solar thermal analysis, the average monthly temperature listed in weather parameters and space heating loads listed in Simulated energy use are tabulated to plot these values on an x-y scatter plot and obtain the intercept (c) and slope (m) from the linear curve-fit 'y = mx + c'. The slope '-m' denotes the BuildingUA and the ratio of intercept and slope '-c/m' denotes  $T_{bal}$ . This procedure was followed for both the base-case house and the off-grid, off-pipe house in order to compare the reduction in building heat loss coefficient.

### **I.4. Harvestable Renewable Energy**

This table lists the renewable energy harvestable from different sizes/capacities of wind turbines, photovoltaic panels and solar thermal system. A 2.5 kW and a 7.5 kW wind turbine, mono-crystalline and thin-film photovoltaic panels tilted at 0°, latitude – 15°, latitude and latitude + 15°, and flat-plate and evacuated solar thermal collectors. In addition, space heating and domestic water heating loads, and

electricity loads for the off-grid, off-pipe house are listed to facilitate comparison of supply and demand and determine/select the appropriate renewable system size.

### **I.5. Selection/Sizing of Renewable Energy Systems**

First the building's thermal loads are compared with available solar thermal energy. After selecting a size, the unmet thermal loads are added to the electricity loads. Now, based on the wind turbine output, appropriate turbine size was selected and the electricity demand was compared with the turbine output. For the remaining unmet electricity loads, PV system was sized to meet or exceed the loads.

### **I.6. Sizing of Battery Storage System**

This table includes:

1. Minimum available insolation over consecutive day periods of 7 days, 14 days, 21 days and one month.
2. Equivalent number of NO-SUN or BLACK days, with maximum values highlighted for each month
3. Electricity loads in order to calculate storage for NO-SUN days, with the maximum of the 12 monthly values highlighted
4. Available surplus insolation over consecutive day periods of 1-day, 3-day, 7-day, 14-day, 21-day and a month.
5. Equivalent number of SURPLUS days, with maximum values highlighted for each month
6. Electricity generated in order to calculate storage for SURPLUS days, with the maximum of the 12 monthly values highlighted

The maximum of three and six denotes the effective battery capacity for the location under consideration.

### **I.7. Sizing of Rainwater Harvesting System**

This table includes the steps followed for the sizing of rainwater harvesting system based on 12 years of measured rainfall data. It includes:

1. Rainfall statistics, which includes: monthly rainfall (inch/month), annual rainfall (inch/yr), number of days with rainfall occurrence, number of days requiring first flush volume diversion). The years corresponding to the maximum and minimum values for these statistics are highlighted. The average minimum and maximum values at the bottom of the tables are also listed.
2. The annual harvestable rainfall per unit area of catchment surface (gal/sq. ft.) considering full utilization of harvested rainwater. This denotes the rainwater supply or maximum demand fulfilled.
3. Storage volume required per unit area of catchment surface (gal/sq. ft.).
4. Catchment area and storage size requirement per unit of water demand.

Table I- 2: Weather Parameters for Minneapolis, MN

	Jan	Feb	Mar	Apr	May	Jun	Jul	Aug	Sep	Oct	Nov	Dec	Average	Total	
<b>WEATHER PARAMETERS</b>															
HDD65°F	F-days	1,661	1,314	986	504	189	23	7	5	133	518	932	1,460	-	7,735
CDD50°F	F-days	0	0	4	79	346	567	670	646	329	74	2	0	-	2,716
Average DBT	F	10.8	17.4	32.5	47.7	60.8	68.9	71.6	70.9	61.0	47.7	33.3	17.2	45.1	-
Average DPT	F	4.5	8.8	22.3	34.0	46.2	55.8	60.6	60.3	51.6	36.0	27.0	10.6	34.9	-
Diurnal Temp. Range	F	9.18	10.98	11.34	15.84	16.92	16.92	14.58	15.48	16.02	16.38	9.36	7.20	13.4	-
Relative Humidity	%	76.0	69.0	67.0	62.0	61.0	65.0	70.0	72.0	73.0	65.0	78.0	75.0	69.4	-
Global Hz. Radiation	kWh/m2-day	1.88	2.84	3.74	4.53	5.96	6.50	6.36	5.45	4.21	2.87	1.74	1.44	3.96	47.50
Wind Speed	mph	8.92	9.18	9.55	10.46	10.02	8.91	8.24	7.85	8.69	9.22	9.00	8.85	9.07	-
Rainfall	inch/mo	0.40	0.43	1.45	2.77	3.79	4.32	3.96	4.62	3.16	2.17	1.05	0.56	-	28.68
Frost Days	% of days	97%	93%	77%	30%	0%	0%	0%	0%	13%	73%	97%		-	145 days
Surface Albedo	0 to 1.0	0.39	0.39	0.23	0.12	0.12	0.12	0.12	0.12	0.12	0.12	0.18	0.30	0.19	-
Daylight Hours	hours	0.38	0.43	0.50	0.56	0.62	0.65	0.63	0.58	0.52	0.46	0.40	0.37	0.51	-
<b>DESIGN PARAMETERS</b>															
Heating On	0 or 1	1	1	1	1	1	1	0	0	1	1	1	1	-	-
Cooling On	0 or 1	0	0	0	0	1	1	1	1	1	0	0	0	-	-
Shade Multiplier	Fraction	0.9	0.9	0.9	0.9	0.7	0.7	0.7	0.7	0.7	0.9	0.9	0.9	-	-
Water Mains Temp.	F	40.7	38.6	39.9	44.0	50.0	56.3	61.2	63.5	62.6	58.7	52.8	46.4	51.3	-
Basecase DHW Use	gal/day	80.1	80.4	80.2	79.5	78.3	76.8	75.5	74.7	75.0	76.2	77.7	79.1	77.8	-

Table I- 3 Monthly Energy Use for the Base-case House and Proposed Design in Minneapolis, MN

MONTHLY ENERGY USE			Jan	Feb	Mar	Apr	May	Jun	Jul	Aug	Sep	Oct	Nov	Dec	TOTAL	
Base-case Thermal Energy Use	Space Heating	MMBtu	16.57	10.98	6.81	1.68	0.03	0.00	0.00	0.00	0.00	1.14	7.13	14.17	58.50	
	Dom. Water Heating	MMBtu	1.62	1.60	1.62	1.61	1.62	1.61	1.62	1.61	1.62	1.61	1.62	1.61	1.62	19.37
	TOTAL	MMBtu	18.18	12.58	8.42	3.29	1.65	1.61	1.62	1.62	1.62	1.61	2.76	8.74	15.79	77.87
Base-case Electricity Use	Lighting	kWh	167	151	167	161	167	161	167	167	161	167	161	167	1964	
	Equipment	kWh	578	522	578	559	578	559	578	578	559	578	559	578	6804	
	Space Cooling	kWh	0	0	6	62	382	710	786	710	377	97	8	0	3138	
	Pumps & Misc.	kWh	13	15	23	20	8	0	0	0	4	22	22	14	141	
	Vent Fans	kWh	409	259	129	45	103	185	202	182	102	47	127	315	2105	
TOTAL	kWh	1,167	947	903	847	1,238	1,615	1,733	1,637	1,203	911	877	1074	14,152		
Reduced Thermal Energy use	Space Heating	MMBtu	8.19	5.61	4.18	1.93	0.28	0.00	0.00	0.00	0.00	0.40	3.50	7.26	31.36	
	Dom. Water Heating	MMBtu	0.93	0.86	0.94	0.86	0.83	0.73	0.70	0.67	0.66	0.73	0.77	0.87	9.56	
	TOTAL	MMBtu	9.12	6.47	5.12	2.80	1.11	0.73	0.70	0.67	0.66	1.13	4.27	8.12	40.91	
Reduced Electricity Use	Lighting	kWh	61	55	61	59	61	59	61	61	59	61	59	61	718	
	Equipment	kWh	385	348	385	373	385	373	385	385	373	385	373	385	4535	
	Space Cooling	kWh	0	4	2	3	32	95	132	135	108	58	14	0	583	
	Pumps & Misc.	kWh	26	25	28	21	8	0	0	0	4	23	29	27	191	
	Vent Fans	kWh	179	109	59	22	9	18	26	27	24	20	51	129	673	
	TOTAL	kWh	651	541	535	478	495	545	604	608	568	547	526	602	6700	



Table I- 5 Calculations for Building UA and  $T_{bal}$  for the Base-case House and Proposed Design in Minneapolis, MN

		Jan	Feb	Mar	Apr	May	Jun	Jul	Aug	Sep	Oct	Nov	Dec	Intcpt.	Slope	R <sup>2</sup>	BldgUA	T <sub>bal</sub>
Monthly Avg. T (F)	F	10.8	17.4	32.5	47.7	60.8	68.9	71.6	70.9	61.0	47.7	33.3	17.2	-	-	-	-	-
Basecase Simulated	MMBtu	22.3	16.3	9.1	2.3	0.0					1.5	9.9	19.0	25.8	-0.47	0.96	469.6	54.9
Max. Eff. Simulated	MMBtu	11.0	8.4	5.6	2.7	0.4					0.5	4.9	9.8	12.9	-0.22	0.95	224.2	57.5

Table I- 6 Monthly Harvestable Renewable Energy from Different Systems in Minneapolis, MN

		Jan	Feb	Mar	Apr	May	Jun	Jul	Aug	Sep	Oct	Nov	Dec	TOTAL
2.5 kW Turbine Output	kWh	107	108	239	231	192	126	85	87	111	174	189	152	1,801
7.5 kW Turbine Output	kWh	182	189	429	424	344	224	144	144	191	308	339	269	3,186
20 m2 Mono-crystalline PV @ Lat.	kWh	310	344	406	402	431	424	450	430	373	333	243	231	4,375
20 m2 Mono-crystalline PV @ Lat.-15	kWh	269	316	397	415	463	465	489	451	372	313	218	203	4,371
20 m2 Mono-crystalline PV @ Lat.+15	kWh	330	352	393	369	377	364	389	388	354	334	253	245	4,148
20 m2 Thin-film PV @ Lat.	kWh	302	338	403	405	439	436	466	444	381	336	240	226	4,414
20 m2 Thin-film PV @ Lat.-15	kWh	261	310	394	418	473	479	507	466	380	315	215	198	4,415
20 m2 Thin-film PV @ Lat.+15	kWh	322	346	390	371	383	373	402	399	361	337	251	240	4,175
12 m2 Evac. Tube Collector Output	MMBtu	0.68	0.75	0.94	0.98	1.03	1.04	1.11	1.10	0.96	0.81	0.56	0.52	10.47
24 m2 Evac. Tube Collector Output	MMBtu	8.16	8.99	11.30	11.75	12.34	12.47	13.30	13.14	11.57	9.68	6.76	6.20	125.65

Table I- 7 Sizing of Renewable Energy Systems for the Proposed Design in Minneapolis, MN

		Jan	Feb	Mar	Apr	May	Jun	Jul	Aug	Sep	Oct	Nov	Dec	TOTAL
Thermal Loads	MMBtu	9.12	6.47	5.12	2.80	1.11	0.73	0.70	0.67	0.66	1.13	4.27	8.12	40.91
40 m2 Evac. Tube Collector Output	MMBtu	8.16	8.99	11.30	11.75	12.34	12.47	13.30	13.14	11.57	9.68	6.76	6.20	125.65
Unmet Thermal Energy Use	MMBtu	0.96	0.00	0.00	0.00	0.00	0.00	0.00	0.00	0.00	0.00	0.00	1.92	2.88
Electric Heat Pump System Perf.	COP	3	3	3	3	3	3	3	3	3	3	3	3	3
Electric Heating Loads	kWh	94	0	0	0	0	0	0	0	0	0	0	0	187
DOE-2 Electric Loads	kWh	651	541	535	478	495	545	604	608	568	547	526	602	6,700
Total Electric Loads	kWh	745	541	535	478	495	545	604	608	568	547	526	789	6,982
7.5 kW Turbine Output	kWh	182	189	429	424	344	224	144	144	191	308	339	269	3,186
Remaining Electric Loads	kWh	469	352	106	54	151	321	460	464	377	239	187	333	3,514
30 m2 Mono-crystalline PV @ Lat.	kWh	464	516	609	603	646	636	675	645	559	499	364	347	6,562

Table I- 8 Sizing of Sizing of Battery Storage System for the Proposed Design in Minneapolis, MN

		Jan	Feb	Mar	Apr	May	Jun	Jul	Aug	Sep	Oct	Nov	Dec
Minimum Available Insolation Over A Consecutive-day Period (% of Avg. Monthly Insolation)	7 day	63.3	59.0	50.5	34.7	47.9	56.4	60.2	50.0	45.9	47.1	54.7	61.0
	14 day	79.9	69.7	61.2	55.8	64.0	64.5	78.9	61.6	53.3	53.5	68.9	63.6
	21 day	82.7	76.5	66.2	66.3	70.6	76.4	81.9	73.6	66.3	60.4	74.5	75.4
	Month	88.6	83.7	83.7	84.5	84.2	92.5	86.3	84.4	83.5	75.2	86.4	84.8
Equivalent Number of NO-SUN Or BLACK Days (days)	7 day	2.6	2.9	3.5	4.6	3.6	3.1	2.8	3.5	3.8	3.7	3.2	2.7
	14 day	2.8	4.2	5.4	6.2	5.0	5.0	3.0	5.4	6.5	6.5	4.4	5.1
	21 day	3.6	4.9	7.1	7.1	6.2	5.0	3.8	5.5	7.1	8.3	5.4	5.2
	Month	3.5	4.6	5.1	4.7	4.9	2.3	4.2	4.8	5.0	7.7	4.1	4.7
Avg. Electricity Load	kWh/day	24.0	19.3	17.3	15.9	16.0	18.2	19.5	19.6	18.9	17.6	17.5	25.5
Storage for NO-SUN days	kWh	87.3	95.4	122.5	112.8	98.6	90.3	82.7	108.7	134.0	146.7	93.9	131.6
Maximum Insolation Over A Consecutive-day Period (% of Avg. Monthly Insolation)	7 day	147	153	160	157	144	142	132	142	149	161	157	132
	14 day	130	129	142	142	136	131	119	130	136	152	142	122
	21 day	118	123	131	130	125	117	120	121	131	130	130	117
	Month	111	114	116	117	120	115	111	115	121	117	116	114
Equivalent Number of Days with Avg. Radiation (days)	7 day	3.3	3.7	4.2	4.0	3.1	2.9	2.2	2.9	3.4	4.3	4.0	2.2
	14 day	4.2	4.1	5.9	5.9	5.0	4.3	2.7	4.2	5.0	7.3	5.9	3.1
	21 day	3.8	4.8	6.5	6.3	5.3	3.6	4.2	4.4	6.5	6.3	6.3	3.6
	Month	3.4	3.9	5.0	5.1	6.2	4.5	3.4	4.7	6.3	5.3	4.8	4.3
Avg. Electricity Generated	kWh/day	15.0	18.4	19.6	20.1	20.8	21.2	21.8	20.8	18.6	16.1	12.1	11.2
Storage for SURPLUS SUN days	kWh	62.9	89.0	127.8	126.6	129.2	95.5	91.5	96.7	121.2	117.2	76.4	48.5



## APPENDIX J

### COST ESTIMATE OF SYSTEMS

The costs associated with the energy-efficiency and water-efficiency measures, and the systems for self-sufficiency is presented for the proposed off-grid, off-pipe house, which could be used to perform life-cycle cost analysis for future studies.

The base-case house is a 2,500 sq. ft., four bedroom, single-family detached unit assumed to be located in a suburban area in each of the selected climate location. The cost of the house was estimated from NAHB House Price Estimator (NAHB 2009). The cost of energy-efficiency measures were estimated as 6% of the base-case cost (Malhotra 2005). The renewable systems/systems required for self-sufficiency include solar thermal, photovoltaic, wind power, battery-storage, rainwater harvesting and sewage disposal systems. Cost of some of these systems was determined from the available total system costs, obtained from several resources. For other systems such as renewable electric systems, consideration of the cost of individual components provided a better estimate. Table J- 1 lists the capital cost estimate of the house and its systems based on an example system sizing requirements, as described below.

A 6.8 kW PV array for peak summer loads, supplemented by a 2 kW wind turbine for overcast days in winter was considered. The battery bank was sized for 10 days with no solar. Considering maximum daily electrical load of 26 kWh, 83% battery efficiency (during charge/discharge cycle), 24V battery bank voltage, 50% maximum depth of discharge, and selecting 2 volt, 1766 Amp-hr batteries, the electricity storage would consist of 10 batteries in series, and a total of 20 batteries. A solar thermal system with 128 sq. ft. evacuated tube collectors and a 120 gallon hot water storage tank (1.875 gallon storage/sq. ft. of collector, storing water at 180 deg F) should provide all of winter heating needs, even during 5 overcast days. In addition, a rainwater harvesting system with a 2,500 sq. ft. roof catchment area and a 10,000 gallon storage tank was assumed. The septic system was a typical residential sized system, with 1,000 gallon underground tank.

*Table J- 1 Capital Cost Estimation for Off-grid, Off-pipe Homes*

Items	Capital (\$)	Source
Base case house	\$272,000	NAHB House Price Estimator (NAHB 2009)
Additional Cost for energy and water-efficiency improvements	\$16,000	5 to 6% of the base-case cost (Malhotra 2005)
Solar thermal system (64 sqft collector, 120 gallon storage tank)	\$4,500	Southface (2008)
Electric system		
PV array (6.8kW)	\$34,000	\$5 per watt (SECO 2009)
Wind turbine (2kW)	\$6,000	\$3 per watt (Shevory 2007)
Batteries (25,000Ah)	\$25,000	\$1/Ah (SECO 2009)
Inverter (5kW)	\$5,000	\$1 per watt (SECO 2009)
Balance of system and installation cost	\$13,000	20% of total system cost (SECO 2009)
SUBTOTAL	\$79,000	
Rainwater harvesting system (10,000 gallon storage tank)	\$15,000	Tanktown (2009)
Septic system (1,000 gallon underground tank)	\$2,500	WQWM (1996)
<b>TOTAL</b>	<b>\$389,000</b>	Not considering rebates, tax credits, maintenance and replacement costs

**VITA****Mini Malhotra**

PO Box 2008, MS 6067  
Oak Ridge, TN 37831-6067  
Email: malhotram@ornl.gov

**Education**

Doctor of Philosophy, December 2009  
Texas A&M University, College Station, Texas

Master of Science in Architecture, December 2005  
Texas A&M University, College Station, Texas

Bachelor of Architecture, May 1999  
Birla Institute of Technology, Mesra, Ranchi, India

**Professional Experience**

R&D Associate, November 2009 – Present  
Oak Ridge National Laboratory, Oak Ridge, Tennessee

Graduate Assistant - Research, June 2004 - October 2009  
Energy Systems Laboratory, Texas A&M University

Graduate Assistant - Teaching, September 2003 – May 2004  
Department of Architecture, Texas A&M University

Graduate Assistant – Non-teaching, June 2003 – August 2003  
Women’s Center, Texas A&M University

Free-lance Architect, April 2002 – December 2002  
Unnao, India

Assistant Architect, August 1999 – March 2002  
Ar. Dharendra K. Mishra, Kanpur, India

**Major Field of Specialization**

Building Energy Simulation and Analysis  
Energy-efficiency and Renewable Energy Technologies for Buildings